

**Investigating the Interdependent Influence of Multiple
Environmental Features of Urban Green Spaces on
Human Thermal Comfort at Microscale Using a Multi-
parameter Approach**

Dissertation

zur Erlangung des Grades eines
Doktors der Naturwissenschaften (Dr. rer. nat.)

am Fachbereich Geowissenschaften
der Freien Universität Berlin

vorgelegt von

Huiwen Zhang

Berlin, Dezember 2023

Erstgutachterin (Betreuerin): Prof. Dr. Sahar Sodoudi

Zweitgutachter: Prof. Dr. Ulrich Cubasch

Tag der Disputation: 14. Juni 2024

TABLE OF CONTENTS

Table of Contents.....	i
List of Figures.....	iii
List of Tables.....	viii
List of Abbreviations.....	ix
Statement of Original Authorship.....	xi
Acknowledgement.....	xii
Abstract.....	xv
Keywords.....	xvii
Chapter 1: Introduction.....	1
1.1 Research Area.....	1
1.2 Research Objective: Enhancing Methodology to Generalize Research Results at Microscale.....	11
1.3 Thesis Structure.....	20
Chapter 2: Multi-parameter Approach vs. Single-parameter Approach	23
2.1 Overview of multi-parameter Approach.....	23
2.2 Comparison with single-parameter Approach.....	44
2.3 Why the multi-parameter Approach is Conducive to the Application and Generalization of Research Results.....	47
Chapter 3: The Influence of Spatial Configuration of Green Space on Microclimate and Human Thermal Comfort.....	53
3.1 Introduction.....	54
3.2 Methodology.....	56
3.3 Results and Discussion.....	62
3.4 Conclusions and Application.....	76
Chapter 4: How Do Walkways in Historic Gardens Affect the Thermal Comfort of Pedestrians? An Example from Berlin's Tiergarten	79
4.1 Introduction.....	81
4.2 Methodology.....	82
4.3 Results.....	86
4.4 Conclusions, Application and Outlook.....	100
Chapter 5: Interdependent Influences of Three Landscape Design Factors on Human Thermal Comfort of Urban Riverside Greenways	103
5.1 Introduction.....	104
5.2 Methodology.....	106

5.3	Results	118
5.4	Further Simulation Experiment on Comparing the Cooling Capability of Waterbody and Trees	123
5.5	Conclusions, Discussion and Application	128
	Chapter 6: Conclusions and Discussion	133
6.1	Overall Conclusion.....	133
6.2	Strengths of the Multi-parameter Approach Represented in Three Studies.....	134
6.3	Comparison with Similar Studies.....	137
6.4	Outreach	140
	Additional Information.....	143
	Publication Bibliography	145

LIST OF FIGURES

Figure 1-1 Hierarchical relationship among the research areas to which this research belongs.....	1
Figure 1-2 Idealized vertical structure of the urban atmosphere over (a) a whole city (mesoscale), (b) a single urban terrain zone (local scale), and (c) a single street canyon (microscale) (Oke, 1997, p. 305).	3
Figure 1-3 An orographic classification of urban sites (Wanner and Filliger,1989).	14
Figure 1-4 Simplified classification of distinct urban forms arranged in approximate decreasing order of their ability to impact local climate [2004 unpublished] (Oke, 2006a).	16
Figure 1-5 LCZ subclasses to represent combinations of surface structure and surface cover (Stewart and Oke, 2012).....	17
Figure 1-6 WUDAPT LCZs classification framework (Xu et al., 2017).....	18
Figure 2-1 A schematic representation of a simple factorial experiment (David Harvey 2013).	25
Figure 2-2 Local Climate Zones containing features of building types and land cover types. (Stewart and Oke, 2012).....	26
Figure 2-3 The idea of LCZ system is consistent with the idea of the factorial design. By integrating different levels of features of different spatial factors, a collection of scenarios in the form of a matrix can then be formed. As this collection expands in terms of factors and levels, it can become increasingly comprehensive to encompass a wider range of urban land surface types.	27
Figure 2-4 Structure of the factorial experiment in the study of Chapter 3.	28
Figure 2-5 An example in Chapter 4 using the Latin Hypercube Sampling (LHS) method for selecting samples from factorial experiment for field measurements. The red dots represent the selected points for field measurement.	29
Figure 2-6 Interface of the Albero Module in ENVI-met 4.3.....	31
Figure 2-7 Schematic overview over the ENVI-met model layout (enviadmin, 2017c).	32
Figure 2-8 Data Flow in ENVI-met V3.1 (enviadmin, 2017b).....	34
Figure 2-9 Composite indicator is a form of data dimensionality reduction.	36
Figure 2-10 Energy fluxes that affect the human energy budget outdoors. M: Metabolism; C: Convection—Moving air removes radiated heat; K: Conduction—direct heat transfer by conduct; E: Evaporation—Loss of heat by evaporation of water; R: Radiation—SW: Short-wave, LW: Long-wave, D: Direct, Di: Diffused, Re: Reflected; Em: emission of	

Long-wave radiation; Ta: air temperature; Ws: Wind Speed; RH: air Relative Humidity; Tsk: Skin Temperature; Ts: Surface Temperature; (+) heat gain (–) heat loss; up arrow: increase, down arrow: decrease (Antoniadis et al., 2020).....	38
Figure 2-11 Flowchart of the human-biometeorological assessment of the thermal environment (Matzarakis et al., 2016).	40
Figure 2-12 Input window of RayMan Pro on the relevant values for the calculation of T_{mrt} and thermal indices (Matzarakis et al., 2007).	42
Figure 2-13 Input window of RayMan Pro on urban environment (Matzarakis et al., 2007).....	43
Figure 2-14 Input window of RayMan Pro on fish-eye photographs (Matzarakis et al., 2007).....	43
Figure 2-15 Single-parameter approach in current urban climatology: analytical extracting isolated indicators of complex objects and finding linear relationships between indicators.	45
Figure 2-16 Comparison of multi-parameter and single-parameter approaches at the technical aspect.....	47
Figure 2-17 The parable of the blind men and an elephant indicates that the whole cannot be accurately perceived by merely the side descriptions (Illustration: Hans Moller; Public Domain).	50
Figure 2-18 The analytical approach is suitable for answering the “how” questions, while the integrative approach is appropriate for the “why” questions.....	51
Figure 2-19 Advantages of multi-parameter methods over single-parameter methods.	51
Figure 3-1 Configuration of studied area on the simulation day.....	57
Figure 3-2 The daily time series of meteorological data (Meteogram) of the weather station located in Berlin Tempelhof (10384) from June 8 to June 9, 2014 (Data from Meteostat.net).....	58
Figure 3-3 (a) The mean hourly 2 m air temperature measured on the walkway surrounded by three vegetation types in Tiergarten (red) and the corresponding simulated air temperature (black); (b) The scatter diagram showing the correlation between the measurement and simulation.	63
Figure 3-4 Mean cooling effect by different scenarios at 2 pm, 10 pm, and 5 am.	64
Figure 3-5 The percentage of the area cooled down by more than 1.5 K, green: a>50% of the whole area, red: <10% of the whole area.	65
Figure 3-6 Mean cooling effect and Max cooling effect of Configurations 1-3.	66
Figure 3-7 Simulated air temperature of Configuration 1-3 at 2 pm (vegetation type: tree-big canopy).	67
Figure 3-8 Mean cooling effect of three selected vegetation types.....	69

Figure 3-9 Simulated air temperature of Configurations 2 and 4 at 2 pm (vegetation type: tree-big canopy).....	70
Figure 3-10 Wind speed and direction in Configurations 4 and 5. The colour indicates the wind speed in m/s and the wind direction is shown by arrows.....	70
Figure 3-11 Mean cooling effect of different vegetation types at 2 pm.	72
Figure 3-12 Mean cooling effect of different vegetation types at 10 pm.	72
Figure 3-13 Mean cooling effect of different vegetation types at 5 pm.	73
Figure 3-14 The mean PET values of 25 scenarios at 2 pm, 10 pm and 5 am.....	74
Figure 3-15 Difference value of PET of different scenarios compared to asphalt at 2 pm, 10 pm, and 5 am.....	75
Figure 3-16 Difference value of PET by trees-big canopy.	75
Figure 3-17 Decision tree derived from the research results.	78
Figure 4-1 Actual views of nine measurement points containing two features: vegetation type and walkway width.....	82
Figure 4-2 Location of the measuring area in Tiergarten (a) and the route of the moving measurement through points (b).....	83
Figure 4-3 The daily time series of meteorological data (Meteogram) of the weather station located in Berlin Tempelhof (10384) from Aug 30 to Aug 31, 2017 (Data from Meteostat.net).....	84
Figure 4-4 The fisheye photos of measuring points and the corresponding Sky View Factor (SVF) calculated by RayMan model.....	85
Figure 4-5 The design of scenarios for multi-variate simulation.....	86
Figure 4-6 Air temperature (T_a) difference between urban weather station at Jagow Street (T_u) and measurement points (T_x) in 7 m, 5 m and 3 m width walkways with Trees&Shrubs, Trees&Grass and Grass at 2 pm and 10 pm on 30, August 2017. The chart at the bottom shows the difference between 10 pm and 2 pm at each measurement point.	87
Figure 4-7 (a) Diurnal variation of the T_a on the 7m wide walkway surrounded by three vegetation types (Grass, Tree & Grass, Tree & Shrubs) from 9am in 30, August 2017 to 8am in 31, August 2017; (b) Diurnal variation of the wind velocities on the three measuring points, (c) SVF on the three measured points.....	89
Figure 4-8 (a) Diurnal variation of the T_a on the 7 m, 5 m, 3 m wide walkway surrounded by Tree & Shrubs from 9am in 30, August 2017 to 8am in 31, August 2017;(b) Diurnal variation of the wind velocities on the three measuring points, (c) SVF on the three measured points.	91
Figure 4-9 (a) The diurnal variation of measured T_a of the different vegetation types (Grass, Tree & Grass, Tree & Shrubs) on the 7 m wide walkway; (b) The diurnal variation of simulated T_a of the scenarios with different vegetation types (Grass, Tree & Grass, Tree & Shrubs).....	92

Figure 4-10 (a) The diurnal variation of measured T_a of the different widths of walkways (7m, 5m, 3m) with the vegetation type of Tree & Grass; (b) The diurnal variation of simulated T_a of the scenarios with different widths of walkways (7m, 5m, 3m).....	93
Figure 4-11 The linear regression between the simulated air temperature and the measured air temperature.	94
Figure 4-12 (a)The physiological equivalent temperature (PET) calculated from the simulated data, and (b) the simulated mean radiant temperature (T_{mrt}) of the scenarios with the same width of walkway (7m), different vegetation types (Grass, Tree&Grass, Tree&Shrubs).	96
Figure 4-13 (a)The physiological equivalent temperature (PET) calculated from the simulated data, and (b) the simulated mean radiant temperature (T_{mrt}) of the scenarios with the same vegetation type (Tree&Shrub), the different widths of walkway (3m, 5m, 7m).....	97
Figure 4-14 The maps of T_{mrt} at 1.1 m height on 2 pm of each simulating scenario.	98
Figure 4-15 The map of T_{mrt} at 1.1 m height at 10 pm in each simulating scenario.	99
Figure 4-16 The map of human thermal comfort of the walkways in Tiergarten at summer daytime. The bottom left chart (SenUVK, 2023) presents the mean wind direction distribution at the Berlin-Tempelhof DWD station for summer season (June, July and August), differentiated by wind speed.....	102
Figure 5-1 Structure of the factorial experimental design for the microclimate simulation. The blue arrows represent the wind directions: 0° (North)—parallel to the greenway, 90° (East)—blowing from the urban area toward the waterbody, 270° (West)—blowing from the waterbody toward the urban area.	107
Figure 5-2 The Latin Hypercube Sampling (LHS) design was used to select five values from the twelve categories of tree species for the factorial simulation experiment.	109
Figure 5-3 Cross-section profile of an urban riverside greenway, illustrating how the greenway trail position is quantified by the <i>Distance from Waterbody</i> (D_w).	110
Figure 5-4 The five basic scenario spaces for simulation were built using ENVI-met, representing the five greenway trail positions ($D_w = 0, D_w = 0.25, D_w = 0.5, D_w = 0.75, D_w = 1$).	112
Figure 5-5 Arrangement of measuring points in the measuring experiment. (a) Location of the experiment field in downtown Shanghai; (b) Measuring points for greenway trail position $D_w = 0$; (c) Measuring points for greenway trail position $D_w = 0.5$	114

Figure 5-6 The daily time series of meteorological data (Meteogram) of the weather station located in Shanghai Hongqiao (58367) on July 30, 2014 (Data from Meteostat.net).....	115
Figure 5-7 Weather stations at measuring point No.5; (b): Spectrum Watchdog 2900ET is a portable weather station with high precision and multifunction; (c): Weather station at the measuring point No.1.	115
Figure 5-8 The space of the measuring fields were reconstructed by SPACES module of ENVI-met 4.3 to evaluate the modeling. (a1): Plane graph; (b1): Aerial view graph.	117
Figure 5-9 The comparison between the mean value of the simulated air temperature (T_a) from the six receptors and the mean value of the measured T_a from the six portable weather stations.	118
Figure 5-10 Air temperature (T_a) at a height of 1.5 m on greenway trails with five greenway trail positions D_w , five types of tree species and wind direction of north (0°).	119
Figure 5-11 Air temperature (T_a) at a height of 1.5 m on greenway trails with five greenway trail positions (D_w), five types of tree species and three wind directions: 0° (N)—parallel to greenway, 90° (E)—from urban street to waterbody, 270° (W)—from waterbody to urban street.	120
Figure 5-12 Physiological Equivalent Temperature (PET), air temperature (T_a) and Mean radiant temperature (T_{mrt}) at a height of 1.5 m on greenway trails with five greenway trail positions (D_w), five types of tree species and three wind directions.	122
Figure 5-13 The spatial layout of the scenarios simulated in ENVI-met for comparing the cooling capability of the waterbody and green areas. a-a, b-b, and c-c refer to cross sections of the green area scenarios (2), (3) and (4).	124
Figure 5-14 The temperature difference (D-value) of the air temperature on the waterbody (T_{a_water}) and that in the green area (T_{a_canopy}) at a height of 1.5 m.	125
Figure 5-15 Spatial and temporal distribution of the air temperature in measuring experiment. (a): the diurnal change of air temperature, (b): the box plot of diurnal air temperature; (1) $D_w=0$; (2) $D_w=0.5$	127
Figure 6-1 Different methods of urban space description can reflect information of different dimensions of space.	138
Figure 6-2 The Kuhn Cycle (Roth and Rosenzweig, 2020).....	141
Figure 6-3 The S-curve of performance and functionality improvement in science development (Filmore, 2008).....	142

LIST OF TABLES

Table 2-1 Ranges of the PET for different grades of thermal perception by human beings and physiological stress on human beings. The assessment classes of PET* (Matzarakis et al., 2009, p. 212).	41
Table 3-1 The configuration of ENVI-MET for the simulation.....	59
Table 3-2 Descriptions and equations for Patch Density and Edge Density (PD & ED).....	61
Table 3-3 The comfort/sensation scale of the physiological equivalent temperature (PET) according to Matzarakis and Mayer (1997).	62
Table 3-4 Patch Density and Edge Density (PD & ED) of Configurations 1-3.....	65
Table 3-5 Patch Density and Land Shape Index (LSI) of Configuration 2 and Configuration 4.	68
Table 3-6 Comparison of configuration 4 and 5 in terms of turbulent fluxes.....	71
Table 5-1 Categories of commonly used tree species represented by the combination of Lead Area Density (LAD) and Foliage Albedo values.....	108
Table 5-2 The general configuration of the simulation conducted using the ENVI-met model.	113
Table 5-3 Recorded data and configuration of weather station Watchdog 2900ET.	116
Table 5-4 Values and classes of the LAD and Foliage Albedo of tree species recorded in ENVI-met model (Bruse, 2017).....	131

LIST OF ABBREVIATIONS

A	
Aspect Ratio (H/W)	137
C	
Climate Change Adaptation (CCA)	1
Climate Change Mitigation (CCM)	1
Computational Fluid Dynamics (CFD)	30
D	
Deutscher Wetterdienst (DWD)	xii
Distance From Waterbody (D _w)	109
E	
Edge Density (ED) [m ha ⁻¹]	60
G	
General Circulation Models (GCMs)	5
Geographic Information System (GIS)	5
I	
Intergovernmental Panel on Climate Change (IPCC)	1
L	
Land Shape Index (LSI)	60
Land Surface Temperature (LST) [°C]	4
Lateral Boundary Conditions (LBC)	32
Latin Hypercube Sampling (LHS)	29
Leaf Area Density (LAD) [m ² m ⁻³]	107
Local Climate Zones (LCZ)	11
M	
Mean Radiant Temperature (T _{mrt}) [°C]	94
Ministry of Housing and Urban-Rural Development (MOHURD)	9
Modified Physiological Equivalent Temperature (mPET) [°C]	37
Munich Energy Balance Model for Individuals (MEMI)	40
N	
National Development and Reform Commission (NDRC)	9
Nearest Neighbor Distances (NND)	5
Normalized Difference Vegetation Index (NDVI)	45
O	
Outdoor Standard Effective Temperature (Out_SET) [°C]	37
P	
Park Cool Island (PCI)	1
Partial Differential Equations (PDE)	31

Patch Density (PD) [ha^{-1}].....	60	(UTCI).....	37
Patch Density and Edge Density (PD & ED).....	54	Urban Boundary Layer (UBL).....	3
Perceived Temperature (pT) [$^{\circ}\text{C}$].....	37	Urban Canopy Layer (UCL).....	3
Physiological Equivalent Temperature (PET) [$^{\circ}\text{C}$].....	37	Urban Climate Zones (UCZ).....	11
Predicted Mean Vote (PMV).....	37	Urban Climatic Map (UCMap).....	18
R		Urban Green Space (UGS).....	1
Regional Climate Models (RCMs).....	5	Urban Heat Island (UHI).....	4
Root Mean Square Error (RMSE).....	118	Urban Open Space (UOS).....	103
S		Urban Riverside Greenway (URG).....	21
Sky View Factor (SVF).....	4	Urban Terrian Zone (UTZ).....	14
Standard Effective Temperature (SET) [$^{\circ}\text{C}$].....	37	W	
U		World Meteorological Organization (WMO).....	6
Universal Thermal Climate Index		World Urban Database and Portal Tool (WUDAPT).....	18

STATEMENT OF ORIGINAL AUTHORSHIP

The work contained in this thesis has not been previously submitted to meet requirements for an award at this or any other higher education institution. To the best of my knowledge and belief, the thesis contains no material previously published or written by another person except where due reference is made.

Signature: Huiwen Zhang

Date: 21.12.2023

ACKNOWLEDGEMENT

This research was funded by the scholarship of China Scholarship Council (CSC) for full-time doctoral study abroad.

The Study mentioned in Chapter 3: *The Influence of Spatial Configuration of Green Space on Microclimate and Human Thermal Comfort*” contributes to the research program “Urban Climate Under Change ([UC]2)”, funded by the German Ministry of Research and Education (FKZ01LP1602 A). The authors are grateful to the project “Cooling effect of the historical garden ‘Tiergarten’ in Berlin” financed by Berlin-Brandenburg Academy of Science (BBAW), German Weather Service - Deutscher Wetterdienst (DWD) for the data of the station Tempelhof, and China Scholarship Council (CSC) for the financial support. They also thank David Mottram for his valuable proofreading of this paper.

The Study mentioned in Chapter 4: *How Do Walkways in Historic Gardens Affect the Thermal Comfort of Pedestrians? An Example from Berlin's Tiergarten* was funded by Berlin-Brandenburg Academy of Science (BBAW) for the project *Historische Gärten im Klimawandel: Die interdisziplinäre Arbeitsgruppe untersuchte die Folgen des Klimawandels für historische Gärten, Parkanlagen und Kulturlandschaften*.

The Study mentioned in Chapter 5: *Interdependent Influences of Three Landscape Design Considerations on Human Thermal Comfort of Urban Riverside Greenways* was funded by the key project of the National Natural Science Foundation of China (NSFC): *Theory and Methodology of Climate-adaptative Landscape Design at Microscale for a Liveable Urban Environment (No.51338007)*.

The beginning of this dissertation coincided with the onset of the COVID-19 pandemic. Although I encountered difficulties in the process of completing the thesis, upon its completion, I realized that I should be grateful for this dissertation and my doctoral journey. These experiences represent the most valuable lessons I have ever acquired. Therefore, I sincerely express my gratitude to all the individuals who have supported me throughout this journey of personal development. I also hope that the world will soon recover from this pandemic and move towards a brighter future.

I would like to express my gratitude to my first supervisor, Prof. Dr. Sahar Sodoudi. She has consistently provided me with all the help I needed in a remarkably professional

and passionate manner. Without her assistance, I could not have secured this invaluable opportunity for study. I also extend my thanks to Prof. Dr. Ulrich Cubasch for his professionalism, patience, and friendliness, which greatly contributed to enhancing this dissertation. Additionally, I appreciate the support of Prof. Dr. Uwe Ulbrich for his substantial help in my doctoral project and for dedicating his time to reviewing my dissertation. I would like to thank Prof. Dr. Andreas Matzarakis for his thoughtful review and constructive suggestions, which have significantly improved this dissertation.

I would also like to express my gratitude to my post-graduate supervisor, Prof. Dr. Deshun Zhang. My dedication to urban climatology originated from my participation in the key project of the National Natural Science Foundation of China: *Theory and Methodology of Climate-adaptive Landscape Design at Microscale for a Liveable Urban Environment* (No.51338007), in which he was involved. Prof. Dr. Deshun Zhang played a crucial role in facilitating my Ph.D. project. His rigorous academic attitude has consistently influenced my approach to academic work.

I would also like to thank Prof. Dihua Li, who had generously hosted me for an academic visit at Peking University. This visit provided inspiration for this thesis at the philosophical level and shaped the planned direction of my future research.

Thanks to my colleagues: Dr. Huidong Li, Dr. Xiaoli Chi, Dr. Ines Langer, Felix Müller, Jochen Werner, Elham Fakhariyade. Without the support of the group, I could not have achieved any of the results. I would also like to extend my thanks to Ingo Kirchner for providing important assistance in data at the final stage of my thesis.

Thanks to the Fayad Daher family: Sophia, Ugarit, Inanna, and Juliana. I wrote this dissertation while living with them. Without their provision of a stable and comfortable family-like environment, I wouldn't have completed my doctoral work in such a pleased and peaceful state.

I am very grateful to my family. Although they are more eager than anyone else to have me finish my studies and return to them as soon as possible, they always hid their expectations to avoid putting more pressure on me. They provided great financial support and encouragement when I was engaged in writing the thesis. Their love is the inexhaustible motivation for me to move forward.

Thank Dr. Zhen Wang for all of your warm support throughout my entire doctoral period.

Thanks to all the people who helped me. The doctoral research process has taught me that any result is a collective effort involving many individuals. The present dissertation would not have been possible without the contribution of any of the above-mentioned people. In gratitude, I aspire to use what I have learned to benefit others.

ABSTRACT

The three studies in this dissertation investigate the interdependent influence of various environmental features in Urban Green Space (UGS) on human thermal comfort at the microscale. This research pertains to microscale urban climatology. Urban climatology is an interdisciplinary field focused on advising urban construction to achieve the preferred urban climate.

Microscale urban climatological studies have more application potential than those at meso- and local scales. Yet, current limitations in microscale urban climatological research hinder realizing this potential. Firstly, the costs of microscale studies are generally high. Secondly, it is difficult to apply the research results elsewhere. As a result, the high-cost microscale studies must be continuously repeated in various locations. The challenge of generalizing research results is a common limitation in urban climatology. Approaches have been proposed to alleviate this limitation in urban climatological studies at meso- and local scales. However, there is a lack of such attempts at the microscale.

This research aims to propose an approach contributing to the generalization of research results in microscale urban climatological studies. This approach upgrades from the previous single-parameter approach to a multi-parameter approach. The multi-parameter approach views the UGS holistically by exploring the interdependent influence of various environmental features on human thermal comfort. The interdependent influence can enhance the comprehensiveness of results, improve the results generalization, and facilitate the knowledge transfer into specific guidelines for climate-adaptive UGS design and planning.

To explore the interdependent influence, the multi-parameter approach utilizes the factorial experimental design. The microclimate model ENVI-met is used to simulate scenarios in the factorial experiments. The simulations are conducted on idealized and simplified scenarios to minimize the research costs. To control the research cost, the Latin Hypercube Sampling (LHS) design is adopted to sample a subset of scenarios from the factorial experiment for field measurement and simulation. For result applicability, this research evaluates UGS cooling effects using both climatic parameters and biometeorological index -- Physiological Equivalent Temperature (PET). PET values in this research are calculated using the RayMan model.

This thesis comprises three independent studies on the interdependent influence of various environmental features of UGS on human thermal comfort. The following common conclusions can be drawn from these three studies. Firstly, different environmental features influence the cooling effects of UGS in an interdependent way. Specifically, the correlation between an environmental feature and the PCI effect depends on various environmental features. Secondly, the multi-parameter approach is significantly superior to the single-indicator approach in comprehensively and accurately capturing the interdependent influence. Additionally, these three studies provide specific and generalizable suggestions for the climate-adaptative UGS design and planning, demonstrating the capability of the multi-parameter approach to enhance the applicability and generalizability of findings in urban climatological studies.

The characteristics of the multi-parameter approach include the following three aspects. At the practical level, it can provide specific guidelines for practical UGS design and planning; at the research level, it explores the interdependent influence of multiple environmental features on human thermal comfort; and at the philosophical level, it adopts the holistic view. This research is not only an attempt to enhance methodology and promote the application of research results, but also a manifestation of the philosophical paradigm shift in urban climatology.

KEYWORDS

- Climate Change Adaptation (CCA)
- Urban Climatology
- Microclimate
- Microscale Modelling / Simulation
- Urban Green Space (UGS)
- Climate-adaptative Urban Design
- Park Cool Island (PCI) effect
- Human Thermal Comfort
- Physiological Equivalent Temperature (PET)

Chapter 1: Introduction

1.1 Research Area

This research belongs to the area focusing on the influence of spatial morphology of Urban Green Space (UGS) on human comfort at the microscale. It is a subfield of urban climatology that concentrates on the Park Cool Island (PCI) effects of UGS. Urban climatology is a manifestation of Climate Change Adaptation (CCA) in urban spaces. CCA and Climate Change Mitigation (CCM) are the two main branches of the field of climate change. The hierarchical relationship among these research areas is illustrated in Figure 1-1.

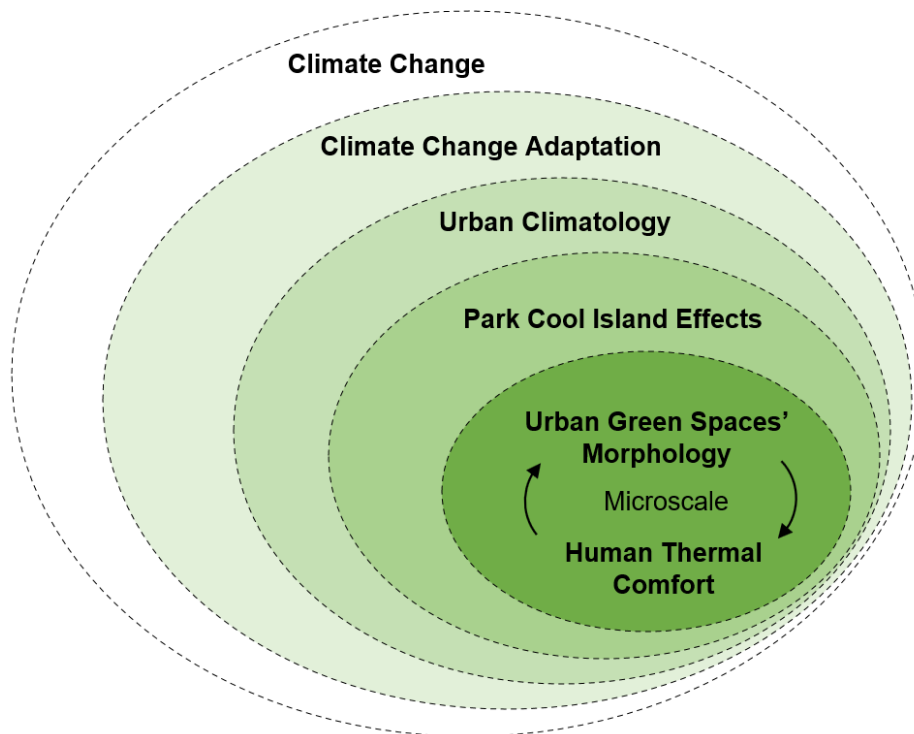


Figure 1-1 Hierarchical relationship among the research areas to which this research belongs.

1.1.1 Climate Change Adaptation (CCA) in Urban Areas

Global warming poses a serious threat to humankind's survival and development. Despite significant efforts to mitigate this crisis, the pace of climate change has not slowed as expected. The reality that humans will inevitably live in a changing climate for a long period has been acknowledged (Klein et al., 2007; Verbruggen, 2007). In this context, rapid adaptation to climate change is important. In its 2014 glossary, the Intergovernmental Panel on Climate Change (IPCC) defined *Adaptation* as:

The process of adjustment to actual or expected climate and its effects. In human systems, adaptation seeks to moderate or avoid harm or exploit beneficial opportunities (IPCC, 2018, p. 1758).

Cities, serving as dense human settlements, house 55% of the world's population (United Nations, 2018). Due to the high density of human activities, the climatic environment in cities is significantly worse than in other regions. Particularly in recent decades, rapid urbanization and global warming are jointly rendering urban climates around the world less liveable (Meehl and Tebaldi, 2004). The worsening urban climate is causing thermal discomfort and health risks for urban dwellers (Mihalakakou et al., 2004; Pantavou et al., 2011; Patz et al., 2005). Urban heat waves have shown a strong correlation with morbidity and mortality among the elderly living in urban areas (Åström et al., 2011; Fouillet et al., 2006). Furthermore, the air conditioning and electricity used to cool down cities is exacerbating global warming (Kolokotroni et al., 2007). All the above factors underscore the urgent need to implement Climate Change Adaptation (CCA) in urban areas. Over the past approximately 40 years, research intensity in urban climatology has been increasing, parallel to the growing attention to climate change (Hebbert and Mackillop, 2013).

1.1.2 Brief Overview of Urban Climatology

1.1.2.1 Definition of Urban Climatology

Urban climatology, a branch of climatology, is specifically concerned with urban areas. Rather than being a separate discipline, urban climatology is more of a “cross-disciplinary field” (Hebbert and Mackillop, 2013, pp. 1542–1543). Janković defines urban climatology as “a study of anthropogenic processes in urban atmospheres” (Janković, 2013, p. 540), considering urban form and function as environmental factors and modifiers of local climate. Urban climatology also examines how urban spatial structures, such as buildings, blocks, and landscapes influence airflow, turbulence, air temperature, humidity etc., shaping the specific local climate pattern. Oke (1984a), on his part, defined urban climatology in terms of a comparison with urban meteorology:

The study of the physical, chemical and biological processes operating to produce, or change the state of, the atmosphere in cities is called urban meteorology. The study of the resulting preferred states of their atmospheres is urban climatology.

From the above, we can see that urban climatology is characterized by its concern with how urban anthropogenic processes affect the urban climate. The motivation behind this

concern is to achieve the “preferred states” of the urban atmosphere by adjusting anthropogenic urban infrastructure (Brazel and Quatrocchi, 2005; Oke, 1984a).

1.1.2.2 Horizontal Scale and Vertical Scope

Urban climatology primarily studies the atmospheric boundary layer. When researchers study the urban infrastructure at different scales, they investigate its influence on corresponding atmospheric layers within the boundary layer. The urban infrastructure at the microscale, including individual buildings, streets, and trees, primarily influences the Urban Canopy Layer (UCL), i.e., the layer of air below the mean height of the urban rooftop, as well as the roughness sublayer. At the local scale, large neighborhoods with street canyons, buildings, and gardens influence the air at the *surface layer*. At the mesoscale, distinct urban terrain zones and large urban green patches influence the *internal boundary layers* in each zone. These components mix together and form the Urban Boundary Layer (UBL)(Figure 1-2) (Oke, 1984a, 1997, 1998).

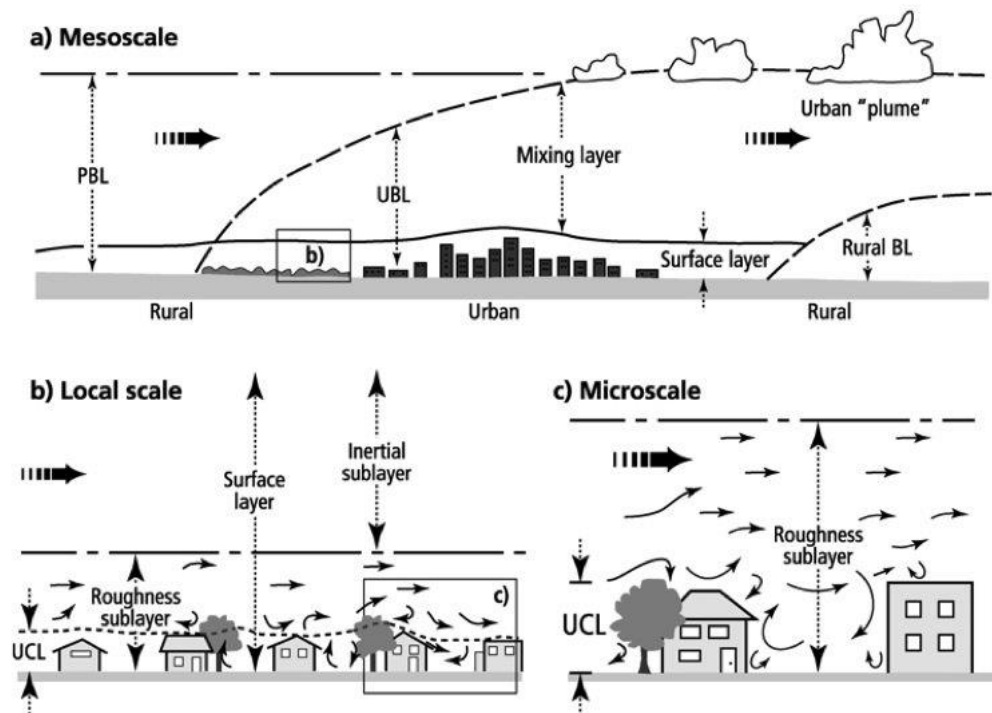


Figure 1-2 Idealized vertical structure of the urban atmosphere over (a) a whole city (mesoscale), (b) a single urban terrain zone (local scale), and (c) a single street canyon (microscale) (Oke, 1997, p. 305).

1.1.2.3 Evolution of Research Objects and Methods

Objects in urban climatology were roughly categorized by Oke into three aspects: *climatography*, *physical climatology*, and *applied climatology*. *Climatography* refers to the description and presentation of urban climate information. *Physical climatology* indicates the

meteorological explanation of climatic features. *Applied climatology* refers to the use of climatic knowledge in practical problem-solving (Oke, 1984a). Since the 1980s, with the growing urgency of global warming, the focus of urban climatological research has shifted to applied climatology. Numerous studies have explored the relationship between urban environmental features and the urban atmosphere to identify the urban land-surface form that can create the preferred urban climate (Bärring et al., 1985; Johnson and Watson, 1984; Oke, 1981).

From the 1950s to the 1970s, major studies in urban climatology were descriptive, attempting to optimize data collection methods to obtain a more comprehensive and accurate description of the Urban Heat Island (UHI) effect. For instance, Sundborg (1950) and Chandler (1965) studied the UHI effects of Lund and London using the transect method, which enables the observation of meteorological variables that respond more conservatively in shorter time. With the increase in the amount and accuracy of observational data, empirical research on relationships between urban climatic parameters and urban environmental and economic parameters began to emerge. Chandler (1967) investigated the effect of urban form on air temperature in Leicester; Daniels (1965) examined the correlations between the UHI effect and air pollution; Oke (1973) explored the empirical numerical relationship between urban population and UHI intensity.

In the 1980s, with Oke's research being representative, the study of urban climate forcing factors gradually shifted focus to the geometry and morphology of urban space. In 1981, Oke studied the influence of building height, street width and Sky View Factor (SVF) on UHI intensity. He also constructed an empirical numerical model applicable to different cities (Oke, 1981). For a long time after that, the urban canyon, with SVF and aspect ratio (H/W) as the main environmental parameters, was one of the most studied urban climate modifiers in urban climatology (Bärring et al., 1985; Johnson and Watson, 1984).

Urban climatology's development is inseparable from technological advances. Technical advances in satellite remote sensing in the 1980s and in climate modeling in the 1990s propelled urban climatological research into a highly active phase. Urban climatological research after the 1980s exhibited a broader scope, more diverse methods, and higher precision and accuracy compared to previous studies.

Since 1982, when the multispectral scanning radiometer Landsat Thematic Mapper (TM) was carried on board Landsat 4 (European Space Agency, 2020), it has been possible to derive continuous Land Surface Temperature (LST) from the data collected by this TM sensor (Price,

1984; Zhengming and Dozier, 1989). Since that time, the empirical study of urban climatology has reached a new level beyond the limitations of land surface observation. By combining Landsat TM data with geospatial analysis techniques, which were developed around the same time as the Geographic Information System (GIS), researchers can study the influence of urban morphology on the urban climate on a larger scale. For example, some studies have introduced parameters such as Land Shape Index (LSI), Edge Density (ED), and Nearest Neighbor Distances (NND) to describe the influence of the shape, fragmentation and connectivity of green patches on the thermal environment (Connors et al., 2013; McGarigal and Cushman, 2002; Zhou et al., 2011). Ecology, urban planning, landscape architecture, and other related disciplines increasingly participate in urban climatology.

With the rapid improvement in computer processing capacity (Moore, 1998), the physical climatological aspect of urban climatology has advanced significantly through climate models. The development of climate models has greatly expanded the possibilities of urban climatological research, making it possible to predict future urban climates and simulate scenarios which do not yet exist, thus providing suggestions for future decisions.

Currently, two main types of models are used in urban climatological research. One type refers to climate models on urban scale, which are represented by WRF/UCM (Chen et al., 2011), COSMO/CLM (Schubert and Grossman - Clarke, 2014), MUKLIMO_3 (DWD, 2024a; Sievers, 2012). The spatial resolution of these models is in most cases larger than 100 meters. This means that these models are generally used to study an urban neighborhood or an entire city. Since 2016, the German research program [UC]² has been developing the high-resolution urban climate model PALM-4U, with grid spacing ≤ 10 meters, capable of building-resolving simulation (DWD, 2024b; Steuri et al., 2020). When nested with Regional Climate Models (RCMs) and General Circulation Models (GCMs), these top-down models make it possible to predict urban climate for the coming decades. The other type refers to the CFD models that are specifically applicable to microclimate. They are represented by ENVI-met (Bruse and Fler, 1998; Sebastian and Bruse, 2009), ANSYS Fluent (Gromke et al., 2015), and STAR-CCM+ (Santiago et al., 2014). These models typically conduct three-dimensional simulations on small urban spaces, with spatial resolution as high as 1 meter. Studies at this microscale usually consider human thermal comfort. 3D radiation models such as RayMan (Matzarakis et al., 1999), SkyHelios (Matzarakis et al., 2021; Matzarakis and Matuschek, 2011), and SOLWEIG (Lindberg et al., 2008) are often used to calculate the human thermal comfort indices.

Over its approximately 200 years of development, urban climatology has evolved from the first simple observations of the UHI effect to the current extensive research on the climatic effects of various urban spatial factors at various scales. With the increasing amount of data and advanced modeling techniques, the reliability of the current description, interpretation, and prediction of urban climate has reached a high level. To optimize the urban environment, more and more specific suggestions derived from urban climatological research have been proposed. Urban climatology is moving closer to the definition given by Oke in 1984, “a discipline that aims at the preferred status of urban atmosphere” (Brazel and Quatrocchi, 2005; Oke, 1984a).

1.1.2.4 Expectations for Applying Urban Climatological Knowledge

In the early stages of urban climatology development, scientists broadly acknowledged the significance of applying urban climatological knowledge to civilian contexts, particularly in planning, designing, and constructing urban infrastructure. Landsberg has termed this matter “knowledge circulation”, denoting the flow of knowledge from scientific meteorology to the practical construction of urban infrastructure (Hebbert and Mackillop, 2013). It is also regarded as a facet of applied meteorology directed towards urban construction (Bitan, 1984; Oke, 2006b).

Since the mid-20th century, numerous eminent researchers in urban climatology have endeavored to facilitate the transfer of urban climatological knowledge. In 1947, Helmut Landsberg proposed:

one of the surest ways of improving the performance of individual buildings and whole cities would be to incorporate microclimatic knowledge into their design (Landsberg, 1947, p. 119),

advocating for the thoughtful consideration of microclimate in architectural design and urban planning. In *The Urban Climate* (Landsberg, 1981), he emphasized:

the knowledge we have acquired about urban climates should not remain an academic exercise on an interesting aspect of the atmospheric boundary layer. It should be applied to the design of new towns or the reconstruction of old ones (Landsberg, 1981, p. 255),

underlying the significance of knowledge transfer in urban climatology. In 1976, Tony Chandler asserted in World Meteorological Organization (WMO) Technical Note 149 (Chandler, 1976) the imperative and urgency of considering climate as a design factor in urban design and planning. He stated:

faced with the exponential growth of the world's population and the accelerating pace of urbanization it is clear that our cities must, where appropriate, be purposefully planned in order to optimize the environment of urban areas and avoid a series of structural and functional design failures. Climate is an essential element in this planning (Hebbert, 2014).

Das Stadtklima written by Albert Kratzer is a representative book in the field of urban climatology. A primary argument in this book is that “urban climate does not need to be accepted as a fact but could, and should, influence the public benefit” (Hebbert, 2014; Kratzer, 1956).

Timothy Richard Oke stands out among the numerous representatives of urban climatology, notably for his substantial contributions to the knowledge circulation in this field. Over more than two decades, from 1984 to 2006 (Oke, 1984b, 2006b), Oke has consistently underscored the importance of applying urban climatology in urban design and planning through a number of articles. Moreover, the majority of his studies have been committed to advancing the application of urban climatological knowledge from various perspectives.

Urban planners and architects also assign significant importance to integrating climatic knowledge in their work. Fundamentally, one of the primary objectives of urban design and planning is to create human settlements that maximize livability. The climate is undoubtedly an important factor affecting the livability of settlements. Consideration of climatic elements dates back to the early history of architecture. In Roman times, Vitruvius's *De Architectura*, which was afterwards widely known as *The Ten Books on Architecture*, deliberated on the correlation between wind direction and street orientation, noting that “if the streets run straight in the direction of the winds then their constant blasts rush in and sweep the streets with great violence” (Erell, 2008; Vitruve et al., 1999). In many locations, it is not difficult to find details in local traditional building that show how people considered climatic factors (Brown, 2010; Foruzanmehr, 2015; Pozas and González, 2016; Xu et al., 2016).

In contemporary architecture, landscape architecture, and urban planning, the consideration of climatic factors is indicative of an advanced approach. With the ongoing process of climate change, an increasing number of urban design and planning projects demand climate knowledge, leading to greater involvement of urban planners and designers in urban climatological research (Eliasson, 2000; Ng, 2012; Page, 1968).

In 1963, architect Victor Olgyay published his book *Design with Climate: Bioclimatic Approach to Architectural Regionalism*, which is recognized as a cornerstone of bioclimatic architecture (Olgyay and Olgyay, 1963; Olgyay, 2015). This book provides step-by-step guidance on understanding and applying bioclimatic principles to achieve climate-comfort in architectural designs across different climatic zones. Over the past 60 years, these principles have been built upon and expanded. For outdoor environments, landscape architect Robert Brown, in his book *Design with Microclimate: The Secret to Comfortable Outdoor Space*, discusses how a thermally comfortable microclimate is fundamental to a well-loved and well-used outdoor space. He also proposes general processes and specific guidelines for designing outdoor spaces that optimize human thermal comfort (Brown, 2010). Brown's strategies for modifying microclimate primarily focus on using landscape elements to influence solar radiation, terrestrial (long-wave) radiation, wind, and humidity. Andre Santos Nouri (2018) aggregates possible approaches for modifying outdoor thermal comfort into four Measure Review Frameworks (MRFs): Green MRF (using urban vegetation), Sun MRF (using artificial shelter canopies), Surface MRF (using cool materials), and Blue MRF (using water and misting systems).

A growing number of countries and cities worldwide are recognizing the importance of incorporating climate adaptation into the urban planning process and are working to promote this integration through the development of regulations, standards, guidelines and tools.

In Germany, the *Bundesbaugesetz* (BBauG, Federal Building Act) amended in 1976 for the first time included a requirement that “climate” must be taken into account when drafting urban land-use plans (§ 1 para. 6 of BBauG, 1976). Following the enactment of the *Bundes-Klimaschutzgesetz* (KSG, Federal Climate Protection Act) in 2019, the current version of the BBauG (last amended in 2023) now mandates that urban land-use plans should contribute to ensure “climate protection” and “climate adaptation” (§ 1 para. 5 of BauGB, 2017). In response to the development of these statutes, guidelines and tools have been created to support climate-friendly urban planning. In 1977, the state of Baden-Württemberg published the first version of *Städtebauliche Klimafibel* (Urban Planning Climate Primer) to provide urban planning practitioners with essential climatic knowledge. This primer kept been updated according to frequently asked questions from planning practice and became available online since 2007 (Ministerium für Landesentwicklung und Wohnen Baden-Württemberg, 2012). In 2008, the Urban Climatology Department of Stuttgart and the Association of the Stuttgart Region published the *Klimaatlas* (Climate Atlas), which provides a spatial inventory of the current

climate in the Stuttgart region, covering an area of 3654 km². The atlas includes not only maps of geographical and climatic data but also analytical maps, such as bioclimatic information (Stadtlima Stuttgart, 2008). The *Klimafibel* and the *Klimaatlas* are closely related and complement each other to offer comprehensive climate information and analysis for urban planning in Stuttgart region (Nora, 2018). The experience in Stuttgart has demonstrated the potential for climatic knowledge to influence urban planning through the phrases of municipal-level urban land-use planning and the urban development framework planning (Landeshauptstadt Stuttgart, 2022).

In China, the National Development and Reform Commission (NDRC), in collaboration with eight other ministries, published the first *National Climate Change Adaptation Strategy* in 2013. This document provides guidance and serves as the foundation for national climate adaptation efforts from 2014 to 2020. One of the key tasks outlined in this strategy is the improvement of urban habitat environments to ensure human well-being (NDRC, 2013, p. 21). In response to this national strategy, in 2016, the Ministry of Housing and Urban-Rural Development (MOHURD) published the *Action Program on Urban Adaptation to Climate Chang*. This document provides specific guidance for integrating climate adaptation into urban-rural development efforts. Key requirements include considering climate change in urban planning processes (§ 2 para. 1 sentence 1), using public open spaces to improve ventilation and mitigate the urban heat island effect (§ 2 para. 1 sentence 2) and leveraging urban greenery to adjust the microclimate (§ 2 para. 4) (NDRC and MOHURD, 2016). In 2019, the recommendatory national standard (GB/T 37529-2019)—*Technical for Climatic Feasibility Demonstration in Master Planning*—was published. This standard demonstrates the potential and outlines methods for incorporating climatic knowledge during the feasibility study phase of urban planning. In addition to establishing standards, accumulating experience through pilot cities is another key approach for the widespread implementation of climate adaptation. In 2024, 39 cities and districts were selected as pilot climate-adaptive cities. According to the second *National Climate Change Adaptation Strategy* (NDRC, 2022, p. 40), by 2035, prefecture-level cities and above will fully adopt the climate-adaptive initiatives tested by the pilot cities.

In summary, whether in the realm of urban climatology or urban design and planning, there is a collective anticipation for the expansion of climatological knowledge to enhance the urban built environment. The aim is to improve the urban climate and create liveable environment in an efficient and scientific manner.

1.1.3 Urban Green Space (UGS) and Park Cool Island (PCI) Effects

Urban climatological research on urban geometry and morphology has been conducted not only for anthropogenic urban elements such as buildings and streets, but also for natural elements such as vegetation and water bodies. Due to the evapotranspiration and shading effects of vegetation, Urban Green Space (UGS) are considered an important means of mitigating the UHI effect and alleviating urban heat stress (Boukhabl and Alkam, 2012; Terjung and O'Rourke, 1981). Abundant research indicates that green spaces lower ambient air temperature and regulate humidity in surrounding areas (Bowler et al., 2010; Chang et al., 2007; Spronken-Smith and Oke, 1998), creating an “oasis effect”. This effect, known as the Park Cool Island (PCI) effect, has gradually become an important branch of urban climatology.

Studies of PCI effects primarily investigate numerical relationships between the PCI intensity and environmental features of UGS, such as vegetation structure, vegetation density (Cao et al., 2010; Hardin and Jensen, 2007) , and layout of green spaces (Wilmers, 1990; Yu et al., 2015; Zhang et al., 2009). This subfield of urban climatology has attracted an increasing number of landscape architects and urban planners, who have directed research in this subfield into a more practical direction, i.e., identifying UGS morphology for optimal PCI effects (Bowler et al., 2010; Jáuregui, 1990; Wong and Yu, 2005). The expectation behind these studies is that the results can be used to guide the design and planning of UGS. These studies align with “climate-adaptive design and planning” in urban planning and landscape architecture (Cerra, 2016; Kleerekoper, 2017; Schuetze and Chelleri, 2011).

1.1.4 UGS & PCI at Microscale: Influence of Morphological Features of UGS on Microclimate and Human Thermal Comfort.

This study specifically investigates how morphological features of UGS impact microclimate and human thermal comfort at the microscale. The horizontal spatial resolution at this scale ranges from 1 to 100 meters. The temporal resolution ranges from 1 hour to 1 day. The atmosphere studied is at the Urban Canopy Layer (UCL). Since humans can tangibly perceive space at this scale, many studies evaluate the microclimate in terms of human thermal comfort using human biometeorological thermal indices.

Two main types of methods are used in this field: one is microscale numerical simulation, and the other is field measurements, including questionnaires. Numerical simulation involves using CFD microclimate models, as mentioned in the previous section (1.1.2). The microclimate model used in this study is ENVI-met, a three-dimensional non-hydrostatic prognostic model (Bruse and Fleer, 1998), which is statistically the most frequently used model

in this field (Jänicke et al., 2021; Tsoka et al., 2018). Studies using the ENVI-met model for microclimate simulation in this field can be categorized into two types. One type uses ENVI-met to simulate the environment of the entire investigated site (Erlwein et al., 2021; Sun et al., 2017; Tang et al., 2022). The other type uses the model to simulate various simplified and idealized scenarios (Deng et al., 2019; Morakinyo and Lam, 2016; Tang et al., 2022).

Studies employing field measurement methods typically utilize portable meteorological monitoring devices for mobile traverse measurements (Ali and Patnaik, 2019; Yan et al., 2014), or short-term, multi-fixed-point measurements (Amani-Beni et al., 2018; Cheung and Jim, 2019). Studies assessing human comfort also incorporate questionnaires to gather pedestrians' subjective perceptions of the thermal environment (Chan et al., 2017; Manavvi and Rajasekar, 2022). Additionally, some studies employ scaled outdoor experiments, which is based on dynamic similarity theory. In this method, researchers use concrete to build outdoor models simulating urban neighborhoods, with potted plants placed in between to simulate urban trees (Chen et al., 2020; Chen et al., 2021).

1.2 Research Objective: Enhancing Methodology to Generalize Research Results at Microscale

Overall, the current research on the microscale cooling effects of UGS encounters the limitations of high research costs and challenges in generalizing research results. In fact, the challenge of generalizing research results and the consequent difficulty of results application is a commonly faced problem in urban climatological research. Many researchers in urban climatology have attempted to address this problem.

Among them, Oke's research results stand out as particularly representative. He has emphasized the importance of methodological enhancement in addressing the difficulty in results generalizability and application. He has actively engaged in the methodological exploration and has developed methods for categorizing and summarizing urban space, including Urban Climate Zones (UCZ) and Local Climate Zones (LCZ). These methods have proven valuable for the generalizing research results at the urban mesoscale. Yet, these methods have not been applied to the urban microscale.

The microscale of urban climate and human thermal well-being has been attracting increasing attention in recent years. Nouri has argued in several articles that the top-down approach in urban climatology is inadequate for guiding decision-making at the local scale (Nouri et al., 2021; Nouri and Bártolo, 2013; Nouri and Matzarakis, 2019). This is because

GCM and RCM models often overlook fundamental climatic issues relevant to microscale phenomena. To practically promote urban climate adaptation, it is essential to adopt a bottom-up approach alongside the top-down method. The bottom-up approach is more human-centered, focusing on identifying and adjusting local microclimatic factors to create thermally responsive urban environments. Consequently, the human biometeorological system plays a crucial role in the bottom-up approach.

This study attempts to extend Oke's methods from the mesoscale to the microscale. The objective is to propose methodology applicable to the microscale, enhancing the generalization of research results. This methodology aims to meet three objectives: achieving comprehensive results, providing actionable suggestions, and ensuring reasonable research costs.

1.2.1 High Cost and Low Generalizability of Microclimate Studies

Presently, studies on the microscale cooling effects of UGS encounter a gap of implementation. The study incurs high costs in time, manpower, and financial due to the high precision required and the spatial complexity of the microscale urban space. However, the results of microscale studies are often not comprehensive enough to serve as guidelines for generalizable design behaviors.

Field measuring experiments entail significant financial and manpower costs. In particular, the mobile traverse measurements demand substantial manpower to establish a measurement campaign to rapidly traverse all measured points every hour of a 24-hour period. Multi-fixed-point measurements involve high financial cost. Employing as many high-precision sensors as possible is crucial in these measurements. Scaled outdoor experiments are costly in both financial and manpower terms. The method of constructing an outdoor experiment site is not widely replicable. However, despite the high research costs, the potential for generalizing the results from field measurement experiments is limited. This is because field measurements can be a description of the phenomenon, but it is difficult to explain the reasons behind it. In addition, field measurements provide only a point-by-point description rather than a global description. Due to the low cost-effectiveness in terms of generalization, increasing number of microclimate studies are turning to numerical simulations.

In simulation experiments, the entire site simulations can provide specific decision-making recommendations for a particular site, but they are time-consuming. Simulating a 36-hour period (24 hours plus 8 hours spin-up time) for a 500-meter-diameter neighborhood can take approximately a month. But the results of these studies are difficult to generalize to other

sites. Therefore, many studies have started to incorporate the idealized scenario simulation method. However, while the idealized simulation method can decrease simulation time costs, it demands meticulous experimental design to generalize the results. The scenarios need to be designed properly to ensure that important influencing factors are not overlooked. Furthermore, it is necessary to find a realistic space that can reflect the idealized scenario and to conduct field measurement experiments to evaluate the simulation results. Numerous studies employing idealized simulations have the problem of overly simplistic scenario design or inadequate field measurements.

1.2.2 Common Difficulties in Generalizability of Research Results

Although there are many studies on the climatic effects of UGS, the application potential of these studies remains low. Most of the studies addressing the climate effects of UGS suggest that the results can serve as guidelines for the urban design and planning (Eliasson, 2000; Hebbert, 2014; Oke, 1984a). However, the recommendations from these urban climatological studies are rarely considered in UGS design and planning. At present, it has been a consensus that urban climatology has encountered an impasse in the knowledge circulation and application (Erell, 2008; Frommes, 1982; Hebbert and Mackillop, 2013; Mills, 2006).

The low generalizability of the research results is a key factor contributing to the challenges in applying urban climatological findings. When environmental conditions, study scales, and study methods change, different studies investigating the same relationship can come to completely different conclusions (one example can be seen in section 3.1). However, each city is unique in its land surface and its climatic context. The lack of results universality has made urban climatology research unavoidably fall into endless case studies (Munn, 1973; Oke, 2006b). If the findings of a study cannot be generalized, then there is little chance for them to be transferred into applicable guidelines.

The undesirable consequences of the low generalizability of research results include not only the implementation gap, but also the waste of research effort. In order to effectively consolidate the research efforts of urban climatology to practically promote the climate change adaptation at urban scale, the problem of generalizability of urban climatological findings needs to be addressed.

Oke has expressed his concern about the lack of sound methodology in urban climatology research to tackle the challenge of generalizing results. In his 2006 study, he noted that Lowry's framework for estimating the impact of cities on climate variables (Lowry, 1977) is almost the

only statement that involves methodology in urban climatology. Few studies have attempted a methodological exploration after Lowry's work. In Oke's view, a unified methodological guidance (e.g. in the form of an experimental control or manual) to aid the design of research and experiments would make a significant contribution to raising the standard of work in urban climate (Oke, 2006b, p. 187).

1.2.3 Previous Efforts on Methodological Enhancements

Some researchers, represented by Oke, have started to try to make methodological enhancements in the field of urban climatology to facilitate the application of the results. Wanner and Filliger (1989) developed an orographic classification on urban sites at intermediate scales, considering the combination of built urban area and orographic elements (Figure 1-3). Ellefsen (1991) designed Urban Terrian Zone (UTZ) types to classify urban space at local scales. This classification is initially according to building contiguity and subdivides into 17 sub types by function, location in the city, height, construction type, and etc. (Ellefsen, 1991; Oke, 2006b).

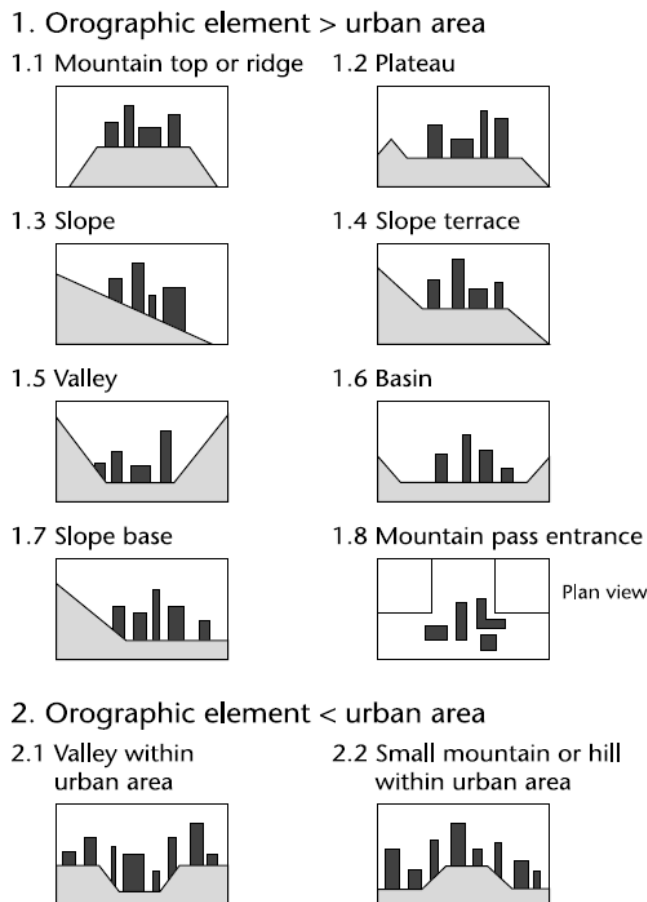
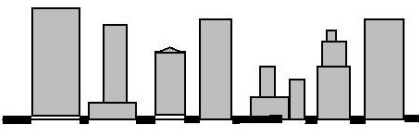
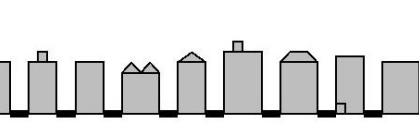
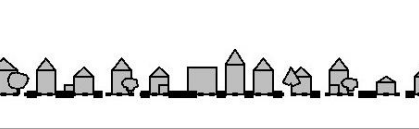
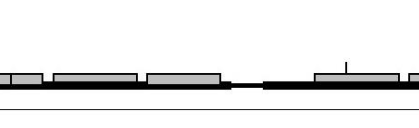
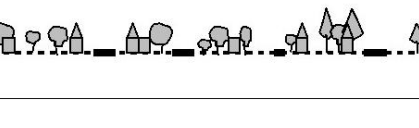

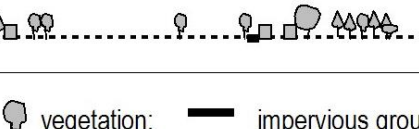



Figure 1-3 An orographic classification of urban sites (Wanner and Filliger,1989).

In 2006, Oke proposed the Urban Climate Zone (UCZ) based on the UTZ types. He argued that a spatial classification system for urban climatology needs to include spatial features that significantly influence urban climate, namely the urban structure, urban terrain, urban texture, and urban metabolism. Based on this idea, in addition to the UTZ type, the UCZ adds a structural measure, aspect ratio (z_H/W), indicating the vertical spatial character, and a measure of the surface cover (% Built), representing surface permeability in terms of ratio of anthropogenic to natural surfaces (Figure 1-4).

Urban Climate Zone, UCZ ¹	Image	Roughness class ²	Aspect ratio ³	% Built (impervious) ⁴
1. Intensely developed urban with detached close-set high-rise buildings with cladding, e.g. downtown towers		8	> 2	> 90
2. Intensely developed high density urban with 2 – 5 storey, attached or very close-set buildings often of brick or stone, e.g. old city core		7	1.0 – 2.5	> 85
3. Highly developed, medium density urban with row or detached but close-set houses, stores & apartments e.g. urban housing		7	0.5 – 1.5	70 - 85
4. Highly developed, low or medium density urban with large low buildings & paved parking, e.g. shopping mall, warehouses		5	0.05 – 0.2	70 - 95
5. Medium development, low density suburban with 1 or 2 storey houses, e.g. suburban housing		6	0.2 – 0.6, up to >1 with trees	35 - 65
6. Mixed use with large buildings in open landscape, e.g. institutions such as hospital, university, airport		5	0.1 – 0.5, depends on trees	< 40
7. Semi-rural development, scattered houses in natural or agricultural area, e.g. farms, estates		4	> 0.05, depends on trees	< 10

Key to image symbols:  buildings;  vegetation;  impervious ground;  pervious ground

- 1 A simplified set of classes that includes aspects of the schemes of Auer (1978) and Ellefsen (1990/91) plus physical measures relating to wind, thermal and moisture controls (columns at right). Approximate correspondence between UCZ and Ellefsen's urban terrain zones is: 1(Dc1, Dc8), 2 (A1-A4, Dc2), 3 (A5, Dc3-5, Do2), 4 (Do1, Do4, Do5), 5 (Do3), 6 (Do6), 7 (none).
- 2 Effective terrain roughness according to the Davenport classification (Davenport *et al.*, 2000); see Table 2.
- 3 Aspect ratio = z_H/W is average height of the main roughness elements (buildings, trees) divided by their average spacing, in the city centre this is the street canyon height/width. This measure is known to be related to flow regime types (Oke 1987) and thermal controls (solar shading and longwave screening) (Oke, 1981). Tall trees increase this measure significantly.
- 4 Average proportion of ground plan covered by built features (buildings, roads, paved and other impervious surfaces) the rest of the area is occupied by pervious cover (green space, water and other natural surfaces). Permeability affects the moisture status of the ground and hence humidification and evaporative cooling potential.

Figure 1-4 Simplified classification of distinct urban forms arranged in approximate decreasing order of their ability to impact local climate [2004 unpublished] (Oke, 2006a).

In 2012, Steward turned Oke's vision of UCZ into a reality, building the Local Climate Zones (LCZ) classification system. Based on Grigg's theory of classification (Grigg, 1965), the LCZs divide the landscape with two properties that influence urban climate, namely *surface*

structure and *surface cover*. *Surface structure* refers to the vertical properties of buildings and trees, affecting local climate through the modification of airflow, atmospheric heat transport, and shortwave and longwave radiation balances. *Surface cover* mainly distinguishes pervious and impervious, anthropogenic and natural surfaces, influencing local climate through albedo, moisture availability, and heating/cooling potential of the ground (Stewart and Oke, 2012, p. 1884). The combination of these two properties constitutes dozens of prototype classes, moreover, enabling users to create much more diverse subclasses based on needs (Figure 1-5). This flexibility allows the LCZs to provide a more detailed and comprehensive description of urban spaces than other climate-based classification systems.

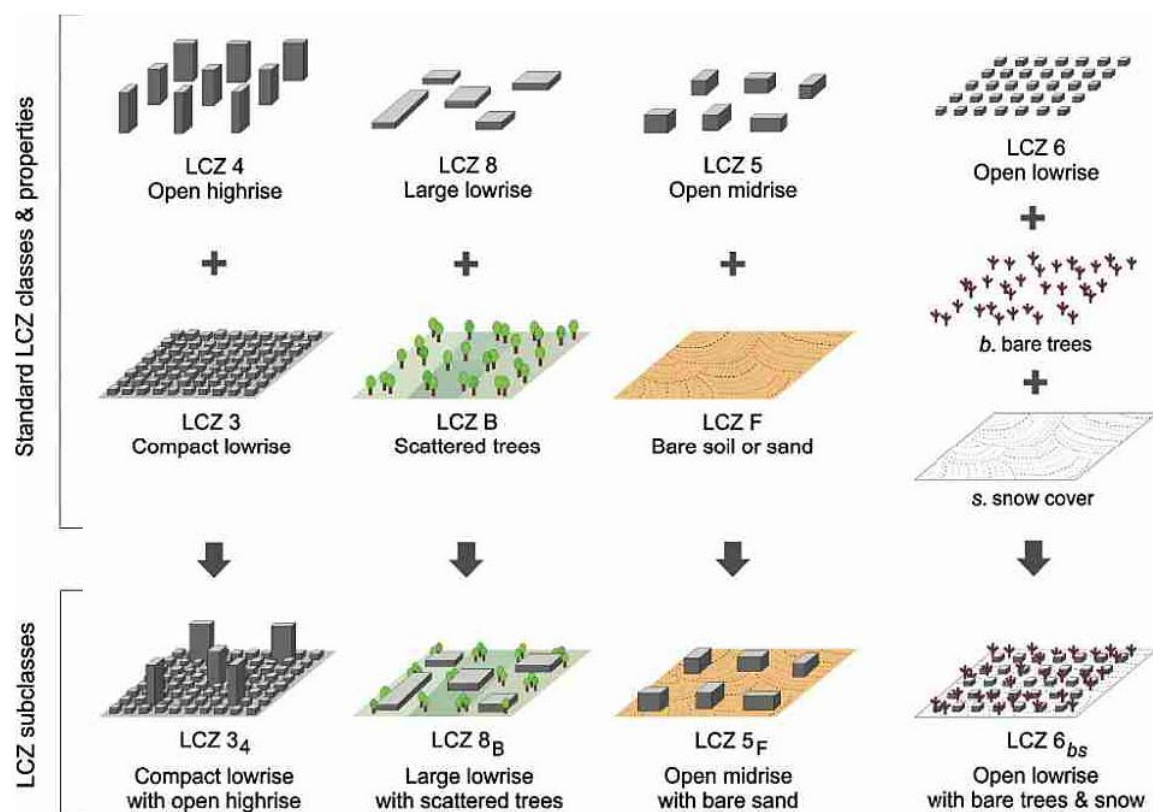


Figure 1-5 LCZ subclasses to represent combinations of surface structure and surface cover (Stewart and Oke, 2012).

The original purpose of the LCZs classification system was to facilitate consistent documentation of site metadata and provide an objective protocol for measuring the magnitude of the urban heat island effect (Stewart and Oke, 2012). Due to its universal applicability, compatibility with numerical climate models, and integration with urban design theory, the LCZs have shown potential for a much wider range of applications than it was originally designed for. It can be used to improve the parameterization of urban canopy in numerical

climate models and weather prediction schemes, help quantify the thermal and morphological layers of an Urban Climatic Map (UCMap). This application potential has, in a few short years, led to the widespread use of LCZs in urban climatological studies around the world (Bechtel et al., 2015; Lehnert et al., 2015; Xu et al., 2017).

In 2015, Milles et al. began their work on the World Urban Database and Portal Tool (WUDAPT) project (Mills et al., 2015). Based on LCZ classification system, the WUDAPT provides a portal that enables autonomous participation of worldwide urban climate researchers in building and sharing a global database of urban characteristics (World Urban Database, 2020). Through WUDAPT portal, participants are able to create LCZs for their respective cities in a consistent manner, collect parameters for city characteristics, and aggregate the data to a user-specified reference grid and compare cities around the world (Figure 1-6). The WUDAPT portal further extended the advantages of the LCZ classification system and realized the standardization of climate-based classification of urban spaces on a global scale.

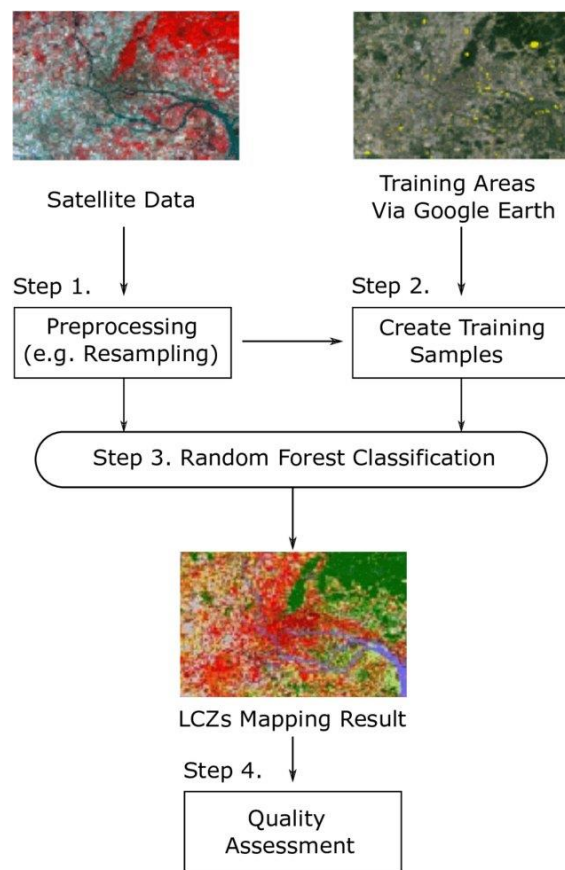


Figure 1-6 WUDAPT LCZs classification framework (Xu et al., 2017).

The above attempts of methodological enhancement are mainly focused on local and urban scales, and there are few methodological enhancements at microscale yet. In fact, the

microscale is the most conducive scale for applying research results among the three scales in urban climatology. In urban decision-making, decisions become less difficult to achieve as the scale decreases and fewer considerations come into play. Hence, it is necessary to explore methodological enhancements specifically at the microscale in urban climatology.

1.2.4 Proposing the Multi-parameter Approach

The purpose of this study is to propose a methodology that contributes to the generalization of research results from studies on the cooling effects of UGS at the microscale. This methodology adopts the idea of spatial summarization and classification of Local Climate Zones at mesoscale. It advances from the previous single-parameter approach to the multi-parameter approach. The multi-parameter approach views the UGS as a whole and investigates the interdependent influence of its various environmental features on human thermal comfort. The interdependent influence allows the results to be more comprehensive and therefore easier to generalize. In addition, the results derived from the factorial experiments can be easily translated into specific and actionable guidelines for climate-adaptive UGS design and planning.

To explore the interdependent influence, the multi-parameter approach uses the factorial experimental design as its basic framework. A factorial design is an experimental setup that enables researchers to study the effects of two or more factors (variables) simultaneously. In a factorial experiment, all possible combinations of the levels of each factor are investigated. This design allows for the examination of not only the effect of each factor on the dependent variable but also the interdependence between the factors. In this study, to examine the combinations in the factorial experiment, the microclimate model ENVI-met is utilized. To minimize research costs, the simulation is conducted on simplified and idealized scenarios. The field measurements adopt the Latin Hypercube Sampling (LHS) design, i.e., selecting several scenarios from the factorial experiment to conduct field measurement according to the conditions of the measuring sites.

In comparison to the original single-parameter approach, this multi-parameter approach can more comprehensively encompass various UGS types, explore in greater depth the nuanced relationships between UGS morphology and human thermal comfort, and give specific recommendations for climate-adaptive UGS design and planning. Leveraging these advantages, the multi-parameter approach is expected to address the difficulty of results' application and generalization in urban climatology at the microscale.

1.3 Thesis Structure

This thesis is composed of three main parts: Methodology (Chapter 2), Case Studies (Chapters 3 to 5), and Conclusions & Discussion (Chapter 6):

Chapter 2 introduces the multi-parameter approach in detail. It includes the technical details of the multi-parameter approach, a comparison with the single-indicator approach, and an illustration of why the multi-parameter approach is helpful in applying research results.

Chapters 3 to 5 showcase the effectiveness of the multi-parametric approach through three specific studies:

- 1) The study in Chapter 3 investigates the interdependent influence of vegetation type, landscape index and green-belt direction of UGS on cooling effects and human thermal comfort. It addresses the question of whether a centralized or a scattered UGS leads to higher Park Cool Island (PCI) effects. Previous studies have not reached a consensus on this question. Some studies conclude that the more fragmented the green space is, the higher its cooling effects will be, while others have come to the opposite conclusion: the compact green space leads to higher cooling effects. The results of this study show that the vegetation density of the UGS is a crucial factor influencing the climatic effects of the UGS layout. When the vegetation density is high, fragmented green space provides higher PCI effects than compact green space. When the vegetation density of green space is low, the PCI effects of compact green space is higher than that of fragmented green space. This study unveils the joint influences of vegetation density and layout of UGS on the PCI effects, thus demonstrating the multi-parameter approach's superiority in deriving comprehensive correlations compared to the conventional single-parameter approach.
- 2) Chapter 4 describes a study applying the multi-parameter approach in the historical park Tiergarten in Berlin. It explores how the spatial features of walkways in Tiergarten influence the human thermal comfort of the pedestrians traversing the park. Three environmental parameters are considered in the factorial experiment, including the walkway width, the vegetation density, and the Sky View Factor (SVF). The joint influence of these factors varies between daytime and nighttime. At daytime of a hot summer day, the narrower walkways covered by dense canopy and surrounded by dense vegetation have the lowest PET values. During the nighttime,

the wider walkways covered by sparser canopy and surrounded by less dense vegetation have the lowest PET values. The results are illustrated as a map of human thermal comfort for Tiergarten, which can be used to assist the pedestrians in selecting the comfortable walkways for their outdoor activities during hot summer days. This study serves as an example of employing the multi-parameter approach to provide specific climate-adaptive suggestions for a real UGS case.

- 3) Chapter 5 details the third study, which investigates the joint influences of three common design factors on the thermal comfort of Urban Riverside Greenway (URG). The three factors include the urban prevailing wind direction, the tree species, and the position of greenway trails. The results show that these three factors function as an interconnected whole to determine the PCI effects of the URG. The first consideration in a climate-adaptive design of an URG should be the prevailing wind direction of the city. When the prevailing wind moves from the urban area to the waterbody, the nearer the greenway trail is to the waterbody, the better the human thermal comfort on the trail is. When the prevailing wind moves from the water body to the urban area, the preferable position of the greenway trail depends on the vegetation density. Through the multi-parameter approach, this study investigates simultaneously two cooling resources: vegetation and the water body. Furthermore, it takes the wind direction into consideration. This complexity of research subjects is not possible with the previous single-parameter approaches. This study gives further evidence of the potential of multi-parameter approaches to solving complex microscale urban climatological issues.

Chapter 6 includes the overall conclusions, comparison with similar studies, advantages and limitations of this study, application of research results, and the outreach.

Chapter 2: Multi-parameter Approach vs. Single-parameter Approach

Multi-parameter approach means using multiple parameters simultaneously to describe the spatial configuration of urban green space and exploring the interdependent influence of these parameters on the urban climate. The key difference between multi-parameter and single-parameter approaches is not the number of parameters, but the perspective from which urban green space and its influence on urban climate are viewed. The multi-parameter approach considers urban space as a whole and attempts to explore the interdependent effects of different spatial features on urban climate. The single-parameter approach, on the other hand, attempts to extract the linear relationship between individual spatial features on urban climate indicators.

2.1 Overview of multi-parameter Approach

2.1.1 Brief Description

The specific methodology of the multi-parameter approach consists of the following aspects:

- 1) To derive the interdependent influence of multiple spatial features, using the method of factorial experiment to combine different levels of considered parameters in the form of a multidimensional matrix to form multiple experimental units.
- 2) To control research costs, using the Latin Hypercube Sampling (LHS) method to select a subset of scenarios in the full factorial experimental design to conduct field measurement experiment or simulation experiment. The LHS-designed field measurement selects scenarios based on the circumstances of the measurement site. The LHS-designed simulation experiment is employed when there are too many levels of a factor in the factorial experimental design. In this condition, we select a subset of the levels to form the final factorial design for the microclimate simulation.
- 3) To ensure that each experimental unit can be studied under the same conditions, using the microscale climate model ENVI-met to build idealized models for each experimental unit and run the microclimate simulation.

- 4) In accordance with the holistic perspective of the multi-parameter approach, composite indicators with the same holistic perspective are used to describe the urban climate. The composite indicator selected for this study is the biometeorological index—Physiological Equivalent Temperature (PET). The model used to calculate the PET value is RayMan model.

2.1.2 Factorial Experiment: Comprehensive Description of Urban Land Surface

In statistical perspective, the multi-parameter approach corresponds to the multivariate analysis. Factorial experiment is a frequently used type of multivariate analysis. When a researcher wishes to study the effects of k independent variables, where $k > 1$, the most common method that would be used is the factorial experiment (Collins et al., 2009; Oehlert, 2010). In a factorial experimental design, “all levels of each independent variable are combined with all levels of the other independent variables to produce all possible conditions” (California State University, 2018).

If a factorial experiment contains k factors ($k > 1$), each of which contains n levels ($n > 1$), then a total of n^k experimental units are included in the factorial experiment. These experimental units take on all possible combinations of these levels across all such factors. Thus, a full factorial design can also be called a fully crossed design. For example, the simplest factorial experiment contains two factors, each of which has two levels. In this case, a total of four (2^2) experimental units needs to be executed. When the number of factors grows to three, the complexity increases by a power of three (2^3) (Figure 2-1).

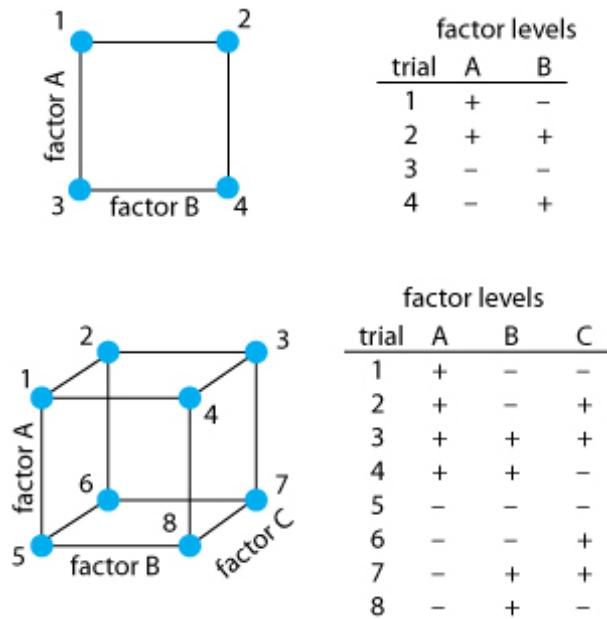


Figure 2-1 A schematic representation of a simple factorial experiment (David Harvey 2013).

The factorial experiment enables the study of effect of each factor on the response variable and the effects of interactions between factors on the response variable. Therefore, the factorial experiment is selected as the statistical framework in this study to investigate the independent and joint effects of multiple spatial parameters (factors) on the urban climate index (response variables).

An example of the application in urban climatology is the system of Local Climate Zone (LCZ) (Stewart and Oke, 2009). The LCZ system classifies urban land surface by permuting different qualitative features of the land surfaces (Figure 2-2). Theoretically, this permutation of multi-variables makes it possible to achieve an exhaustive enumeration of urban land surface types as long as the spatial features are rich enough and the degree within each feature is detailed enough. In fact, the LCZ system did provide room for expansion so that this classification system can be further broadened. Although it has not been explicitly stated, it is obvious that the LCZ system adopts the factorial design. The LCZ system contains several factors including building height, compactness, and land cover properties. Each factor is divided into classes, including high, medium and low (Figure 2-3).

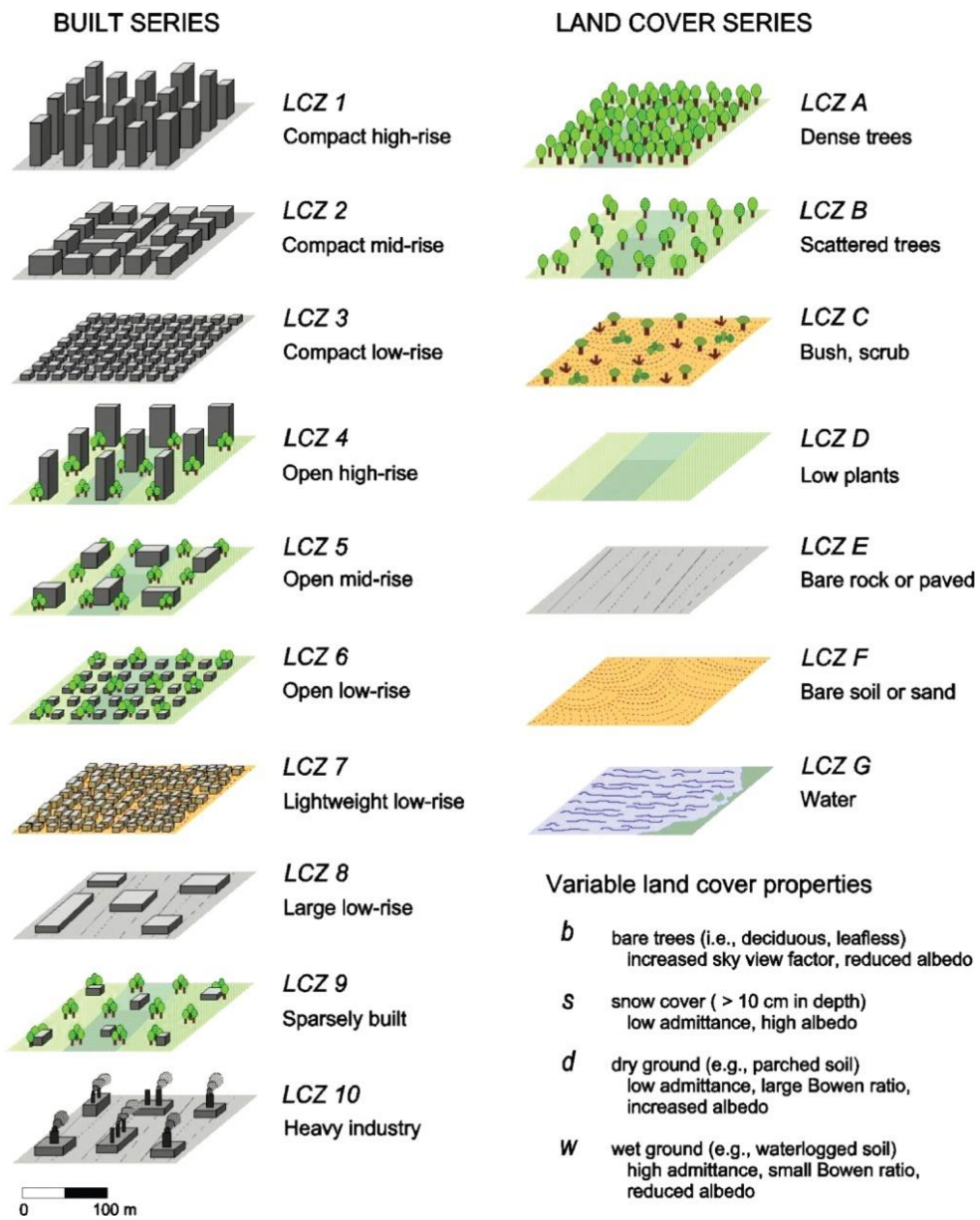


Figure 2-2 Local Climate Zones containing features of building types and land cover types. (Stewart and Oke, 2012).

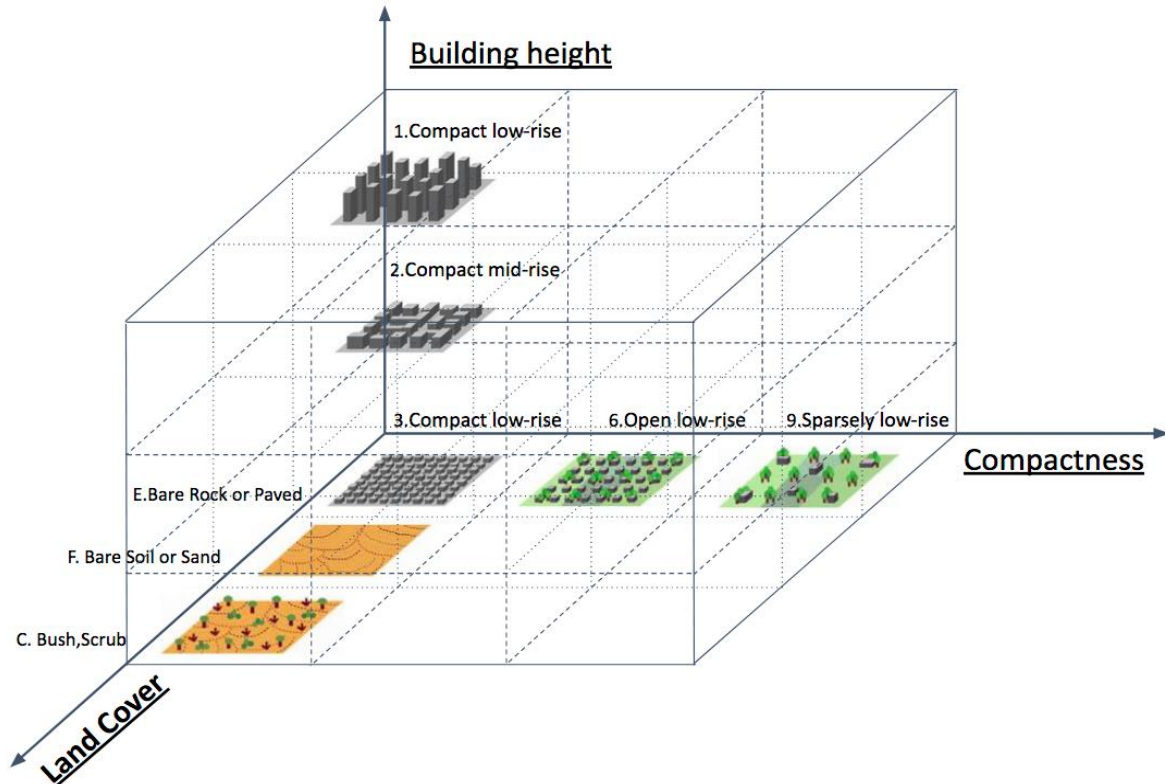


Figure 2-3 The idea of LCZ system is consistent with the idea of the factorial design. By integrating different levels of features of different spatial factors, a collection of scenarios in the form of a matrix can then be formed. As this collection expands in terms of factors and levels, it can become increasingly comprehensive to encompass a wider range of urban land surface types.

For example, the factorial experimental design of the study described in Chapter 3 is shown in Figure 2-4. This study investigated the interdependent influence of three different landscape morphological parameters and vegetation type on the cooling effect and human thermal comfort. The three different landscape morphological parameters include Patch Density and Edge Density (PD & ED), Land Shape Index (LSI) and Green-belt Orientation. This study employs three separate factorial experiments to conduct the simulation.

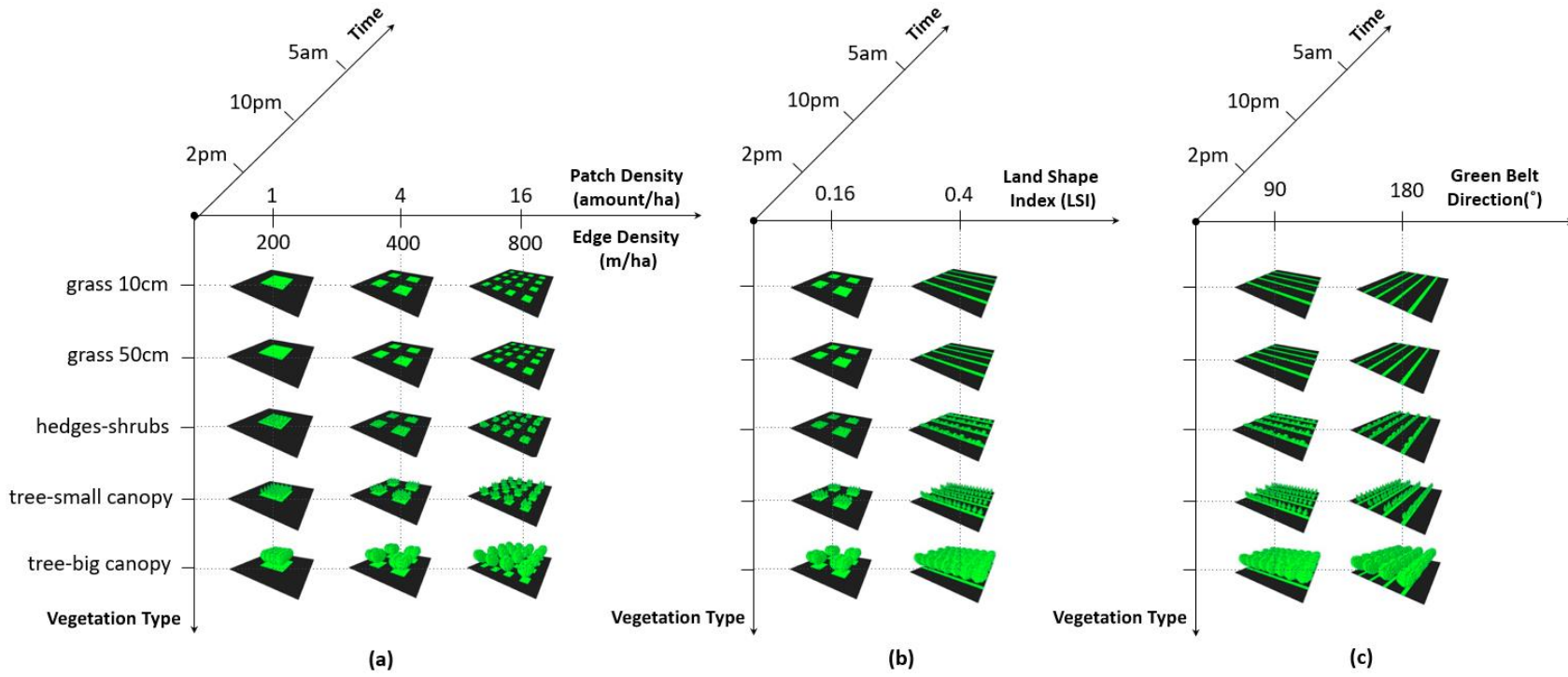


Figure 2-4 Structure of the factorial experiment in the study of Chapter 3.

2.1.3 Latin Hypercube Sampling (LHS) Experimental Design

Latin Hypercube Sampling (LHS) is a statistical method for generating a near-random sample of parameter values from a multidimensional distribution (Mckay et al., 1979). In statistical sampling, a square grid containing sample positions is a Latin square if (and only if) there is only one sample in each row and each column. A Latin hypercube is the generalization of this concept to an arbitrary number of dimensions. LHS is commonly employed in experimental design to cover a broad range of variables with as few experiments as possible (Helton and Davis, 2003). Multidimensional factorial experiments in multi-parameter approach can easily result in a large number of experimental units. To control research costs, LHS design is employed to select scenarios from factorial design for field measurements and simulation experiments.

The LHS-designed field measurement selects scenarios based on the circumstances of the measurement site. For example, in the study in Chapter 4, we used LHS design to select 9 points from the total 15 scenarios from the factorial experimental design for field measurement (Figure 2-5). The number of selected measuring points are more than the least required number of LHS design. This is a result of the actual circumstances of the field measurement site.

The LHS-designed simulation experiment is employed when there are too many levels of a factor in the factorial experimental design. An example can be found in Chapter 5. We used LHS design to sample 5 levels from the full 12 levels of the factor *tree species* to reduce the scenarios for simulation from 180 to 75 (Figure 5-2).

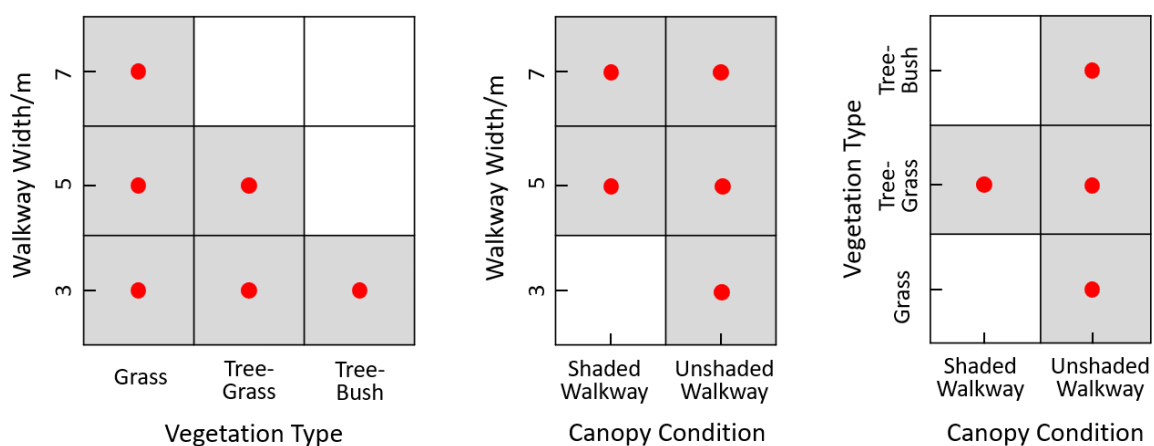


Figure 2-5 An example in Chapter 4 using the Latin Hypercube Sampling (LHS) method for selecting samples from factorial experiment for field measurements. The red dots represent the selected points for field measurement.

2.1.4 Microclimate Simulation through ENVI-met® Model

ENVI-met® is a holistic three-dimensional microclimate model designed to simulate the surface-plant-air interactions in urban environment with a typical horizontal resolution from 0.5 to 10 m and a typical time frame of 24 to 48 hours with a time step of 1 to 5 seconds. This resolution allows to analyze small-scale interactions between individual buildings, surfaces and plants (enviadmin, 2023a).

2.1.4.1 Integrated Modules

ENVI-met integrates the atmospheric module, the soil and waterbody module, the vegetation module, and the building module to simulate the interaction between different urban land surface features and microclimates. In the atmospheric model, the wind field includes a full 3D Computational Fluid Dynamics (CFD) model, which solves the Reynolds-averaged non-hydrostatic Navier-Stokes equations for each spatial grid and for each time step.

In the soil model, ENVI-met dynamically solves the soil hydraulic state of the soil based on Darcy's law considering evaporation, water exchange inside the soil and water uptake by plant roots. Water bodies are considered as a special type of soil in ENVI-met. The calculated processes inside the water include the transmission and absorption of shortwave radiation in the waterbody.

The vegetation model of ENVI-met allows complex 3D vegetation geometries. ENVI-met has a vegetation geometry interface — *Albero*, which allow users to configure the vegetation's 3D morphology and physical parameter, including Leaf Area Density and foliage albedo (Figure 2-6). ENVI-met also uses a sophisticated model to simulate the stomata behaviour of the vegetation in response to microclimate, CO₂ availability and water stress level. These features placed ENVI-met in an unique position for studies on PCI effects at micro scale (Bruse and Fleer, 1998; Hedquist and Brazel, 2014; Lenzholzer, 2012; Perini and Magliocco, 2014; Wania et al., 2012).

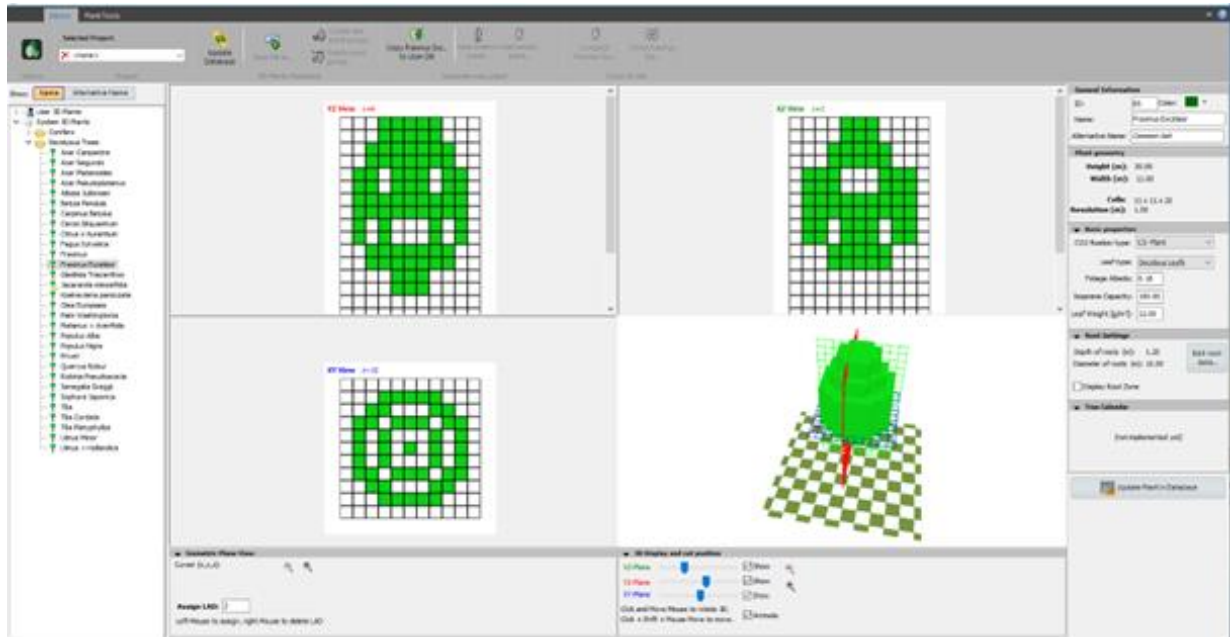


Figure 2-6 Interface of the Albero Module in ENVI-met 4.3.

2.1.4.2 Internal Structure

The numerical discretisation scheme of ENVI-met is an orthogonal Arakawa C-grid. Because of this scheme, ENVI-met only allows straight and rectangular structures. ENVI-met uses the finite difference method to solve the multitude of Partial Differential Equations (PDE) and other aspects in the model. The scheme is partly implicit, partly explicit depending on the sub-system analysed. The atmospheric advection and diffusion equations are implemented in a fully implicit scheme, which allows ENVI-met to use relatively large time steps by still remaining numerically stable. The programming language of ENVI-met is Object Pascal, for WINDOWS using DELPHI.

2.1.4.3 Basic Model Layout

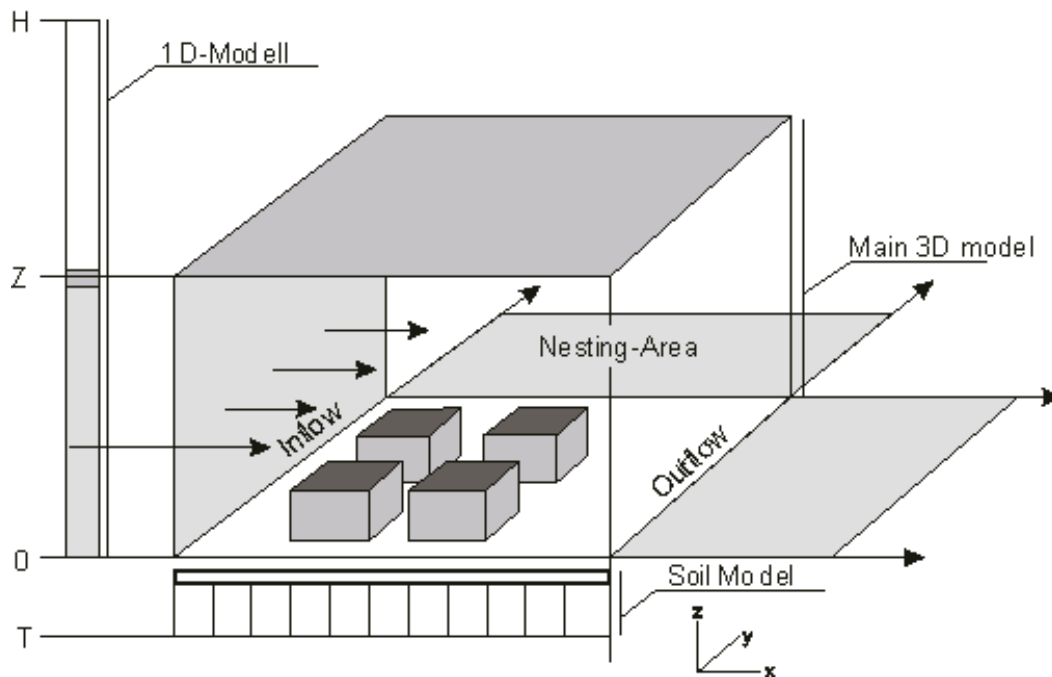


Figure 2-7 Schematic overview over the ENVI-met model layout (enviadmin, 2017c).

The main model of ENVI-met is designed in 3D with 2 horizontal dimensions (x and y) and one vertical dimension (z) (Figure 2-7). Inside this main model, the typical elements that represent the area of interest are placed: buildings, vegetation, different types of surfaces, etc.

Several strategies are used in ENVI-met to cover as much space as possible by using less grid points as possible. One of the strategies is the usage of additional 1D model. To allow an accurate simulation of boundary layer processes, it is necessary to extend the model up to a minimum height of 2500 m. As it is not possible, and not necessary either, to extend the complete 3D model up to this height, the 1D model takes over the calculation from the top of the 3D model and the total model top at 2500 m. In addition, the 1D model provides the vertical profiles of all model variables for the inflow boundary of the 3D model.

2.1.4.4 Lateral Boundary Conditions

There are three kinds of Lateral Boundary Conditions (LBC) in ENVI-met (enviadmin, 2017a).

- 1) Open LBC: the values of the next grid point close to the border are copied to the border for each time step. The open LBC is the condition with the minimum effect of the model boundary to the inner parts of the model. As the open LBC copies the values from the inner parts of the model to the boundaries, there is a certain danger of numerical instabilities. The use of open LBC would represent a situation where

the neighbourhood of the simulation area has a similar structure to the simulation area but is not very close.

- 2) Forced (or closed) LBC: the values of the 1D model are copied to the border. The forced LBC is the most stable condition because the mostly independent 1D model is used to obtain the boundary values which stabilises the 3D model. On the other hand, the 1D profile will have a significant effect on the data in the main model. The use of forced LBC is applicable to simulate isolated scenarios, for example, where a building is placed on a flat plane with nothing around it.
- 3) Cyclic LBC: the values of the downstream model border are copied to the upstream model border. The cyclic LBC assumes that the average conditions upstream of your model area (which produce the inflow profile) are similar to your model area. As the values of the outflow boundary are copied to the inflow boundary there is also a certain danger of undesired feedback inside the model which might cause numerical instabilities. The usage of cyclic LBC represents a situation where the neighbourhood has in average the same structure as the model area. In contrast to the situation using open LBC, the neighbourhood is so close to the simulation area that the modified profile is not recovering before entering the model area.

The studies involved in this dissertation all simulated isolated idealized scenarios. In these scenarios, simulated urban green spaces are assumed to be constructed on open flat land with no interference from other structures around them. Therefore, the LBC type adopted in these studies is the forced (or closed) LBC.

2.1.4.5 Data Flow

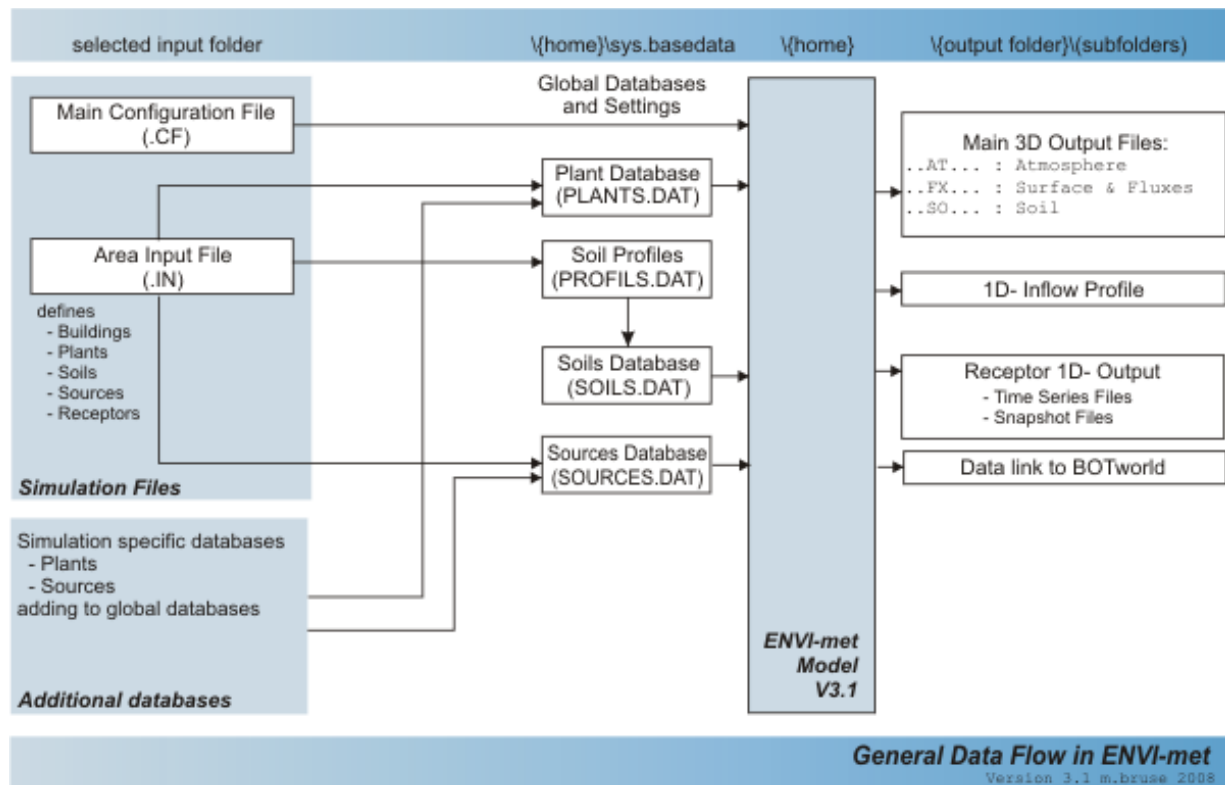


Figure 2-8 Data Flow in ENVI-met V3.1 (enviadmin, 2017b).

The basic data flow of ENVI-met model is shown in Figure 2-8. The main input data can be classified in two types: simulation files and additional database. In the Main Configuration File(.CF) of simulation files, users can define the file name, the forcing meteorological setting, the duration of simulation, etc. In Area Input File(.IN) of simulation files, users can define the spatial configuration of the scenarios and the materials at each grid. In the additional database, users can assign values to the physical characteristics of plants and different surface materials.

There are four types of output files from ENVI-met simulation. The “Main 3D Output Files” are binary files that need to be read with the software package LEONARDO. This software can represent the distribution of meteorological values for a certain facet of the simulated scenario at a certain timepoint. ENVI-met runs a one-dimensional model parallel to the main (3D) model in order to have produce different initial and boundary conditions. The “1D-Inflow Profile” reflects the state of the 1D model, which is saved each time the main data of the model are saved. The “Receptor 1D Output Files” show the state of the atmosphere, the surface and of the soil at selected points inside the model. The receptor data is stored in two ways, the “snapshot files” and the “time series files”. The snapshot files show the present model state at all the receptors, while the time series files represent the evolution of different variables

at one point during the model run. The “Data link to BOTworld” was initially assigned to simulate the thermal conditions for virtual pedestrians. But BOTworld has not developed since then. Instead, BIO-met was developed as a side application after the fourth edition of ENVI-met. BIO-met supports the calculation of various human thermal comfort indices including Predicted Mean Vote (PMV/PPD), Physiological Equivalent Temperature (PET), Dynamic PET (dPET), Universal Thermal Climate Index (UTCI) and Standard Effective Temperature (SET) (enviadmin, 2023b).

2.1.4.6 Limitation of ENVI-met Model

In previous studies evaluating the performance of ENVI-met model, researchers have observed the following limitations. Firstly, the solar radiation inputs are estimated from an internal database. ENVI-met does not allow the input of hourly solar radiation variations. Thus ENVI-met has difficulty in providing an accurate simulation when solar radiation varies (Maggiotto et al., 2014). Similarly, users cannot input measured variation of wind velocity and wind. Thus, when the air flow changes, the difference between the modeled and measured data becomes larger (Acero and Arrizabalaga, 2018; Tsoka et al., 2018). In addition, ENVI-met is not grid-independent. But the model is less dependent on grid resolution than it is on different simulation scenarios. Therefore, when exploring the differences between simulation scenarios, the conclusions of ENVI-met are considered not obscured by the effects of the sensitivity of the grid to changes in vertical resolution (Crank et al., 2018).

Some studies have also suggested that relying too much on the default values for vegetation and surface materials within ENVI-met can lead to inaccurate simulation results. The accuracy of the results can be greatly improved if researchers can assign values to the physical parameters of vegetation, such as leaf area density, foliage albedo, and crown shape, and the physical parameter of surface materials based on field measurements (Liu et al., 2021; Ouyang et al., 2022).

These studies have all agreed that despite these shortcomings, ENVI-met is still competent in modeling urban microclimates. The simulation of ENVI-met is still credible in reflecting the differences among scenarios, the distribution of meteorological values within scenarios, and the diurnal trends of measuring points. Furthermore, ENVI-met has the advantage of allowing users to freely set up urban environment. Therefore, ENVI-met is still the prevailing model for simulating complex urban microclimates with high accuracy.

2.1.5 Human Biometeorological Thermal Index—PET

2.1.5.1 Human biometeorological thermal indices

In accordance with the holistic perspective of the multi-parameter approach, the composite indicator with holistic perspective is used to describe the urban climate. From the holistic point of view, the more comprehensively the system can be viewed, the more accurate conclusions can be drawn (Auyang, 1998; Fang and Casadevall, 2011; Systems Innovation, 2020b). By using composite indicator, it is possible to encapsulate as many object characteristics as possible with the least amount of data. The composite indicator is formed “when several individual indicators are compiled into a single index, on the basis of an underlying model of the multi-dimensional concept that is being measured” (United Nations Economic Commission for Europe, 2017). The synthetic way of thinking in composite metrics is often applied in complexity science and manifests itself in data dimensionality reduction (van der Maaten et al., 2009) (Figure 2-9).

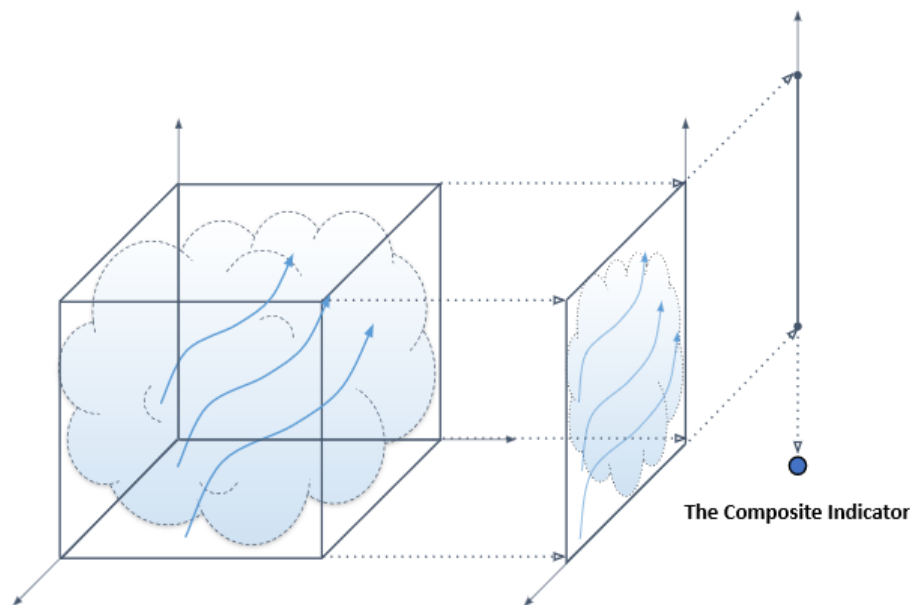


Figure 2-9 Composite indicator is a form of data dimensionality reduction.

The idea of human biometeorological thermal indices is a concrete expression of the idea of holistic thinking and dimensionality reduction. By using only one indicator, it can project the multiple characteristics of the atmosphere. Moreover, human biometeorological thermal indices are formulated with human comfort and well-being as the main consideration. This consideration would be specifically beneficial for the application of the research results of urban climatology. As a human settlement, it is the natural duty of a city to ensure human well-being. Efforts that are consistent with the duty of a city will inevitably receive higher priority

in urban decision making. Also, the original aim of urban climatology was to help human beings cope with the life safety crisis brought about by climate change. Therefore, thermal safety, health, and well-being of humans should be the primary motivation for urban climatology research.

Human Biometeorology is a cross-disciplinary field stemming from epidemiology and physiology and can be extended outward to building heating and ventilation, urban design and planning, and etc. It mainly studies the interactions between human bodies and the atmosphere (Munn, 2013). For urban climatology, human biometeorology plays an important role that links urban climate closely to human health and well-being (American Meteorological Society, 1972). According to Hebbert, bio-meteorologists constituted the main global network of urban climatology in the late 1980s (Hebbert and Mackillop, 2013). When applied to urban climatology, commonly used thermal indices include:

“Predicted Mean Vote (PMV) (Fanger, 1972), Physiologically Equivalent Temperature (PET) (Höppe, 1999; Matzarakis et al., 1999; Mayer and Höppe, 1987), modified Physiologically Equivalent Temperature (mPET) (Chen and Matzarakis, 2018), Standard Effective Temperature (SET) (Gagge et al., 1986) or Outdoor Standard Effective Temperature (Out_SET) (Spagnolo and Dear, 2003), Perceived Temperature (pT) (Staiger et al., 2012) and Universal Thermal Climate Index UTCI (Jendritzky et al., 2012).” (Matzarakis et al., 2015; Matzarakis and Amelung, 2008)

The basis for the human biometeorological thermal indices is the energy balance equation for the human body (Matzarakis, 2007, p. 141) (Figure 2-10).

$$M + W + R + C + E_D + E_{Re} + E_{Sw} + S = 0 \quad (2-1)$$

M : metabolic rate (internal energy production)

W : the physical work output,

R : the net-radiation of the body,

C : the convective heat flow,

E_D : the latent heat flow to evaporate water diffusing through the skin (imperceptible perspiration),

E_{Re} : the sum of heat flows for heating and humidifying the inspired air,

E_{Sw} : the heat flow due to evaporation of sweat, and S the storage heat flow for heating or cooling the body mass.

S: the storage heat flow for heating or cooling the body mass.

The unit of all heat flows is in Watt (Höppe, 1999).

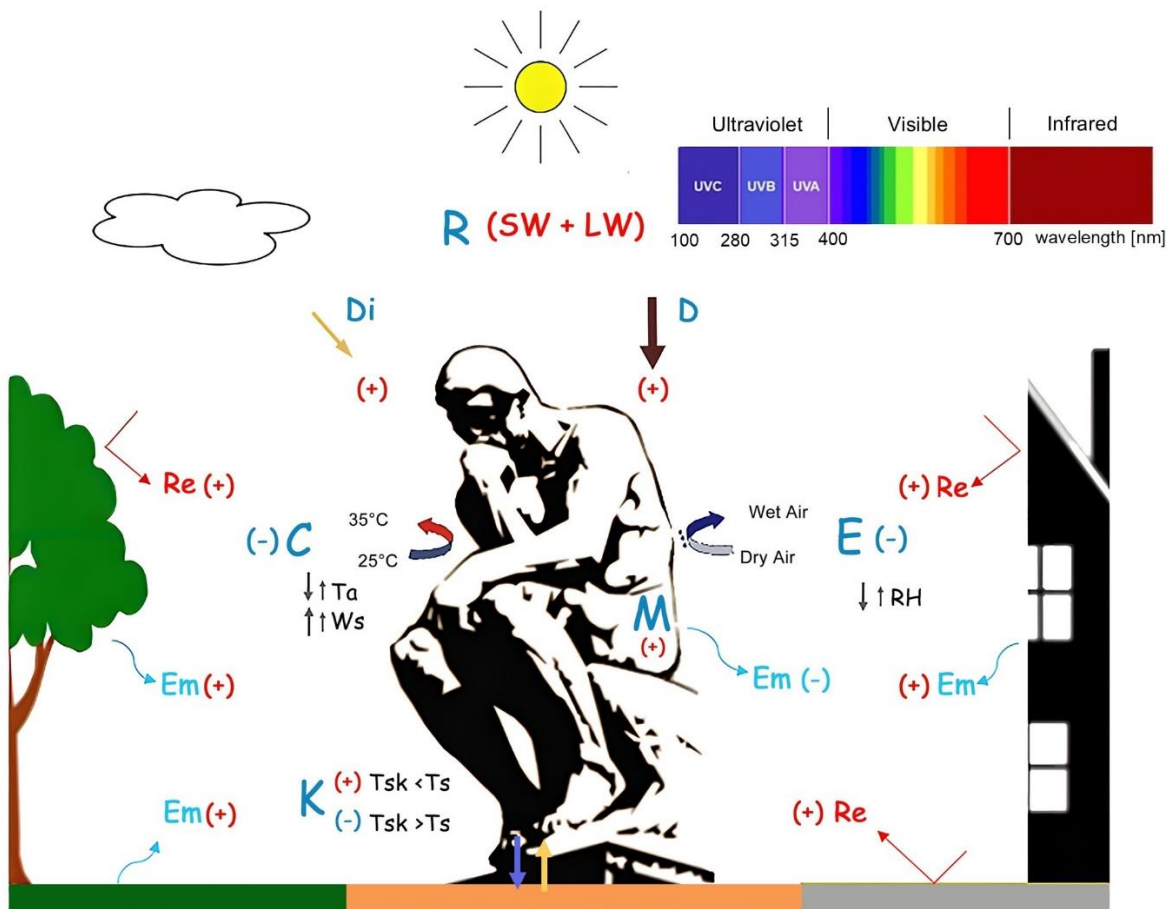


Figure 2-10 Energy fluxes that affect the human energy budget outdoors. M: Metabolism; C: Convection—Moving air removes radiated heat; K: Conduction—direct heat transfer by conduct; E: Evaporation—Loss of heat by evaporation of water; R: Radiation—SW: Short-wave, LW: Long-wave, D: Direct, D_i : Diffused, Re : Reflected; Em : emission of Long-wave radiation; T_a : air temperature; W_s : Wind Speed; RH : air Relative Humidity; T_{sk} : Skin Temperature; T_s : Surface Temperature; (+) heat gain (-) heat loss; up arrow: increase, down arrow: decrease (Antoniadis et al., 2020).

According to Höppe, the temperatures of human skin and blood are influenced by the integrated effect of all meteorological parameters (Höppe, 1999). Thus, these thermal indices differ in the way they are calculated, but require the same meteorological input parameters: air temperature, air humidity, wind speed, short and long wave radiation fluxes (Matzarakis et al., 2016). In addition, the real situation of human thermal perception, the heat resistance of clothing (clo) and activity of humans (in W) are also required. (Figure 2-11).

The first classic human thermal comfort model is the Predicted Mean Vote (PMV) model developed by Fanger in the 1970s (Fanger, 1972). The PMV model uses four physical variables (air temperature, air velocity, mean radiant temperature, and relative humidity) and two personal variables (clothing insulation and activity level) to obtain an index that corresponds to the seven-point ASHRAE thermal sensation scale (ranging from -3 to 3, where 0 is neutral, -3 is cold, and 3 is warm) (Charles, 2003). The PMV model and results have been included in the modern thermal comfort standard ISO 7730 (ISO, 2005).

The mean radiant temperature (T_{mrt}) is an important meteorological input parameter for the human energy balance during sunny weather in summer. T_{mrt} is defined as “the uniform temperature of a surrounding surface giving of blackbody radiation (emission coefficient $e = 1$) which results in the same radiation energy gain of a human body as the prevailing radiation fluxes which are usually very varied under open space conditions.” (Matzarakis and Rutz, 2000). T_{mrt} can either be measured with a globe thermometer or calculated from short-wave and long-wave radiation fluxes.

To calculate T_{mrt} , the entire surroundings of the human body are divided into n thermal surfaces with the temperatures T_i ($i = 1, n$) and emission coefficients e_i , to which the solid angle proportions (angle factors) F_i are to be allocated as weighting factors. Long-wave radiation ($E_i = e_i \times s \times T_{Si}^4$), with s the Stefan-Boltzmann constant ($5.67 \times 10^{-8} \text{ W/m}^2\text{K}^4$) and T_{Si} the temperature of the i^{th} surface), diffuse short-wave radiation D_i are emitted from each of the n surfaces of the surroundings (2-2).

$$T_{mrt} = \left[\frac{1}{\sigma} \times \sum_{i=1}^n (E_i + a_k \times \frac{D_i}{\varepsilon_p}) \times F_i \right]^{0.25} \quad (2-2)$$

ε_p is the emission coefficient of the human body (standard value 0.97). D_i is the total diffuse solar radiation and diffusely reflected global radiation. a_k is the absorption coefficient of the irradiated body surface for short-wave radiation (standard value 0.7).

If there is value of direct solar radiation, T_{mrt} is replaced by T_{mrt}^* (2-3).

$$T_{mrt}^* = \left[T_{mrt}^4 + f_p \times a_k \times \frac{I^*}{(\varepsilon_p \times \sigma)} \right]^{0.25} \quad (2-3)$$

I^* is the radiation intensity of the sun on a surface perpendicular to the incident radiation direction. The surface projection factor f_p is a function of the incident radiation direction and the body posture. For practical application in human-biometeorology, is it generally sufficient

to determine f_p for a rotationally symmetric person standing up or walking. f_p ranges from 0.308 for 0° of the angle of the solar altitude and 0.082 for 90° (Matzarakis and Rutz, 2000).

2.1.5.2 Physiological Equivalent Temperature (PET)

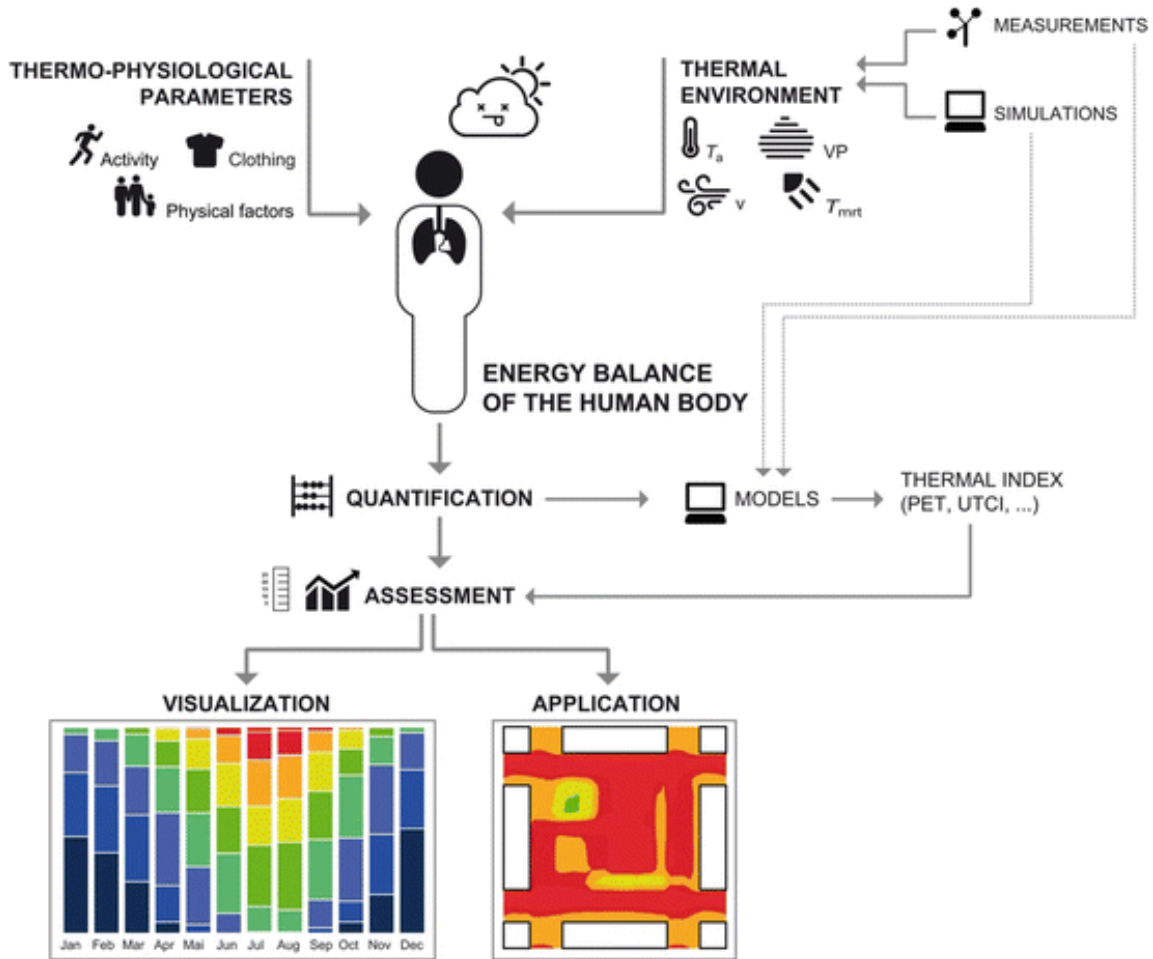


Figure 2-11 Flowchart of the human-biometeorological assessment of the thermal environment (Matzarakis et al., 2016).

The thermal index adopted in the studies addressed in this thesis is the Physiological Equivalent Temperature (PET). Even though the index PMV is widely used in the scientific community, it is specifically designed for indoor environments. For outdoor environments, one of the most widely used indices is PET, which is defined as:

equivalent temperature at a given place (outdoors or indoors) to the air temperature in a typical indoor setting with core and skin temperatures equal to those under the conditions being assessed. (Höppe, 1999)

Its calculation is based on the thermo-physiological heat-balance model: Munich Energy Balance Model for Individuals (MEMI) (Höppe, 1993). The reason for choosing PET as the thermal index in this study is that PET is an “application-friendly” indicator. It presents the

results through easily accepted Celsius degrees ($^{\circ}\text{C}$), making it simple for decision makers, planners, and citizens without a background in meteorology to understand (Table 2-1) (Matzarakis et al., 1999). This feature is consistent with the idea of the multi-parameter approach mentioned in this study, i.e., to describe the object as comprehensively as possible, but to present the results as simply as possible.

Table 2-1 Ranges of the PET for different grades of thermal perception by human beings and physiological stress on human beings. The assessment classes of PET* (Matzarakis et al., 2009, p. 212).

PET [$^{\circ}\text{C}$]	Thermal perception	Grade of Physiological Stress
≤ 4	Very cold	Extreme cold stress
4.1 - 8	Cold	Strong cold stress
8.1 - 13	Cool	Moderate cold stress
13.1 - 18	Slightly cool	Slight cold stress
18.1 - 23	Neutral (Comfortable)	No thermal stress
23.1 - 29	Slightly warm	Slight heat stress
29.1 - 35	Warm	Moderate heat stress
35.1 - 41	Hot	Strong heat stress
$41 >$	Very hot	Extreme heat stress

*Note: The classes are valid only for the assumed values of internal heat production (80 W) and thermal resistance of the clothing (0.9 clo). The meteorological input parameters have to be measured or transferred to the average height of a standing person's gravity center, 1.1 m above ground. (Matzarakis et al., 2009)

2.1.5.3 RayMan model for calculating T_{mrt} and PET

In this study, PET was calculated by using RayMan model (Matzarakis et al., 2007, 2010). RayMan is a microscale model for the calculation and estimation of the most modern thermal indices used in human biometeorology, as well as Sky View Factor (SVF), sunshine duration, shadow and in general radiation fluxes. This model is developed to calculate outdoor short wave and long wave radiation fluxes affecting the human body. RayMan model enables the consideration of complex building structures and the effects of clouds. The output of the model is the calculated mean radiant temperature, which is required in the human energy balance model and for the assessment of human biometeorological thermal indices. Most of the

commonly used thermal indices can be calculated through RayMan, including Predicted Mean Vote (PMV), Standard Effective Temperature (SET), Physiological Equivalent Temperature (PET), Universal Thermal Climate Index (UTCI) and Perceived Temperature (pT) (Matzarakis, 2012).

In the input windows of RayMan Pro, users can input the relevant values for calculating T_{mrt} (Figure 2-12), as well as the urban environment around the measuring point (Figure 2-13). Users can also import fish-eye photographs to calculate the SVF and estimate the sunshine duration at the measuring point (Figure 2-14). RayMan allows users to consider the effect of clouds on radiant fluxes in two ways, either by freely drawing the shape of clouds in the input window of fish-eye photographs or by giving a value to “Cloud cover (oktas)” in the input window of relevant values. Calculation of hourly, daily and monthly averages of sunshine duration, short wave and long wave radiation fluxes with and without topography, and obstacles in urban structures can be carried out with RayMan model.

Figure 2-12 Input window of RayMan Pro on the relevant values for the calculation of T_{mrt} and thermal indices (Matzarakis et al., 2007).

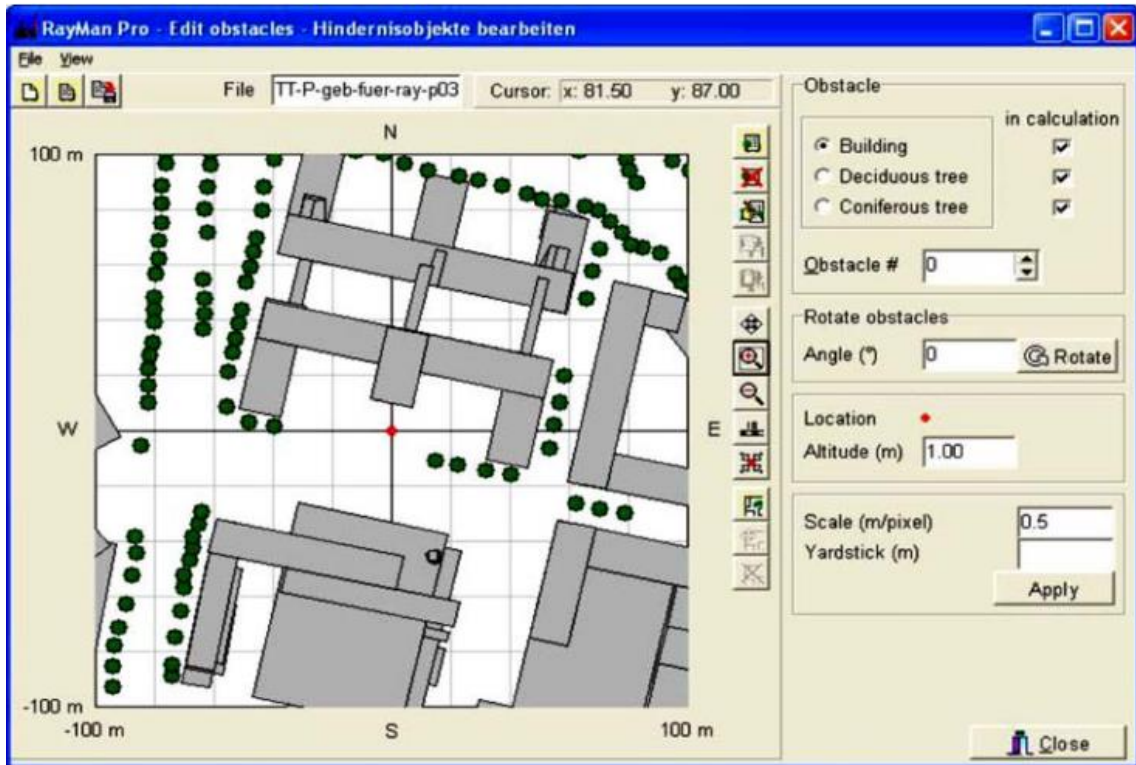


Figure 2-13 Input window of RayMan Pro on urban environment (Matzarakis et al., 2007).

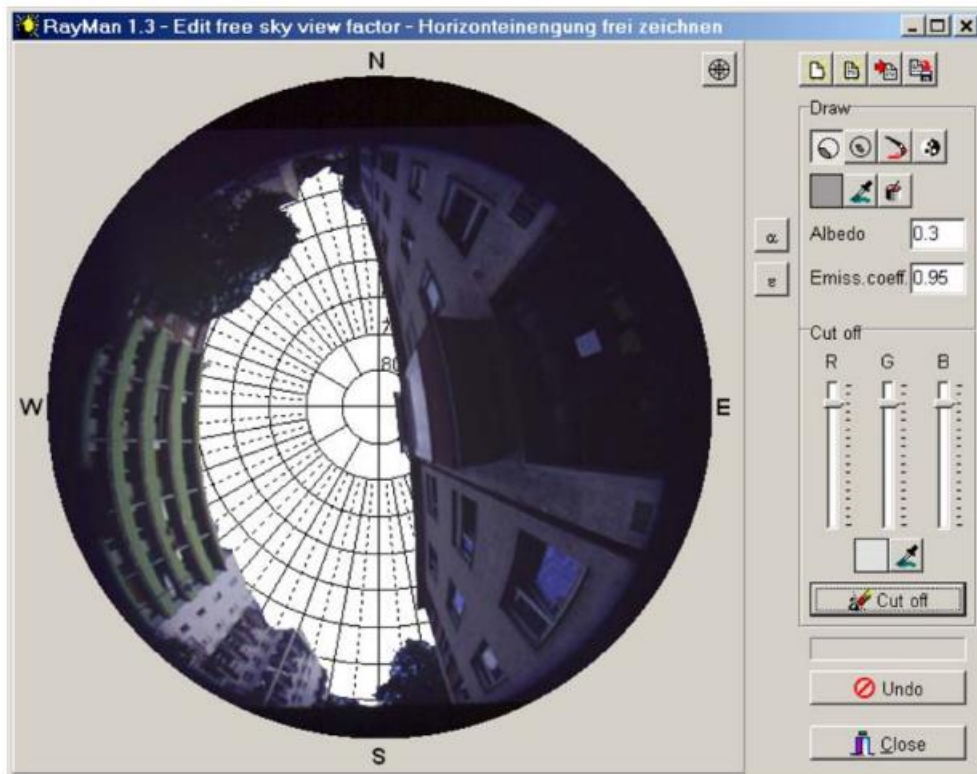


Figure 2-14 Input window of RayMan Pro on fish-eye photographs (Matzarakis et al., 2007).

The advantage of RayMan model is that it specializes in the radiative fluxes related to human thermal comfort. RayMan model is also able to consider the effects of SVF and cloud cover on the radiative flux at the measuring point. These advantages can exactly compensate for the shortcomings of the ENVI-met model in calculating radiative fluxes. The disadvantage of RayMan is that it can only calculate the values at a single point, which can also be compensated by ENVI-met model. Therefore, we have chosen to use RayMan model in combination with ENVI-met model. ENVI-met was used to derive the 3D distribution of meteorological values for the idealized scenarios, and RayMan was used to calculate the PET at a point.

2.2 Comparison with single-parameter Approach

2.2.1 Single-parameter Approach's Disadvantages

In previous studies of PCI effects, researchers commonly choose one single parameter to represent the spatial characteristic of UGS and attempt to derive a numerical relationship between this spatial parameter and the climatic parameter.

In recent years, there is still many urban climatological studies using regression analysis to investigate the linear relationship between land surface features and atmospheric characteristics of a particular city. The phenomenon is summarized by Oke as “never-ending case studies, regression analysis in the absence of physical explanation” (Oke, 2006b, p. 188).

The single-parameter approach manifests itself in by reducing the complex objects (urban land surfaces & urban atmosphere) to independent characteristic indicators, and then exploring linear relationships between the indicators of urban atmosphere and that of urban land surface (Figure 2-15).

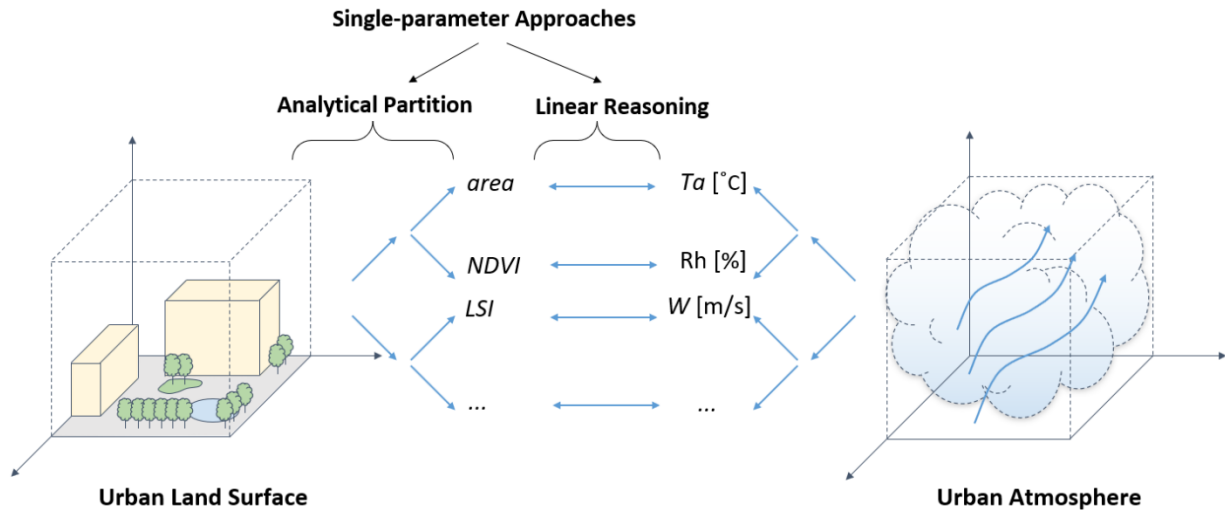


Figure 2-15 Single-parameter approach in current urban climatology: analytical extracting isolated indicators of complex objects and finding linear relationships between indicators.

The often used spatial parameters of UGS include the size, the vegetation density and the morphology indicators (Hardin and Jensen, 2007; Wilmers, 1990; Yu et al., 2015). For example, in 2010, Cao et al. investigated the correlation between the surface area of UGSs and the Land Surface Temperature (LST). They concluded that the significant PCI only exists when the UGS is larger than 2 ha. Dousset and Gourmelon (2003) characterized the vegetation coverage of UGS with the indicator Normalized Difference Vegetation Index (NDVI) and figured out the negative correlation between the LST and NDVI. Zhang et al. (2009) characterized the morphology of UGS with indicators of shape index, perimeter/area, perimeter density, and etc. They investigated the numerical relationship between each of the above indicators and the urban LST and concluded that more aggregated green patches can lead to lower urban LST.

The drawbacks emerged after the repeated usage of this single-parameter approach. Firstly, the derived numerical relationships can hardly be generalized across cities. Since only one parameter was investigated, the results can be contradictory when the environmental context changes. For instance, when investigating the degree of fragmentation of UGS (represented by indicator of Patch Density and Edge Density (PD&ED)), some studies concluded that the more fragmented UGSs have stronger cooling effects (McGarigal and Cushman, 2002; Xu and Yue, 2008), while some other studies found that more compacted UGSs yield greater cooling effects (Cao et al., 2010; Li et al., 2013). Because of the low universality, the urban climatological research is falling into “never-ending case studies” and “regression analysis in the absence of physical explanation” (Munn, 1973; Oke, 2006b).

Secondly, the findings obtained from the single-parameter approach are difficult to be applied to practical design and planning of UGS. The UGS in real world is a complex object, which means, it is impossible to change only one spatial characteristic of it without touching the other characteristics. Thus, the isolated relationship between one single spatial parameter and the microclimate is hardly referential to the climate-adaptative UGS design and planning. Although most of the studies on PCI effects claim that their results can guide the UGS design and planning, the actual application of the research results in practice is still rare (Eliasson, 2000; Hebbert, 2014).

The low generalizability and difficult applicability of the research results are two commonly recognized challenges facing urban climatological research (Erell, 2008; Hebbert, 2014; Mills, 2006; Munn, 1973; Oke, 2006b). The above elaboration illustrates that both the challenges are related to the single-parameter approach. To solve these problems, it is necessary to explore the joint influence of multiple spatial characteristics of UGS on the microclimate through a multi-parameter approach. However, attempts in this regard are still few in previous studies.

2.2.2 Comparison in Methodology

There are three main differences between the multi-parameter and single-parameter methods in terms of technical aspects (Figure 2-16).

- 1) In describing the urban land surface, multivariate experiments, which characterize land surface by the permutations of multiple land surface spatial features, will be conducted instead of the single-variate experiments that were commonly adopted in previous studies.
- 2) In describing the urban atmosphere, composite indicators, which contain as comprehensive characteristics as possible with the smallest possible amount of data, will be used instead of the segmented single index adopted in previous studies.
- 3) In revealing the numerical relationship between urban spatial morphology and urban climate, the multi-parameter approach aims to reveal the interdependent influence of different spatial features on the human thermal comfort, while the single-parameter approach aims to reveal the linear relationship between the single spatial parameter and climatic index.

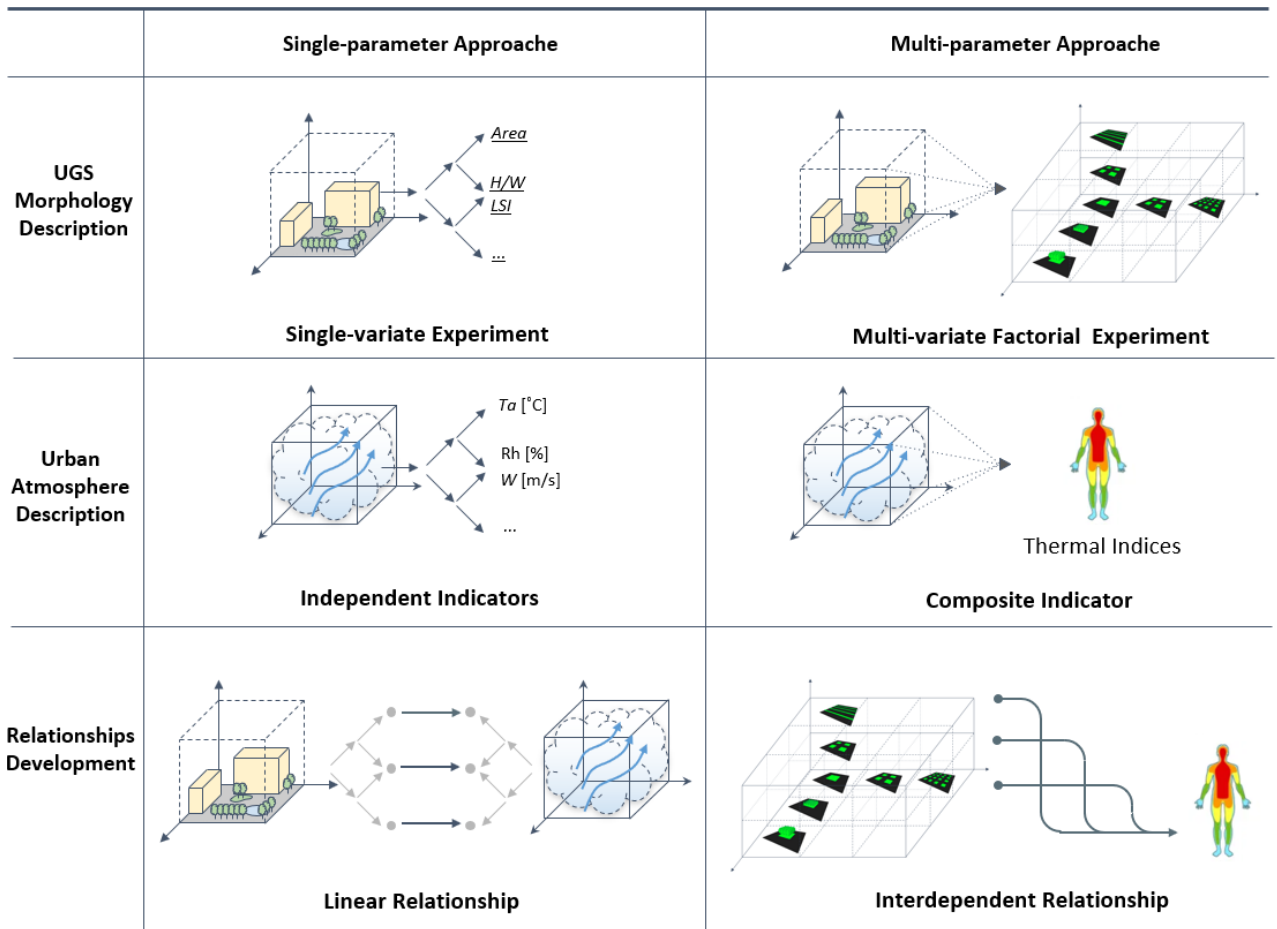


Figure 2-16 Comparison of multi-parameter and single-parameter approaches at the technical aspect.

2.3 Why the multi-parameter Approach is Conducive to the Application and Generalization of Research Results

2.3.1 Reason Analysis of the Implementation Gap in Urban Climatology

In many studies on the application impasse, the communication gap between researchers and urban construction executors was mentioned as a cause of the implementation gap in urban climatology (Chandler, 1976; Hebbert, 2014). This communication gap can be interpreted from the following three aspects in which the researchers and executors hold different views:

2.3.1.1 Specific Action vs. Numerical Relationship

If it is expected that the results of urban climatological research will be used in the practical construction of cities, then urban planners and designers will need to know exactly what to do. However, most of the climatologist-led research in this area only goes so far as to show the numerical relationship between a particular feature of the land surface and the urban

climate index. They do not go further to translate the findings into concrete guidelines for action in urban design and planning. This gap between scientific knowledge and concrete what-to-do is one of the main reasons for the application impasse.

A questionnaire study conducted by Eliasson among urban planners revealed how wide this gap is (Eliasson, 2000). In the opinion of the urban planners interviewed, there is a need for the application of climatological research in urban planning. But they do not have enough climatological knowledge to be able to interpret the results obtained by climatologists. On the other hand, urban planners believe that most climatologists do not understand the urban planning process (Eliasson, 2000; Golany, 1996; Mills, 2006). The results of many climatologist-led urban climatological studies do not correspond to any of the urban decision-making steps that can implement these results. Therefore, the results of many urban climatology studies have no real potential for application.

Mills once noted that most research results are not “designer-friendly”. Namely, they are not readable and usable enough for urban planners and designers (Mills, 2014). What can solve this problem is a tool like a “translator” that can translate the climatological research results into a design language that enables a direct change to the urban space (Givoni, 1998, p. 250; Hebbert, 2014). As early as 1984, Oke has noticed the lack of a practical predictive tool in urban climatology that can assist the designers in configuring green space, orienting roads, optimizing aspect ratios, etc. (Hebbert and Mackillop, 2013; Oke, 1984b). Oke has even personally devoted much effort to the development of tools for urban climatological knowledge transfer (Oke, 1984b, 2006a, 2006b). Errell (2008) proposed a vision to this tool, envisaging that it should be “formulated so that the inputs include parameters related directly to the architect’s decision-making process”. However, so far there is no evidence that such a tool has been developed and is in use by urban planners and designers.

2.3.1.2 Need for Generalization vs. Case-by-case Studies.

Another important reason for this application difficulty is the low degree of generalizability of the findings of urban climatological studies. When environmental conditions, study scales, and study methods change, different studies investigating the same relationship can reach completely different conclusions. The manifestation is that the findings of an urban climatological study conducted in one city are not valid in other places (Cao et al., 2010; Li et al., 2013; McGarigal and Cushman, 2002; Xu and Yue, 2008) (see Chapter 3 for a specific example). The problem of low universality stems from the inevitable fact that the urban land surface is incredibly complex and variable. Sometimes a seemingly insignificant change

in surface features can make the shape of a city's UHI effect radically different. Thus, as Munn has stated: “The search for results that are transferable from one city to another and from one climatic zone to another is therefore difficult.” (Munn, 1973, p. 91)

In contrast, urban planning and urban design must follow strict industrial standards. The ideal way to influence urban construction practices is to incorporate the results of urban climatology studies into urban design and planning standards. But this undoubtedly requires that the results be highly generalizable. Therefore, the difficulty of generalizing urban climatological research results inevitably hinders the knowledge transfer. Although a climatological consultation for a specific city or a specific urban construction project is also a possibility for knowledge transfer, this kind of spot application is still far from the expected large-scale impact of urban climatology on urban construction.

2.3.1.3 Complex System vs. Linear Relationship

Existing single parameter approaches are characterized mainly by using a single parameter independent of each other to describe the space and trying to extract a linear relationship between this single indicator and the urban climate. However, this approach is oversimplified. Both the urban atmosphere and the urban space are complex systems. The way to reveal the interrelationship between the two with a single parameter can undoubtedly reveal only a very small aspect of it. When environmental conditions, study scales, and study methods change, different studies investigating the same relationship can come to completely different conclusions (one example can be seen in Chapter 3). However, each city is unique in its land surface and its climatic context. The low universality has made urban climatology research unavoidably fall into endless case studies (Munn, 1973; Oke, 2006a, 2006b). If the findings of a study cannot be generalized, then there is little chance for them to be transferred into applicable guidelines. Trying to characterize the whole object by reducing only one aspect is like a blind man feeling an elephant, once the perspective changes, different conclusions will be drawn (Ireland, 2007, pp. 81–84; John Godfrey Saxe, 1872) (Figure 2-17).

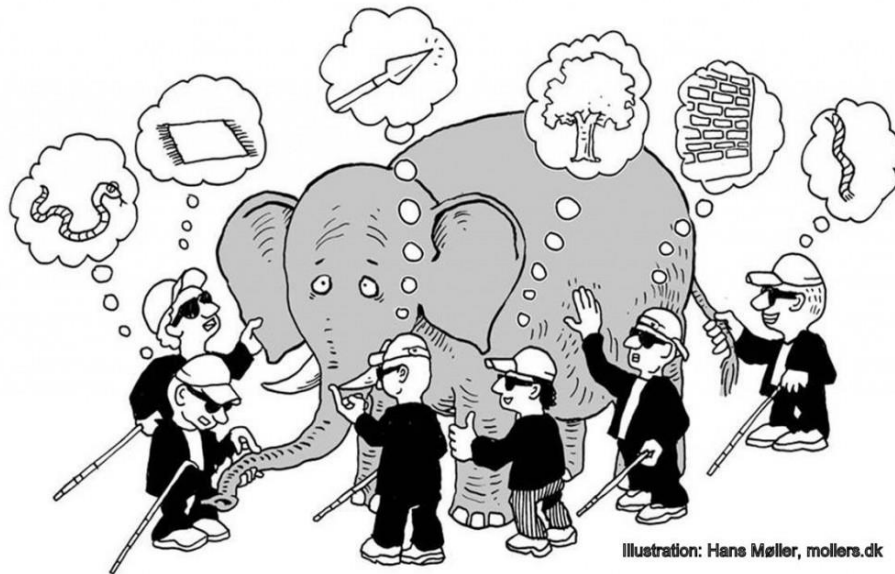


Figure 2-17 The parable of the blind men and an elephant indicates that the whole cannot be accurately perceived by merely the side descriptions (Illustration: Hans Møller; Public Domain).

The main reason why many regression analysis studies are flourishing in urban climatology is that this linear relationship fulfills the needs of practical application. For applications in urban construction, a simple and clear linear relationship is the most expected. The main concern of decision makers is: what kind of space can cause which local climate conditions? Therefore, researchers in the field of urban climate are always enthusiastic about regression analysis or even exploring simple linear correlations.

However, the relationships derived from such regression analysis have been shown to be instable across cities. Based on these studies, it is remarkably difficult to derive climate-adaptative guidelines for urban spatial design that are applicable to various cities. The underlying reason is that the researchers have confused the idea of addressing the “how” question and addressing the “why” question. To practically apply the research results to urban construction is a “how” problem, whose solution requires the analytical reductionist methodology. On the other hand, to summarize a law that can be universally applied is a “why” problem, the solution of which requires a synthetic holistic methodology (Figure 2-18) (Systems Innovation, 2016).

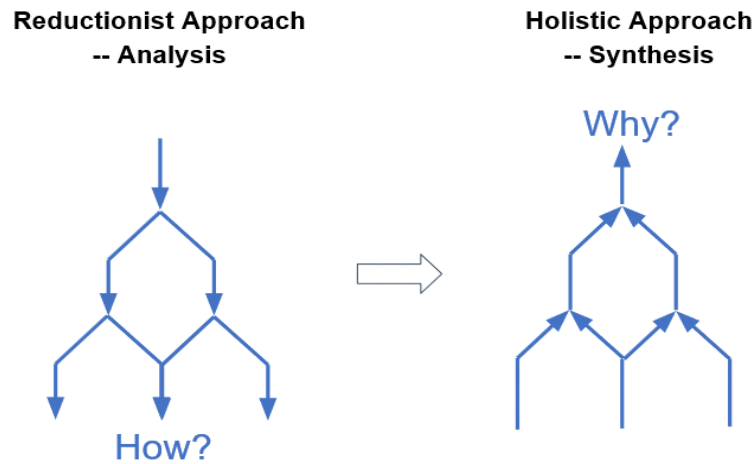


Figure 2-18 The analytical approach is suitable for answering the “how” questions, while the integrative approach is appropriate for the “why” questions.

Those urban climate studies that rely on regression analysis have employed exactly the reductionist approach, which is not suitable for addressing the “why” question.

2.3.2 Applicability of the Multi-parameter Approach to Addressing the Implementation Gap

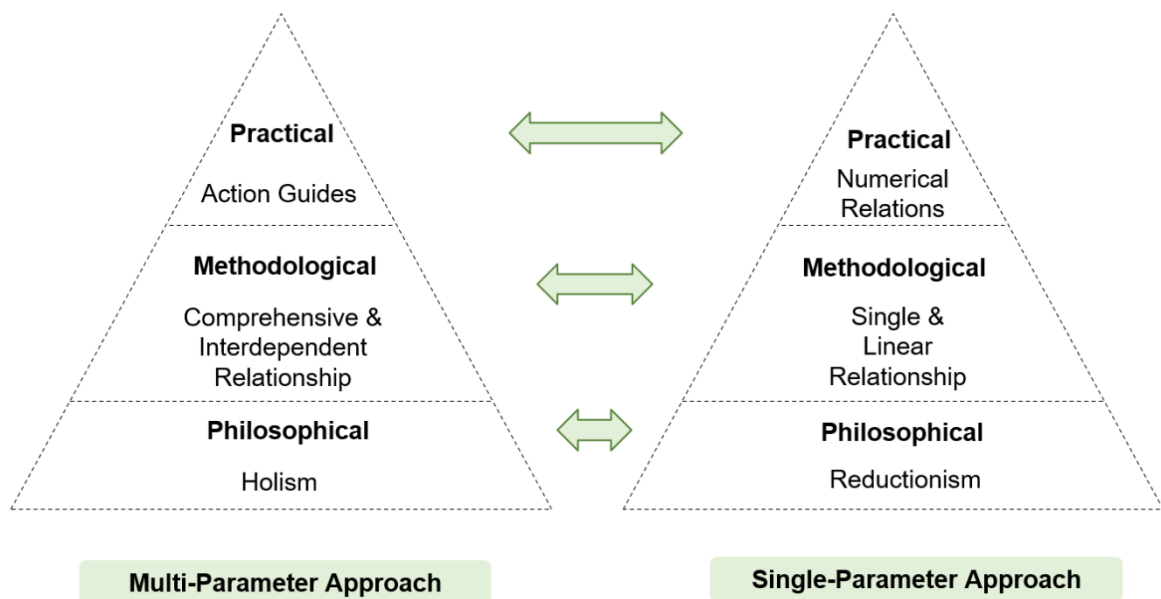


Figure 2-19 Advantages of multi-parameter methods over single-parameter methods.

The main reasons why the multi-parameter approach is more suitable for addressing the current implementation gap in urban climatology can be divided into three aspects: firstly, it compensates for the existing single-indicator approach being too one-sided, secondly, its results can easily be used to provide specific guidelines for action, and thirdly, its holistic philosophical

basis is more suitable for solving complex urban climatology problems (Figure 2-19). These three strengths help to address exactly the causes of the difficulties in generalizing and applying urban climatological research results.

Chapter 3: The Influence of Spatial Configuration of Green Space on Microclimate and Human Thermal Comfort

Abstract¹

Many cities are facing the prospect of increasing air temperatures and heat load because of the urbanization and the consequent Urban Heat Island (UHI) effect. Previous studies on the mitigation strategies focused on the cooling effect of vegetation and green areas, which were investigated as Park Cool Island (PCI). It has been shown that the spatial configuration of a green area can strongly influence its cooling effect. However, the specific correlation has not been sufficiently studied. To systematically clarify the correlation between the spatial configuration and the cooling effect of green areas, 25 idealized scenarios representing green areas with five different spatial configurations and five vegetation types, are designed and simulated using the microclimate model ENVI-met. The cooling effect of each scenario is calculated by comparing the mean air temperature at 2 m height of each scenario with that of an open space completely covered by asphalt. The human thermal comfort of each scenario is evaluated by means of physiological equivalent temperature (PET) using RayMan. The results reveal the influence of the fragmentation degree (quantified by the Patch Density and Edge Density (PD & ED)), shape complexity (quantified by the land shape index), orientation of green belt, and vegetation type on the cooling effect of a green area. The spatial configuration and the vegetation type of green areas are found jointly affecting the efficiency of the green areas' cooling effect. The conclusions of this paper provide suggestions for the climate-adaptive design and planning of urban green areas in the future.

¹ The study described in this chapter has been published as:

Soudoudi, S., Zhang, H., Chi, X., Müller, F. and Li, H. (2018) 'The influence of spatial configuration of green areas on microclimate and thermal comfort', *Urban forestry & urban greening*, vol. 34, pp. 85–96. Available at <https://doi.org/10.1016/j.ufug.2018.06.002>.

This work is licensed under the [CC BY-NC-ND 4.0](https://creativecommons.org/licenses/by-nc-nd/4.0/).

3.1 Introduction

The intensity and frequency of heat waves will increase in the future (Meehl and Tebaldi, 2004). Especially in urban areas, the heat waves are further enhanced by growing Urban Heat Island (UHI) effect (Li, Wolter et al., 2018; Li, Zhou et al., 2018). The rise of air temperature can result in many issues, including the reduced urban thermal comfort and the health of citizens (Bai et al., 2014; Bi et al., 2011; Kovats and Hajat, 2008; Mihalakakou et al., 2004), the increased consumption of energy and power (Chang et al., 2007; Kolokotroni et al., 2007), the increased risk of air pollution (Sarrat et al., 2006), and the interference on the composition and distribution of urban biological species.

Faced with problems caused by increasing urban heat waves, mitigation and adaptation strategies were extensively explored. Since being firstly proposed by Chandler (1962), the cooling effects of urban green areas have aroused considerable interest as a potential method to mitigate urban heat waves (Park et al., 2012). A wealth of studies has shown that green areas can lower the ambient air temperature and adjust the humidity of surrounding areas (Bowler et al., 2010; Chang et al., 2007; Spronken-Smith and Oke, 1998), forming a kind of ‘oasis effect’, which is described as Park Cool Island (PCI) (Cao et al., 2010; Jáuregui, 1990). The observed PCI amplitude ranges from 2 K to 8 K (temperature difference in Kelvin) (Taha, 1997; Wong and Yu, 2005), and varies according to the properties of the green area.

The spatial configuration is defined by the shape, arrangement and layout of green areas (Wilmers, 1990). It has been found that the spatial configuration of a green area significantly affects the intensity of PCI (Cao et al., 2010; Li et al., 2012). However, the influence of the spatial configuration of green areas has not been sufficiently explored (Weng et al., 2004; Zhang et al., 2009). It is suggested that more studies on the influence of green configuration should be conducted in the future (Li et al., 2012; Middel et al., 2014).

The quantification of the spatial configuration of green areas is mainly through the landscape metrics (Chen et al., 2014a; Connors et al., 2013). The landscape metrics is a concept from landscape ecology. It includes a series of indices that quantitatively describing the spatial configuration of green patches. The landscape metrics commonly used in the studies of PCI include the Land Shape Index (LSI) expressing the complexity of the patch shape (Cao et al., 2010; Chen et al., 2014b), and the Patch Density and Edge Density (PD & ED) representing the fragmentation of green patches (Maimaitiyiming et al., 2014; Zhang et al., 2009).

A number of studies were conducted on the correlations between the land surface temperature and PD & ED of green areas. However, the results of these studies were contradictory. Some studies concluded that the cooling effect increased as PD & ED increased (Gomez-Munoz et al., 2010; Maimaitiyiming et al., 2014), while others drew the reverse conclusion (Cao et al., 2010; Li et al., 2013; Zhou et al., 2011). This disagreement between studies is a consequence of the empirical approach. To provide an explanation for this disagreement, numerical modelling is necessary as methodology.

As a widely used model in the studies of microclimate (Hedquist and Brazel, 2014; Perini and Magliocco, 2014; Wania et al., 2012), the holistic three-dimensional non-hydrostatic model ENVI-met ® (ENVI_MET GmbH, Germany) is utilized in this study to investigate the influence of configuration on the cooling effects of green areas. Because of its strength in simulating the plant-air interactions (Bruse and Fleer, 1998), ENVI-met is optimally suited for exploring the cooling effect of the vegetation (Middel et al., 2014; Wang and Zacharias, 2015).

The cooling effect of vegetation primarily comes from three effects—evapotranspiration, ventilation and shade (Boukhabl and Alkam, 2012). ENVI-met enables the simulation of all of these processes. ENVI-met can calculate sensible heat flux, evapotranspiration flux of liquid water on leaves, and transpiration flux (Wania et al., 2012). Jansson (2006) utilized ENVI-met to research water transport processes in the urban microclimate. The effect of vegetation on wind speed and wind direction is usually studied with regard to thermal comfort and air pollution problems (Vailshery et al., 2013; Wang and Zacharias, 2015). As ENVI-met is a model based on CFD, it can also work well in the investigation of the ventilation. The most obvious influence of vegetation on heat waves is as a shelter against solar radiation. It is found that the mean radiant temperature under foliage is much lower than that of the surrounding area (Perini and Magliocco, 2014). The three-dimensional SPACES module and the specific plant module Albero of ENVI-met enable the study on the shade of vegetation.

As the heat waves in urban area significantly influence the human thermal comfort of urban residents (Gabriel and Endlicher, 2011), the physiological equivalent temperature (PET) (Höppe, 1999; Matzarakis et al., 1999; Mayer and Höppe, 1987) is taken as the thermal indices in this study to evaluate the cooling effect of green areas from the point of view of the human thermal comfort. Wide variety of studies were undertaken to explore human thermal comfort by PET in different regions and climate zones (Ahmed, 2003; Eludoyin, 2014; Farajzadeh and Matzarakis, 2012; Li and Chi, 2014; Nikolopoulou and Lykoudis, 2006). Because of its comprehensive and effective assessment of thermal comfort, PET has been widely used to

evaluate the thermal environment of urban regions (Andreou, 2013; Taleghani et al., 2014; Thorsson et al., 2011).

The idea of this study comes from the redevelopment plan for the former Tempelhof Airport in Berlin, Germany. After years of debate, Berliners voted against the redevelopment of the former airport in a public referendum in May 2014. 65% of voters voted against the Senate's plans, and secured the use of the site as a public park (Hilbrandt, 2017). As the site of Tempelhof Airport also faces with risk of overheating, before it is re-constructed as a green area, the following questions should be answered: Which is the optimal layout of this green area, one integrated green area or several smaller distributed green areas? What is the optimal shape of the green areas, belt or square? What is the optimal vegetation type of the green areas, shrubs or trees?

In order to answer these questions and further explore the systematic correlations between the cooling effects and spatial configurations of green areas, in this study, 25 idealized scenarios representing green areas with five layouts and five vegetation types were designed and simulated by numerical model ENVI-met. The landscape metrics were utilized to quantitatively describe the spatial configurations, aiming at generalizing the results of the present study. The PET of each scenario was calculated using RayMan model, to evaluate the cooling effect from the point of human thermal comfort. The results of this study can provide suggestions for the redevelopment plan of Tempelhof Airport Berlin, as well as for the climate-adaptive design of urban green areas adapting to the heat waves.

3.2 Methodology

3.2.1 Study Area

The study was conducted in Berlin (52.52°N, 13.38°E), Germany. Berlin has large urbanized areas and displays pronounced Urban Heat Island effect (Li et al. 2017; 2018). On hot days, people living in the city centre suffered from increased heat stress risk (Gabriel and Endlicher, 2011). This study was conducted for the former Berlin Tempelhof Airport located near the centre of Berlin.

3.2.2 Design of Scenarios

By use of the SPACES module of ENVI-met, 25 idealized scenarios of green areas with five different configurations and five vegetation types were constructed (Figure 3-1). The configuration types included Configuration 1—one central green area, Configuration 2—four

dotted green areas, Configuration 3—sixteen dotted green areas, Configuration 4—four belt-shaped green areas aligned South to North, and Configuration 5—four belt-shaped green areas aligned West to East. The whole domain of each scenario is 10000 m² and the total green area in all scenarios was equal to 2500 m². The five configurations were combined with five different vegetation types: trees with big canopies (Height/Diameter of canopy: 20 m/15 m), trees with small canopies (Height/Diameter of canopy: 10 m/5 m), hedges and shrubs, 50 cm grass, and 10 cm grass. The spaces excepting the green areas in the scenarios were covered by asphalt to imitate the city areas.

In order to evaluate the cooling effect of each scenario, one control scenario completely covered by asphalt was simulated. The difference of the mean air temperature on 2 m height between the control scenario and the objective scenarios was calculated.

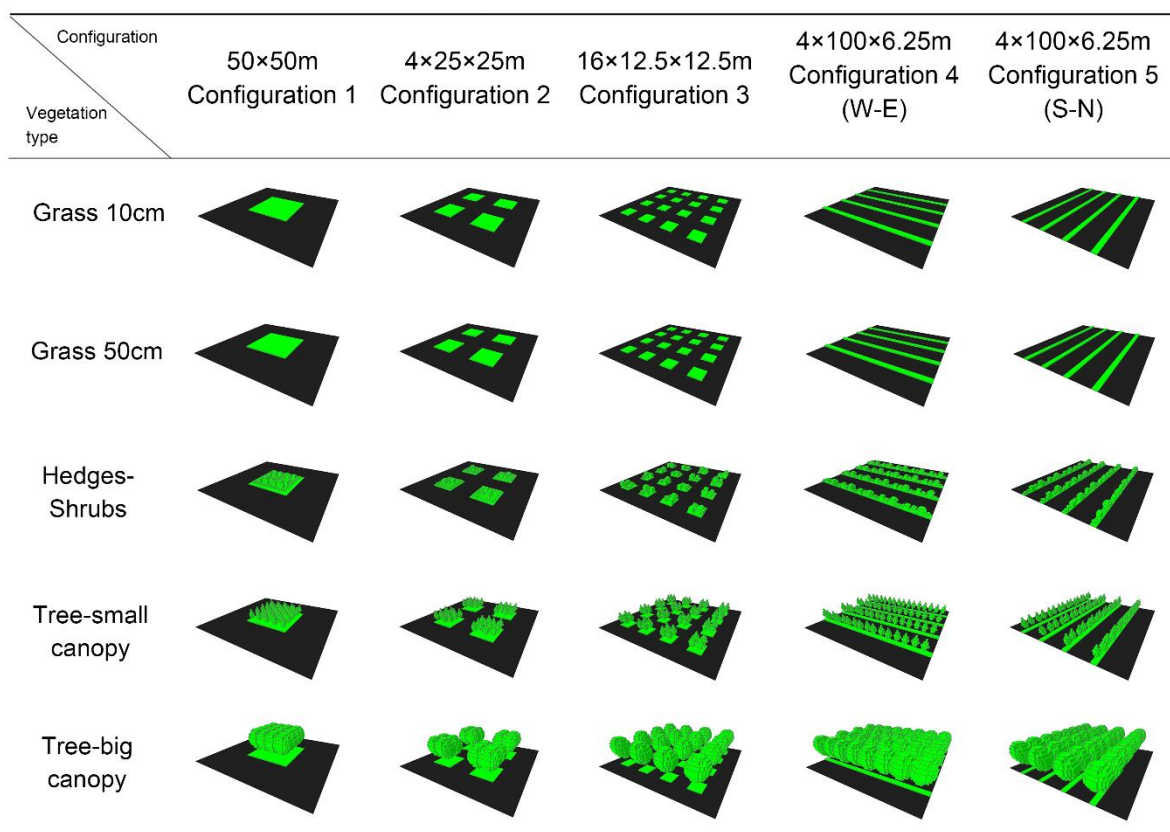


Figure 3-1 Configuration of studied area on the simulation day.

3.2.3 Numerical Modelling

3.2.3.1 Configuration of the ENVI-met

In this study, the micro-climatic conditions of the 25 green areas were simulated using ENVI-met 4.0. Two hot and sunny days in Berlin (8th/9th June 2014) were selected to explore the potential cooling effect of the green areas in this site during heat waves (Figure 3-2). The daytime lasts for around 16 h during this summertime. According to the meteorological observation at Tempelhof meteorological station (52.27°N, 13.38°E), the maximum air temperature at 2 m height was 31 °C, with an average of 23 °C combined with calm wind (2.06 m/s at 10 m height) and low relative humidity (27%). Based on the meteorological condition of study area and the designed scenarios, the configuration file of the model is shown in Table 3-1.

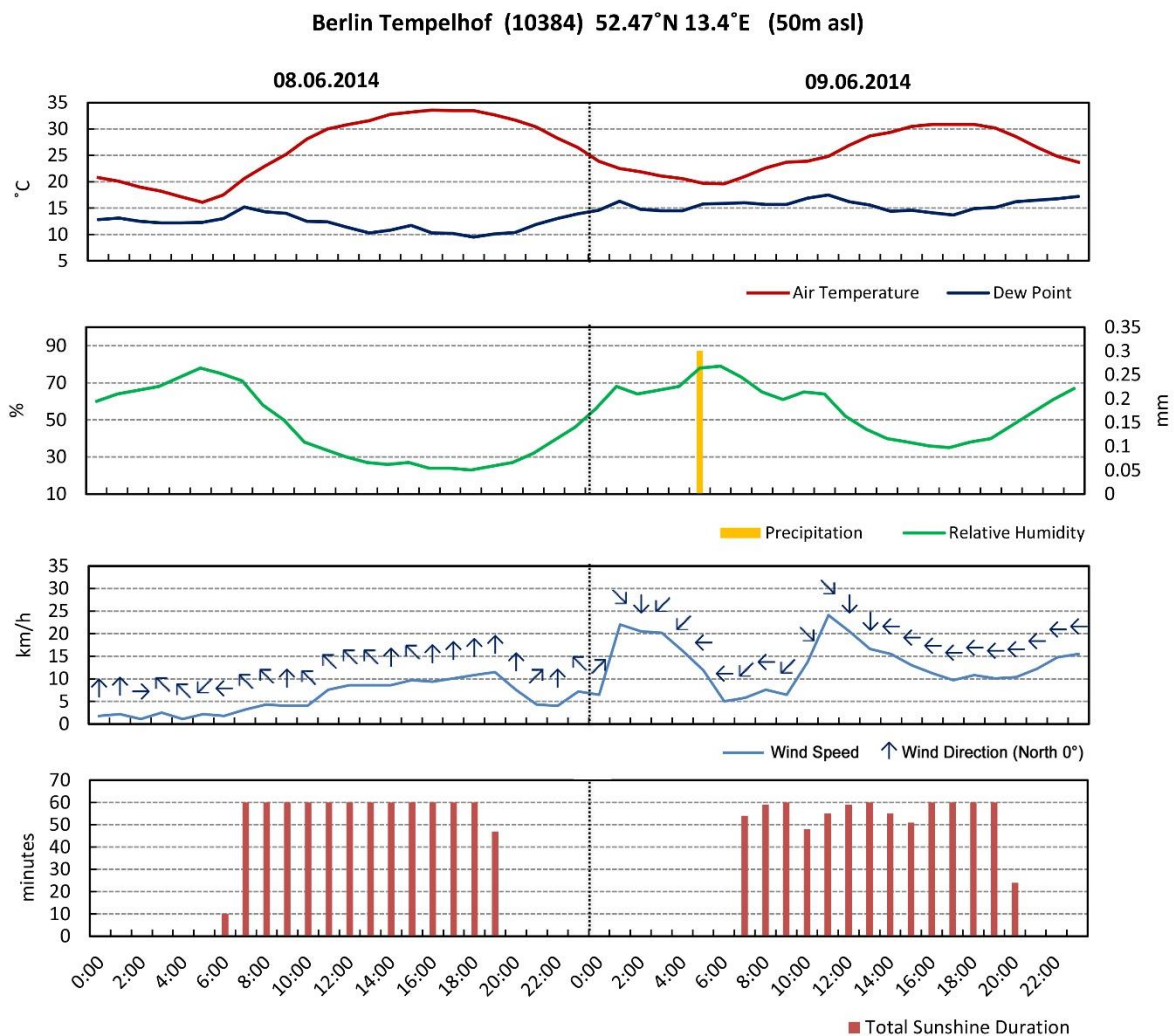


Figure 3-2 The daily time series of meteorological data (Meteogram) of the weather station located in Berlin Tempelhof (10384) from June 8 to June 9, 2014 (Data from Meteostat.net).

Table 3-1 The configuration of ENVI-MET for the simulation.

city	Berlin
longitude, Latitude	52.52°N, 13.38°E
elevation (m)	34
simulation date	08-09.06.2014
wind speed at 2 m (m/s)	2.06
wind direction (0: N 90: E 180:S 270:W)	210 (Southwest)
roughness length (m)	0.01
initial temperature atmosphere (K)	298.5
whole domain (m ²)	10,000
vegetation domain (m ²)	2,500
vegetation types	5
configuration types	5

3.2.3.2 Evaluation of the ENVI-met

The performance of the ENVI-met model in simulating air temperature at green areas in Berlin was evaluated using the measured and simulated data of the project of Berlin-Brandenburg Academic of Science (BBAW): The historical garden in climate change (Hüttl et al., 2020). The measurement was carried out in Tiergarten -- the central park of Berlin with various vegetation types and configurations of green areas. The air temperatures at 2 m height in 24 h were recorded in three measuring points respectively in the vegetation types of grass, tree-grass and tree-shrub-grass. The corresponding simulated air temperature using ENVI-met were compared with the measured data.

3.2.4 Analysis of the Simulated Data

The simulated meteorological condition of the 25 scenarios were analyzed at three time points: 2 pm, 10 pm, and 5 am. As the greenery is well known as a strategy to mitigate the urban heat island, these three time points were selected as samples because of their representativeness in the mitigation of urban heat island. At 2 pm, the cooling influence of the

shades and evapotranspiration are the highest. At 10 pm after sunset, there is no more cooling effect from shades in the 25 scenarios, while the urban heat island intensity of the reference asphalt scenario is still high. At 5 pm before sunrise, there is also no cooling effect from shades in the 25 scenarios, but the reference asphalt scenario has been cooled down because of the heat dissipation. These time points were also used as samples in the previous studies (Lehmann et al., 2014; Mathey et al., 2015).

3.2.5 Quantification of the Spatial Configuration through the Landscape Metrics

The green spaces in the scenarios were quantified by three landscape metrics: Patch Density (PD), Edge Density (ED) and Land Shape Index (LSI).

PD & ED are significant landscape metrics describing the fragmentation of green spaces (Li et al., 2013; Liu and Weng, 2008). PD represents the number of green patches divided by total landscape area, while ED represents the total length of edges per unit area (Table 3-2).

Table 3-2 Descriptions and equations for Patch Density and Edge Density (PD & ED)

	Abbreviation	Definition	Equation	Unit
Patch Density	PD	Densities of patches	$PD = \frac{n}{A} \times 10^4$ n= total number of patches A= total area	number/ha
Edge Density	ED	Total length of all edge segments of green space per hectare.	$ED = \frac{10000}{A} \times \sum_{i=1}^n e_i$ n=number of segment e _i =edge length A=total area	m/ha

Land Shape Index (LSI), which is designed by Patton (1975), describes the complexity and compactness degree of the patch shape. It was known as a factor affecting the Park Cool Island (PCI) (Liu and Weng, 2008; Cao et al., 2010). A concentrated shape has a low LSI value, while a complicated shape has a high LSI value. The equation for LSI is shown as below.

$$LSI = \frac{P_t}{2\sqrt{\pi \times A}} \quad (1)$$

P_t is the total perimeter, and A is the total area.

3.2.6 Assessment of Human Thermal Comfort

In this study, the physiological equivalent temperature (PET) is taken as the thermal indices to assess the cooling effect of green areas from the point of view of the human thermal comfort. PET is defined to be equivalent to the air temperature that is required to reproduce in a standardised indoor setting and for a standardised person the core and skin temperature that are observed under the conditions being assessed (Höppe, 1999). PET applied in this study assessed human thermal comfort (Table 3-3) by considering the meteorological conditions, human metabolic heat exchange rate, and other individual-related parameters such as age, gender, height, weight, and clothing, allowing a comprehensive assessment of the effectiveness of adaptation measures.

Table 3-3 The comfort/sensation scale of the physiological equivalent temperature (PET) according to Matzarakis and Mayer (1997).

PET/°C	Thermal perception	Grade of physiological stress
≤4.0	Very cold	Extreme cold stress
4.1-8.0	Cold	Strong cold stress
8.1-13.0	Cool	Moderate cold stress
13.1-18.0	Slightly cool	Slight cold stress
18.1-23.0	Comfortable/Neutral	No thermal stress
23.1-29.0	Slightly warm	Slight heat stress
29.1-35.0	Warm	Moderate heat stress
35.1-41.0	Hot	Strong heat stress
41.1≤	Very hot	Extreme heat stress

The model RayMan Pro version 2.1 was used to calculate PET in this study (Matzarakis, 2012). RayMan is well suited for determining microclimatic changes in different urban structures, as it calculates the radiation fluxes of different surfaces and their changes (Gulyás et al., 2006). In this study, the RayMan model was driven by the meteorological data, which are exported from ENVI-met, including air temperature, relative humidity, mean radiant temperature and wind velocity.

3.3 Results and Discussion

3.3.1 Evaluation of the Simulation

Figure 3-3 shows the diurnal variations of the simulated and measured air temperature (left), and the corresponding linear fitting (right). It can be observed that the simulated air temperature consists with the measured air temperature well, with the correlation coefficient of 0.92 ($P < 0.05$), RMSE=1.26 (Middel et al., 2014). With the relatively low RMSE and high correlation coefficient, the simulation model ENVI-met in the study of green areas can be evaluated as reliable.

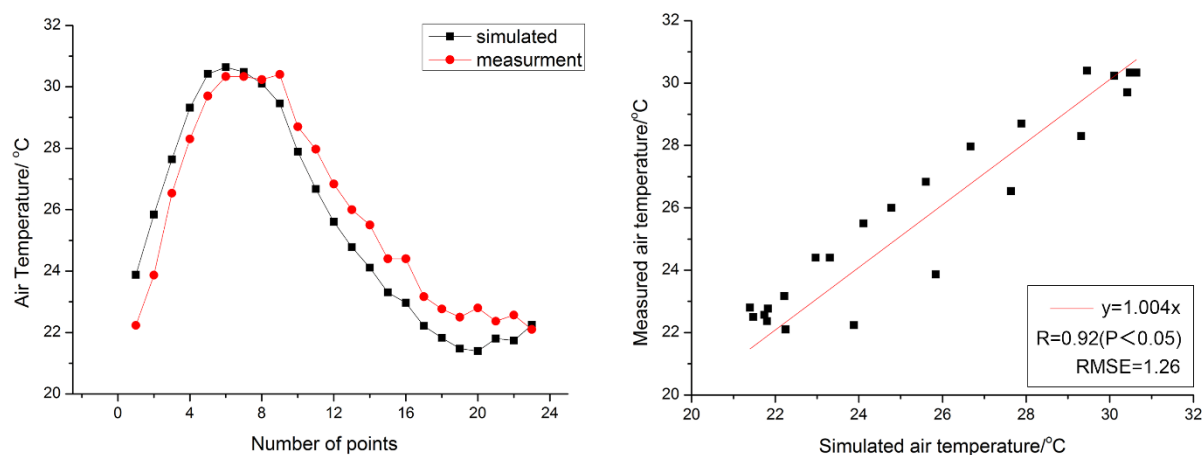


Figure 3-3 (a) The mean hourly 2 m air temperature measured on the walkway surrounded by three vegetation types in Tiergarten (red) and the corresponding simulated air temperature (black); (b) The scatter diagram showing the correlation between the measurement and simulation.

3.3.2 General Conditions of Cooling Effects in 25 Scenarios

Figure 3-4 shows the diurnal variation of the mean cooling effect of 25 scenarios at 2 pm, 10 pm, and 5 am. The mean cooling effect was calculated by the difference of the mean 2 m height air temperatures between each green area scenario and the control area covered by asphalt. In every scenario, the mean cooling effect decreases as the time goes on from 2 pm to 5 am. The cooling value is the greatest at 2 pm in all scenarios. Cooling effects at 10 pm are greater than that at 5 am. The highest mean cooling value appears at 2 pm, reaching 6.3 K in the scenario of Configuration 4 with tree-big canopy, while the lowest one appears at 5 am, with 1.2 K for Configuration 1 with 10 cm grass.

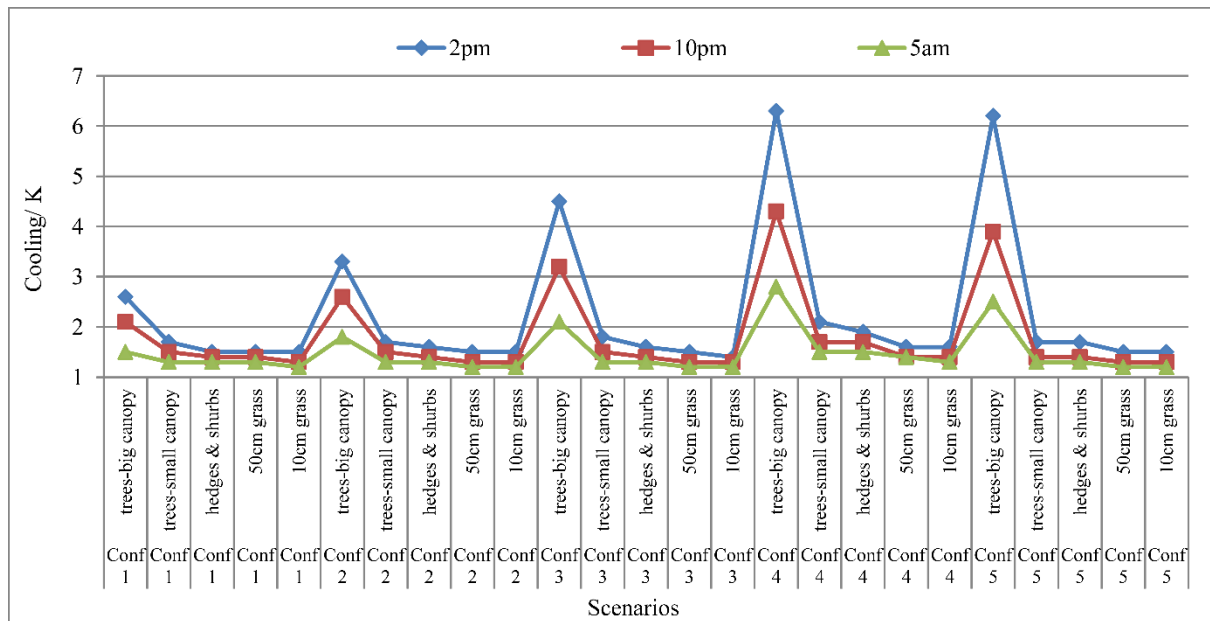


Figure 3-4 Mean cooling effect by different scenarios at 2 pm, 10 pm, and 5 am.

The differences in cooling effects between different scenarios were greater in daytime than that at nighttime (Figure 3-4). The difference in cooling effects between different scenarios decreased after sunset. Every scenario exerted obvious diurnal variation. This was because of strong daytime radiation, leading to greater evapotranspiration and a larger difference between shaded areas and un-shaded areas. At night, the stomata close due to the lack of radiation, and vegetation has no cooling effect from transpiration. Naturally, there is no shades to distinguish green and impervious area at nighttime. Trees also inhibit nocturnal long-wave radiative cooling because of smaller sky view factor, while excess moisture increases the thermal capacity of the soil and slows down surface cooling.

In every scenario, the total green area was equal, although the configuration and vegetation type were different. In order to compare the cooling effect of different scenarios, the size of areas with cooling in excess of 1.5 K was estimated. Figure 3-5 shows the percentage of the total cooled down area featuring cooling in excess of 1.5 K.

In Figure 3-5, green values indicated a percentage greater than 50%, while red values indicated a percentage lower than 10%. Most of the percentages greater than 50% were related to scenarios with trees with canopies and scenarios with scattered or belt-shaped configuration.

Configuration/ Vegetation	Time	50×50m Configuration1	25×25m Configuration2	12.5×12.5m Configuration3	100×6.25m Configuration4	100×6.25m Configuration5
Grass 10cm	2 pm	31.8	40.7	45.9	74.4	55.6
	10 pm	27.7	27.9	13.2	42.2	12.4
	5 am	24.4	17.4	3.8	20.2	0.0
Grass 50cm	2 pm	32.2	43.1	51.0	70.9	55.1
	10 pm	28.8	29.7	12.5	41.3	6.6
	5 am	26.7	22.5	6.3	31.2	0.0
Hedges- Shrubs	2 pm	32.4	46.8	59.6	79.2	67.7
	10 pm	30.4	39.1	36.7	79.1	45.9
	5 am	27.9	29.8	19.7	60.2	25.4
Tree-small canopy	2 pm	34.6	50.2	68.9	83.7	82.1
	10 pm	32.2	45.0	60.0	81.8	67.4
	5 am	27.0	30.3	19.2	50.3	20.3
Tree-big canopy	2 pm	92.0	100	100	100	100
	10 pm	100	100	100	100	100
	5 am	34.7	100	100	100	100

Figure 3-5 The percentage of the area cooled down by more than 1.5 K, green: a>50% of the whole area, red: <10% of the whole area.

3.3.3 Effect of Patch Density and Edge Density (PD & ED) of Green Area on Cooling Effect

Configurations 1-3 were configurations with different Patch Density (PD) and Edge Density (ED). As the number of patches raised from 1 to 16, the PD increased from 1/ha to 16/ha, and the ED increased from 200 m/ha to 800 m/ha (Table 3-4). In order to concisely illustrate the influence of PD & ED on the cooling effect, the mean cooling effect and maximum cooling effect of Tree-big canopy, Tree-small canopy and 50 cm Grass scenarios, which were the most representative vegetation types, were compared (Figure 3-6).

Table 3-4 Patch Density and Edge Density (PD & ED) of Configurations 1-3.

	Configuration 1	Configuration 2	Configuration 3
Patch Density (PD)			
(number/ha)	1	4	16
Edge Density (ED)			
(m/ha)	200	400	800

In terms of the mean cooling effect, when the vegetation type is Tree-big canopy, there is a clear increase in cooling effect as PD & ED increase. At 2 pm, the cooling of configuration 1 is significant lower (1.96 K) than configuration 3, for trees with big canopy. However, when the vegetation type changes, the trend starts to turn. When the vegetation type is changed to Tree-small canopy, the stronger cooling effect of Configuration 3 is no longer obvious. The difference between Configurations 1 and 3 is only 0.13 K at 2 pm. This slight difference is barely noticeable at 10 pm and 5 am. When the vegetation type is Grass 50 cm, a reverse trend can be observed: the cooling effect decreases as PD & ED increases. The cooling effect of Configuration 1 at 2 pm is 0.04 K higher than Configuration 3. These reversed differences expand to 0.1 K at 10 pm and 0.9 K at 5 am.

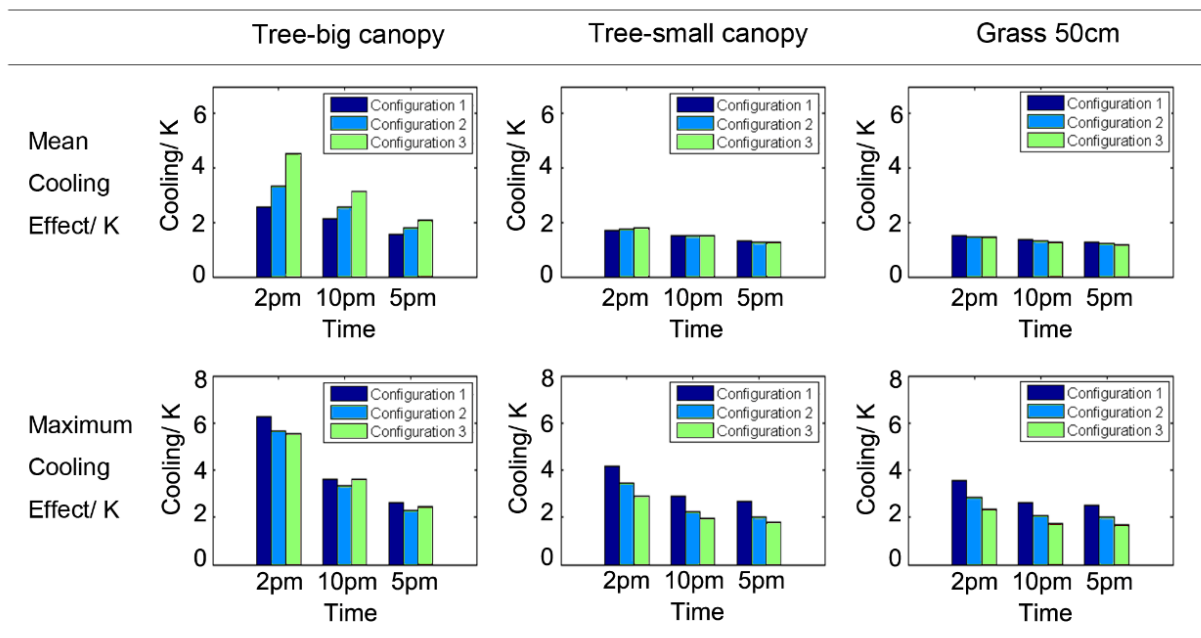


Figure 3-6 Mean cooling effect and Max cooling effect of Configurations 1-3.

The previous study (Forman, 1995) indicated that an increase in the PD & ED of a green space enhanced shade, and the interactions between the green space and its surrounding area. Therefore, more scattered green spaces led to greater cooling effects. The results of this study indicate that this conclusion is only valid when the vegetation type contains trees with big canopies. When the vegetation type includes trees with small canopies, or even hedges and grass, this trend tends to reverse.

It can be estimated that when the cooling ability and shade of a single green patch is large enough, more scattered green spaces perform better in terms of mean cooling effects. This is because the scattered green spaces provide more shade, and interact more with the surrounding

impervious area. The opposite effect emerges when the cooling ability and shade of a single patch is too small, the more scattered green spaces have worse mean cooling effect, due to the reduction of the area of a single patch.

In terms of the maximum cooling effect (the difference between the coolest point in the scenario and the control asphalt scenario), green spaces with lower PD & ED perform better in most cases. The maximum cooling effect of Configuration 1 is always higher than that of Configuration 3. This is to say, when total area is constant, green spaces with a more centralised configuration have lower central air temperature (Figure 3-7).

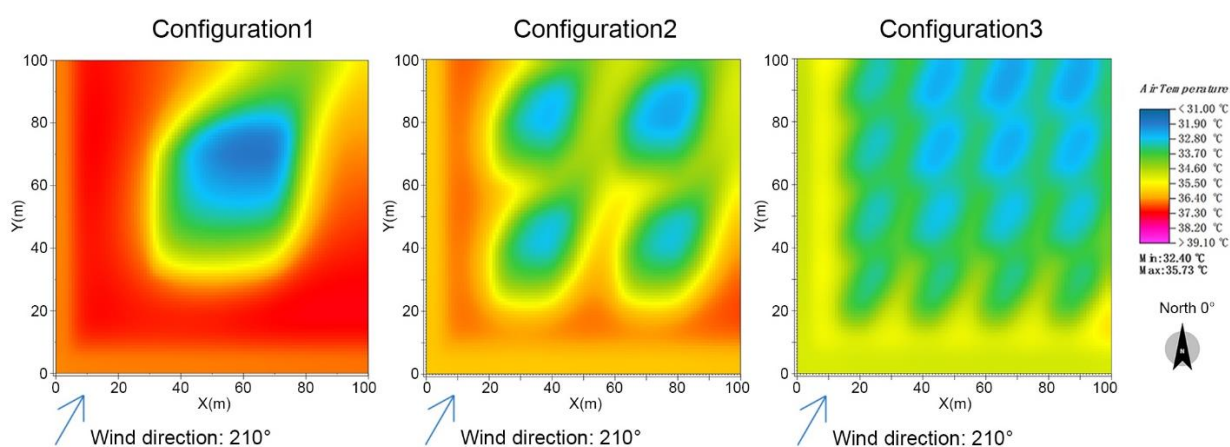


Figure 3-7 Simulated air temperature of Configuration 1-3 at 2 pm (vegetation type: tree-big canopy).

3.3.4 Effect of Land Shape Index (LSI) of Green Areas on Cooling Effect

In the comparison of configurations with vegetation types “Trees-big canopy”, “Trees-small canopy” and “Grass 50 cm” (Figure 3-8), Configurations 4 and 5 always show clear advantages in terms of mean cooling effect. The green areas in Configurations 4 and 5 both indicated the belt shape. This greater cooling effect can come from the stretched green space shape and the higher Land Shape Index (LSI).

Studies in ecology have claimed that green patches with higher LSI led to greater ecological benefits, because of better interactions with the surrounding area (Vos et al., 2008). In a similar way, in this study, green spaces with more complex shapes can provide a greater cooling effect.

To analyse the influence of LSI, Configurations 2 and 4 were compared. As shown in Table 3-5, despite having the same patch density and total area, the LSI of Configuration 4 is much higher than that of Configuration 2. This phenomenon is caused by the more stretched

shape of Configuration 4. According to the simulation data (Figure 3-9), Configuration 4 always performs better in terms of mean cooling effect. This advantage is clearer when the vegetation type is Trees-big canopy. Therefore, it can be concluded that when the area and patch density are constant, belt patterns with higher LSI perform better than those with dotted patterns, in terms of cooling effects. This result agrees with previous studies (Cao et al., 2010; Liu and Weng, 2008). When the total area and vegetation type are fixed, the longer the perimeter a single patch has, the more shade is provided, and the greater the interactions with the surrounding areas. In another words, high LSI increases the cooling efficiency of an integrated patch (Zhou et al., 2011).

Table 3-5 Patch Density and Land Shape Index (LSI) of Configuration 2 and Configuration 4.

	Configuration 2	Configuration 4
Patch Density (number/ha)	4	4
Land Shape Index	0.16	0.4

In the comparison shown in Figure 3-8, the mean cooling effect of Configuration 4 is always higher than that of Configuration 5. The only difference between these two configurations is the direction of tree belts, which directly affects the ventilation conditions. The wind direction was blowing from South-West (210°). Configuration 4, with North-South (180°) tree belts, is closer to parallel with the wind direction than Configuration 5 with West-East (90°) tree belts.

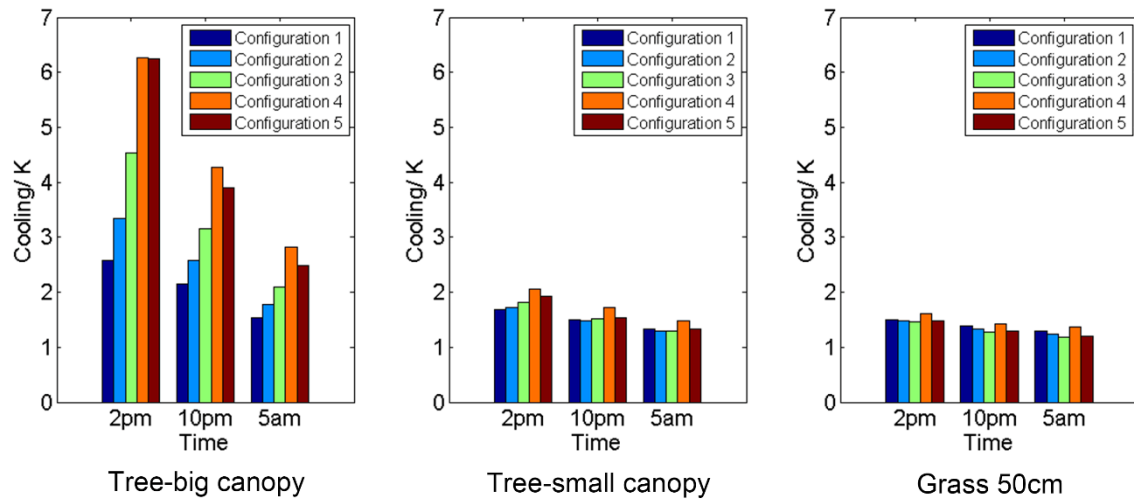


Figure 3-8 Mean cooling effect of three selected vegetation types.

According to former research, vegetation with big canopies can substantially affect ventilation (Wania et al., 2012). As shown in the simulated wind field, the ventilation conditions of Configuration 4 are better than those of Configuration 5, out of the direction of tree belts (Figure 3-10). The maximum wind speed in Configuration 4 is 2.45 m/s and the maximum wind speed in Configuration 5 is 2.2 m/s. The mean wind speed in the canyon of Configuration 4 is 1.65 m/s, and the mean wind speed in the canyon of Configuration 5 is 1.33 m/s. Tree belts which are close to parallel to the wind direction tend to form straight-forward air channels. On the contrary, tree belts which are closer to perpendicular to the wind direction are more likely to block the airflow.

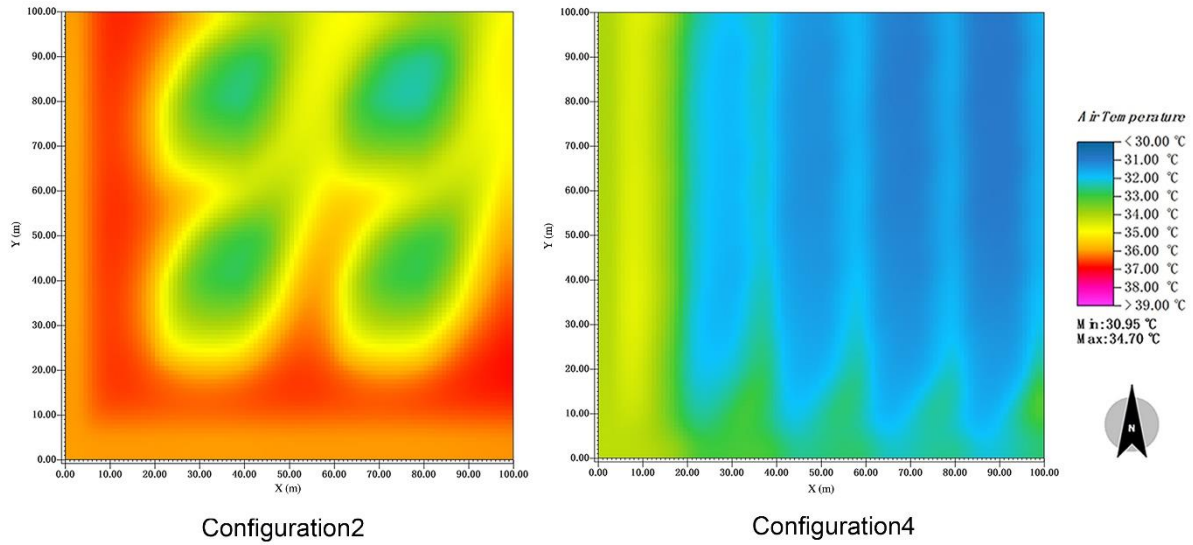


Figure 3-9 Simulated air temperature of Configurations 2 and 4 at 2 pm (vegetation type: tree-big canopy).

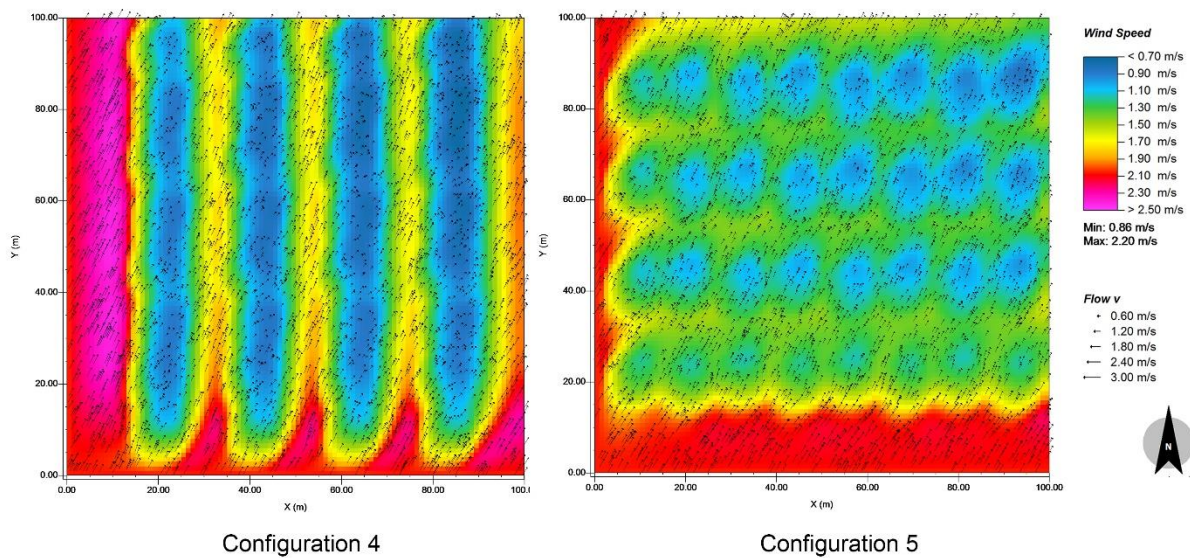


Figure 3-10 Wind speed and direction in Configurations 4 and 5. The colour indicates the wind speed in m/s and the wind direction is shown by arrows.

As ventilation is critical to heat dissipation, configurations with less ventilation store more heat internally. In addition, as shown in Table 3-6, higher winds in the green belt in Configuration 4 carry heat (sensible heat) and moisture (latent heat) away from the surface and increase these heat fluxes. It results in the lower mean air temperature in Configuration 4.

Table 3-6 Comparison of configuration 4 and 5 in terms of turbulent fluxes.

Variable (W/m^2) Conf.	Sensible heat	Latent heat
	Configuration 4	187.81
Configuration 5	162.80	97.44

3.3.5 Effect of Vegetation Type on Cooling Effect

There were five common vegetation types in the simulated scenarios. The mean cooling effect of different vegetation types in each scenario were compared at 2 pm, 10 pm and 5 am. The results show that “Tree-big canopy” vegetation generates the largest cooling effect, followed in descending order by Tree-small canopy, Hedges-shrubs, Grass 50 cm and Grass 10 cm (Figure 3-11).

It is notable that the difference in mean cooling effect between Tree-big canopy and the other vegetation types is particularly large. In comparison, the difference between the other four vegetation types is not obvious enough. In particular, at 2 pm in Configuration 4, the mean cooling effect of Tree-big canopy is three times larger than the other vegetation types. This result indicates that when it comes to the influence of vegetation type on cooling effect, canopy is the most effective factor, directly blocking incoming short-wave radiation, thereby reducing the absorbed energy.

On the other hand, when there is no significant difference in canopy, as the total leaf area increases, the cooling effects of vegetation increase. Quite an amount of research has observed this positive correlation between cooling effect and leaf area index (LAI). Because the increased LAI of vegetation lead to increased shade and evapotranspiration (Hardin and Jensen, 2007; Li et al., 2016; Shashua-Bar and Hoffman, 2000). At 10 pm and 5 am (Figure 3-12 and Figure 3-13), the cooling ranking of different configurations is the same as at 2 pm. Due to the lack of shade and transpiration, the differences between different configurations decrease.

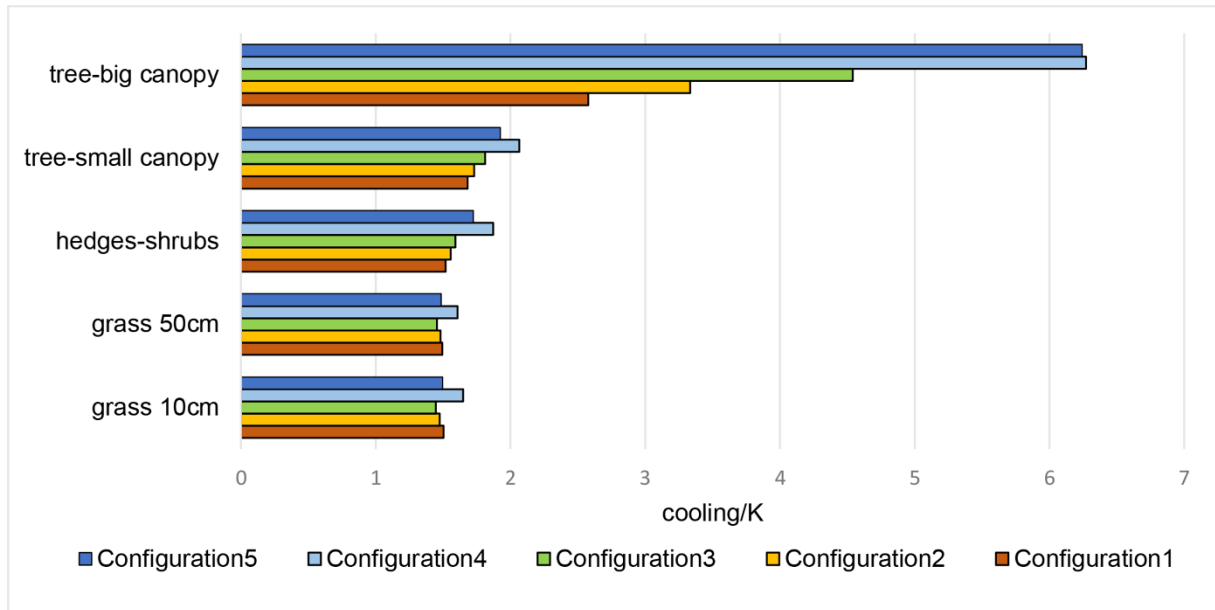


Figure 3-11 Mean cooling effect of different vegetation types at 2 pm.

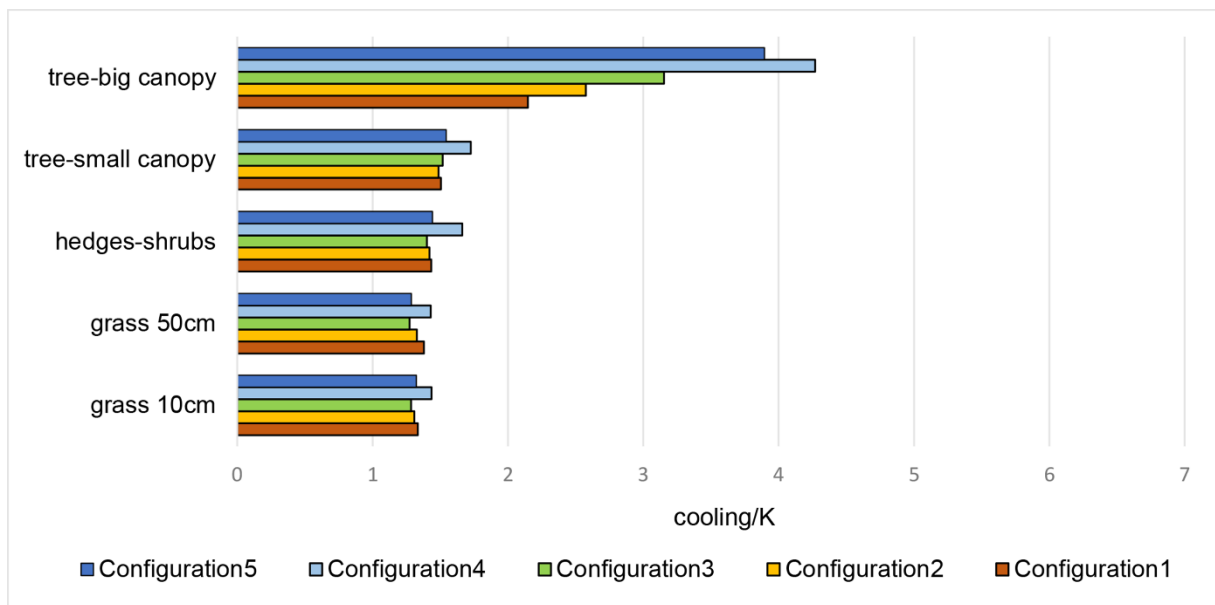


Figure 3-12 Mean cooling effect of different vegetation types at 10 pm.

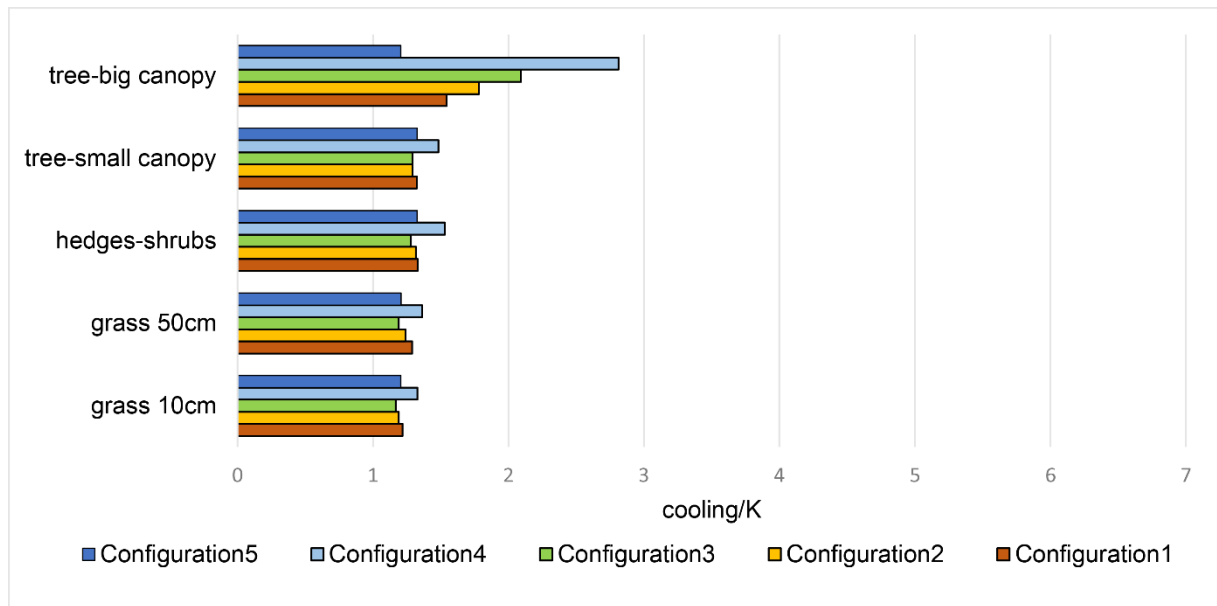


Figure 3-13 Mean cooling effect of different vegetation types at 5 pm.

3.3.6 Human Thermal Comfort of Green Areas

The mean PET values of each scenario at three representative times are shown in Figure 3-14. The PET values of 2 pm, 10 pm and 5 am are distributed in the range of 38.3–53 °C, 23–26.8 °C, and 23–26.8 °C. According to (Table 2-1), PET values from 13 °C to 29 °C are classed as pleasant, 35 °C to 41 °C as strong heat stress, and greater than 41 °C as extreme heat stress. The variation of PET values at 10 pm and 5 am are very small; the values are between 20.7 °C and 26.8 °C, which are all pleasant. At 2 pm, the PET values are very high (average value is 50.6 °C); all of them are in the heat stress range. The lowest PET values appear in tree-big canopies scenarios, particularly at 2 pm. Tree-big canopy scenarios clearly show cooler PET values. Figure 3-15 shows that vegetation type tree-big canopy can improve PET by more than 15 K, confirming the importance of using shade trees in urban green areas.

The PET differences (D-value) of 25 scenarios, compared with a surface covered by asphalt, were calculated (Figure 3-16). The PET differences at 5 am and 10 pm are very small, in every scenario at any time, except for the scenarios with trees-big canopies at 2 pm. At that time, the D-value is much higher than other times. These results also highlight the importance of shade in improving thermal comfort.

As shown in the Figure 3-15, the difference value of PET in trees-big canopy scenarios is clearer at 2 pm than at any other time. The PET difference between trees-big canopy scenarios and an asphalt surface varies between 5.3 K and 15.9 K at 2 pm. At other time, the difference range is lower than that at 2 pm (ranging from 2.1–4.9 K), but still higher than in other

scenarios. The trend of PET difference in every scenario with tree-big canopy, shows the rising tendency at 2 pm. The range is from 5.4 K (Configuration 1 with tree-big canopy) to 15.9 K (Configuration 5 with tree small canopy) (Figure 3-16). The highest PET difference is shown in Configuration 5, although the highest temperature difference is seen in Configuration 4 (Figure 3-8, left) at 2 pm. At other times, PET differences show a similar result as for temperature (Figure 3-16; Figure 3-8, left).

This is due to the jointly effect of shade and ventilation. The prevailing wind in every scenario blows from the South-West (210°) direction, providing better ventilation in Configuration 4. As good ventilation helps to reduce heat, in every trees-big canopy scenario, almost at every time, the Configuration 4 scenario is the best in terms of both PET and temperature. At 2 pm, although the cooling effect of Configuration 4 is higher than Configuration 5 (Figure 3-11 to Figure 3-13), the PET of Configuration 5 is higher than Configuration 4 (Figure 3-16). This is due to another influence factor—shade. The sun is in the South at 2 pm. Configuration 4 has a smaller amount of shade than Configuration 5, fixing the disparity induced by wind direction. At 2 pm, Configuration 5 has 196 m², about 2 % more shade than Configuration 4. The shade reduces the incoming short-wave radiation and the mean radiant temperature. Mean radiant temperature shows a direct relationship with thermal comfort (Höppe, 1999; Thorsson et al., 2011).

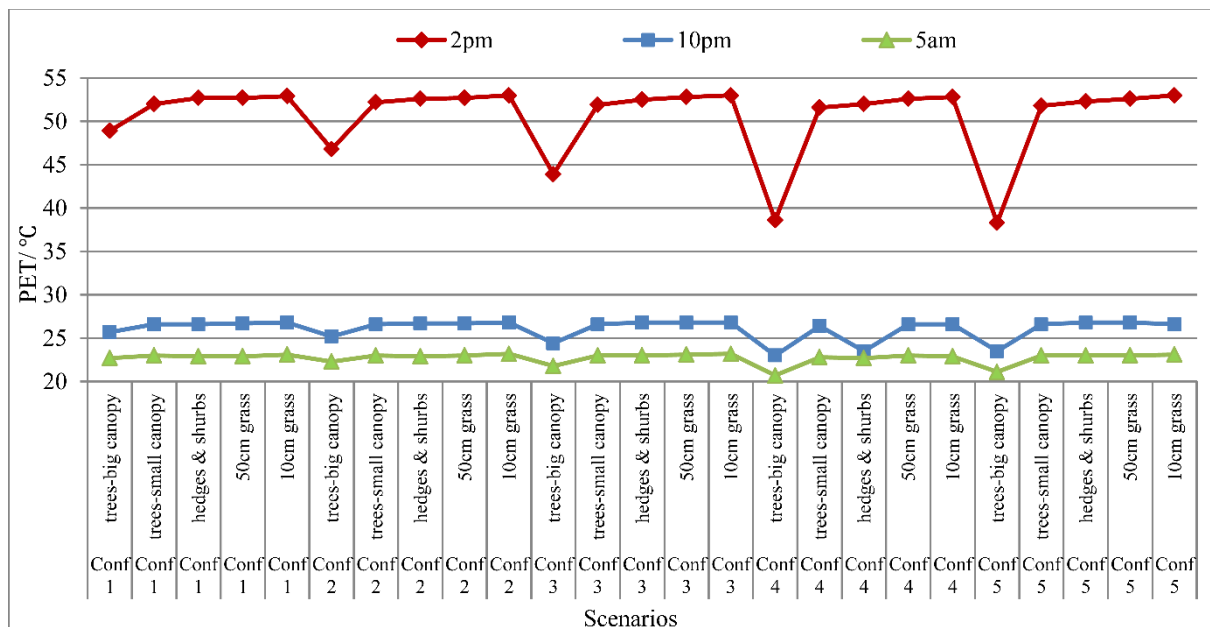


Figure 3-14 The mean PET values of 25 scenarios at 2 pm, 10 pm and 5 am.

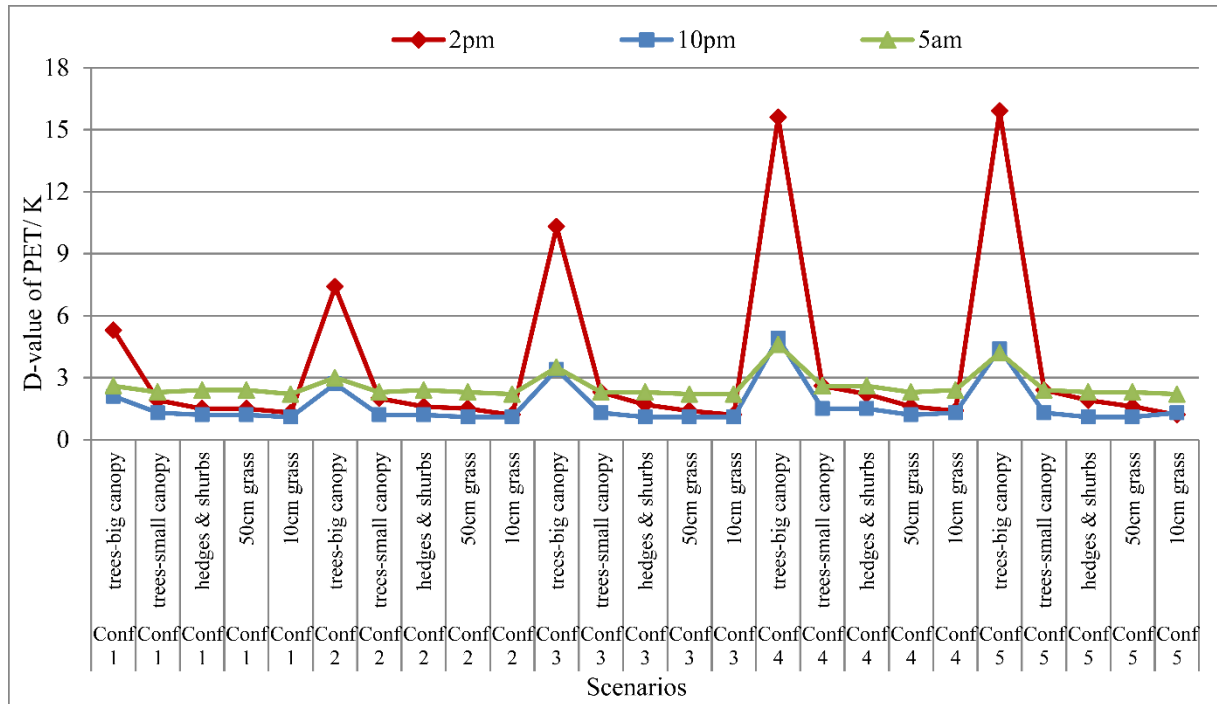


Figure 3-15 Difference value of PET of different scenarios compared to asphalt at 2 pm, 10 pm, and 5 am.

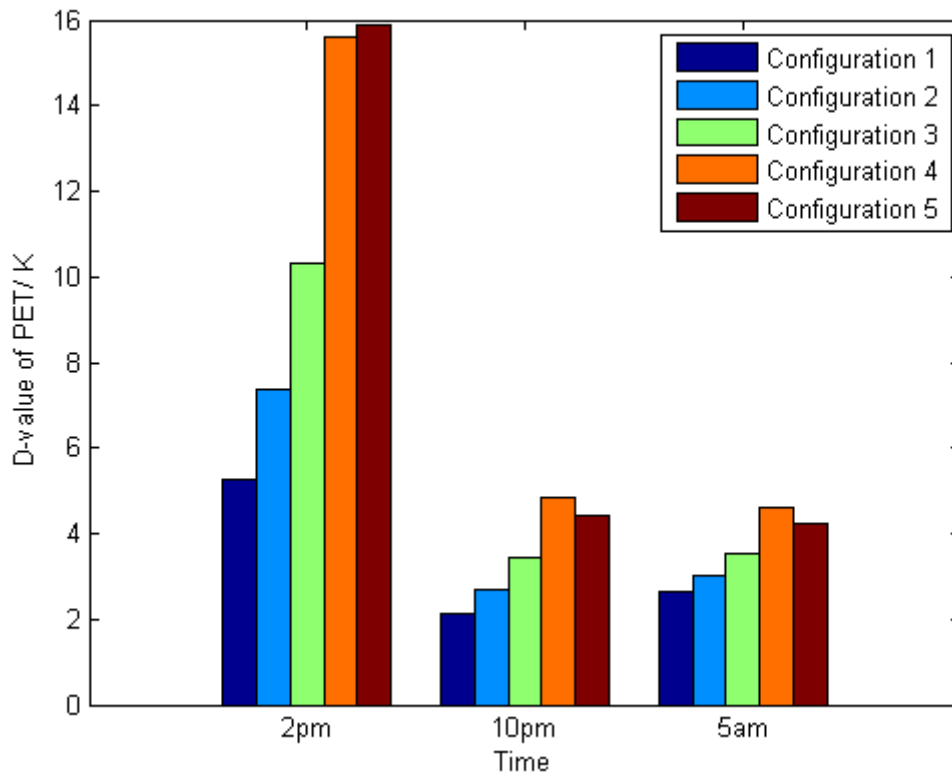


Figure 3-16 Difference value of PET by trees-big canopy.

3.4 Conclusions and Application

This study investigated the influence of spatial configurations of green areas on the microclimate and thermal comfort. The major conclusions are summarized as follows:

Green areas can generate cooling effects and improve the thermal comfort, especially at the daytime of hot summer days. The shade of vegetation is the dominant factor of the cooling effect. In addition, the ventilation and leaf area index of green areas also influence the cooling effect obviously. By affecting the shade, ventilation and leaf area index, the spatial configuration influences the cooling effect of green areas on microclimate and human thermal comfort.

The belt-shaped green areas with the orientation parallel to the direction of the wind produce the strongest cooling effect. The trees with big canopies have the best cooling effect. The combination of trees with big canopy and belt-shaped green areas along wind direction can achieve the largest improvement of the microclimate and thermal comfort.

The influence of fragmentation of green areas depends on the vegetation type. When the vegetation type is Tree-big canopy, the cooling capacity of each green patch is large enough. At this time, the mean cooling effect grows as the fragmentation of green areas increases, because more shade and interactions can be generated. When the vegetation type is Shrubs and Grass, the cooling capacity of a single patch is not large enough. In this case, the mean cooling effect decreases as the fragmentation of green areas increases, due to the reduction of the area of a single patch.

In terms of the maximum cooling effect, green spaces with lower fragmentation performs better in most cases. Because green spaces with more integrated layout can achieve lower central air temperature.

The belt-shaped green area with higher shape complexity forms lower mean air temperature, compared with the dotted green area with lower shape complexity. Because the green areas with more complex shape provided more interactions with the surrounding city area.

The results of this study can be summarized in the following decision tree. The data used for this decision making is the cooling effects at 2:00 pm. This decision tree provides the importance (weights) of each decision parameter and scores the different variables for each decision parameter (Figure 3-17).

The weights of the parameters are calculated as follows:

- 1) calculating the mean of cooling effects for all levels of each parameter.
- 2) expressing the dispersion of the mean cooling effects of each parameter using variance.
- 3) normalizing all the variances values representing the dispersions. The weights of different parameters can be then obtained.

The scoring of the different variables in each parameter is calculated as follows:

The ratio of the mean of the cooling effects of each variable in one parameter to the sum of the means of all the variables of that parameter is calculated. This ratio is used to characterize the cooling intensity score of that variable in the parameter.

This decision tree can be used in two ways: firstly, to give the best combination. That is, choosing variables with the highest scores from each of the parameters for decision-making. For example, in this study, the best combination is Tree big canopy + stretched land shape + scattered layout + green-belt parallel to wind. Secondly, to compare candidate schemes. The final decision can be easily achieved by comparing the total scores of the candidates.

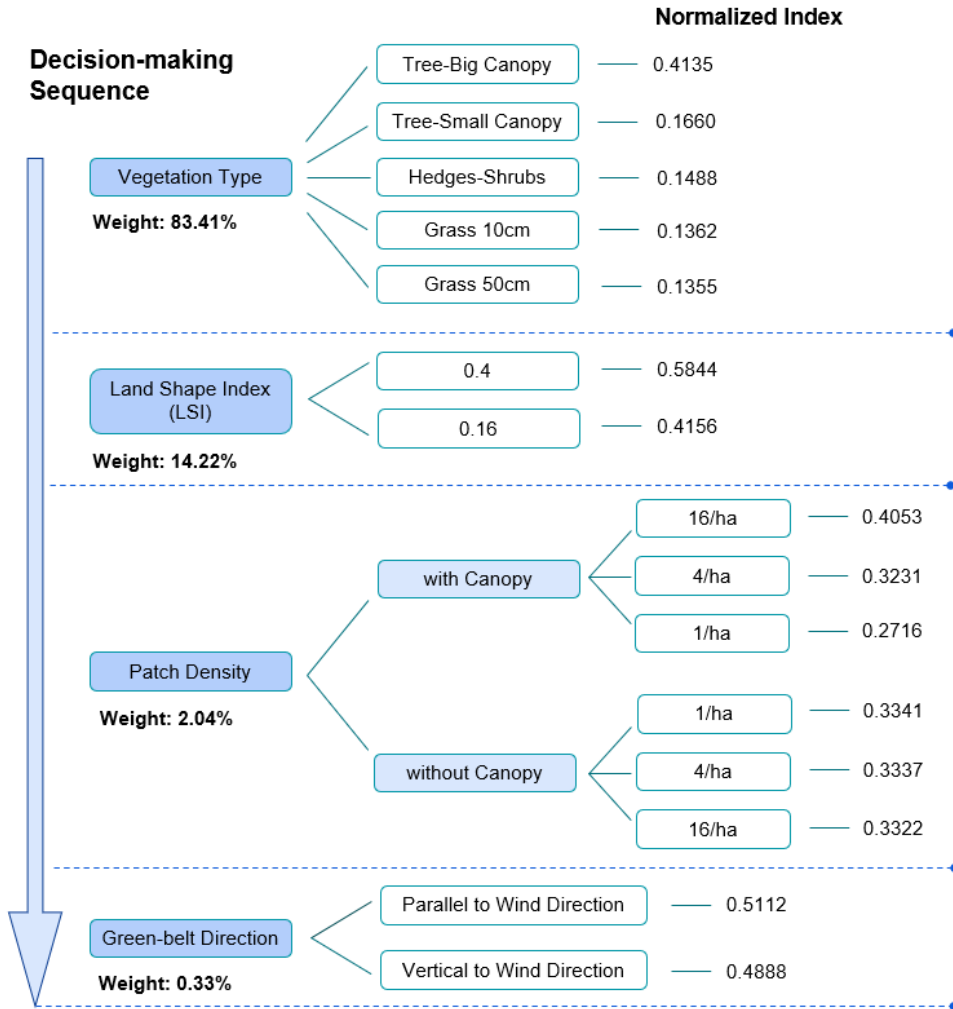


Figure 3-17 Decision tree derived from the research results.

Chapter 4: How Do Walkways in Historic Gardens Affect the Thermal Comfort of Pedestrians? An Example from Berlin's Tiergarten

Abstract²

Along with the global climate change and the accelerating Urban Heat Island (UHI) effect, people living in mega-cities are facing growing heat pressures. As a consequence, the outdoor activities of citizens are increasingly conducted in the green spaces that can mitigate the local heat pressures and form the comfort microclimate. The cooling effects of green spaces on the people are influenced by many properties of green spaces, including the Sky View Factor (SVF), the density and structure of the vegetation, and the width of the walkway in the green space, etc. In order to explore the optimal spatial configuration of the green space for the outdoor microclimate, this study investigates the Tiergarten, which is the central historical park of Berlin, Germany, containing multiple types of green areas, and enabling diverse outdoor activities for the citizens of Berlin. The study consists of two parts: the in-situ measurement and the numerical simulation. In the phase of the measurement, the meteorological data was measured in nine types of green spaces in the Tiergarten, combining three widths of walkways (3m, 5m, 7m) and three vegetation types (Grass, Tree&Grass, Tree&Shrubs). In the part of the simulation, 15 idealized scenarios of green spaces containing different SVF, vegetation types,

² This study described in this chapter has been published as:

Zhang, H., Chi, X., Müller, F., Langer, I., & Sodoudi, S. (2019). Wie wirkt sich der Tiergarten Berlin auf das Wohlbefinden der Menschen aus? Eine Studie über den Kühlungseffekt von Grünflächen und den thermischen Komfort der Fußgänger. In Reinhard F. Hüttl/Karen David/Bernd Uwe Schneider (Hrsg.): *Historische Gärten und Klimawandel: eine Aufgabe für Gartendenkmalpflege, Wissenschaft und Gesellschaft*. –ISBN: 978-3-11-060748-2.–Berlin/Boston: De Gruyter Akademie Forschung, 2019 (Forschungsberichte/Interdisziplinäre Arbeitsgruppen der Berlin-Brandenburgischen Akademie der Wissenschaften; 42) (pp. 167-179). De Gruyter Akademie Forschung. Available at <https://doi.org/10.1515/9783110607772-015>.

This publication was in German. The published article did not present all results due to length constraints. In this chapter, we present more detailed results than were available in the published version.

and widths of walkways were simulated using the micro-climatic model ENVI-met. In addition, the Physiological Equivalent Temperature (PET) was calculated using RayMan model to evaluate the cooling effect of each type of green spaces. The results show that the human thermal comfort in the green space is jointly affected by the SVF and the open degree of the space. The SVF is determined by the canopy density, and the open degree is determined by the width of a walkway and the vegetation type. The green space combining the low SVF and the high open degree is optimal for the human thermal comfort against the heat pressure. The conclusion of this study can give advice to the citizens in selecting the superior green space for outdoor activities, as well as provide suggestions for the climate-adaptive landscape design of green spaces in the future.

4.1 Introduction

Tiergarten is the central park and one of the largest parks in the city of Berlin. As a historical park in Berlin, the beginning of Tiergarten can be traced back to the 16th century. Nowadays, with its dense forest, Tiergarten has become an important natural recreation area for the residents of downtown Berlin. The main open spaces in Tiergarten are the walkways, where the citizens engage in various outdoor activities, including strolling, jogging, and bicycling. It is interesting for the pedestrians to know which walkways in the Tiergarten are cooler for exercising on hot summer days. Under the heat stress, how can people choose the thermally comfortable walkways in Tiergarten for outdoor activities? In addition, it will also be useful for landscape architects to know why some walkways are cooler than others, and what inspiration it can bring to the future climate-adaptive walkway design.

To answer these questions, this study attempted to explore that the walkways in which area in the park is more thermal-comfortable for pedestrians to execute the outdoor activities in the hot summer days. To achieve this goal, this study is going to explore the joint effects of three spatial features: width of walkways, vegetation density along walkways, and the Sky View Factor (SVF) above walkways, on human thermal comfort on the garden walkways.

This study was conducted in roughly four steps:

1. Classification of Walkway Spaces: Through field surveys, the walkways in the park were roughly classified into nine types according to the walkway width and the vegetation type along the walkway.

2. Field Measurement: For each type, one measuring point was selected for 24-hours field measurements. The results of the measurement were used to explore the general spatial-atmosphere relationships and evaluate the subsequent simulation.

3. Climatic Modeling: 15 idealized scenarios embracing the combination of three spatial features: walkway width, vegetation type along the walkway, and the Sky View Factor (SVF), were constructed and simulated for 24 hours by ENVI-met model.

4. Evaluation and Generalization: The simulation outcomes were evaluated by PET to derive the joint effects of the three spatial features on human thermal comfort. The results can be generalized to the whole park according to the spatial classification done in the first step. Then the map of human thermal comfort of the park can be drawn accordingly.

4.2 Methodology

4.2.1 Field Measurement

Tiergarten occupies ca. 520 acres of land, with 12.76 km long walkways. After a thorough investigation on all the walkways, it was found that the walkways can be classified by two features: the widths of walkways and the surrounding vegetation types. Therefore, nine measuring points were selected in Tiergarten, demonstrating three widths of walkways (3 m, 5 m, 7 m) and three surrounding vegetation types (Grass, Tree & Grass, Tree & Shrubs) (Figure 4-1).

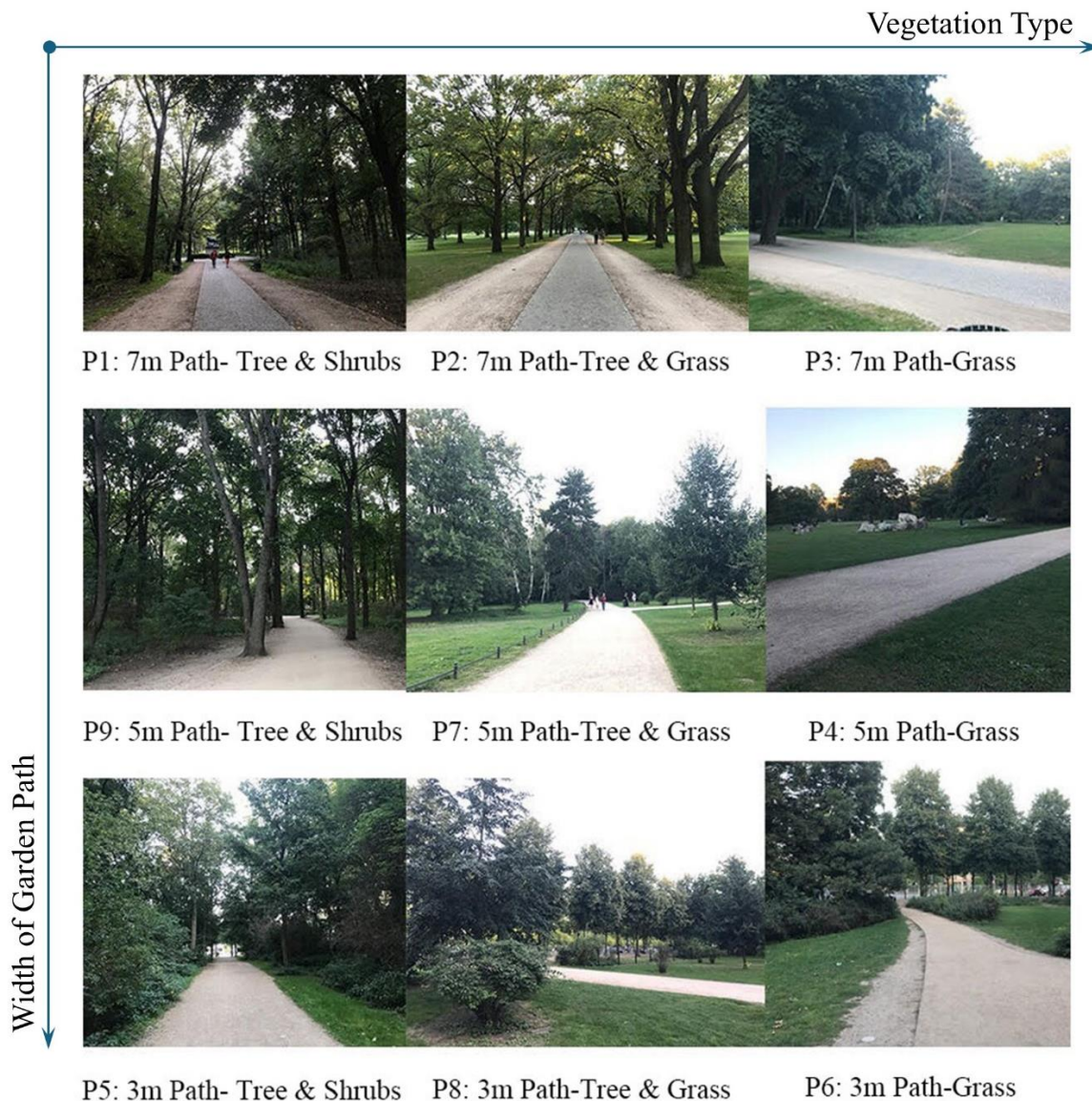


Figure 4-1 Actual views of nine measurement points containing two features: vegetation type and walkway width.

The mobile measurements were made in the middle of the walkway, representing the people walking on the walkway. The measuring site was set in the southeast corner of Tiergarten, because of the diversity of types of walkways in this area. The nine measuring points were selected along a circle route so that one round of moving measurement can be completed within 30 minutes (Figure 4-2). At hourly intervals, two members of the measuring team walked from point 1 to point 9 in sequence to measure the data at each point. One of them measured the data and the other recorded the data.

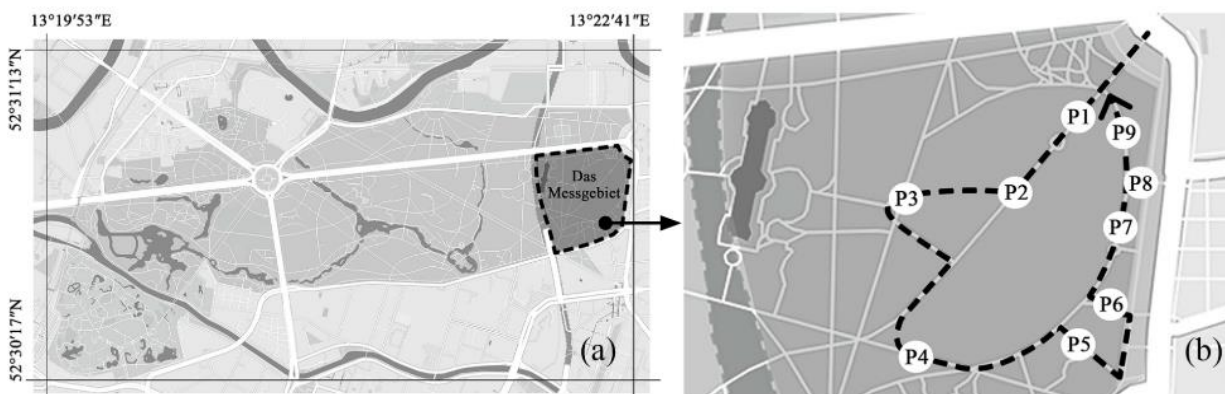


Figure 4-2 Location of the measuring area in Tiergarten (a) and the route of the moving measurement through points (b).

The measurement was conducted from Aug 30 to Aug 31, 2017 (Figure 4-3). During the measuring day, the highest air temperature exceeded 30 °C, representing that it was a typical summer day. The measurement period was from 9 am to 9 am (+1 day), lasting 24 hours with one hour measuring interval. The measured data included the air temperature (T_a), globe temperature (T_g), relative humidity (RH), wind speed (v), infrared surface temperature (IR) and the Sky View Factor (SVF) (Figure 4-4). All the measurements were taken at 1.1 m height, representing the middle of the human body.

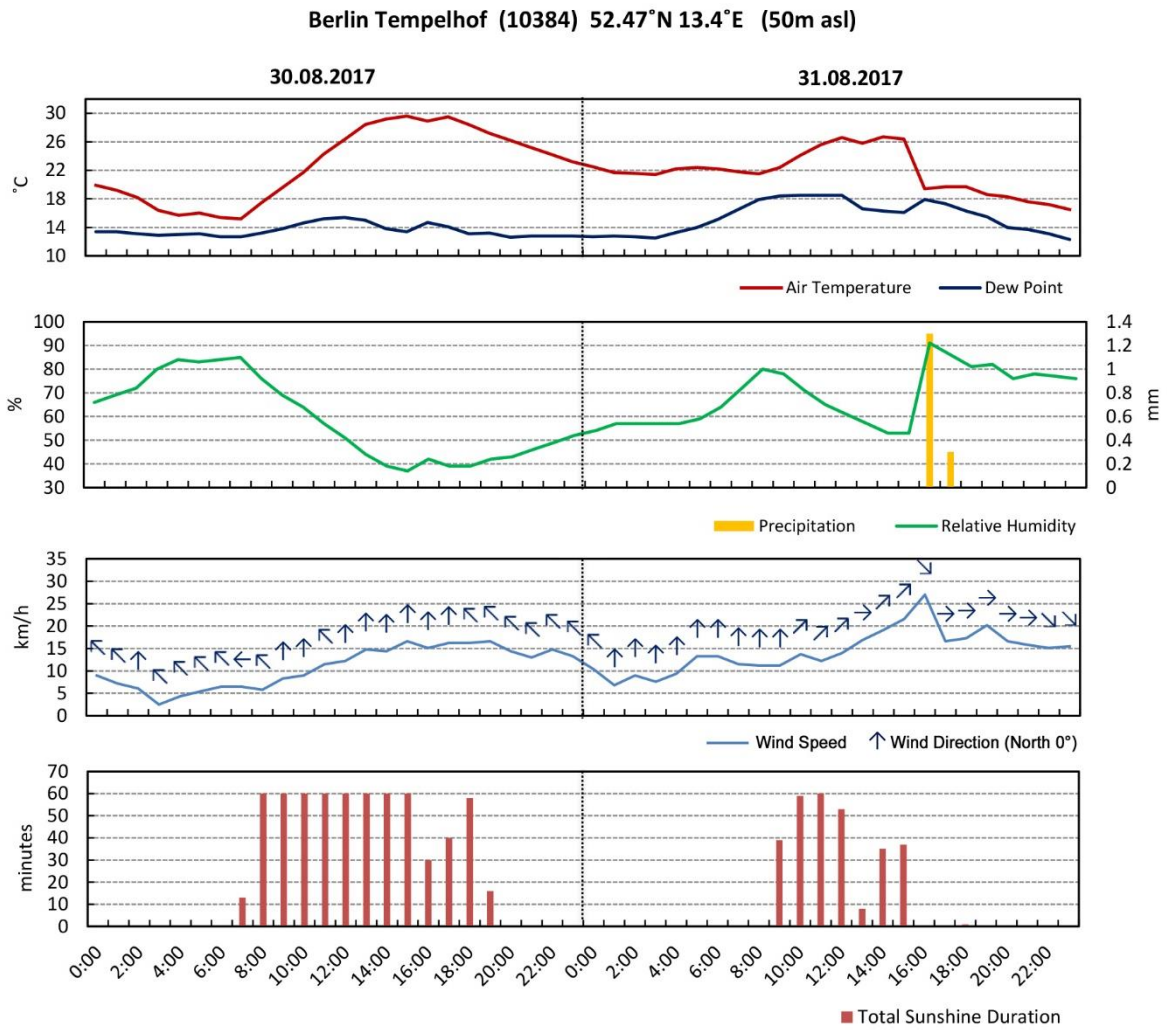


Figure 4-3 The daily time series of meteorological data (Meteogram) of the weather station located in Berlin Tempelhof (10384) from Aug 30 to Aug 31, 2017 (Data from Meteostat.net).

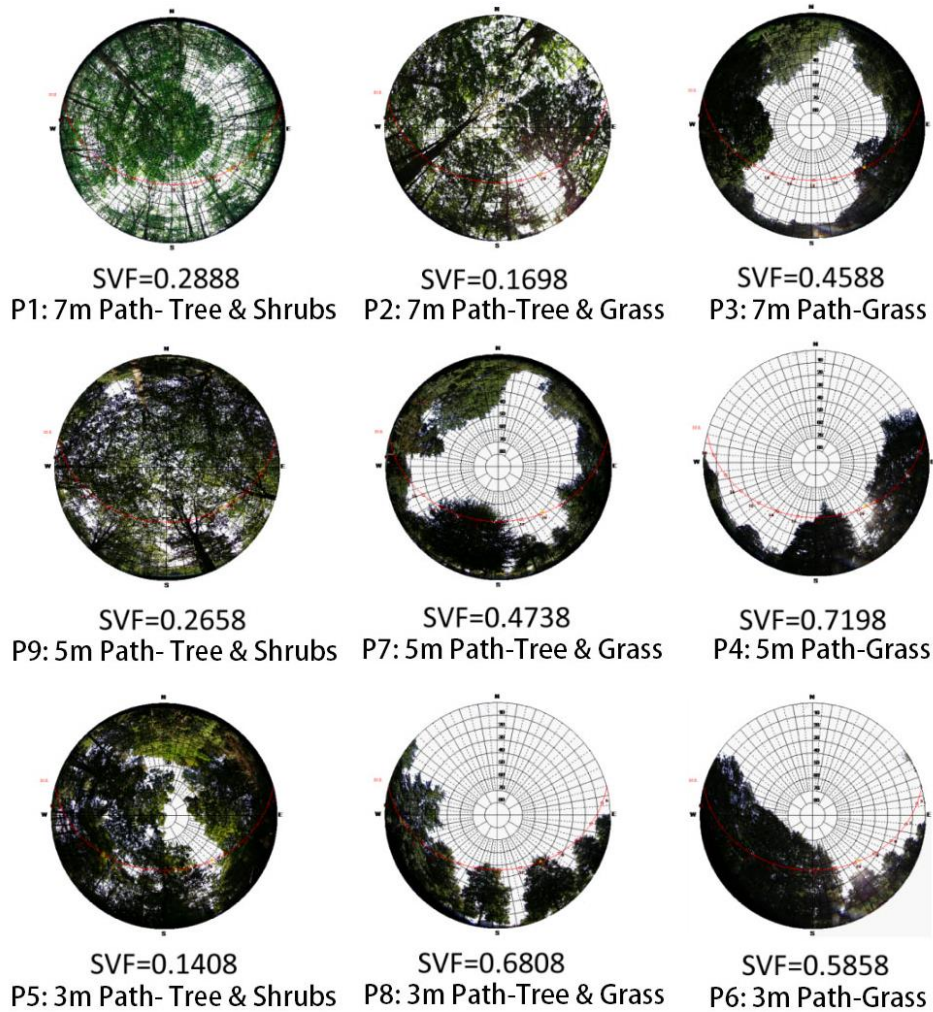


Figure 4-4 The fisheye photos of measuring points and the corresponding Sky View Factor (SVF) calculated by RayMan model.

4.2.2 Multivariate Modeling Experiments

According to the preliminary analysis of the measured data, a hypothesis was formulated. The human thermal comfort on the walkway is jointly influenced by three properties: the Sky View Factor (SVF) above the walkway, the width of the walkway, and the vegetation type. Therefore, a system of scenarios for the simulation is designed based on these three properties. As shown in Figure 4-5, the scenario system for the simulation contains three dimensions: three widths of walkways (3 m, 5 m, 7 m), three surrounding vegetation types (Grass, Tree & Grass, Tree & Shrubs), and two SVFs (low SVF with tree canopy on the walkway, high SVF without tree canopy on the walkway).

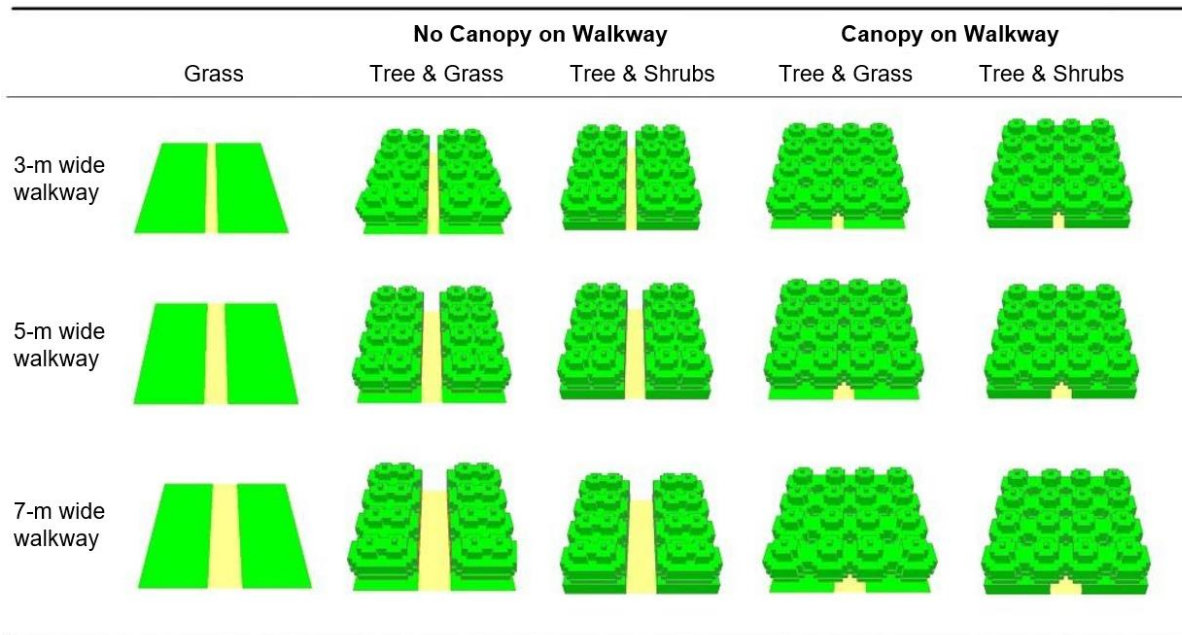


Figure 4-5 The design of scenarios for multi-variate simulation.

4.3 Results

4.3.1 Results of Field Measurement

4.3.1.1 Overall Measured Results

The D-values of the 1.1 m high air temperature (T_a) between the nine measuring points in Tiergarten (T_x) and the weather station in urban space (T_u) are presented in Figure 4-6. At daytime (2 pm), some of the measuring points in Tiergarten show higher T_a than the urban weather station. At night (10 pm), all the measuring points are cooler than the urban weather station. The T_a difference within the measuring points at daytime are larger than that at nighttime.

This phenomenon is closely related with the Sky View Factors (SVF) of the measuring points (Figure 4-4). At daytime, all the measuring points which are warmer than the urban weather station have the SVF higher than 0.4, while the SVF of the measuring points which are cooler than the urban weather station are all lower than 0.3. The high SVF leads to strong short-wave radiation at daytime, which will directly increase the quantity of heat. Furthermore, the walkways in Tiergarten are paved by sands, which have low specific heat capacity. The temperature of the sand surface increases faster than the other material under the same heat. Therefore, the measuring points in the middle of the walkways under the high SVF show higher temperature than the urban weather station.

At night, the T_a difference caused by the SVF vanished. The T_a of the measuring points are more like each other. The Figure 4-6-bottom shows the T_a difference between 2pm and 10pm, indicating the ability of the heat dissipation of each scenario. It can be found that the scenario with higher SVF also shows higher heat dissipation after sunset.

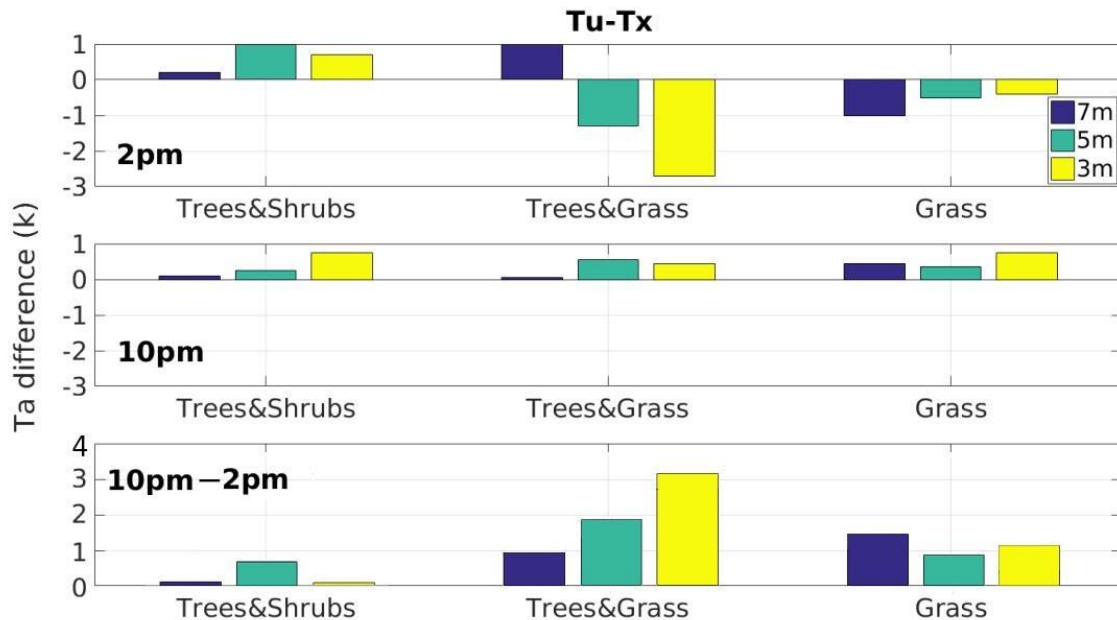


Figure 4-6 Air temperature (T_a) difference between urban weather station at Jagow Street (T_u) and measurement points (T_x) in 7 m, 5 m and 3 m width walkways with Trees&Shrubs, Trees&Grass and Grass at 2 pm and 10 pm on 30, August 2017. The chart at the bottom shows the difference between 10 pm and 2 pm at each measurement point.

4.3.1.2 Difference Among Vegetation Types

The Figure 4-7 demonstrate the comparison of measured data among three different vegetation types (Grass, Tree & Grass, Tree & Shrubs) along the 7 m wide walkway. The SVF of each compared measuring point is shown in Figure 4-7-c.

Through the diurnal variation of the T_a at 1.1 m height (Figure 4-7-a), it can be figured out that, at daytime, the T_a on the walkway surrounded by Grass is obviously higher than that surrounded by Tree & Grass and Tree & Shrubs, but this difference of T_a is no more obvious at nighttime. The difference of T_a among the vegetation types at daytime is in line with the difference of their SVF. As shown in Figure 4-7-c, the SVF of walkway surrounded by Grass is also much higher than the others, while the SVF of Tree & Grass and Tree & Shrubs are close to each other. These results agree with the regularity found in the overview of measured data (Figure 4-6), that the T_a difference at daytime is mainly caused by the different SVF,

because of the different intensity of short-wave radiation. Correspondingly, the T_a difference vanished at nighttime because of the disappearance of the short-wave radiation.

The Figure 4-7-b shows the diurnal variation of the wind velocity among different vegetation types. The wind velocity on the walkway surrounded by the Tree & Shrubs can be found lower than that surrounded by Grass and Tree & Grass. It reveals that the ventilation on the walkway can be blocked by the shrubs on the side, and by the canopy on the top. The high SVF can also increase the ventilation on the walkway. Furthermore, even with the dense canopy, the walkway surrounded by Tree & Grass still shows the same good ventilation with the walkway surrounded by the Grass. It demonstrates that the absence of shrubs can improve the ventilation condition.

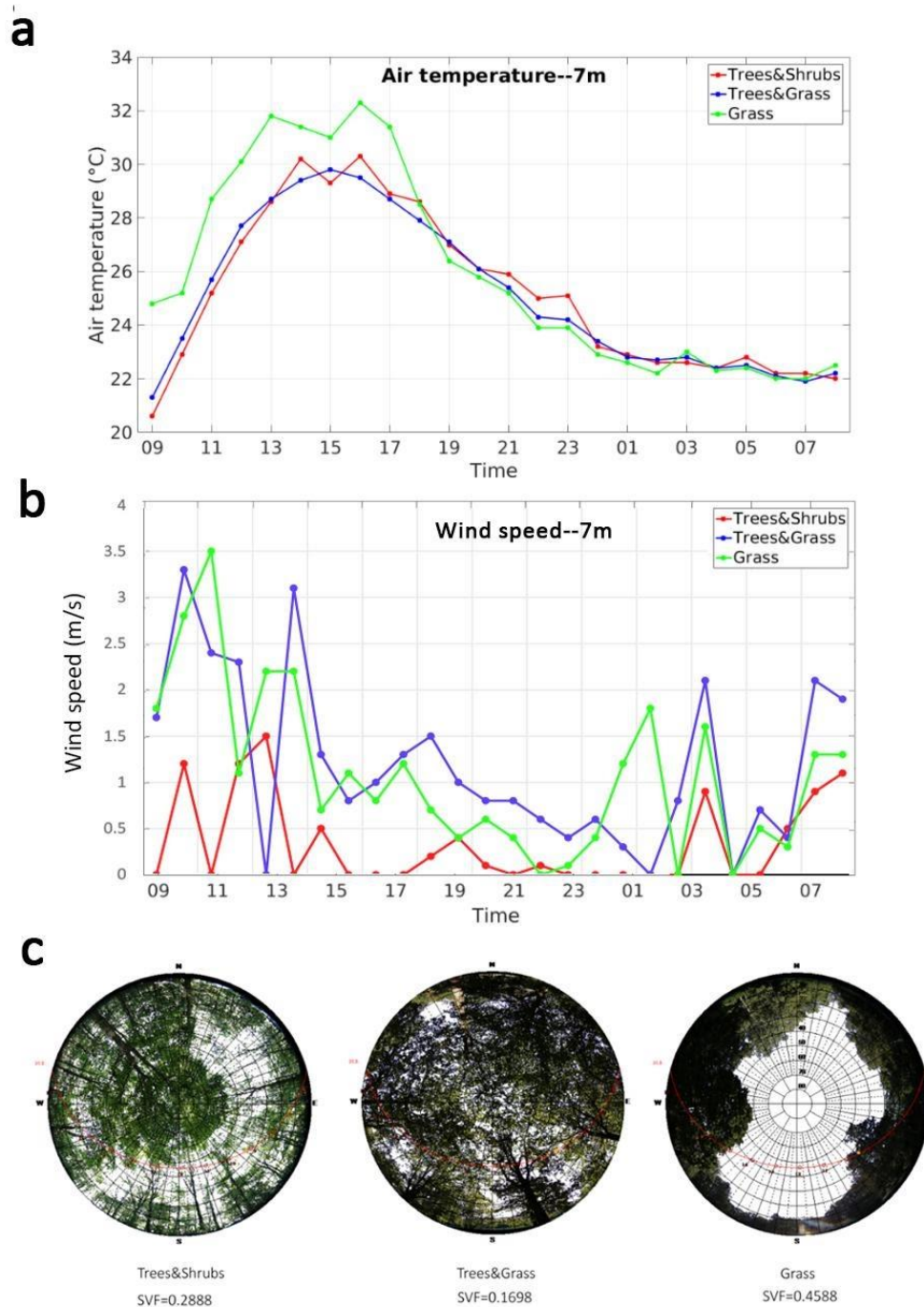


Figure 4-7 (a) Diurnal variation of the T_a on the 7m wide walkway surrounded by three vegetation types (Grass, Tree & Grass, Tree & Shrubs) from 9am in 30, August 2017 to 8am in 31, August 2017; (b) Diurnal variation of the wind velocities on the three measuring points, (c) SVF on the three measured points.

4.3.1.3 Difference Among Walkway Widths

The Figure 4-8 demonstrate the comparison of measured data among three different widths of walkways (3 m, 5 m, and 7 m) with the vegetation type of Tree & Shrubs. The sky

view factor of each compared measuring point is shown in Figure 4-8-c. When the SVF is similar with each other, the diurnal variation of each width of walkway T_a is also close to each other (Figure 4-8-a). It indicates that the influence of the width of walkway on the T_a is not as strong as the SVF. However, as shown in Figure 4-8-b, the wind velocity on the 7 m wide walkway is obviously higher than that on the 3 m and 5 m wide walkway, representing that the width of walkway has obvious influence on the ventilation. When the vegetation is Tree & Shrubs and the SVF is similar, the wider the walkway is, the higher the wind speed is on the walkway.

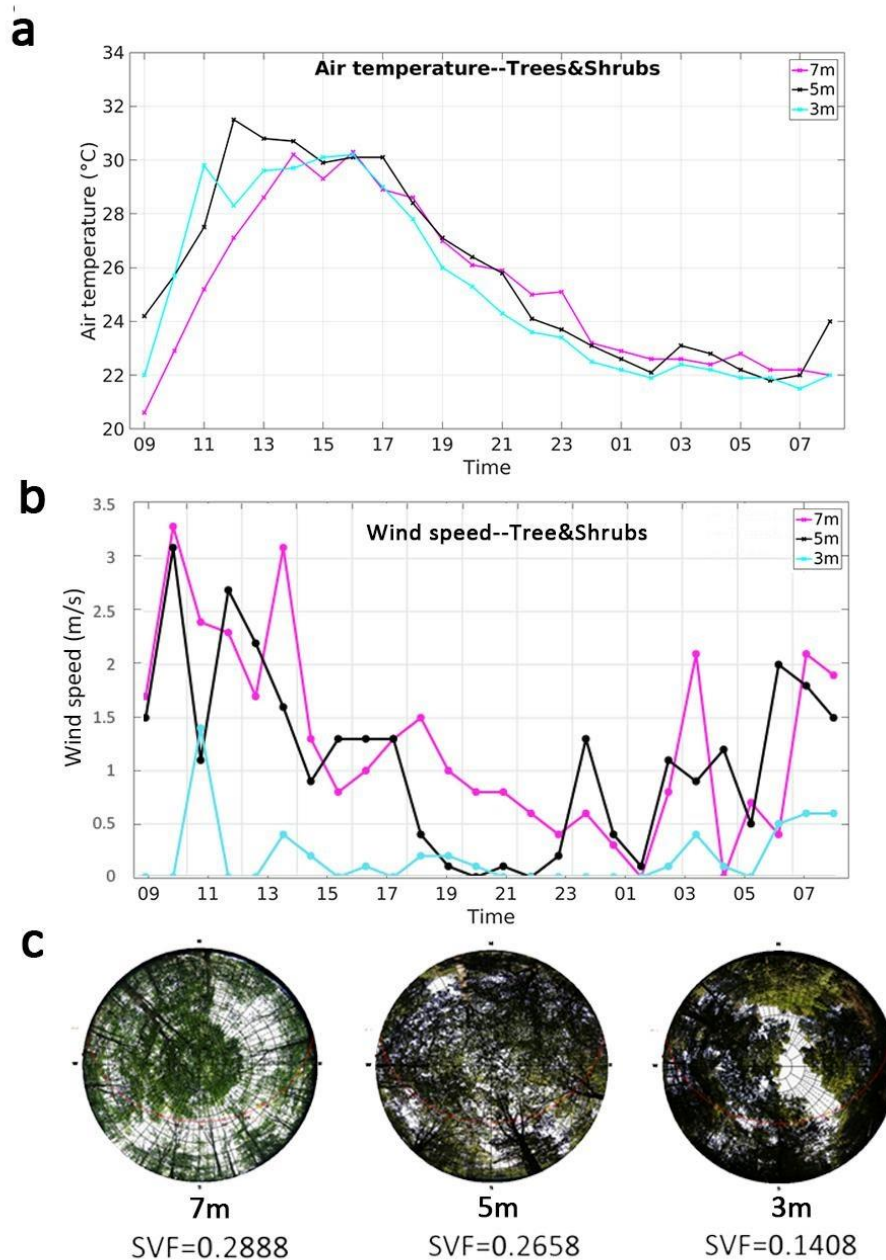


Figure 4-8 (a) Diurnal variation of the T_a on the 7 m, 5 m, 3 m wide walkway surrounded by Tree & Shrubs from 9am in 30, August 2017 to 8am in 31, August 2017;(b) Diurnal variation of the wind velocities on the three measuring points, (c) SVF on the three measured points.

4.3.2 Results of the Simulation

4.3.2.1 Evaluation of the Modelling

To evaluate the performance of the simulation, the simulated data was compared with the corresponding measured data. As shown in Figure 4-9, the diurnal variation of the T_a of the measuring points with the 7 m wide walkways and three different vegetation types were

compared with that of the simulated scenarios which have the same widths, vegetation and canopy condition. It can be seen that ENVI-met has an underestimation in terms of T_a during the daytime. In particular, the underestimation is greater at mid-day when solar radiation is strong and in scenarios that lack canopy cover. This bias has been mentioned in previous studies (Maggiotto et al., 2014). ENVI-met still relies on an internal database for its solar radiation data and does not allow the user to manually enter hourly solar radiation data. Therefore, when solar radiation fluctuates, the difference between simulated and measured values becomes larger. However, ENVI-met is still able to accurately represent the differences between scenarios and the diurnal trends.

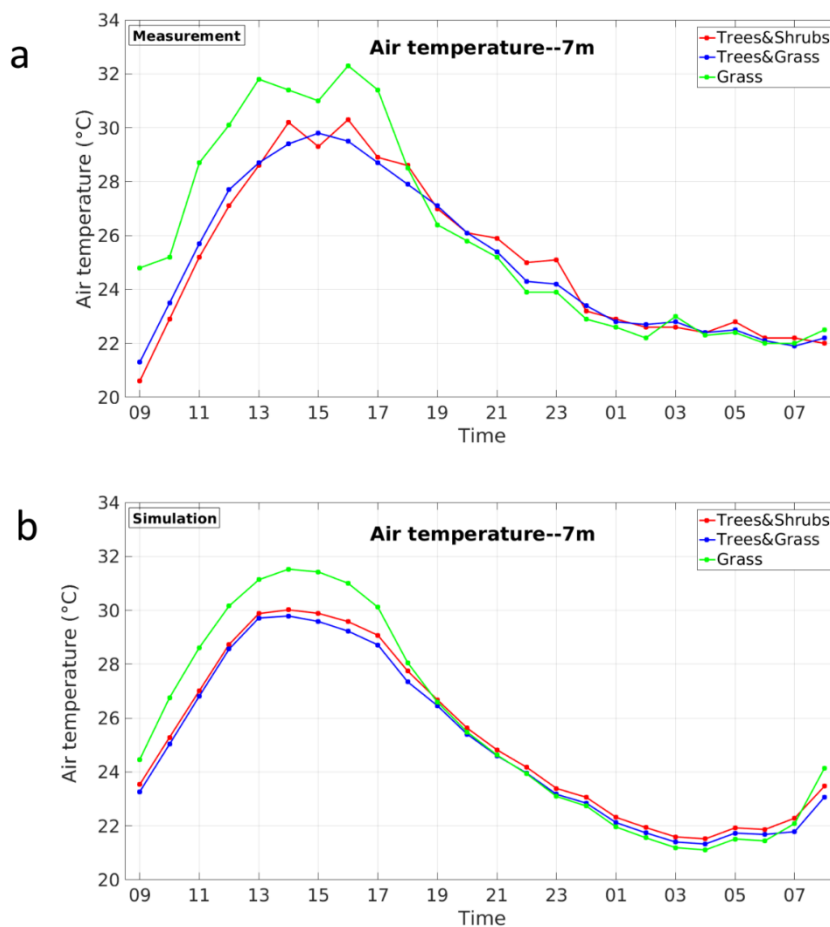


Figure 4-9 (a) The diurnal variation of measured T_a of the different vegetation types (Grass, Tree & Grass, Tree & Shrubs) on the 7 m wide walkway; (b) The diurnal variation of simulated T_a of the scenarios with different vegetation types (Grass, Tree & Grass, Tree & Shrubs).

As shown in Figure 4-10, the diurnal variation of the T_a of the measuring points with different widths of walkways under the same the vegetation type of Tree & Grass were compared with that of the simulated scenarios which have the same widths, vegetation and

canopy condition. In this case, ENVI-met overestimates the daytime air temperature more significantly for the 5 m wide walkway and the 3 m wide walkway. As can be seen in Figure 4-4, the SVF for the 7 m wide walkway is significantly smaller than that for the 5 m and the 3 m wide walkways, which means the 7 m wide walkway is less affected by solar radiation. Therefore, this underestimation is still a result of ENVI-met's reliance on an internal database for solar radiation value input.

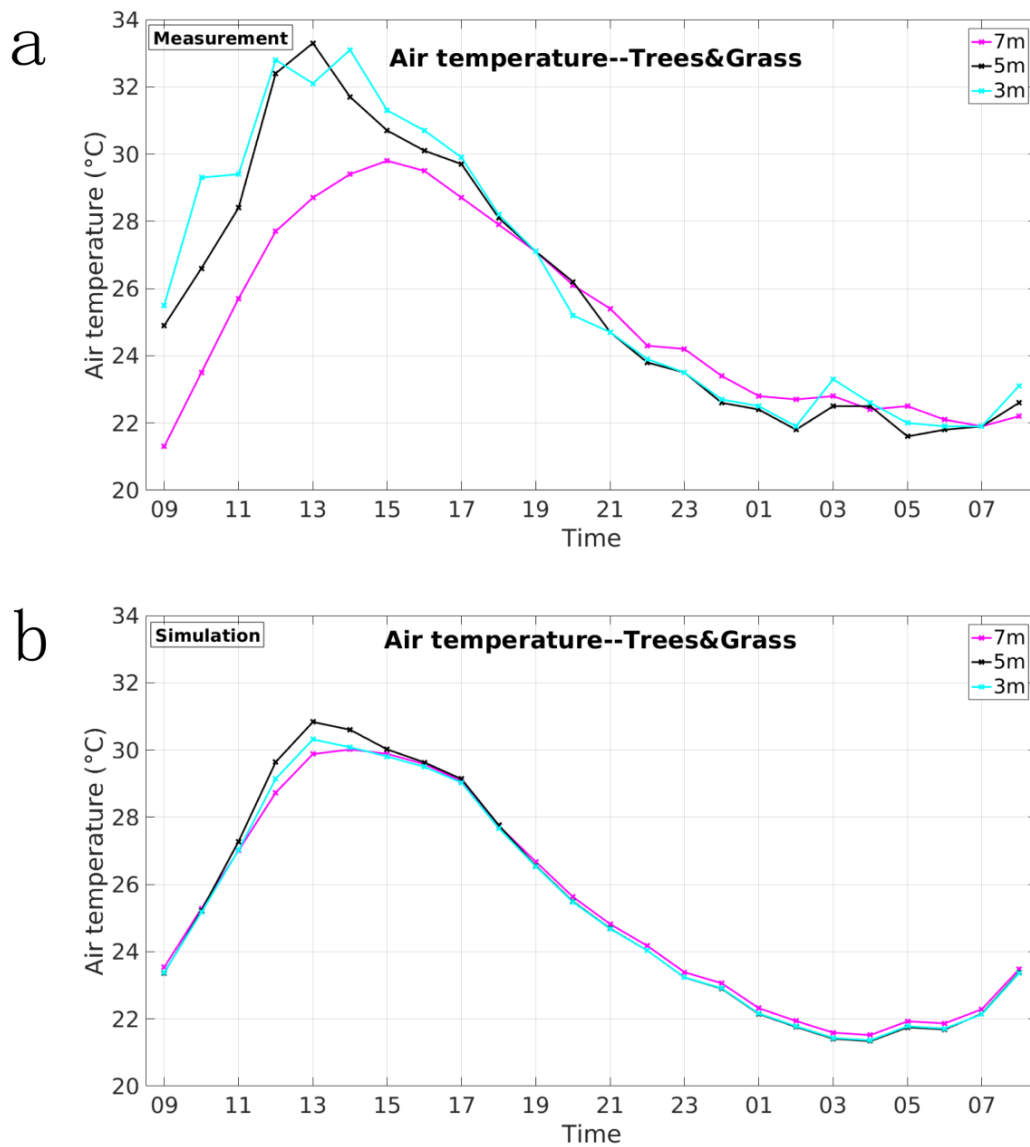


Figure 4-10 (a) The diurnal variation of measured T_a of the different widths of walkways (7m, 5m, 3m) with the vegetation type of Tree & Grass; (b) The diurnal variation of simulated T_a of the scenarios with different widths of walkways (7m, 5m, 3m).

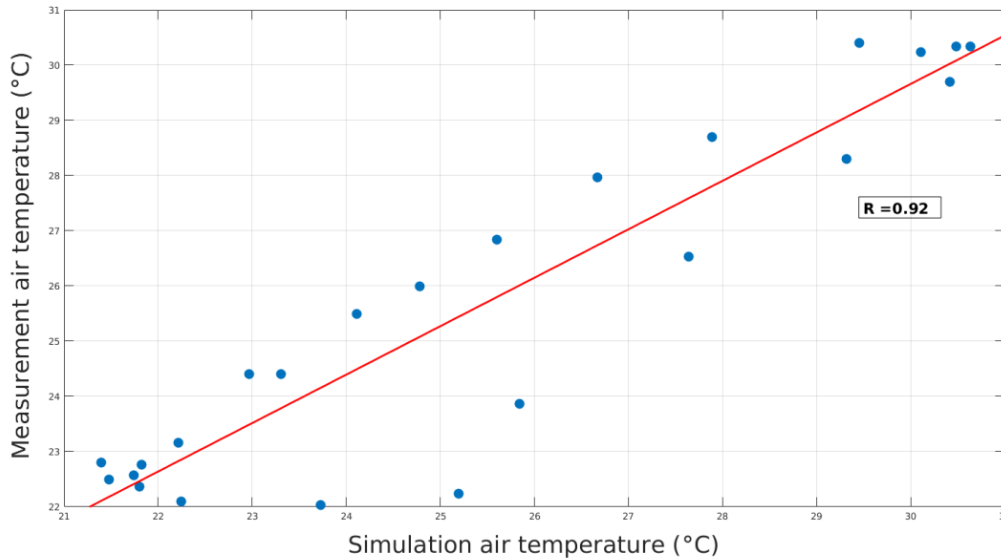


Figure 4-11 The linear regression between the simulated air temperature and the measured air temperature.

To specifically verify the simulation model, the mean air temperature of the above-mentioned points is selected to be compared (Figure 4-11). In this comparison, regression coefficient $R=0.92$ ($P < 0.05$, $n=24$), representing high correlation between simulated and measured data. Additionally, $RMSE=1.26$ and bias is -0.22 between the simulation data and measurement data. Therefore, with the high correlation coefficient and lower bias, the simulation model ENVI-met in this research can be seen as accurate and reliable.

4.3.2.2 Influence of the SVF and Vegetation Types on the Human Thermal Comfort

To illustrate the human thermal comfort on the simulated walkway, the PET of the simulating scenarios were calculated using RayMan model with the simulated air temperature (T_a), wind velocity (v), relative humidity (RH) and the mean radiant temperature (T_{mrt}).

Figure 4-12 shows the diurnal variation of the PET of the scenarios with the same width of walkway and the different vegetation types and canopy conditions. At daytime, it can be found that the canopy condition is the dominant factor of the PET. The PET of the Grass is the highest because there is completely no canopy in the scenario. The PET of the scenarios without the canopy on the walkway is obviously higher than the scenarios with canopy on the walkway. When the canopy condition is the same, the PET of the Tree & Shrubs is lower than the Tree & Grass, but the difference is not as obvious as the difference caused by the canopy conditions. At night, the PET conditions are revised compared with daytime. The scenario with the Grass has the lowest PET, while the scenarios with Tree & Shrubs and with canopy on the walkway

has the highest PET. The difference of PET among different scenarios is not as strong as the daytime.

This phenomenon is because the canopy of trees can directly block the short-wave radiation at daytime, reducing the heat arriving the walkway. At nighttime, the canopies and shrubs block the dissipation of the long-wave radiation, trapping the heat on the walkway. This explanation is supported by the diurnal variations of the T_{mrt} of the scenarios (Figure 4-12-b). During all the simulated data used for the calculation of the PET, the T_{mrt} was found the most correlative and similar with the PET results. The agreement between the T_{mrt} and the PET shown in Figure 4-12 has proved that the human thermal comfort of the simulating scenarios can be represented by the T_{mrt} .

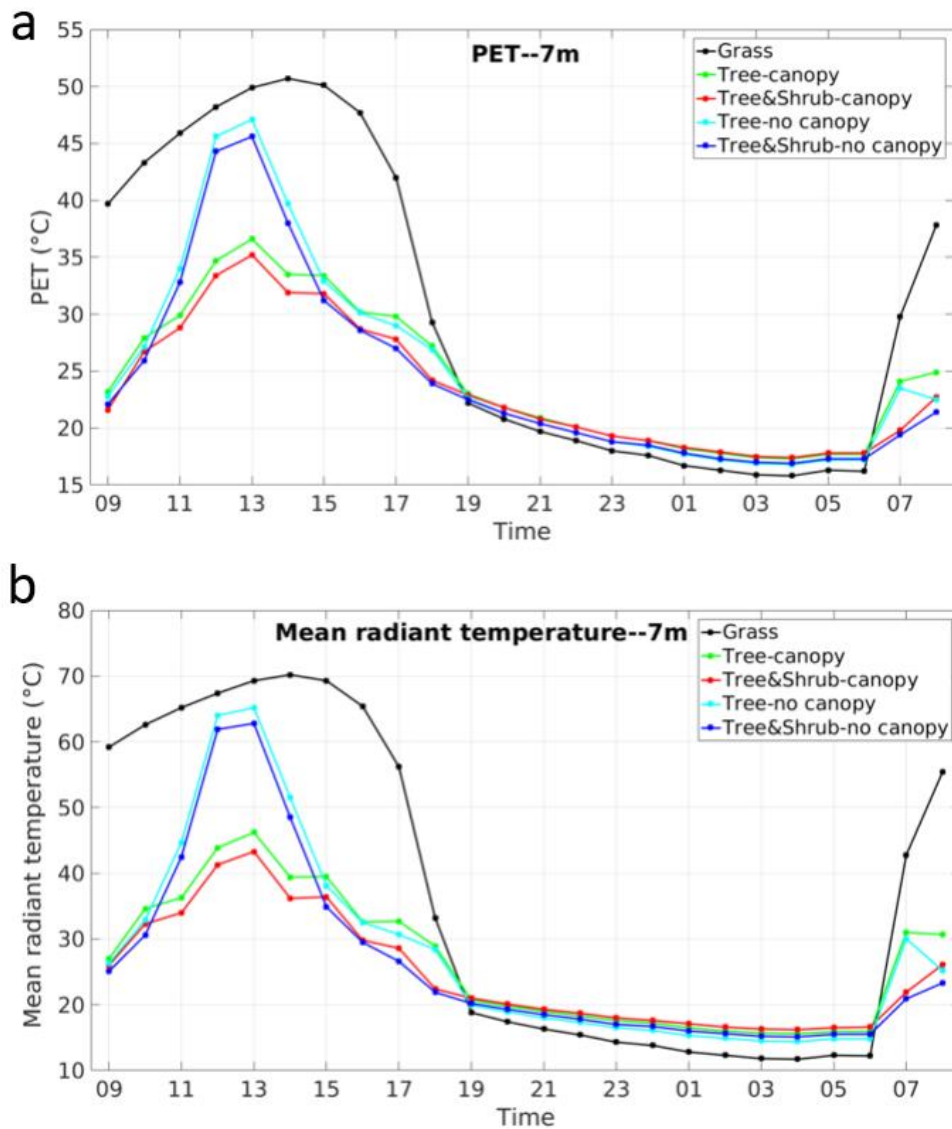


Figure 4-12 (a) The physiological equivalent temperature (PET) calculated from the simulated data, and (b) the simulated mean radiant temperature (T_{mrt}) of the scenarios with the same width of walkway (7m), different vegetation types (Grass, Tree&Grass, Tree&Shrubs).

4.3.2.3 Influence of the Width of Walkways on Human Thermal Comfort

Figure 4-13-a shows the diurnal variation of the PET of the scenarios with the same vegetation type (Tree & Shrubs) and the different widths of walkways (3 m, 5 m, 7 m) and canopy conditions. At daytime, the canopy condition is also the dominant factor of the PET. When the canopy condition is the same, with the walkway getting wider, the PET on the walkway increases. The PET on the 7 m wide walkway is slightly higher than that on the 5 m and 3 m walkways in sequence at daytime. However, the PET difference caused by the width of walkway is very small compared with that caused by the canopy condition. At night the PET conditions are reversed, too. The PET on the 7 m wide walkway turns to be the lowest

and the PET on the 3 m wide walkway becomes the highest. However, the difference among scenarios at nighttime is even slighter than that at daytime. The results are because the wider walkway represents the opener space, which can accept more short-wave radiation at daytime and trap less long-wave radiation at nighttime. This explanation can also be proved by the diurnal variations of the T_{mrt} of the scenarios (Figure 4-13-b).

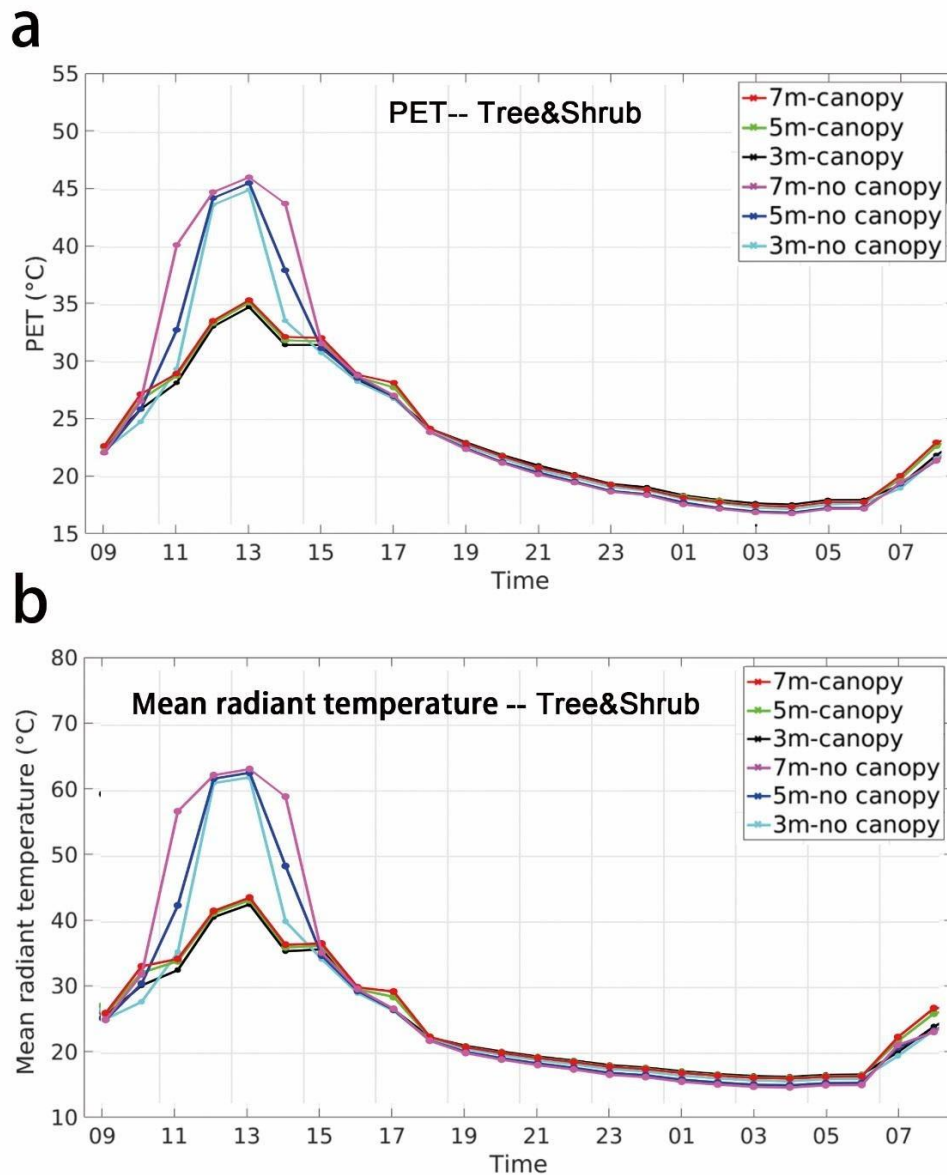


Figure 4-13 (a) The physiological equivalent temperature (PET) calculated from the simulated data, and (b) the simulated mean radiant temperature (T_{mrt}) of the scenarios with the same vegetation type (Tree&Shrub), the different widths of walkway (3m, 5m, 7m).

4.3.2.4 Overview of the Simulated Human Thermal Comfort

As already been proven in the Figure 4-14 and Figure 4-15, the simulated mean radiant temperature (T_{mrt}) can approximately represent the human thermal comfort conditions. Therefore, to overview the human thermal comfort conditions in all the simulating scenarios, the maps of T_{mrt} at 1.1 meter of every scenario were extracted at daytime (2pm) and nighttime (10pm).

The Figure 4-14 demonstrates the comparison of T_{mrt} maps at 2pm. It can be figured out that, at daytime, the dominant factor of the human thermal comfort on the walkway is the canopy condition. All the T_{mrt} on the walkways covered by canopies are lower than that on the walkways without canopy. Meanwhile, the highest T_{mrt} appears in the scenarios with Grass, which are completely exposed to the short-wave radiation. The second-important factor of human thermal comfort at daytime is the vegetation type. When the canopy condition is the same, all the T_{mrt} on the walkways surrounded by Tree & Shrubs are lower than the Tree & Grass. The third-important factor at daytime is the width of walkway. When the canopy condition and the vegetation type are the same, the T_{mrt} on the walkway increase with the walkway getting wider.

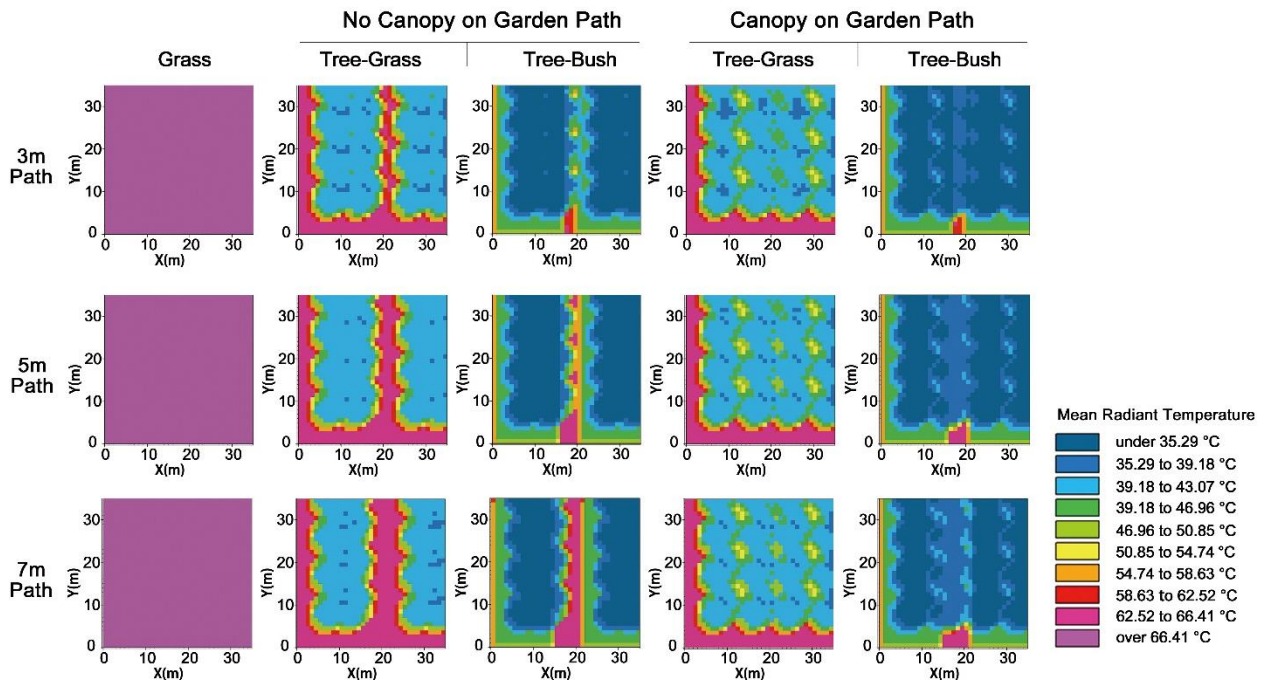


Figure 4-14 The maps of T_{mrt} at 1.1 m height on 2 pm of each simulating scenario.

The Figure 4-15 shows the comparison of T_{mrt} maps at 10pm. It can be figured out that, at nighttime, the dominant factor of the human thermal comfort on the walkway turns to be the

vegetation type. All the T_{mrt} on the walkways surrounded by Tree & Shrubs are higher than that surrounded by Tree & Grass. The walkways surrounded by Grass show the lowest T_{mrt} at nighttime. The second-important factor at nighttime is the canopy condition, when the vegetation type is the same, all the walkways covered by canopies have higher T_{mrt} than the walkways without canopy. The third-important factor of human thermal comfort at nighttime is still the width of walkway. When the vegetation type and the canopy condition is the same, the T_{mrt} decrease with the walkways getting wider.

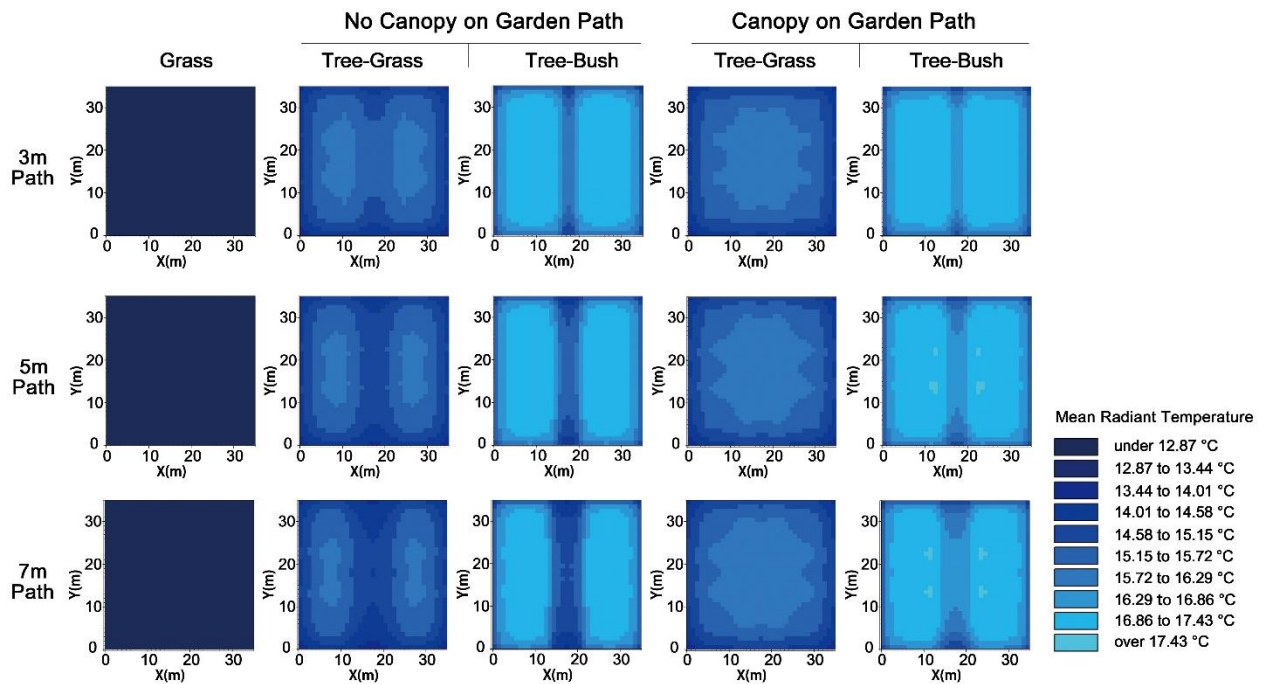


Figure 4-15 The map of T_{mrt} at 1.1 m height at 10 pm in each simulating scenario.

By comparing the Figure 4-14 and Figure 4-15, it can be found that the human thermal conditions at nighttime are thoroughly reversed from the conditions at daytime. The coolest scenario at daytime (3 m walkway covered by canopy and surrounded by Tree & Shrubs) turns to be the warmest at night. Correspondingly, the warmest scenario at daytime (7 m walkway surrounded by Grass) becomes the coolest scenario at nighttime. The human thermal comfort of the other scenarios also turns to their opposites from daytime to nighttime. This is because, the canopy and shrub, which block the short-wave radiation, can at the same time trap the dissipation of the long-wave radiation. This trapping effect is not obvious at daytime but becomes the dominant factor of the thermal condition at nighttime, when there is no more influence from the short-wave radiation.

4.4 Conclusions, Application and Outlook

The human thermal comfort on the walkway is found jointly influenced by the Sky View Factor (SVF) above walkways, the vegetation density along walkways, and the width of walkways. The results show that the SVF is the dominant factor influencing human thermal comfort, followed by the vegetation density and then the walkway width. The joint influence of the three factors differs from the daytime and nighttime.

During the daytime of a hot summer day, the walkway covered by dense canopy, surrounded by dense vegetation and with narrower width can provide more optimal human thermal comfort against the heat stress at daytime. At night, the walkway covered by sparser canopy, surrounded by less vegetation, and with wider width has lower PET values. This is because the tree canopy and shrub can block the short-wave radiation and trap the dissipation of the long-wave radiation at the same time. The blocking of the short-wave radiation plays the dominant role during the daytime and the trapping of long-wave radiation becomes dominant at nighttime.

A map of human thermal comfort of Tiergarten was generated according to the above conclusion (Figure 4-16). In this map, all the walkways in Tiergarten were classified by their width, canopy condition and vegetation type, and arranged different color to demonstrate their human thermal comfort at daytime of a hot summer day. This map of human thermal comfort can help the pedestrians in Tiergarten to select a comfortable walkway for their outdoor activities against heat waves.

Since this study simulates idealized scenarios, the conclusions can be applied to other park walkways as long as the main characteristics of the walkway match those of the idealized scenarios. The results are particularly applicable to large parks in open fields that are not shaded by neighboring buildings. In addition, the results can be used by landscape architects to design garden walkways. The higher generalizability of the results is an advantage of the idealized scenario simulation.

The field measurements in this study are performed on a typical summer day in Germany when the daytime maximum air temperature exceeds 30 °C. In recent years, the summer temperatures in Germany have frequently exceeded 30 °C. According to Deutscher Wetterdienst (DWD, German Weather Service), the maximum temperature in 2023 was 38.8 °C, observed on July 15 in Möhrendorf-Kleinseebach (Bavaria) (DWD, 2023). The highest temperature that has been recorded in Germany so far is 41.2 °C, which was observed on July

25, 2019, in Duisburg-Baerl and Tönisvorst (DWD, 2020). The results of this study are applicable to other hot and sunny summer days in Germany, as well as to regions with a similar climate type.

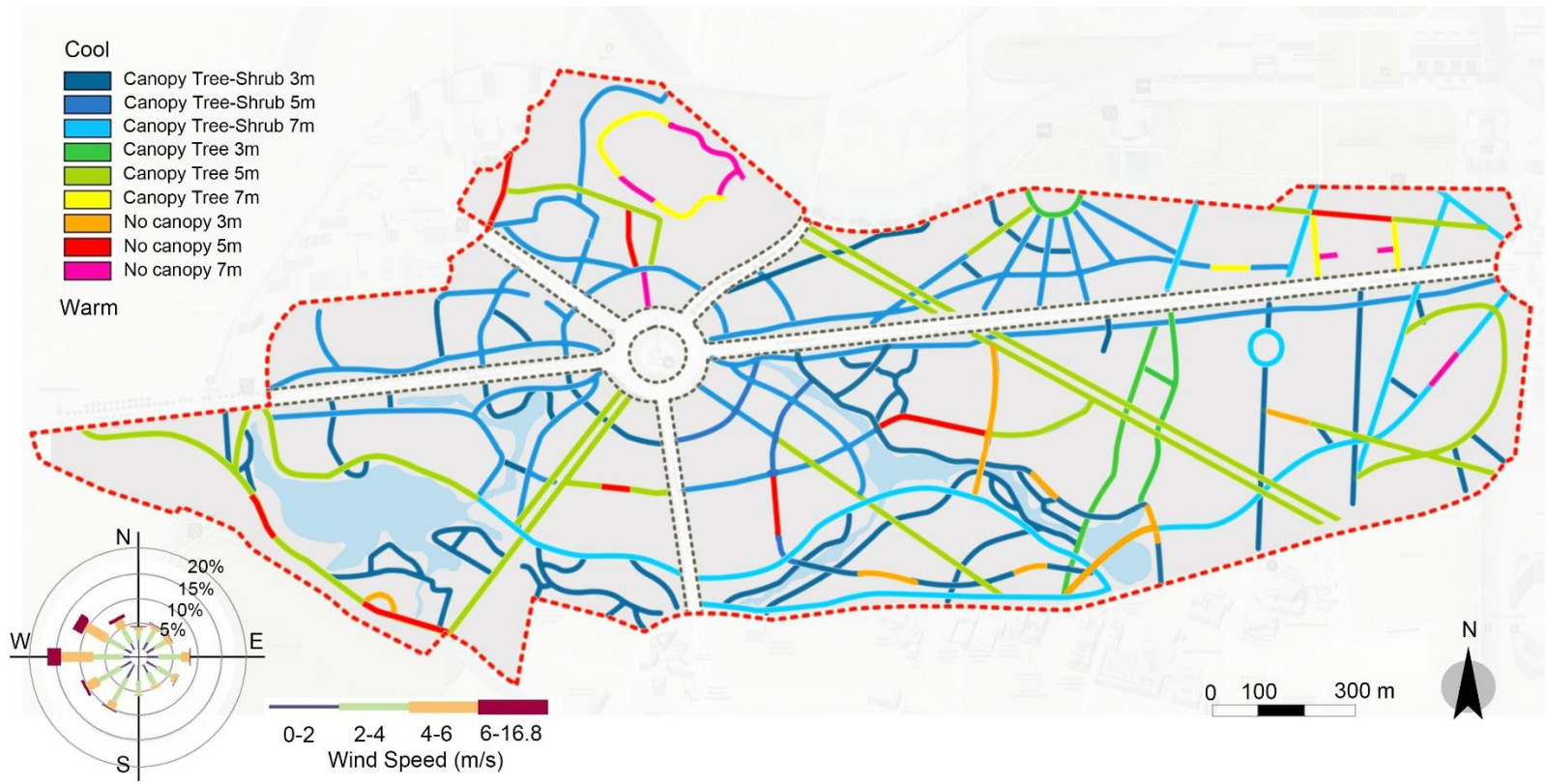


Figure 4-16 The map of human thermal comfort of the walkways in Tiergarten at summer daytime. The bottom left chart (SenUVK, 2023) presents the mean wind direction distribution at the Berlin-Tempelhof DWD station for summer season (June, July and August), differentiated by wind speed.

Chapter 5: Interdependent Influences of Three Landscape Design Factors on Human Thermal Comfort of Urban Riverside Greenways

Abstract

Urban Riverside Greenway (URG) is a specific linear Urban Open Space (UOS) that attracts a substantial body of outdoor activities. To maintain the well-being and health of the users of the greenways under the warming urban climate and growing heat stress, climate-adaptive design of the urban riverside greenway is becoming important. The purpose of this study is to clarify the interdependent influences of three landscape design considerations on the thermal comfort of urban riverside greenways. The three factors include the urban prevailing wind direction, tree species, and the greenway trail position, referring to both the site condition and the spatial morphology of an urban riverside greenway. 75 simulating scenarios are designed with different combinations of three prevailing wind directions, five types of tree species, and five positions of greenway trail. These scenarios are simulated using ENVI-met[®] model V4.3.2 science version. The simulated results are evaluated and verified through a field measurement conducted on the riverside of Suzhou River in Shanghai. To represent the human thermal comforts, the physiological equivalent temperatures (PET) are calculated through RayMan model Pro Version 2.3 Beta. The results support that the three factors of landscape design jointly influence the thermal environment. Following climate-adaptive design strategies for an URG are derived from the results: (1) The first consideration in a climate-adaptive design of an URG should be the prevailing wind direction. (2) The relative relationship between the cooling capability of green area and that of the waterbody is crucial to determining the coolest greenway trail position in an URG. (3) Any greenway trail position in an URG can be optimal for human thermal comfort on hot summer days when combined with proper tree species and prevailing wind direction. The results can be conveniently applied in both the replanting of the existing urban waterfront greenways and the design of the future ones.

5.1 Introduction

Concurrent with global climate change, the incidence of heat waves is escalating worldwide (Cowan et al., 2014; Habib et al., 2015; Meehl and Tebaldi, 2004). Simultaneously, rapid urban expansion is intensifying Urban Heat Island (UHI) effects (Jusuf et al., 2007; Li et al., 2019; Oke, 1995). These changes induce increasing heat stress on urban residents, posing a threat to public health (Bustinza et al., 2013; Morabito et al., 2012). Increasing attention is being paid to the climate-adaptive design of Urban Open Space (UOS) to ensure outdoor thermal comfort amid the changing urban climate (Doick et al., 2014; Middel et al., 2015; Tan et al., 2016).

Greenways are a specific type of urban open space characterized by their belt shape and ecological corridor function (Brown et al., 2014; Larson et al., 2016). In urban areas, greenways usually accommodate outdoor activities and recreation, such as commuting, jogging, walking and bicycling (Gobster, 1995; Lindsey and Nguyen, 2004; Shafer et al., 2000). Many researchers have discovered that, outdoor activities conducted in greenways positively impact the livability and the public health of a city (Chiesura, 2004; Fabos, 1995; Larson et al., 2016; Tzoulas et al., 2007). With the increasing awareness of the significance of greenways, there is an anticipation of more greenway constructions in the future (Fabos, 2004; Hellmund and Smith, 2013; Tan et al., 2016). Urban Riverside Greenway (URG) is a special kind of urban greenway. Different from common greenways, river-scape is brought into the scenery of the URG. Because of people's aesthetic preference for the river-scape and the diverse visual experience, the URGs attract more outdoor activities than common greenways (Litton, 1977; Pflüger et al., 2010; Zhao et al., 2013). However, the majority of current URGs are designed without considering the thermal comfort of greenway users. According to a 2016 study by Giannakis, although many greenway users anticipated the thermal environment in riverside greenways to be more comfortable in summer than in other urban areas, measurements revealed that URGs were not as cool as expected. Some areas in the URG were even warmer than the other urban areas. He also projected that, this type of riverside greenway will be less comfortable in the warming future (Giannakis et al., 2016). Therefore, it's important to incorporate climate adaptation into the design of the URGs to ensure the thermal comfort and health of greenway users in the warming future (Giannakis et al., 2016).

The climate-adaptive design of an urban open space is normally achieved through the proper arrangement of spatial morphology, which includes the layout (Hong and Lin, 2014), the shape of vegetated areas (Sodoudi et al., 2018), and the vegetation species (Emmanuel et

al., 2007; Shashua-Bar et al., 2010). Previous studies have found that, with efficient spatial morphology of the urban open space, the air temperature can vary significantly (Gobster, 1995; Shafer et al., 2000). For instance, Hong and Lin (2014) studied the influence of the layout on the cooling effects and found that the air temperature of the dispersed vegetated areas can be 0.78 K higher than that of the centralized areas. Sodoudi et al. (2018) have shed light on the influence of the shape of green space and found that belt-shaped green spaces show higher cooling effects than square-shaped green spaces. The influence of vegetation species is usually studied in combination with planting density. For example, Shashu-Bar et al. (2010) have found that the air temperature in the densely planted *Ficus* grove is up to 2.9 K lower than in a sparsely planted Palm grove.

Although numerous studies have investigated the influences of various morphological features on the cooling effects of urban open space, only a few studies have explored the interdependent influences of multiple environmental factors on cooling effects. The results from these studies have demonstrated the existence of interdependent influences, i.e., the way an environmental factor influences the cooling effects depends on the values of other factors. For instance, Sodoudi et al. (2018) found that the vegetation type is crucial when discussing the influence of spatial layout of Urban Green Space (UGS) on cooling effects. Their study also found that the interdependent influence of multiple factors is easier to transfer to specific guidelines for climate-adaptive UGS design and planning.

The aim of this study is to investigate the interdependent influence of three environmental factors on human thermal comfort of URG. The three factors include: tree species, greenway trail position, and prevailing wind direction. We used the distance from waterbody (D_w) to describe the greenway trail position and used the combination of Leaf Area Density (LAD) and the Foliage Albedo to quantify the tree species. To realize this complex investigation, we adopted the factorial experimental design for simulation experiment. To control the computational cost, we employed the Latin Hypercube Sampling (LHS) design to limit the number of scenarios from 180 to 75. The microclimate model ENVI-met was used to simulate these 75 scenarios. And the simulated results were evaluated through a field measurement conducted in the URG alongside the Suzhou River in Shanghai, China.

5.2 Methodology

5.2.1 Factorial Experimental Design

5.2.1.1 Structure of the Factorial Experiment

The factorial experiment of simulation in this study encompassed three factors: tree species, greenway trail position, and prevailing wind direction. Tree species in this study were quantified and categorized by Leaf Area Density (LAD) ($D\#$) and Foliage Albedo ($A\#$), with five levels: D0.5A0.2, D0.5A0.4, D1A0.2, D1.5A0.4, D2A0.6. Greenway trail position was categorized by the parameter D_w , quantifying the distance of trail to waterbody, with five levels: $D_w = 0$, $D_w = 0.25$, $D_w = 0.5$, $D_w = 0.75$, $D_w = 1$. Prevailing wind direction has three levels: 0° (N)—parallel to greenway, 90° (E)—from urban street to waterbody, 270° (W)—from waterbody to urban street (Figure 5-1). The following two sections will interpret in detail how the factors: greenway trail position and tree species are quantified and categorized for the factorial experimental design.

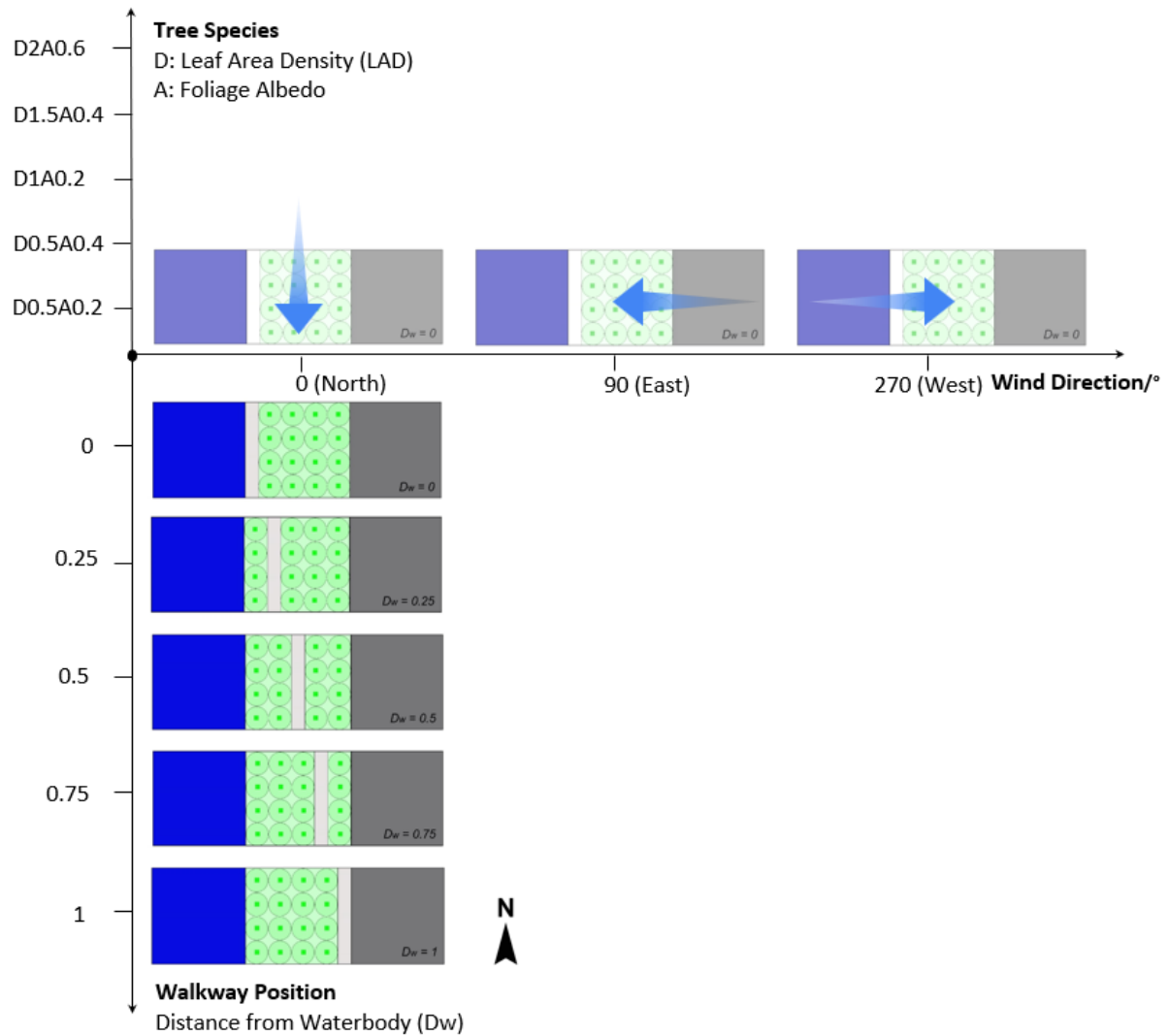


Figure 5-1 Structure of the factorial experimental design for the microclimate simulation. The blue arrows represent the wind directions: 0° (North)—parallel to the greenway, 90° (East)—blowing from the urban area toward the waterbody, 270° (West)—blowing from the waterbody toward the urban area.

5.2.1.2 Quantification of Tree Species through Leaf Area Density (LAD) and Foliage Albedo

Two parameters commonly used to describe the canopy characteristic of a tree are the Leaf Area Density (LAD) (Lalic and Mihailovic, 2004; Meir et al., 2000; Ross et al., 2000) and the Foliage Albedo (Stadt and Loeffers, 2000). These two parameters are involved in the studies of various processes of the energy and water balance within the vegetation and the atmosphere (Bruse, 2004; Bruse and Fleer, 1998). According to previous studies, the database of ENVI-met model provides values of these two parameters for some tree species commonly used in

Europe (Bruse, 2017). The data show that the LAD values of the commonly used plants vary between 0.5 and 2, while the Foliage Albedo values vary between 0.2 and 0.6.

We employed another factorial design to categorize these commonly used tree species based on the combination of the two factors: LAD and Foliage Albedo. LAD (D#) has four levels ranging from 0.5 to 2 with a step of 0.5. Foliage Albedo (A#) has three levels ranging from 0.2 to 0.4 with a step of 0.2 (Table 5-1). The twelve values of D#A# can represent the canopy conditions of most tree species mentioned in ENVI-met model. However, if all the twelve values of D#A# are included in the factorial experiment of simulation, the number of simulated scenarios will be 180. To control the computational load, we used the Latin Hypercube Sampling (LHS) method to select five values from the twelve D#A# combinations for the factorial simulation experiment (Figure 5-2). Then, the number of simulated scenarios were limited to 75.

Table 5-1 Categories of commonly used tree species represented by the combination of Leaf Area Density (LAD) and Foliage Albedo values.

		Foliage Albedo		
Leaf Area Density (LAD)		A_0.2	A_0.4	A_0.6
	D_0.5	D0.5A0.2	D0.5A0.4	D0.5A0.6
	D_1	D1A0.2	D1A0.4	D1A0.6
	D_1.5	D1.5A0.2	D1.5A0.4	D1.5A0.6
	D_2	D2A0.2	D2A0.4	D2A0.6

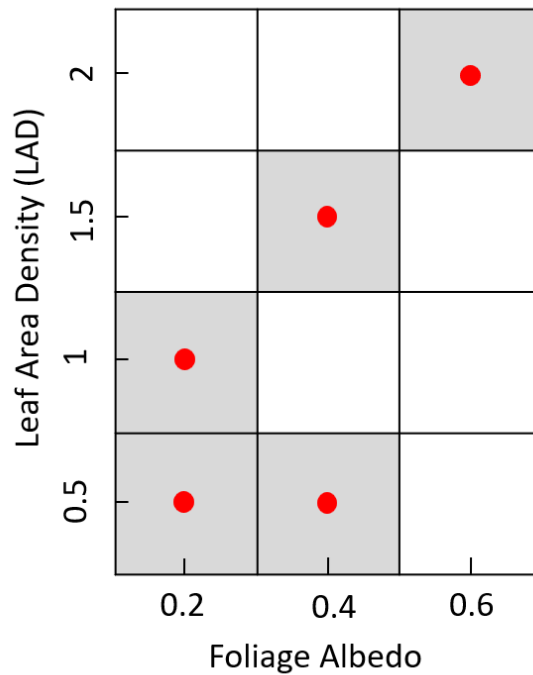


Figure 5-2 The Latin Hypercube Sampling (LHS) design was used to select five values from the twelve categories of tree species for the factorial simulation experiment.

5.2.1.3 Quantification of Greenway Trail Position

Due to the linear form of the Urban Riverside Greenway (URG), the position of the trail in the urban riverside greenway can be represented as a point on a line segment using the cross-section. As shown in Figure 5-3, we simplified the cross-section of an URG as a line segment \overline{WU} . One endpoint represents the waterbody (W), and the other represents the urban street (U). On this line segment, the distance from the near-to-waterbody edge of the trail to the endpoint W can be set as d_w , and the distance from the near-to-urban-street edge of the trail to the endpoint U can be set as d_u . The sum of d_w and d_u represents the total width of the greenway excluding the trail. The ratio of the d_w in the sum represents the *Distance from Waterbody* (D_w) of the trail. As shown in (1)

$$D_w = \frac{d_w}{d_w + d_u} \quad (1)$$

, when $D_w = 0$, the trail is adjacent to the waterbody; when $D_w = 1$, the trail is adjacent to the urban street; when $D_w = 0.5$, the trail is located at the center-point of the greenway. In this study, overall five values of D_w were adopted, including $D_w = 0, D_w = 0.25, D_w = 0.5, D_w = 0.75, D_w = 1$, respectively representing the positions: *Adjacent to Waterbody*,

Centered with Deviation to Waterbody, Center-point, Centered with Deviation to Urban Street, and Adjacent to Urban Street.

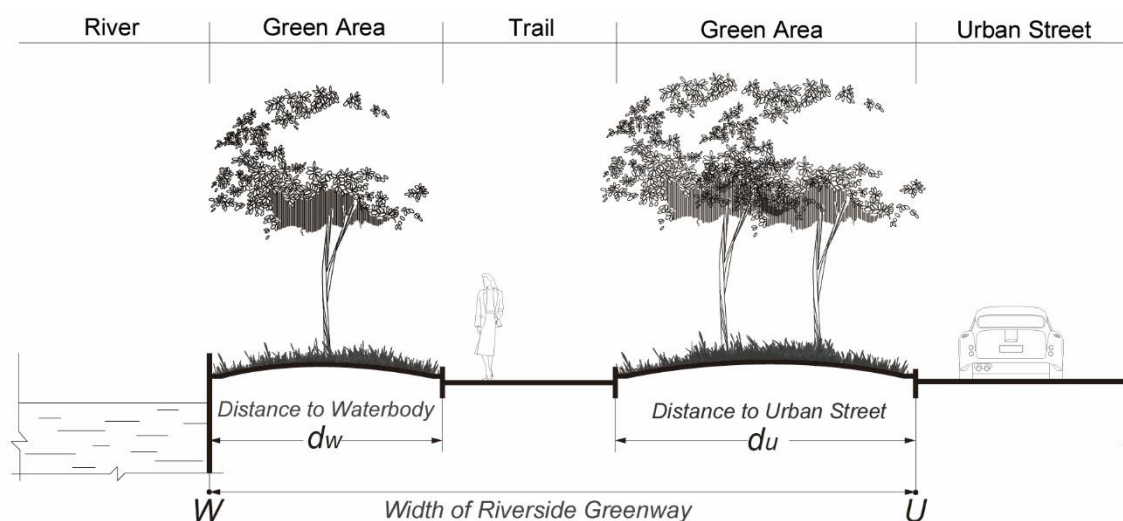


Figure 5-3 Cross-section profile of an urban riverside greenway, illustrating how the greenway trail position is quantified by the *Distance from Waterbody* (D_w).

5.2.2 Microclimate Simulation through ENVI-met® Model

In this study, the microclimate simulation was conducted using ENVI-met® V4.3.2 Science version. ENVI-met is a holistic three-dimensional non-hydrostatic prognostic model for the high-resolution microscale numerical simulation of surface-plant-air interactions in the lower part of the atmosphere (Bruse and Fler, 1998). The basic concept of the atmospheric model of ENVI-met is derived from a combination of equations, which includes the non-hydrostatic incompressible Navier-Stokes equations, the combined advection-diffusion equation and the equations for the local turbulence and their dissipation rate (Yamada and Mellor, 1975). According to this concept, the ENVI-met is able to simulate the “soft” wind field modifications (porous shelters) such as vegetation and is therefore known to be a good measurement tool for understanding the climatic influence of the greenery in urban areas (Huttner et al., 2008; Ozkeresteci et al., 2003; Wania et al., 2012).

There were in total 75 scenarios for microclimate simulation in this study. Five sections of urban riverside greenway were set as basic scenario spaces representing five greenway trail positions ($D_w = 0$, $D_w = 0.25$, $D_w = 0.5$, $D_w = 0.75$, $D_w = 1$) (Figure 5-4). The basic scenario space measured 20m×60m, including 20m×20m waterbody, 20m×20m greenway and 20m×20m urban street paved by asphalt. Each space was configured with five types of tree

species (D2A0.6, D1.5A0.4, D0.5A0.4, D1A0.2, D0.5A0.2). All the above-mentioned scenarios were simulated three times with three different prevailing wind directions (0° North, 90° East, 270° West). To minimize the interference of the shades of the tree canopy, we designated the direction of the urban riverside greenway as North-South and only analyzed the data at mid-noon (12:00 pm), when no shades were cast on the greenway trails. The initial wind velocity was set as 1 m/s at a height of 10 meters, classified as *light air* on the Beaufort scale (Beaufort, 1805).

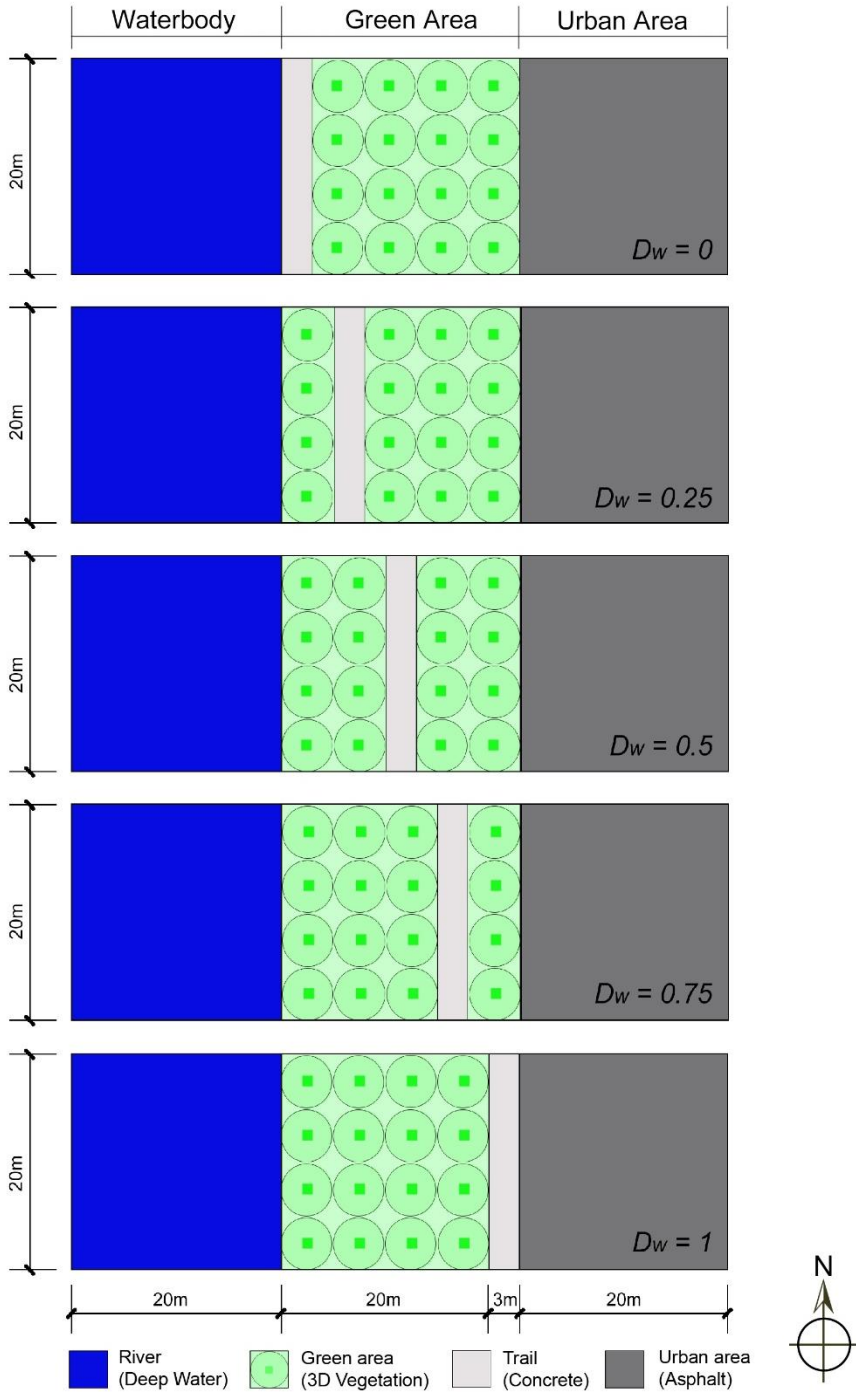


Figure 5-4 The five basic scenario spaces for simulation were built using ENVI-met, representing the five greenway trail positions ($D_w = 0$, $D_w = 0.25$, $D_w = 0.5$, $D_w = 0.75$, $D_w = 1$).

The 24-hour forcing data of all the scenarios was obtained from field measurements conducted on July 30, 2014, in Shanghai, China. The simulation time ranged from 7:00 to 13:00 with five-hour spin-up time. We selected the data of mid-noon (12:00 pm) for analysis to

eliminate the influence of the shadings on the trails. The basic configuration of the scenarios is represented in Table 5-2.

Table 5-2 The general configuration of the simulation conducted using the ENVI-met model.

City:	Shanghai
Longitude, Latitude:	31.23°N, 121.47°E
Elevation (m):	4
Start simulation at day:	30.07.2014
Start simulation at time:	7:00 am
Total simulation time in hours:	8
Wind speed at 10m (m/s):	1
Wind direction (0: N; 90: E; 180:S; 270:W):	0; 90; 270
Roughness length (m):	0.01
Initial temperature atmosphere (K):	304.13
Specific humidity in 2500m (g water/kg air):	7.0
Relative humidity in 2m (%)	50

5.2.3 Evaluation of ENVI-met Model through Field Measurements

To evaluate the results of the ENVI-met model, a field measurement was conducted in Shanghai (E120°52'-122°12', N30°40'-31°53'), on the floodplain of the Yangtze River delta of China, characterized by a humid subtropical climate and four distinct seasons. Shanghai is a typical megacity with high density (downtown reaches 16828 people per km²). Consequently, the Urban Heat Island (UHI) effect and heat stress in Shanghai are notably severe. In recent years, increasing occurrences of extreme heat are evident. The highest recorded air temperature was 40.9 °C on July 21, 2017. In 2018, the air temperatures of 67 days were observed higher than 30 °C (Shanghai Meteorological Service, 2018).

We conducted the measuring experiment in a segment of the riverside greenway along the Suzhou River near Heng Feng Road (Figure 5-5). The Suzhou River is one of the major

rivers flowing through downtown Shanghai. The total channel length of the Suzhou River inside Shanghai is 53 km, and the average channel width is around 47 m. The width of the riverside greenway where the measurement takes place is 13 m. As shown in Figure 5-5, a total of six weather stations (WatchDog® 2900ET) were divided equally into two groups. One group (Stations No.1~3) measured the greenway trail position with $D_w = 0$, and the other group (Stations No.4~6) measured the greenway trail position with $D_w = 0.5$. In each group, three stations were arranged equidistantly traversing the riverside greenway. Additionally, one more station was placed in a nearby open space to record the forcing data for the simulation.

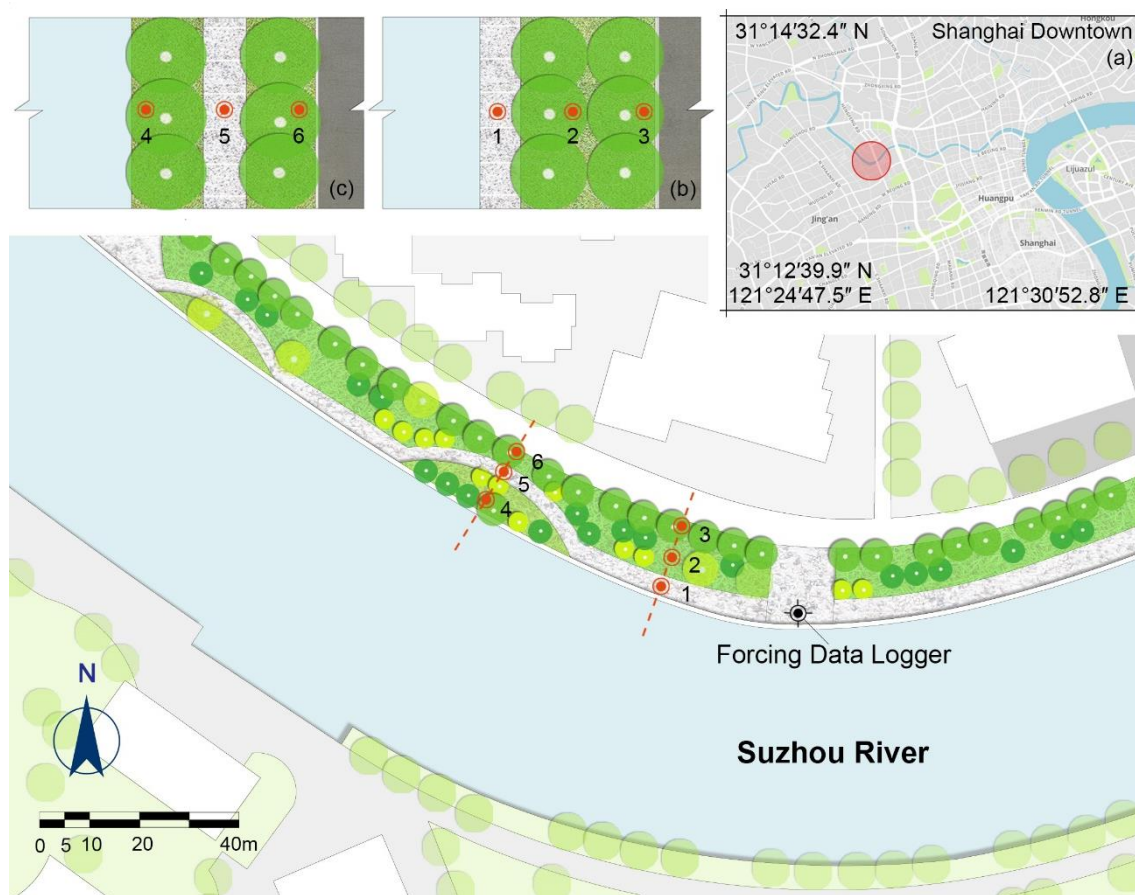


Figure 5-5 Arrangement of measuring points in the measuring experiment. (a) Location of the experiment field in downtown Shanghai; (b) Measuring points for greenway trail position $D_w = 0$; (c) Measuring points for greenway trail position $D_w = 0.5$.

Three consecutive sunny summer days with calm winds were selected as measuring days. Meteorological data at each measuring point were recorded automatically at 10-minutes interval. The measuring period of the experiment extended from 10 am to 6 pm on July 30, 2014. The daily air temperature on the measuring day in Shanghai ranged from 27 °C to 35 °C (Figure 5-6). The measured data included solar radiation, wind speed/direction, air temperature and relative humidity (RH) (Table 5-3). The measurement was conducted using seven portable

weather stations—Spectrum Watchdog 2900ET (Spectrum-Technologies, 2017). The weather stations were placed at a height of 1.5 meters above the ground (Figure 5-7).

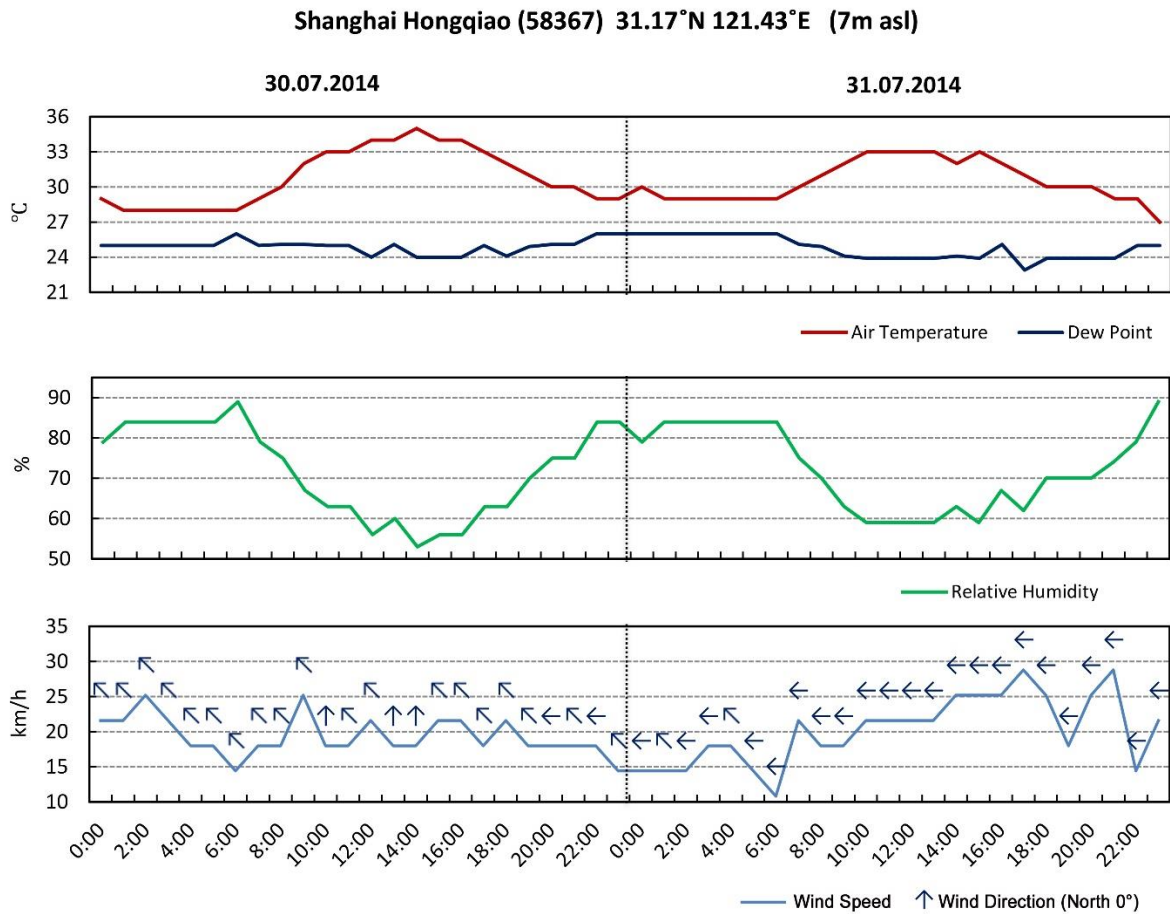


Figure 5-6 The daily time series of meteorological data (Meteogram) of the weather station located in Shanghai Hongqiao (58367) on July 30, 2014 (Data from Meteostat.net).

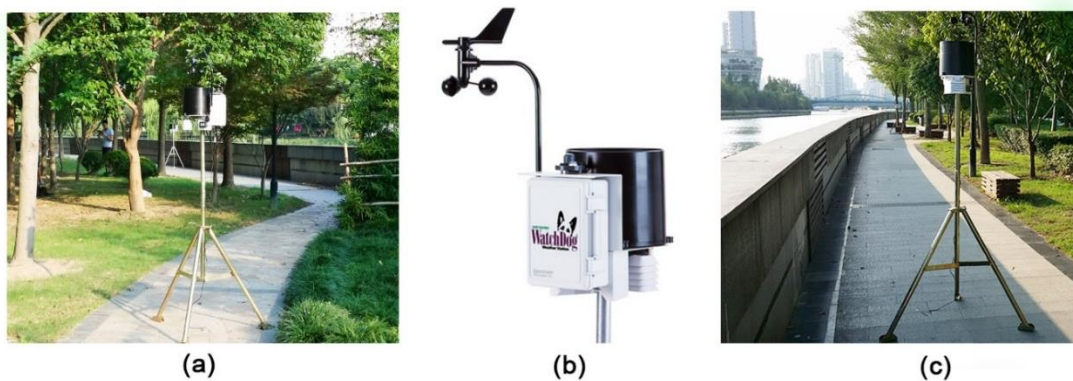


Figure 5-7 Weather stations at measuring point No.5; (b): Spectrum Watchdog 2900ET is a portable weather station with high precision and multifunction; (c): Weather station at the measuring point No.1.

Table 5-3 Recorded data and configuration of weather station Watchdog 2900ET.

Air/Surface temperature/°C		Wind direction/°	
Measuring Range	-32-+100	Measuring Range	0-360
Measuring Precision	±0.6	Measuring Precision	±4
Resolution	0.1	Resolution	1
Relative humidity /%		Wind speed / km/h	
Measuring Range	10-100 (5-50°C)	Measuring Range	0.3-241
Measuring Precision	±3	Initial wind speed	3
Resolution	0.1	Measuring Precision	±5%
Solar Radiation/ W/m2		Resolution	0.1
Measuring Range	0-1500	Atmospheric pressure/ hPa	
Measuring Precision	±5%	Measuring Range	880-1080
Resolution	1	Measure Precision	±1.7

We modeled the space of the measuring field using the SPACES module of ENVI-met model V4.3.2 (Figure 5-8). In the model, six receptors were set corresponding to the measuring points in the field experiments. The forcing data came from the forcing data logger in the measuring experiment. These forcing data were also used for the factorial simulation experiment in this study. To evaluate the simulation, the average diurnal air temperatures of six measuring points (from 10 am to 6 pm) were compared with the corresponding average diurnal air temperatures of the six receptors in the simulation. The correlation coefficient Pearson's R and RMSE between simulated and measured data were calculated as the evaluation indices.

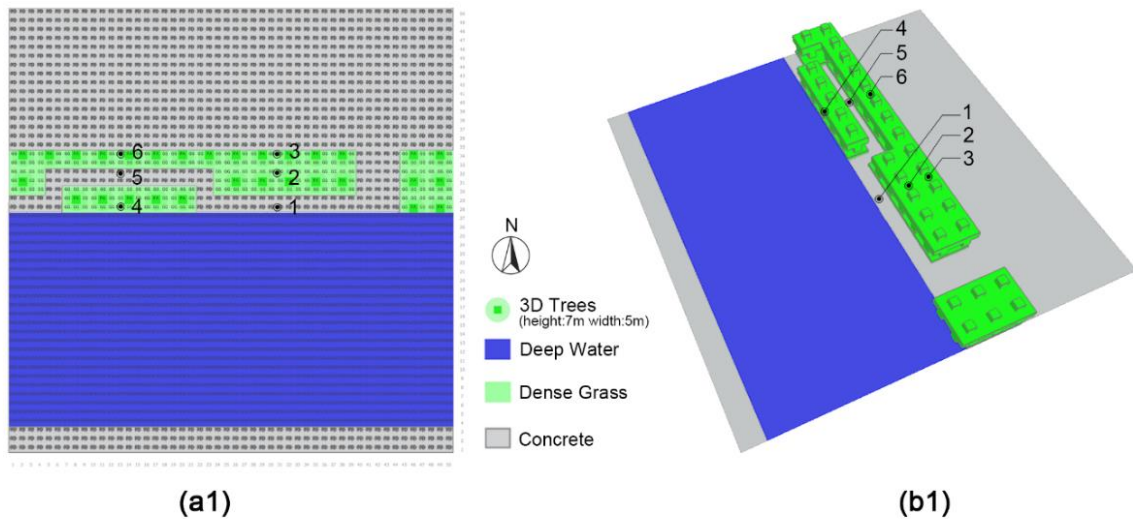


Figure 5-8 The space of the measuring fields were reconstructed by SPACES module of ENVI-met 4.3 to evaluate the modeling. (a1): Plane graph; (b1): Aerial view graph.

5.2.4 Calculation of PET through RayMan model

In this study, we used Physiological Equivalent Temperature (PET) to assess human thermal comfort of URGs. PET is a human biometeorological thermal index defined as:

“the air temperature at which, in a typical indoor setting (without wind and solar radiation), the heat budget of the human body is balanced with the same core and skin temperature as under the complex outdoor conditions to be assessed.” (Höppe, 1999, p. 71)

The RayMan Pro Version 2.3 Beta was used in this study to calculate PET in this study. RayMan is a model for calculating human biometeorological thermal indices from the relevant meteorological variables (Matzarakis et al., 2007, 2010). It was developed based on the German VDI-Guidelines 3789 (Environmental meteorology-Interactions between atmosphere and surfaces-Calculation of spectral short-wave and long-wave radiation) and VDI-3787, Part 2 (Environmental meteorology-Methods for human-biometeorological evaluation of the thermal component of the climate) (Verein Deutscher Ingenieure, 2019, 2022). RayMan model has been widely used in studies on human thermal comfort in urban areas of various climate zones (Müller et al., 2014; Shashua-Bar et al., 2012; Thorsson et al., 2011). The meteorological variables adopted in the calculation of PET included air temperature (T_a), relative humidity (RH), wind velocity (v), and the mean radiant temperature (T_{mrt}).

5.3 Results

5.3.1 Evaluation of the ENVI-met Model

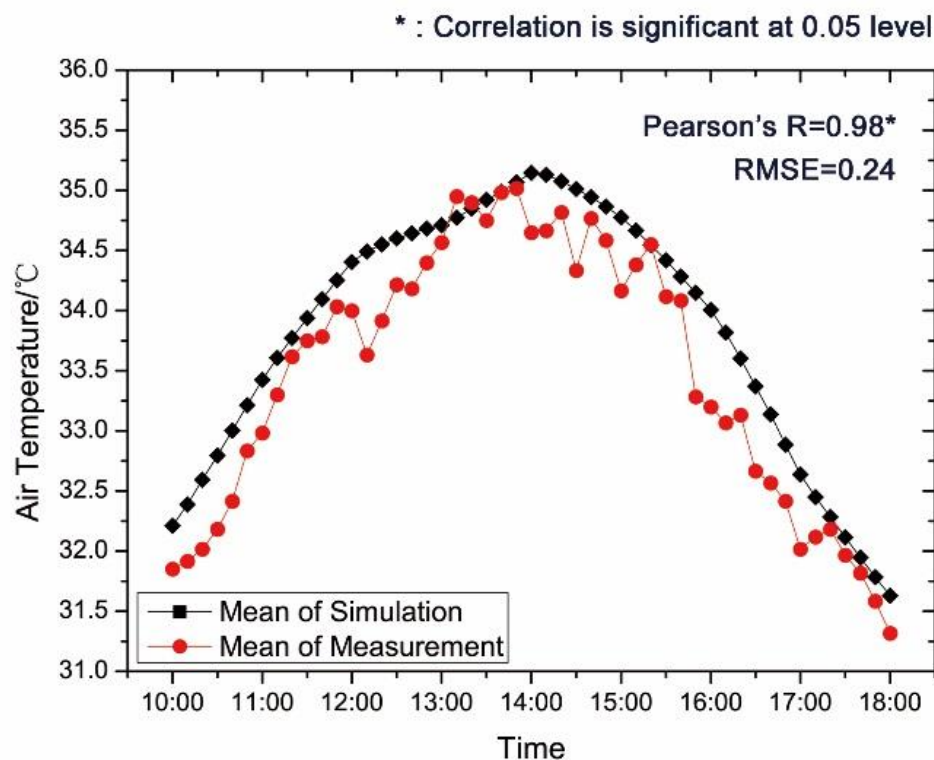


Figure 5-9 The comparison between the mean value of the simulated air temperature (T_a) from the six receptors and the mean value of the measured T_a from the six portable weather stations.

Figure 5-9 shows the comparison between the mean value of the simulated air temperature (T_a) from the six receptors and the mean value of the measured T_a from the six portable weather stations. The simulated data are slightly over-estimated and smoother compared to the measured data. However, the diurnal profiles of the measured and simulated T_a are still very close, with a Pearson's correlation coefficient (R) of 0.98 ($P < 0.05$) and a Root Mean Square Error (RMSE) of 0.24. In a previous evaluation of ENVI-met (Middel et al., 2014), this model was deemed reliable with a RMSE of 3.42. In this study, the high correlation coefficient and the low RMSE indicate that the EMVI-met model and the simulations can be considered credible.

5.3.2 Influence of Tree Species on Air Temperature of Greenway Trails

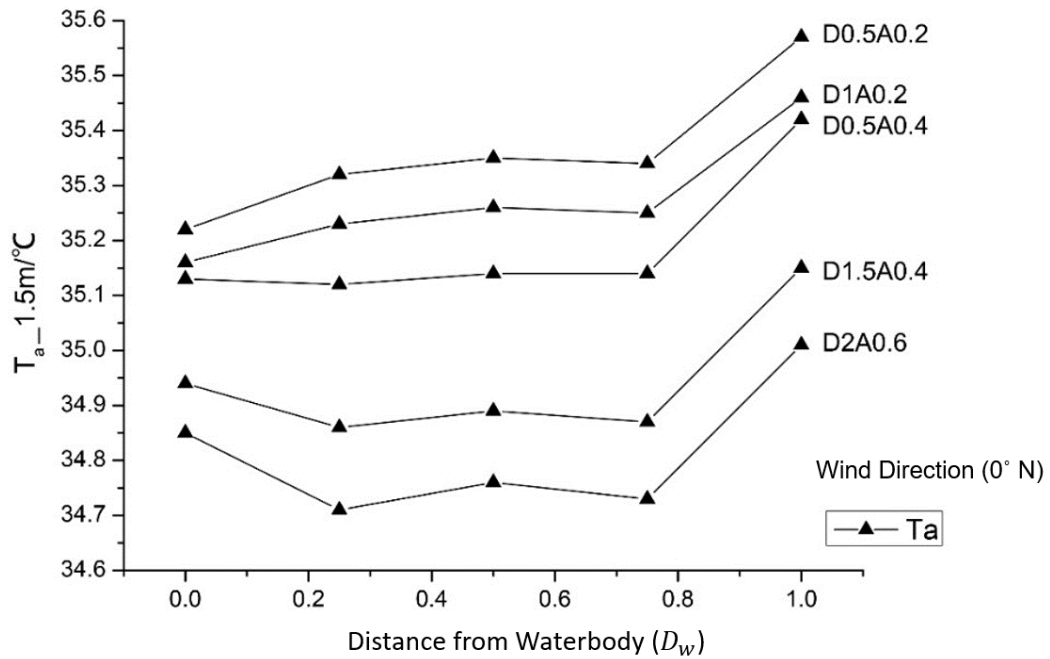


Figure 5-10 Air temperature (T_a) at a height of 1.5 m on greenway trails with five greenway trail positions D_w , five types of tree species and wind direction of north (0°).

Figure 5-10 demonstrates the simulated air temperatures (T_a) at a height of 1.5 m on the greenway trails at different positions ($D_w = 0$, $D_w = 0.25$, $D_w = 0.5$, $D_w = 0.75$, $D_w = 1$) with five types of tree species (D2A0.6, D1.5A0.4, D0.5A0.4, D1A0.2, D0.5A0.2) and wind direction from the north (0°). The T_a on the greenway trails in these scenarios range from to 34.76 °C to 35.55 °C. When the type of tree species is D0.5A0.2, the difference between the highest and the lowest T_a is 0.29 K. When the type of tree species is D2A0.6, the T_a difference is 0.27 K.

The data indicate that, when the prevailing wind direction is parallel to the Urban Riverside Greenway (URG) (0° N), the greenway trail position resulting in the lowest T_a varies depending on the tree species. For tree species D0.5A0.4, D1A0.2, and D0.5A0.2, the lowest T_a is observed on the greenway trails that are *Adjacent to Waterbody* ($D_w = 0$). For tree species D2A0.6 and D1.5A0.4, the lowest T_a is observed on the greenway trails that are *Centered with Deviation to Waterbody* ($D_w = 0.25$). Across all tree species, the greenway trails that are *Adjacent to Urban Street* consistently exhibit the highest T_a .

5.3.3 Joint Influences of Three Factors on Air Temperature on Greenway Trails

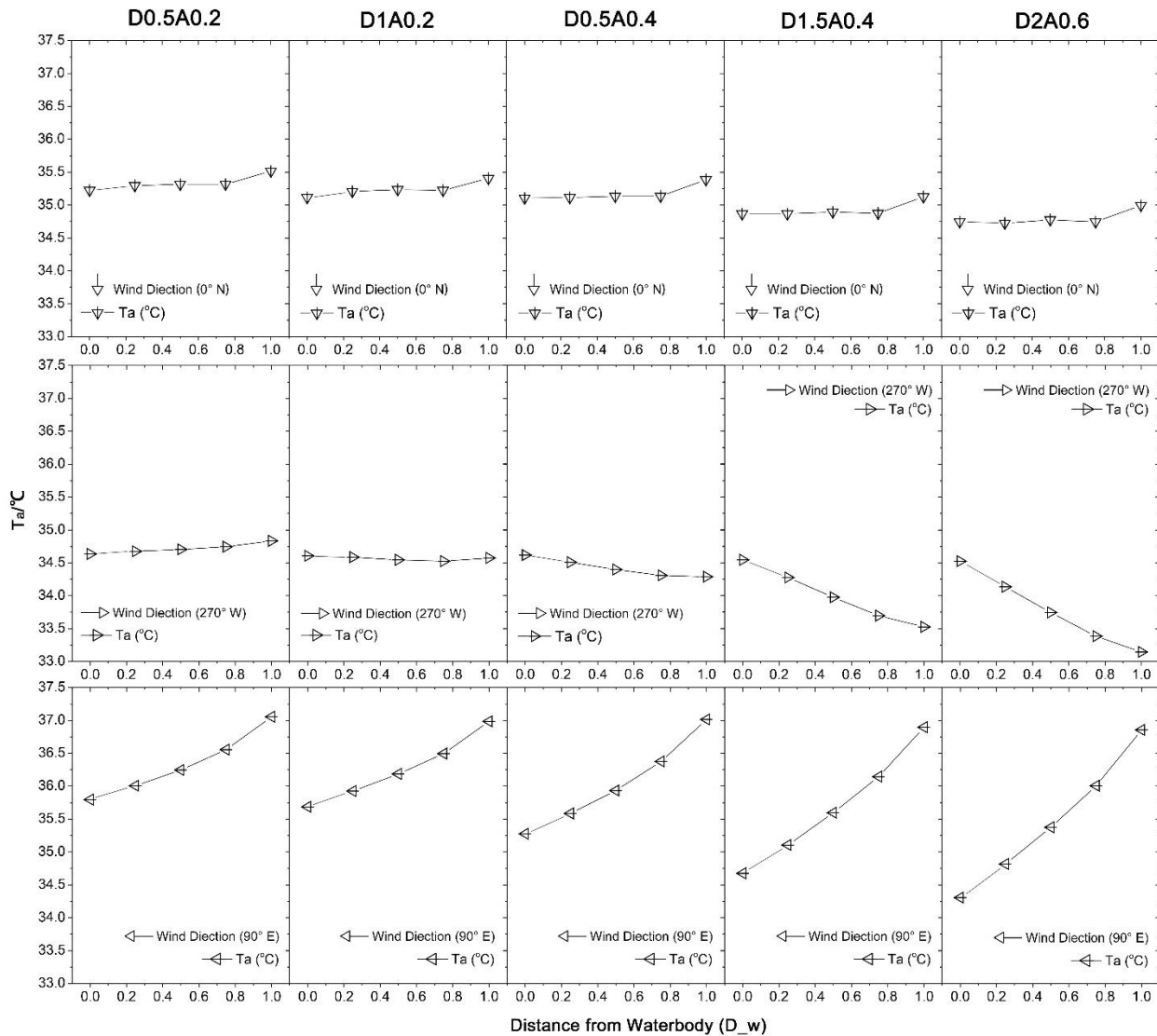


Figure 5-11 Air temperature (T_a) at a height of 1.5 m on greenway trails with five greenway trail positions (D_w), five types of tree species and three wind directions: 0°(N)—parallel to greenway, 90°(E)—from urban street to waterbody, 270°(W)—from waterbody to urban street.

Figure 5-11 shows the air temperature (T_a) at 1.5m height on greenway trails from all the simulated scenarios, including five greenway trail position, five tree species, and three prevailing wind directions. The highest T_a , 37.09°C, occurs on the greenway trail *Adjacent to Urban Street* ($D_w = 1$), with tree species D0.5A0.2, under the wind direction 90°(E)—from urban street to waterbody. The lowest T_a , 33.18°C, occurs on the greenway trail *Adjacent to Urban Street* ($D_w = 1$), with tree species D2A0.6, under the wind direction 270°(W)—from

waterbody to urban street. The temperature difference between the highest and the lowest T_a of all the scenarios is 3.91K.

The data indicates that, when the prevailing wind direction is perpendicular to the URG, the greenway trail position resulting in the lowest T_a varies depending on the moving direction of the wind. When the wind moves from the urban street to the waterbody (90° E), the T_a on the greenway trails consistently decreases when the D_w values decrease (Figure 5-11_bottom row). When the wind moves from the waterbody to the urban street (270° W), there are the following three conditions. For the tree species D0.5A0.2, the T_a on the greenway trails increases when the greenway trails are positioned further from the waterbody (i.e., as D_w value increases). For tree species D2A0.6, D1.5A0.4, and D0.5A0.4, the T_a on the greenway trails decrease when the greenway trails are positioned further from the waterbody. For the tree species D1A0.2, the T_a on the greenway trails remains nearly constant across all greenway trail positions with a temperature difference of 0.08 K (Figure 5-11_middle row).

5.3.4 Joint Influences of Three Factors on PET on Greenway Trails

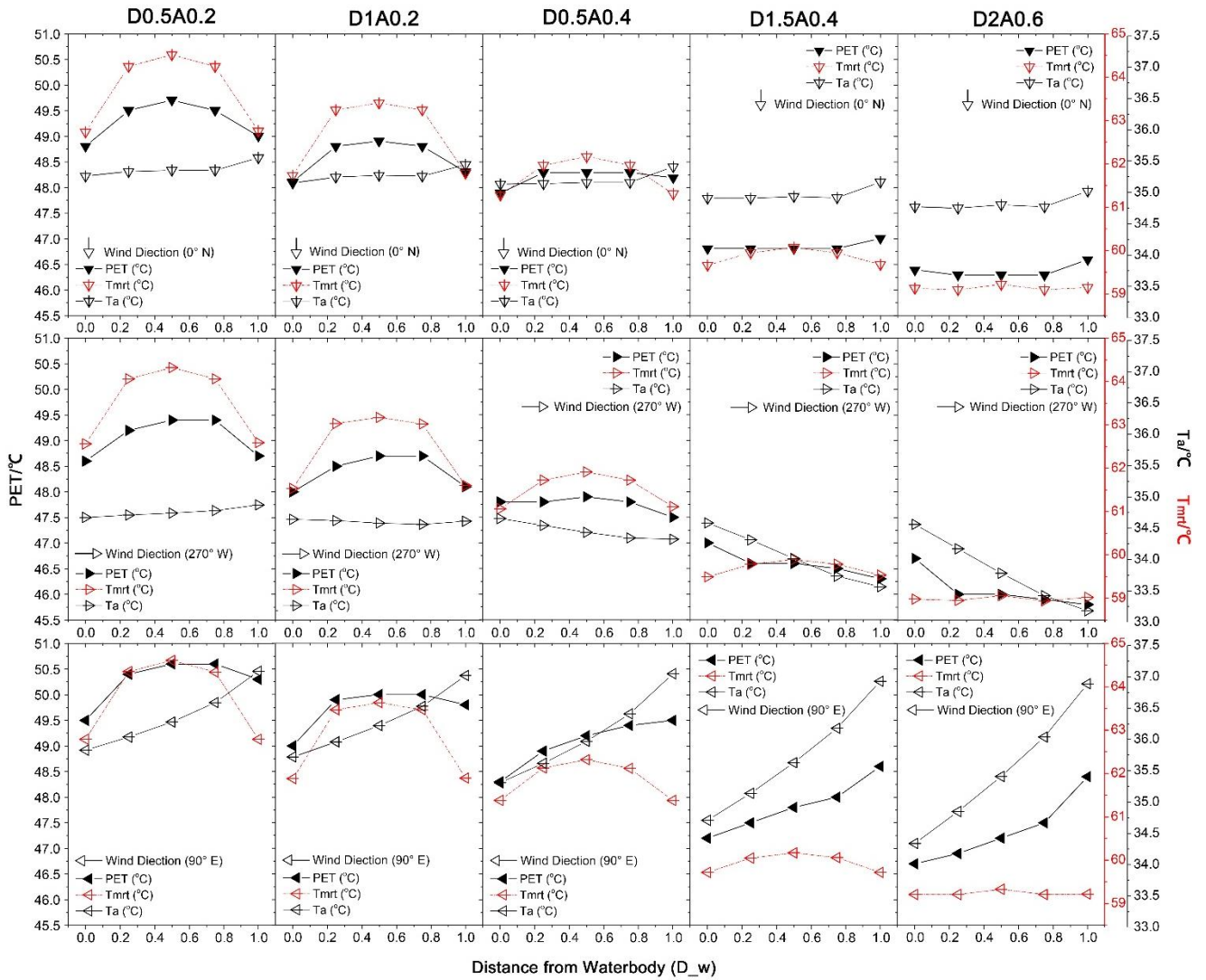


Figure 5-12 Physiological Equivalent Temperature (PET), air temperature (T_a) and Mean radiant temperature (T_{mrt}) at a height of 1.5 m on greenway trails with five greenway trail positions (D_w), five types of tree species and three wind directions.

The PET values of the 75 scenarios are illustrated in Figure 5-12, along with the corresponding values of the Air Temperature (T_a) and the Mean Radiant Temperature (T_{mrt}). T_{mrt} is a significant factor in PET calculation, indicating the intensity of the radiant convection. The data show that the T_{mrt} values remain consistent regardless of wind direction. T_{mrt} on the greenway trails located on *Center-point* ($D_w = 0.5$) is higher than located *Adjacent to Waterbody* ($D_w = 0$) and *Adjacent to Waterbody* ($D_w = 1$). When the canopy condition of tree species gets denser (from D0.5A0.2 to D2A0.6), the T_{mrt} decreases, and the range of the T_{mrt} on trails with different positions decreases. When tree species change from D0.5A0.2 to D2A0.6, the highest T_{mrt} varies from 64.5 °C to 59.2 °C, and the difference of T_{mrt} among different greenway trail positions decreases from 1.8 K to 0.1 K.

Figure 5-12 reveals that, the variation trend of PET sometimes follows the variation trend of the T_{mrt} , and at other times, it follows the variation trend of the T_a . This is determined by the tree species. For tree species D0.5A0.2 and D1A0.2, the variation of the PET is closer to that of T_{mrt} , i.e., PET on trails located on *Center-point* ($D_w = 0.5$) is the highest. Conversely, for tree species D2A0.6 and D1.5A0.4), the variation trend of PET follows that of T_a . The turning point occurs for the tree species D0.5A0.4, where the variation trend of PET is neither same as that of T_{mrt} nor T_a .

5.4 Further Simulation Experiment on Comparing the Cooling Capability of Waterbody and Trees

From the above-mentioned results, it can be noticed that a turning point exists between the tree species D1A0.2 and D0.5A0.4. The variation trends of T_a , T_{mrt} , and PET change when tree species shift from D1A0.2 to D0.5A0.4. We hypothesized that this phenomenon could result from changes in the relative relationship between the cooling capability of the waterbody and green areas. To examine this hypothesis, we designed and conducted the following simulation experiment.

5.4.1 Methodology—Experimental Design of Simulation

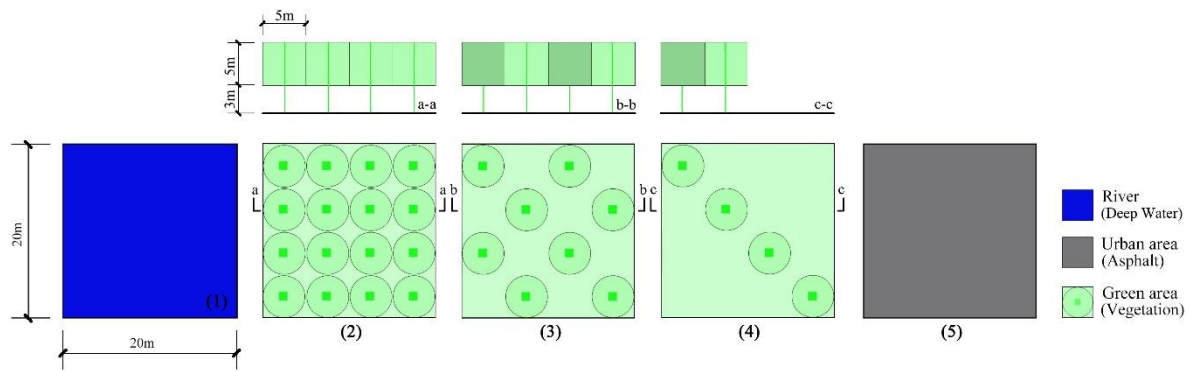


Figure 5-13 The spatial layout of the scenarios simulated in ENVI-met for comparing the cooling capability of the waterbody and green areas. a-a, b-b, and c-c refer to cross sections of the green area scenarios (2), (3) and (4).

Figure 5-13 illustrates the scenarios for simulations made to estimate the relative relationship of cooling capability of the water body and green areas. The scenarios include five spatial layouts. Space (1) and Space (5) represent the waterbody resp. the asphalted urban street. Space (2) to (4) represent different planting patterns. Space (2) represents the homogeneous planting green areas (100%), while Space (3) and Space (4) represent medium-planting (50%) and sparse-planting (25%) green areas. The dimensions of the spaces were 20m×20m. The tree canopies were designated with a size of 5m×5m×5m and a clear bole height of 3 m. On homogeneous Space (2), all twelve tree species ranging from D0.5A0.2 to D2A0.6, as mentioned in section 5.2.1.2 (Table 5-4), were simulated. For Space (3) and Space (4), only the tree species D0.5A0.2, D2A0.6, and D1.5A0.4 were simulated, corresponding to the minimum, the maximum and the median of all twelve types of tree species.

5.4.2 Results—Comparison of the Cooling Capabilities of the Waterbody and Green Areas

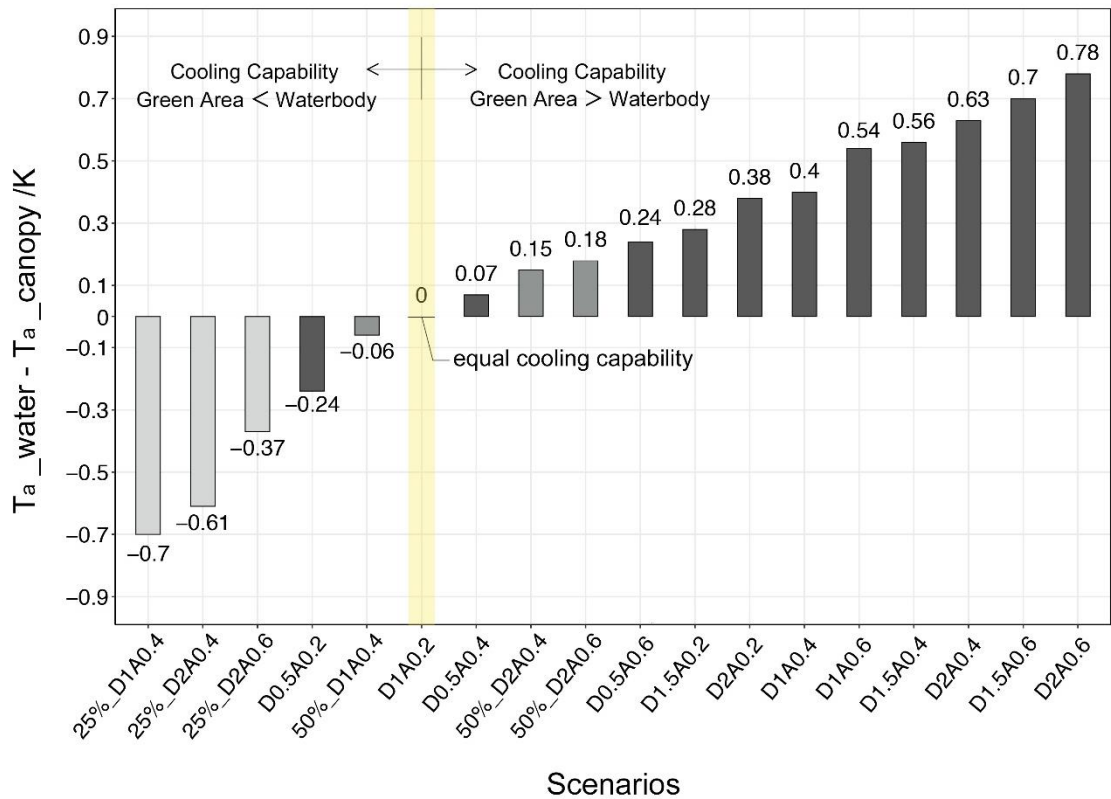


Figure 5-14 The temperature difference (D-value) of the air temperature on the waterbody (T_{a_water}) and that in the green area (T_{a_canopy}) at a height of 1.5 m.

The Figure 5-14 illustrates temperature difference (D-value) of the air temperature above the waterbody (T_{a_water}) and that in the green area (T_{a_canopy}) with different tree species and planting patterns. The positive values on the right represent that the T_{a_canopy} is lower than the T_{a_water} , indicating that the cooling capability of green areas is higher than that of waterbody. The negative values on the left represent the T_{a_canopy} is higher than the T_{a_water} , indicating that the cooling capability of green areas is lower than that of waterbody. The bars colored with the deepest grey represent the homogeneous planting pattern (100%), and those with the light grays represent the medium-planting (50%) and sparse-planting (25%) patterns. The turning point appears at canopy D1A0.2, which shows the same cooling capability as the waterbody. Besides, the cooling capability of tree species D0.5A0.4 is very close to the waterbody with a difference of 0.07 K.

For the homogeneous planting pattern, the D-values between the T_{a_water} and T_{a_canopy} range from -0.24 K to 0.78 K with a range of 1.02 K. Most green areas show higher

cooling capability than the waterbody. Only the T_a of tree species D0.5A0.2 (LAD=0.5, Foliage Albedo=0.2) is warmer than the T_a above waterbody. In the Medium-planting pattern (50%), the D-values range from -0.56 K to 0.18 K with a range of 0.74 K. The T_a under the median canopy D1.5A0.4 is 0.06K lower than that above waterbody, indicating that more than half of the canopies under Medium-planting pattern show lower cooling capability than the waterbody. For the Sparse-planting pattern (25%), the D-values range from -0.94 K to -0.37 K with a range of 0.57 K. The T_a under the densest canopy D2A0.6 with the Sparse-planting pattern is lower than the T_a above waterbody, indicating that all the green areas with the Sparse-planting pattern have lower cooling capability than the waterbody.

The data show that the turning point of results between the tree species D1A0.2 and D0.5A0.4 is exactly where the cooling capability of the waterbody and green areas is equal. This result supports the hypothesis that the change of variation trends of T_a , T_{mrt} , and PET among different tree species is due to the relative relationship between the cooling capability of the waterbody and green areas. When this relative relationship changes, the variation trends of T_a , T_{mrt} , and PET also change accordingly.

5.4.3 Verification of Results through Field Measurement

The results of this study revealed the interdependent influences of the greenway trail position, tree species and the urban prevailing wind direction on the air temperature and thermal comfort of urban riverside greenways. If the above-mentioned results are correct, it is possible to estimate the optimal solution of any one of the three factors according to the other two known factors. Therefore, we used the field measurement data to verify the results. Firstly, we analyzed the prevailing wind direction and tree species in the measuring field. Based on these conditions and the abovementioned results, we estimated the optimal greenway trail position with the lowest air temperature. Subsequently, we used the measuring data to examine whether this estimation is accurate.

According to the meteorological records, the prevailing wind direction of the measuring field at the measuring day is 115° , namely approximately parallel to the riverside greenway. The vegetation in the measuring site is the mid-densely planted (50%) ash trees (*Fraxinus Chinensis*). The canopy property of an ash tree is approximately D1A0.2. According to the above results, the cooling capability of the vegetated area is lower than that of the waterbody. Therefore, it can be estimated that the greenway trail position *Adjacent to Waterbody* ($D_w = 0$) is the coolest position of the greenway trail under the given conditions.

The Figure 5-15 illustrates the spatial and temporal distribution of the T_a at each measuring point in the field measurement. The mean T_a on Point 5 ($D_w = 0.5$) is 34.3 °C, which is 0.7 K higher than the mean T_a on Point 1 ($D_w = 0$). The maximum T_a on Point 5 ($D_w = 0.5$) is 36.6 °C, 1.4 K higher than that on Point 1 ($D_w = 0$). These D-values show that the greenway trail adjacent to waterbody is cooler than that in the centered-point, supporting the estimation derived from the results of this study.

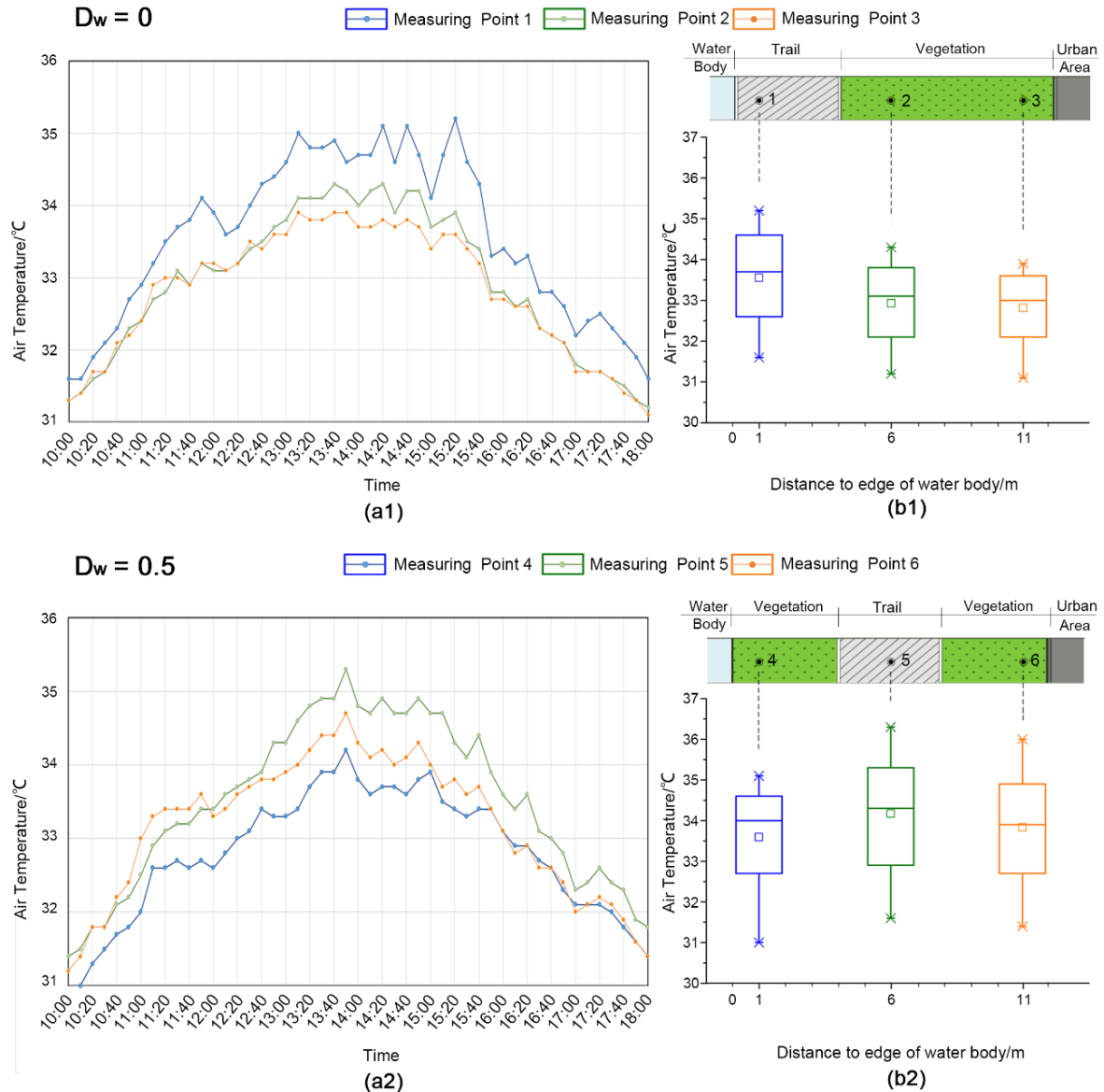


Figure 5-15 Spatial and temporal distribution of the air temperature in measuring experiment.

(a): the diurnal change of air temperature, (b): the box plot of diurnal air temperature; (1)

$D_w=0$; (2) $D_w=0.5$.

5.5 Conclusions, Discussion and Application

5.5.1 Overall Conclusions

This study investigated the greenway trail position, tree species and the urban prevailing wind direction on the human thermal comfort of Urban Riverside Greenways (URG) during summer daytime. The results support the hypothesis that these three factors interdependently influence the thermal environment in URG. Climate-adaptive design strategies for an URG based on these three design factors can be drawn based on these interdependent influences.

The first consideration in a climate-adaptive design of an URG should be the prevailing wind direction. When the prevailing wind moves from the urban street to waterbody, the closer the greenway trail locates to the waterbody, the lower the air temperature on the greenway trail. When the prevailing wind moves from waterbody to the urban street, the coolest greenway trail position depends on the cooling capability of the green area. The relative relationship between the cooling capability of green area and that of the waterbody is crucial to determining the coolest greenway trail position in an URG. When the cooling capability of the waterbody is stronger than that of the green area, the greenway trail located adjacent to waterbody ($D_w = 0$) has a lower air temperature than the trail located inside the green area ($D_w = 0.25; 0.5; 0.75$). Conversely, when the cooling capability of the vegetated area is stronger than that of the waterbody, the trail inside the green area has lower air temperature than the trail adjacent to waterbody.

The tree species and planting pattern determine the cooling capability of the green area in an URG. Most of the medium planted (50%) green area and all the sparse planted (25%) green area have lower cooling capabilities than the waterbody. For the homogeneous planting pattern (100%), the cooling capability of the green area with tree species D1A0.2 and D0.5A0.4 is the closest to the cooling capability of waterbody. According to Table 5-4, the tree species with similar Leaf Area Density (LAD) and Foliage Albedo values include the European ash, Bitter orange, Black poplar, Privet, etc.

In summary, any greenway trail position in an URG can be optimal for human thermal comfort on hot summer days when combined with proper tree species and prevailing wind direction.

The position of greenway trail $D_w = 0$ (*Adjacent to Waterbody*) can be optimal when the prevailing wind blows from urban street to waterbody OR when the cooling capability of the green area is lower than that of the water body.

Positions of greenway trail $D_w = 0.25$, $D_w = 0.5$, $D_w = 0.75$ (Inside Green Area) are optimal when the prevailing wind blows from waterbody to urban street AND the cooling capability of the green area is stronger than that of the water body. Among these three positions, $D_w = 0.5$ is warmer than the other two positions.

The position of greenway trail $D_w = 1$ (*Adjacent to Urban Area*) can be optimal when the prevailing wind blows from waterbody to urban area AND the cooling capability of the green area is stronger than that of the water body.

5.5.2 Discussion

The results support that the relative relation between the cooling capabilities of the waterbody and the green area is critical to the optimal greenway trail position in an Urban Riverside Greenway (URG). This relative relation is determined by canopy characteristics of the vegetated area due to the mechanisms of cooling effects of the waterbody and the vegetation. The cooling effects of the waterbody come from the high heat capacity, the high evaporation and the low roughness of the waterbody (Du et al., 2016; Xu et al., 2010), while the cooling effects of the vegetated area mainly come from the resistance to the incoming short-wave radiation via canopies, the high heat storage of the soil, and the evapotranspiration of the leaves and soil (Bowler et al., 2010; Declet-Barreto et al., 2013). Because the evaporation capacity of the water is much higher than that of the leaves and soil, the Bowen Ratio of the water body is lower than that of the vegetated area (Malek and Bingham, 1993). Therefore, the air temperature above the waterbody is expected to be lower than the above the unshaded vegetated area, i.e., the waterbody shows stronger cooling capability than the vegetated area. However, when the vegetated area is shaded by tree canopies, the advantage of the waterbody in cooling capability is counteracted by the short-wave radiation blocking capacity of the tree canopies. As the density of the tree canopy increases, the air temperature of the vegetated area can be lower than that above the waterbody, and the vegetated area can show stronger cooling capability than the waterbody. This is how the canopy characteristic determines the magnitude relation between the cooling capacities of the waterbody and the vegetated area.

The shrubs were not discussed in this study due to the following reasons. Firstly, the shrubs can interfere the heat convection on the pedestrian level. This interference is disadvantageous for our study, which considers the turbulence. Secondly, the influence of the shrubs on the cooling capability of vegetated area is not as significant as the influence of trees, because of the lack of canopy. Furthermore, the shrubs can cause interferences in other

processes, such as decreasing the Bowen ratio, reducing the wind velocity, reflecting more long-wave radiation, and etc., which will sophisticate this study. Therefore, the effect of the shrubs should be investigated in another independent study, considering many objects including their density, height, planting pattern, etc.

Suzhou River covered in this study is an inner-city river with a width of 40–50 meters. The width of the riverfront green space is 15–20 meters. In green spaces of this scale, there is usually only one trail. The findings of this study are also applicable to other riverside green spaces of similar scales. Notably, there are usually high-rise buildings next to inner-city rivers. The impact of shadows from these buildings needs to be analyzed on a case-by-case basis.

For regional rivers with a width of more than 300 meters, such as the Huangpu River, the width of the waterfront greenway is usually more than 50 meters. In a waterfront greenbelt of this scale, usually more than one trail would be constructed, and even wider impervious space such as plazas are constructed. For a riverside greenway at this scale, the ideas for the experimental design in this study are still applicable. However, the cooling capability of the water body and the equivalent vegetation density may change. In addition, for a riverside green space at this scale, the design considerations also change. The design consideration will no longer be where to place the single trail, but rather the proportion of impervious surfaces. This factor could be implemented in future studies.

5.5.3 Application of Results in Climate-adaptative Design of Urban Riverside Greenways

It has been noticed that many barriers exist in applying climate adaptive strategies in actual design and planning of urban open spaces (Akbari and Taha, 1992; Chang et al., 2007; Givoni, 1997). Eliasson (2000) figured out that the reason for this problem is a communication problem between designers and climatologists. As an interdisciplinary team based on both meteorology and landscape architecture, we conducted this study according to the theories of meteorology and the design considerations and processes of landscape architecture simultaneously, trying to bridge the gap between urban climatic research and practical urban construction. The strategies developed from this study can be applied in both the replanting of the existing urban waterfront greenways and the design of the future ones.

For an existing urban riverside greenway, the research results can be used to evaluate whether the current spatial morphology is optimal in human thermal comfort. If not, it is possible to improve the condition through climate-adaptive replanting. For example, in the measuring field of this study, the greenway trail located in the middle of the green area ($D_w =$

0.5) is warmer than the other trail. According to the research results, the human thermal comfort of that trail can be improved when the cooling capability of the vegetated area is strong enough. Therefore, to adapt to heat stress, this section of trails can be improved through replanting trees denser than D1A0.2 and D0.5A0.4. The replanting tree species can be selected from Table 5-4, in which we classified the tree species recorded in ENVI-met model into ten groups, with the deviation of LAD lower than 0.2 and that of Foliage Albedo lower than 0.1.

For an urban riverside greenway under design, when one or two of the three design considerations are given, the designer can make a proper decision about the unknown design consideration(s) based on these research results. In most cases, the prevailing wind direction of a project will be given. Under this limitation, with the help of the strategies derived from this study, it is convenient for a designer to select the tree species and the position of trails for a climate-adaptive design of an URG. We expect to evaluate the effectiveness of these strategies in a constructed urban riverside greenway in the future.

Table 5-4 Values and classes of the LAD and Foliage Albedo of tree species recorded in ENVI-met model (Bruse, 2017).

Class	Botanical Name	Common Name	LAD	Foliage Albedo
D2A0.2	Acer Campestre	Field maple	2	0.18
	Acer Platanoides	Norway maple	2	0.18
	Robinia Pseudoacacia	Black locust	2	0.18
	Quercus Robur	English oak	1.8	0.18
D1.5A0.6	Pinus Pinea	Stone pine	1.5	0.6
D1.5A0.2	Carpinus Betulus	European hornbeam	1.7	0.18
	Fagus Sylvatica	European beech	1.5	0.18
	Acer Pseudoplatanus	Sycamore maple	1.3	0.18
	Tilia Platyphyllos	Largeleaf linden	1.3	0.18
D1A0.4	Tilia	Linden	1.2	0.4
D1A0.2	Platanus Acerifolia	London plane	1.1	0.18
D1A0.6	Fraxinus	Ash	1	0.6
	Senegalia Greggii	Catclaw acacia	1	0.6

D1A0.2	Fraxinus Excelsior	European ash	1	0.18
	Tilia Cordata	Little leaf linden	1	0.18
	Ulmus Minor	Field elm	1	0.18
	Betula Pendula	Silver birch	0.9	0.18
D0.5A0.6	Koelreuteria paniculata	Golden rain tree	0.7	0.7
	Albizia Julibrissin	Silk tree	0.7	0.6
	Cercis Siliquastrum	Judas tree	0.6	0.6
	Acer Negundo	Manitoba maple	0.6	0.5
	Tamarix Gallica	French tamarisk	0.5	0.6
	Washingtonia filifera	California palm	0.5	0.6
	Olea Europaea	Olive	0.5	0.5
	Jacaranda mimosifolia	Blue jacaranda	0.4	0.6
	Sophora Japonica	Pagoda tree	0.4	0.6
	Populus Alba	Silver poplar	0.4	0.7
D0.5A0.4	Citrus Aurantium	Bitter orange	0.7	0.4
	Populus Nigra	Black poplar	0.7	0.4
	Ligustrum	Privet	0.7	0.4
D0.5A0.2	Abies Alba	Silver fir	0.7	0.18
	Pinus	Pine	0.7	0.18
	Ulmus Hollandica	Dutch elm	0.7	0.18
	Larix Decidua	European larch	0.5	0.18
	Picea Abies	European spruce	0.5	0.18
	Gleditsia Triacanthos	Thorny locust	0.5	0.18
	Cupressus Sempervirens	Cypress	0.4	0.3

Chapter 6: Conclusions and Discussion

6.1 Overall Conclusion

In current studies investigating the cooling effects of Urban Green Space (UGS), there is a common problem of high research costs but low generalizability of the results. It's hypothesized that the underlying reason for the low generalizability is that most studies have not been able to comprehensively examine the non-linear relationships in the complex system of UGS and urban microclimate. Therefore, a holistic multi-parameter approach has been proposed in this research, in contrast to the conventional reductionist single-parameter approach. The purpose of proposing this method is to provide a more comprehensive and accurate description of the complex relationship between environmental features and microclimate in UGS, which can ultimately promote the generalization of the research results.

Three studies that applied the multi-parameter approaches in investigating the interdependent influence of multiple environmental features of UGS on human thermal comfort were presented in this thesis. These studies have come to some common conclusions:

- 1) The influences of multiple environmental features of UGS on urban microclimate and human thermal comfort are interdependent.
- 2) The multi-parameter approach is superior to the single-parameter approach in revealing these interdependent influences.
- 3) When the interdependent relationships are comprehensively revealed, it is possible to reach specific and generalizable suggestions for climate-adaptive design and planning of UGS.

These studies also demonstrated the advantages of the multi-parameter approaches in terms of the following aspects:

- 1) Being capable of explaining issues for which previous linear single-parameter studies have not reached consistent conclusions.
- 2) Being capable of providing specific urban climatological recommendations for both under planning and already built-up UGS.
- 3) Being capable of investigating complex objects, including the combined cooling effects from vegetation and water body, and the influence from the prevailing wind direction.

In summary, the conclusions of the case studies show that the multi-parameter approach, compared to the previous single-parameter approach, is able to provide a more comprehensive description of the complex relationship between the urban environment and the urban climate, and to derive specific suggestions for practical climate-adaptive design and planning. These two advantages determine that the multi-parameter approach helps to promote the generalization of research results from microscale urban climatological studies.

6.2 Strengths of the Multi-parameter Approach Represented in Three Studies

6.2.1 Expanding the Scope of Explainable Phenomena

The study described in Chapter 3 demonstrated the importance of discussing the interdependent influence of multiple environmental features on urban climate with the help of multivariate experiments. This study showed that, for problems that cannot reach precise results, increasing the range of considered influencing elements will allow for a more comprehensive understanding of the problem and thus leading to more reliable conclusions.

This study answered a question that has been actively discussed but not yet reached consensus in previous urban climatological studies: whether the centralized or scattered urban green space has more effective cooling effects? The results of previous studies diverged on this issue. Some studies have found that the more fragmented the green areas is, the better its cooling effect can be (McGarigal and Cushman 2002; Xu and Yue 2008), while the results of other studies showed that the more compact the green space is, the better the cooling effect can be (Cao et al. 2010; Li et al. 2013). This study stated that this disagreement occurred as a result of neglecting the influence of vegetation types (tree-big canopy, tree-small canopy, hedges-shrubs, grass 50 cm, grass 10 cm).

According to the results of this study, the vegetation type is a non-negligible consideration when discussing the influence of spatial layout on the cooling effects of urban green spaces. When the cooling potential and shade area of a single green patch is large enough, the mean cooling effect grows as the dispersion of green space increases. When the cooling potential and shade area of a single green patch is not large enough, the mean cooling effect decreases as the dispersion of green space increase.

When we look at the previous studies in the light of the results of this study, it becomes clear why different research conclusions have been reached on the same question. In the studies of McGarigal and Xu (McGarigal and Cushman 2002; Xu and Yue 2008), the conclusion that

the more dispersed green space can generate better cooling effect is likely concluded due to the high density of vegetation in the green space they studied. On the contrary, in studies of Cao and Li (Cao et al. 2010; Li et al. 2013), the reason why they concluded that the cooling effect of concentrated green space is better is possibly because the vegetation density of the green space they studied is low, or they studied the central temperature of the green space rather than the average cooling effect of the whole green space on the city.

The results of this study demonstrated the importance of discussing the effects of multiple elements on urban climate together with the help of multivariate experiments. For problems that cannot reach precise results, increasing the range of considered influencing elements will allow for a more comprehensive understanding of the problem and thus leading to more reliable conclusions.

6.2.2 Expanding the Scope of Application of Urban Climatological Research

The study described in Chapter 4 investigated the relationship between spatial characters and PET in historic gardens. By means of the multi-parameter approaches, this study applied the findings of urban climatological research to an already-established urban green areas in an innovative way. The results of this study demonstrated the following advantages of the multi-parameter approach:

By mapping the human thermal comfort degree in the historical garden, urban climatological recommendations can also be applied to already established urban open spaces. Previous urban climatological studies have usually provided recommendations only to urban designers, planners, and decision-makers (Eliasson, 2000). This has led to a situation where those urban spaces that can no longer be modified are ignored by urban climatological studies. This study attempted to shift the audience of the recommendations to the users of the space by composite indicator PET. By assessing and mapping the human thermal comfort situation of the historical garden, climate adaptative recommendations can be directly accessible to urban dwellers.

By means of multivariate experiments, this study demonstrated how the multi-parameter approach can be used to generalize the results to a larger space by observing and simulating only a few sample sites. The following process was adopted: Firstly, the green spaces were grouped into several categories; then the sample sites of each category were selected for field measurement; meanwhile, each category was simulated through climate model; and finally, the results were generalized to all the spaces under the same category. In a park like Tiergarten,

which covers a very large area, it would take an enormous amount of time and effort to measure or simulate the entire park. With the above-described research process, the time and cost of the study can be greatly reduced while ensuring the accuracy of the results. The entire space can be understood by only a small number of real measurements and simulations. Thus, this study is a concrete example of how multi-parameter approaches can facilitate the universalization of urban climatology research results and shows how this can be achieved.

6.2.3 Capability of Investigating Multiple Land Surface Materials

The study described in Chapter 5 investigated the interdependent influences of three landscape design considerations on the thermal comfort of urban riverside greenways. The three factors include the urban prevailing wind direction, tree species, and the greenway trail position. The results support that the three factors of landscape design jointly influence the thermal environment. This study investigated the cooling effects of two urban cooling sources that have different physical properties: vegetation and waterbody. The advantage of the multi-parameter approach in this study is mainly manifested in enhancing the scope and complexity of the research object.

This study also demonstrated the necessity of the multi-parameter approach from the following points of view:

The necessity of composite indicator PET: In this study, the results assessed by PET and the results assessed by air temperature can lead to different conclusions. The results obtained from the PET evaluation revealed regularities that cannot be revealed with only air temperature. From this, it can be concluded that the composite indicator, especially the PET, is of great significance for urban climatological research.

The necessity of factorial experiments: Different features of the urban land surface are jointly influencing the urban atmosphere. The effect of one feature variable on the urban atmosphere varies upon the change of another feature variable. Therefore, this complex relationship between urban surface and urban atmosphere cannot be sufficiently explained by the single variate experiments.

6.3 Comparison with Similar Studies

6.3.1 Continuation of Other Holistic Studies

Using multi-parameter approaches to address the application of urban climatology is not unique to this study. In previous urban climatology studies, many researchers have made efforts to enhance the application potential of urban climatology research results. Many of these previous efforts have actually embodied the similar holistic thinking.

For instance, Local Climate Zones (LCZs), proposed by Stewart and Oke (2012), is essentially a holistic way of describing urban space with multidimensional features. Another example is the RayMan Model developed by Matzarakis et al. (2007) for calculating thermal comfort indices and SVF, which also shows the concept of using composite indices to describe the urban surface and urban atmosphere. Last but not least, the ENVI-met model developed by Bruse and Fler (1998) enables three-dimensional simulation of urban climate at the microscale, which greatly expands the possibilities of holistic urban climatological research.

This thesis is based on previous research and summarizes these approaches into a holistic research approach. None of the case studies in this paper would have been possible without these efforts by previous authors. These previous studies reveal a trend that the complex scientific attributes of urban climatology are becoming increasingly evident. In the future, the research approach of urban climatology will evolve toward a holistic, nonlinear, bottom-up emergent complex scientific approach.

In the early studies of urban climatology, the most used spatial descriptor was the aspect ratio (H/W) of urban street canyons. However, the aspect ratio is only able to express the information of a two-dimensional section of urban land surface and considered only the built environment. After that, the Sky View Factor (SVF) gradually became a more widespread indicator, which can convey information about the three-dimensional space. Although the SVF can represent the characteristics of an urban space more comprehensively than aspect ratio, it still cannot reflect the physical properties of the objects on the ground. For example, for the same SVF, whether trees or buildings are shading the sky has a completely different effect on the thermal condition at the measurement point. Furthermore, whether the land surface is covered by sand or vegetation can also have a significant impact on the results. The LCZ system addresses the need to simultaneously describe the spatial characteristics of the land surface and the material

properties of the land surface objects. The application of the factorial experimental approach by the LCZ system also further illustrates the suitability of this method in current and future complex studies of urban climatology (Figure 6-1).

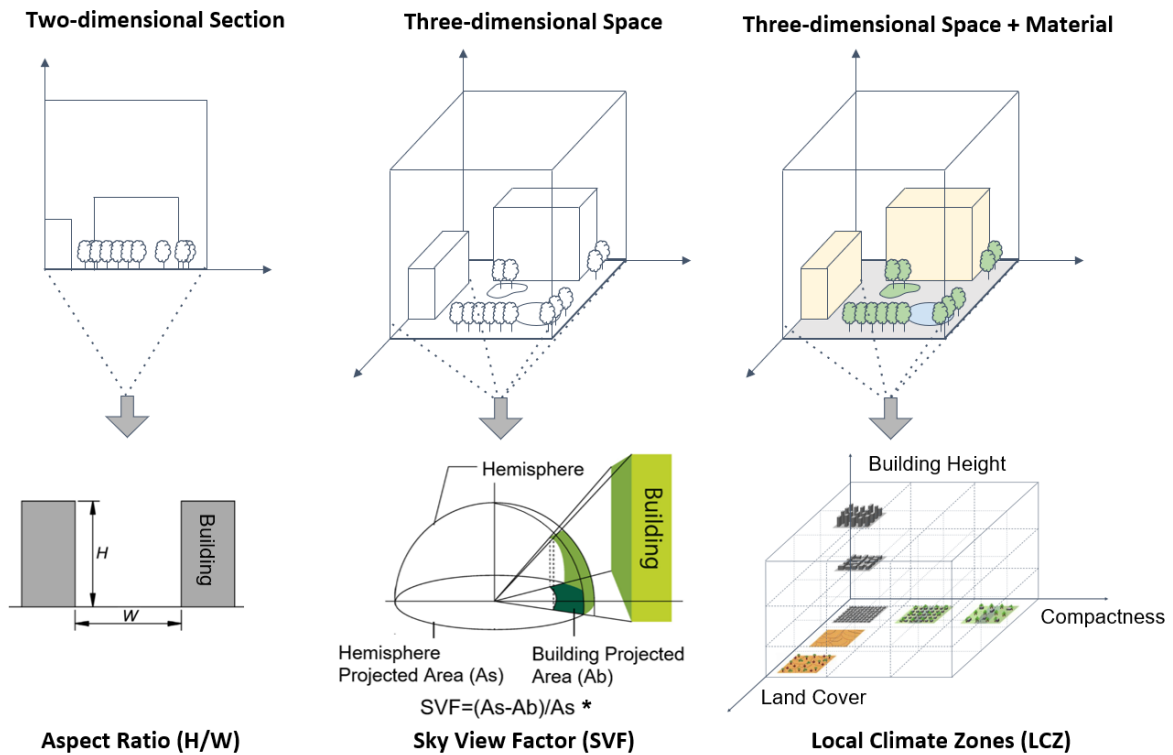


Figure 6-1 Different methods of urban space description can reflect information of different dimensions of space.

**Note: The figure of Sky View Factor (SVF) is adapted from “Proposal of System for Calculating Sky View Factor Using Google Street View”, by Nishio and Ito, 2021, p. 314.*

The comparison with studies similar to the three case studies in this thesis have been mentioned in Chapter 3 to 5.

6.3.2 Enhancements Over Previous Multi-parameter Studies at Microscale

In the field of microscale cooling effects of urban green space, there are already a few studies that simultaneously investigate the influence of multiple environmental parameters. For example, in 2014, Hai Yan et al. investigated the influence of multiple environmental characteristics on air temperature, including percentage of building area, percentage of vegetation cover, sky view factor, distance to park, and distance to water body (Yan et al., 2014). They set up 26 field measurement sites in urban spaces with different spatial characteristics near the Beijing Olympic Park. Their study found that

different spatial features have different degrees of influence on temperature. Moreover, changes in one spatial feature can affect the numerical relationship between another spatial feature and air temperature. Therefore, they concluded, “when testing the effects of the SVF on air temperature, it is important to control for the potential effects from other landscape variables, particularly the land cover features.” However, because this study used only field measurements, they cannot specifically interpret this interdependence among different spatial features. In addition, they concluded with the recommendation that landscape design needs to find a balance among multiple spatial features. But they cannot provide specific recommendations on how to balance these spatial features.

The method used in Morakinyo and Lam's 2016 study is similar to that of the studies in this thesis (Morakinyo and Lam, 2016). They used the ENVI-met model to simulate multiple idealized scenarios to investigate the influence of multiple environmental features on human thermal comfort, including the aspect ratio of street canyon, the prevailing wind condition, and morphological features of trees in the street canyon. In the conclusion, this study also suggests that “tree-selection should not only be based on singular characterization parameter; in conjunction with the LAI values, the leaf density distribution per height and the planting pattern or arrangement should all be adequately combined to achieved desired thermal comfort improvement.” However, similar to the previous study, this study does not specify how this integration should be achieved. Although the interdependent influence of multiple environmental parameters on human thermal comfort can be found in the results of this study, the authors did not describe this interdependence in detail, but rather analysed the influence of each parameter in parallel.

In contrast to previous studies of this type, the studies included in this thesis are more focused on the interdependent influence of multiple environmental parameters on human thermal comfort. By using a systematic factorial experimental approach, this interdependence can be clearly demonstrated. Due to this clarity, the results can also be translated into concrete design recommendations that inform designers in detail how to “balance” the multiple environmental features for a preferred climatic environment.

In addition, compared to previous studies, this research emphasizes the methodological systematicity. That is, it focuses on the completeness of the methodology from the philosophical-theoretical level, the methodological level, and the application level. In short, this study attempts to contribute to the generalizability of the research results from the point of view of two aspects. One aspect is to reveal the interdependent influence of

multiple environmental parameters on human thermal comfort in a more comprehensive and detailed manner. On the other hand, it promotes the methodological advancement of microscale research in urban climatology, which is itself an attempt at the methodological construction of urban climatology advocated by Oke (2006b).

6.3.3 Limitations of the Multi-parameter Approach

The factorial experimental approach used in this study simulates a large number of separate idealized scenarios. This means that the numerical simulation requires substantial manual work. The number of simulated scenarios grows exponentially whenever the investigated parameter or the level of a parameter increases.

For example, in the study described in Chapter 5, the number of scenarios in the full factorial design reaches 180. To control research cost, Latin Hypercube Sampling (LHS) was employed to select a subset of the scenarios for simulation experiment, limiting the simulated scenarios to 75. However, the sampling inevitably results in information loss and an increase in inaccuracy. Therefore, the multi-parameter approach requires the researcher to carefully consider the necessity of each parameter as well as a reasonable number of parameter levels when designing factorial experiments.

For urban climatological study, it is important to balance the expected accuracy and the computing cost. The multi-parameter approach is no exception. To minimize wasting computational costs, the researcher should firstly select a representative small number of scenarios to simulate and analyze the results. If after a first analysis the results are logical, the remaining scenarios can be then simulated to improve accuracy. The multi-parameter approach can enhance the benefit of research results with a moderate research cost. The results can be translated into specific and feasible design recommendations, which represent an increase in the applicability and generalizability of the research results.

6.4 Outreach

The effectiveness of multi-parameter approaches in urban climatology research is not just an isolated case. It is a concrete manifestation of the current paradigm shift triggered by the technological revolution. The alternation of the paradigm is always accompanied by the development of science. This profound fundamental change in paradigm is what we call a *paradigm shift*.

Every scientific development in history, as described by Thomas Kuhn, is a multi-stages process generally consisting of pre-science, normal science and the scientific revolution (Kuhn, 1962; Systems Innovation, 2020a). The pre-science is a domain that the paradigm is not yet formed, and the fundamental philosophical questions are still under debate. The normal science domain represents a period without significant change. Science in this stage is highly conservative and the scientists accept the present paradigm unquestioningly. As Lord Kelvin (1900) stated about the normal scientific stage in his speech: “There is nothing new to be discovered in physics now. All that remains is more and more precise measurement.” (Walfram-Research, 1996)

The scientific revolution occurs when anomalies that cannot be explained with the former paradigm appear. Confidence about the old paradigm is broken down and scientists struggle for a new paradigm. This stage seems like chaos but through which huge scientific progress can appear. These stages form a so-called Kuhn Cycle (Figure 6-2) and perform as a circular pattern that vividly interprets the progress of science.

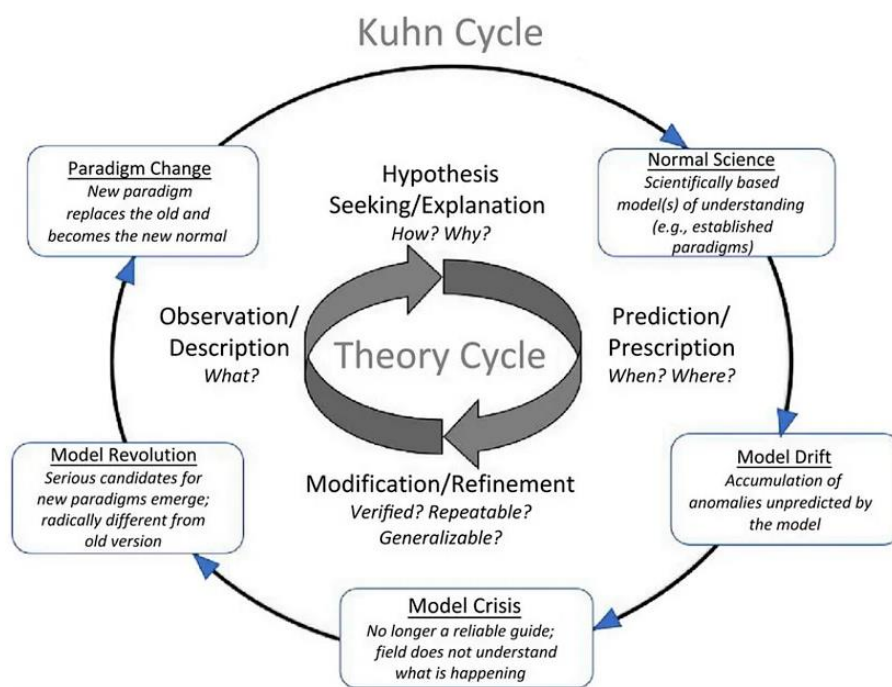


Figure 6-2 The Kuhn Cycle (Roth and Rosenzweig, 2020).

The paradigm shift brings the possibility to break the limitation of the former paradigm and find a new way out to an upper truth (Figure 6-3). Naturally, the accomplishment of a paradigm shift is a long-term work based on a huge amount of work and agreement of a lot of scholars. But it is always important to keep an eye on the

anomalies that appeared in research which have the potential to become a breach to another level of cognition of the world. And the alertness to the paradigm shift should be always ready.

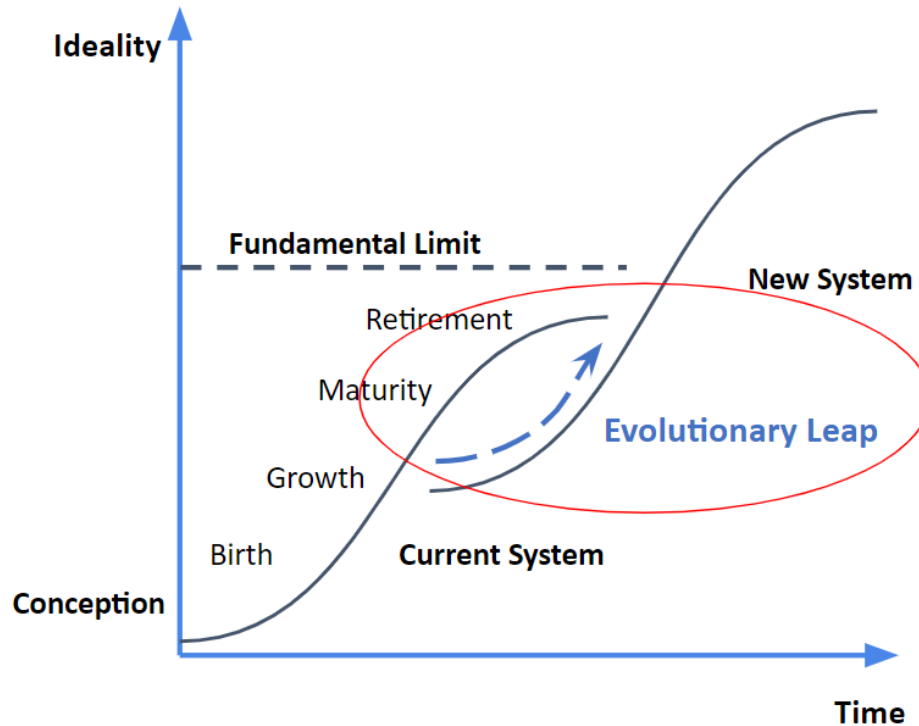


Figure 6-3 The S-curve of performance and functionality improvement in science development (Filmore, 2008).

The concept of paradigm shift is a reminder to scientists that we need to use our thinking, not be used by it. For very often, our thinking itself is the cause of many of the struggles we face. In summary, the problem discussed in this study is therefore a microcosm of the problem of the times. The conclusions generated by this study are also of value not only to urban climatology, but to many interdisciplinary fields, and to the process of the current scientific revolution. In the future, research in urban climatology could be integrated more with complex sciences to shorten the distance between scientific research and practical applications.

Additional Information

Information of coauthors' contribution in Chapter 3:

The candidate drafted the article (except for the PET part); improved it and responded to the peer reviewers' comments; reviewed studies on the relationship between the PCI effects and the morphology of green spaces and found the disagreement among these studies on whether centralized or dispersed green spaces have more intense cooling effects. Using this as an entry point, the candidate analyzed the results of simulation experiments through selected landscape metrics, including Patch Density (PD), Edge Density (ED) and Land Shape Index (LSI). The final results demonstrated, as expected, the advantages of this study in explaining the disagreement in previous studies. The candidate also designed and participated in the outdoor field measurement to evaluate the simulation results. The first author, who is also the candidate's supervisor, proposed the research idea; designed the simulation experiment; and supervised the writing of the article. The co-authors calculated and analyzed the PET values; drafted the part of PET; built and ran the model using ENVI-met; and calculated the sensible and latent heat fluxes.

Information of coauthors' contribution in Chapter 4:

Among the co-authors, Huiwen Zhang's contribution was to design the study and experiment, run the ENVI-met model and to write the English article text. Xiaoli Chi's contribution was to calculate the PET and generate the PET related figures. Felix Müller 's contribution was to translate the English text into German. Ines Langer's contribution was to arrange the measuring campaign. Sahar Sodoudi is the corresponding author and guides the research.

Publication Bibliography

Acero, J. A. and Arrizabalaga, J. (2018) 'Evaluating the performance of ENVI-met model in diurnal cycles for different meteorological conditions', *Theoretical and Applied Climatology*, vol. 131, no. 1, pp. 455–469.

Ahmed, K. S. (2003) 'Comfort in urban spaces: defining the boundaries of outdoor thermal comfort for the tropical urban environments.', *Energy and buildings*, 35(1), pp. 103–110.

Akbari, H. and Taha, H. (1992) 'The impact of trees and white surfaces on residential heating and cooling energy use in four Canadian cities', *Energy*, vol. 17, no. 2, pp. 141–149.

Ali, S. B. and Patnaik, S. (2019) 'Assessment of the impact of urban tree canopy on microclimate in Bhopal: A devised low-cost traverse methodology', *Urban Climate*, vol. 27, pp. 430–445.

Amani-Beni, M., Zhang, B., Xie, G. and Xu, J. (2018) 'Impact of urban park's tree, grass and waterbody on microclimate in hot summer days: A case study of Olympic Park in Beijing, China', *Urban forestry & urban greening*, vol. 32, pp. 1–6.

American Meteorological Society (ed) (1972) *Conference on Urban Environment and Second Conference on Biometeorology: 31 October to 2 November, American Meteorological Society, Philadelphia, PA*.

Andreou, E. (2013) 'Thermal comfort in outdoor spaces and urban canyon microclimate', *Renewable energy*, vol. 55, pp. 182–188.

Antoniadis, D., Katsoulas, N. and Papanastasiou, D. K. (2020) 'Thermal environment of urban schoolyards: current and future design with respect to children's thermal comfort', *Atmosphere*, vol. 11, no. 11, p. 1144.

Åström, D. O., Bertil, F. and Joacim, R. (2011) 'Heat wave impact on morbidity and mortality in the elderly population: a review of recent studies', *Maturitas*, vol. 69, no. 2, pp. 99–105.

Auyang, S. Y. (1998) *Foundations of complex-system theories: in economics, evolutionary biology, and statistical physics*, Cambridge University Press.

Bai, L., Ding, G., Gu, S., Bi, P., Su, B., Qin, D., Xu, G. and Liu, Q. (2014) 'The effects of summer temperature and heat waves on heat-related illness in a coastal city of China, 2011–2013', *Environmental research*, vol. 132, pp. 212–219.

Bärring, L., Mattsson, J. O. and Lindqvist, S. (1985) 'Canyon geometry, street temperatures and urban heat island in Malmö, Sweden', *Journal of climatology*, vol. 5, no. 4, pp. 433–444.

BauGB (2017) *BauGB - Baugesetzbuch ** [Online]. Available at <https://www.gesetze-im-internet.de/bbaug/BJNR003410960.html> (Accessed 27 August 2024).

BBauG (1976) *Bundesbaugesetz 1976, §§ 1- 13* [Online]. Available at <https://www.stadtgrenze.de/s/bbg/1976/bbaug1976-001.htm#001> (Accessed 27 August 2024).

Beaufort, F. (1805) *Beaufort Wind Scale: Developed in 1805 by Sir Francis Beaufort, U.K. Royal Navy* [Online], Storm Prediction Center - National Oceanic and Atmospheric Administration. Available at <https://www.spc.noaa.gov/faq/tornado/beaufort.html> (Accessed 2019).

- Bechtel, B., Alexander, P. J., Böhner, J., Ching, J., Conrad, O., Feddema, J., Mills, G., See, L. and Stewart, I. (2015) 'Mapping local climate zones for a worldwide database of the form and function of cities', *ISPRS International Journal of Geo-Information*, vol. 4, no. 1, pp. 199–219.
- Bi, P., Williams, S., Loughnan, M., Lloyd, G., Hansen, A., Kjellstrom, T., Dear, K. and Saniotis, A. (2011) 'The effects of extreme heat on human mortality and morbidity in Australia: implications for public health', *Asia-Pacific journal of public health*, vol. 23, 2 Suppl, 27S-36.
- Bitan, A. (1984) *Applied climatology and its contribution to planning and building*, Elsevier Sequoia.
- Boukhabl, M. and Alkam, D. (2012) 'Impact of vegetation on thermal conditions outside, Thermal modeling of urban microclimate, Case study: the street of the republic, Biskra', *Energy Procedia*, vol. 18, pp. 73–84.
- Bowler, D. E., Buyung-Ali, L., Knight, T. M. and Pullin, A. S. (2010) 'Urban greening to cool towns and cities: A systematic review of the empirical evidence', *Landscape and urban planning*, vol. 97, no. 3, pp. 147–155.
- Brazel, A. J. and Quatrocchi, D. (2005) 'Urban Climatology', in Oliver, J. E. (ed) *Encyclopedia of World Climatology*, Dordrecht, Springer Netherlands, pp. 766–779.
- Brown, G., Schebella, M. F. and Weber, D. (2014) 'Using participatory GIS to measure physical activity and urban park benefits', *Landscape and urban planning*, vol. 121, pp. 34–44.
- Brown, R. D. (2010) *Design with microclimate: the secret to comfortable outdoor space*, Island Press.
- Bruse, M. (2004) 'ENVI-met 3.0: updated model overview', *University of Bochum*. Retrieved from: www.envi-met.com.
- Bruse, M. (2017) *Knowledge Base: Obtaining Leaf Area Density Data* [Online]. Available at <http://www.envi-met.info/documents/onlinehelpv3/hs890.htm> (Accessed 11 January 2019).
- Bruse, M. and Fleer, H. (1998) 'Simulating surface–plant–air interactions inside urban environments with a three dimensional numerical model', *Environmental modelling & software*, vol. 13, 3-4, pp. 373–384.
- Bustanza, R., Lebel, G., Gosselin, P., Bélanger, D. and Chebana, F. (2013) 'Health impacts of the July 2010 heat wave in Quebec, Canada', *BMC public health*, vol. 13, no. 1, p. 56.
- California State University, F. (2018) *Factorial Designs* [Online]. Available at <https://web.archive.org/web/20120823205710/http://psych.csufresno.edu/psy144/Content/Design/Experimental/factorial.html> (Accessed 2 July 2024).
- Cao, X., Onishi, A., Chen, J. and Imura, H. (2010) 'Quantifying the cool island intensity of urban parks using ASTER and IKONOS data', *Landscape and urban planning*, vol. 96, no. 4, pp. 224–231.
- Cerra, J. F. (2016) 'Inland Adaptation: Developing a Studio Model for Climate-adaptive Design as a Framework for Design Practice', *Landscape Journal*, vol. 35, no. 1, pp. 37–56.
- Chan, S. Y., Chau, C. K. and Leung, T. M. (2017) 'On the study of thermal comfort and perceptions of environmental features in urban parks: A structural equation modeling approach', *Building and Environment*, vol. 122, pp. 171–183.

- Chandler, T. J. (1962) 'London's urban climate', *The Geographical Journal*, vol. 128, no. 3, pp. 279–298.
- Chandler, T. J. (1965) *The climate of London*, Hutchinson.
- Chandler, T. J. (1967) 'Night-time temperatures in relation to Leicester's urban form', *Meteorol. Mag.*, vol. 96, pp. 244–250.
- Chandler, T. J. (1976) 'Urban climatology and its relevance to urban design'.
- Chang, C.-R., Li, M.-H. and Chang, S.-D. (2007) 'A preliminary study on the local cool-island intensity of Taipei city parks', *Landscape and urban planning*, vol. 80, no. 4, pp. 386–395.
- Charles, K. E. (2003) 'Fanger's thermal comfort and draught models' [Online]. Available at <https://nascoinc.com/content/resources/PO-Fanger-Thermal-Comfort.pdf>.
- Chen, A., Yao, L., Sun, R. and Chen, L. (2014a) 'How many metrics are required to identify the effects of the landscape pattern on land surface temperature?', *Ecological indicators*, vol. 45, pp. 424–433.
- Chen, A., Yao, X. A., Sun, R. and Chen, L. (2014b) 'Effect of urban green patterns on surface urban cool islands and its seasonal variations', *Urban forestry & urban greening*, vol. 13, no. 4, pp. 646–654.
- Chen, F., Kusaka, H., Bornstein, R., Ching, J., Grimmond, C. S., Grossman - Clarke, S., Loridan, T., Manning, K. W., Martilli, A. and Miao, S. (2011) 'The integrated WRF/urban modelling system: development, evaluation, and applications to urban environmental problems', *International Journal of Climatology*, vol. 31, no. 2, pp. 273–288.
- Chen, G., Wang, D., Wang, Q., Li, Y., Wang, X., Hang, J., Gao, P., Ou, C. and Wang, K. (2020) 'Scaled outdoor experimental studies of urban thermal environment in street canyon models with various aspect ratios and thermal storage', *The Science of the total environment*, vol. 726, p. 138147.
- Chen, T., Yang, H., Chen, G., Lam, C. K. C., Hang, J., Wang, X., Liu, Y. and Ling, H. (2021) 'Integrated impacts of tree planting and aspect ratios on thermal environment in street canyons by scaled outdoor experiments', *The Science of the total environment*, vol. 764, p. 142920.
- Chen, Y.-C. and Matzarakis, A. (2018) 'Modified physiologically equivalent temperature—Basics and applications for western European climate', *Theoretical and Applied Climatology*, vol. 132, pp. 1275–1289.
- Cheung, P. K. and Jim, C. Y. (2019) 'Effects of urban and landscape elements on air temperature in a high-density subtropical city', *Building and Environment*, vol. 164, p. 106362.
- Chiesura, A. (2004) 'The role of urban parks for the sustainable city', *Landscape and urban planning*, vol. 68, no. 1, pp. 129–138.
- Collins, L. M., Dziak, J. J. and Li, R. (2009) 'Design of experiments with multiple independent variables: a resource management perspective on complete and reduced factorial designs', *Psychological methods*, vol. 14, no. 3, p. 202.
- Connors, J. P., Galletti, C. S. and Chow, W. T. L. (2013) 'Landscape configuration and urban heat island effects: assessing the relationship between landscape characteristics and land surface temperature in Phoenix, Arizona', *Landscape ecology*, vol. 28, no. 2, pp. 271–283.

- Cowan, T., Purich, A., Perkins, S., Pezza, A., Bosch, G. and Sadler, K. (2014) 'More frequent, longer, and hotter heat waves for Australia in the twenty-first century', *Journal of Climate*, vol. 27, no. 15, pp. 5851–5871.
- Crank, P. J., David J. Sailor, George Ban-Weiss and Taleghani, M. (2018) 'Evaluating the ENVI-met microscale model for suitability in analysis of targeted urban heat mitigation strategies', *Urban Climate*, vol. 26, pp. 188–197 [Online]. DOI: 10.1016/j.uclim.2018.09.002.
- Daniels, P. A. (1965) 'The urban heat island and air pollution with applications to Edmonton', *M. &*
- Declat-Barreto, J., Brazel, A. J., Martin, C. A., Chow, W. T. L. and Harlan, S. L. (2013) 'Creating the park cool island in an inner-city neighborhood: heat mitigation strategy for Phoenix, AZ', *Urban Ecosystems*, vol. 16, no. 3, pp. 617–635.
- Deng, S., Ma, J., Zhang, L., Jia, Z. and Ma, L. (2019) 'Microclimate simulation and model optimization of the effect of roadway green space on atmospheric particulate matter', *Environmental pollution (Barking, Essex : 1987)*, vol. 246, pp. 932–944.
- Doick, K. J., Peace, A. and Hutchings, T. R. (2014) 'The role of one large greenspace in mitigating London's nocturnal urban heat island', *Science of the total environment*, vol. 493, pp. 662–671.
- Dousset, B. and Gourmelon, F. (2003) 'Satellite multi-sensor data analysis of urban surface temperatures and landcover', *ISPRS Journal of Photogrammetry and Remote Sensing*, vol. 58, 1-2, pp. 43–54 [Online]. DOI: 10.1016/S0924-2716(03)00016-9.
- Du, H., Song, X., Jiang, H., Kan, Z., Wang, Z. and Cai, Y. (2016) 'Research on the cooling island effects of water body: A case study of Shanghai, China', *Ecological indicators*, vol. 67, pp. 31–38.
- DWD (2020) *DWD stations Duisburg-Baerl and Tönisvorst now top of the list with 41.2 degrees Celsius* [Online]. Available at https://www.dwd.de.translate.goog/DE/presse/pressemitteilungen/DE/2020/20201217_annulierung_lingen_news.html?_x_tr_sl=de&_x_tr_tl=en&_x_tr_hl=en-US (Accessed 2 July 2024).
- DWD (2023) *Wetter und Klima - Deutscher Wetterdienst - Press - The weather in Germany – Summer 2023* [Online]. Available at https://www.dwd.de/EN/press/press_release/EN/2023/20230830_the_weather_in_germany_in_summer_2023_news.html (Accessed 2 July 2024).
- DWD (2024a) *Flow model MUKLIMO_3 (basic version)* [Online]. Available at https://www.dwd.de/EN/ourservices/muklimo_basic/muklimo_basic_en.html (Accessed 4 July 2024).
- DWD (2024b) *Urban climate model PALM-4U* [Online]. Available at https://www.dwd.de/EN/ourservices/palm4u_en/palm4u_en.html; jsessionid=D7E188D7E89CCB8626C68FC724AFA457.live11051 (Accessed 30 August 2024).
- Eliasson, I. (2000) 'The use of climate knowledge in urban planning', *Landscape and urban planning*, vol. 48, 1-2, pp. 31–44.
- Ellefsen, R. (1991) 'Mapping and measuring buildings in the canopy boundary layer in ten US cities', *Energy and buildings*, vol. 16, 3-4, pp. 1025–1049.
- Eludoyin, O. M. (2014) 'A perspective of the diurnal aspect of thermal comfort in Nigeria', *Atmospheric and Climate Sciences*, vol. 4, no. 04, p. 696.

- Emmanuel, R., Rosenlund, H. and Johansson, E. (2007) 'Urban shading—a design option for the tropics? A study in Colombo, Sri Lanka', *International Journal of Climatology*, vol. 27, no. 14, pp. 1995–2004.
- enviadmin (2017a) *Knowledge Base: Lateral Boundary Conditions* [Online]. Available at <https://envi-met.info/documents/onlinehelpv3/hs760.htm> (Accessed 6 August 2023).
- enviadmin (2017b) *Knowledge Base: Overview Model DataFlow* [Online]. Available at <https://envi-met.info/documents/onlinehelpv3/hs810.htm> (Accessed 6 August 2023).
- enviadmin (2017c) *Knowledge Base: Overview Model Layout: Basic Layout of ENVI-met* [Online]. Available at <https://envi-met.info/documents/onlinehelpv3/hs800.htm> (Accessed 22 June 2022).
- enviadmin (2023a) *ENVI-met Model Architecture [A holistic microclimate model]* [Online]. Available at <https://envi-met.info/doku.php?id=intro:modelconcept> (Accessed 11 August 2023).
- enviadmin (2023b) *Thermal Comfort Indices provided by BIO-met [A holistic microclimate model]* [Online]. Available at <https://envi-met.info/doku.php?id=apps:biomet> (Accessed 30 August 2023).
- Erell, E. (2008) 'The application of urban climate research in the design of cities', *Advances in Building Energy Research*, vol. 2, no. 1, pp. 95–121.
- Erlwein, S., Zölch, T. and Pauleit, S. (2021) 'Regulating the microclimate with urban green in densifying cities: Joint assessment on two scales', *Building and Environment*, vol. 205, p. 108233.
- European Space Agency (2020) *Landsat TM/ETM - Historical Missions - Third Party Missions - Earth Online - ESA* [Online]. Available at <https://earth.esa.int/web/guest/missions/3rd-party-missions/historical-missions/landsat-tmetm;jsessionid=1EA2FC7F8965109D179B583259360FF0.jvm1> (Accessed 11 March 2020).
- Fabos, J. G. (1995) *Introduction and overview: the greenway movement, uses and potentials of greenways* [Online], Elsevier.
- Fabos, J. G. (2004) 'Greenway planning in the United States: its origins and recent case studies', *Landscape and urban planning*, vol. 68, 2-3, pp. 321–342.
- Fang, F. C. and Casadevall, A. (2011) 'Reductionistic and Holistic Science ▽', *Infection and Immunity*, vol. 79, no. 4, pp. 1401–1404.
- Fanger, P. O. (1972) *Thermal comfort, analysis and application in environmental engineering* [Online], McGraw Hill, New York.
- Farajzadeh, H. and Matzarakis, A. (2012) 'Evaluation of thermal comfort conditions in Ourmieh Lake, Iran', *Theoretical and Applied Climatology*, vol. 107, pp. 451–459.
- Filmore, P. R. (2008) 'Developing highly effective engineers: The significance of TRIZ', *TRIZCON2008, Kent State University, Ohio, USA*.
- Forman, R. T. T. (1995) *Land mosaics: The ecology of landscapes and regions*, Cambridge [England], Cambridge University Press.
- Foruzanmehr, A. (2015) 'People's perception of the loggia: A vernacular passive cooling system in Iranian architecture', *Sustainable Cities and Society*, vol. 19, pp. 61–67.
- Fouillet, A., Rey, G., Laurent, F., Pavillon, G., Bellec, S., Guihenneuc-Jouyaux, C., Clavel, J., Jouglu, E. and Hémon, D. (2006) 'Excess mortality related to the August 2003 heat wave in

- France', *International archives of occupational and environmental health*, vol. 80, no. 1, pp. 16–24.
- Frommes, B. (1982) 'Urban and building climatology in practice and in professional education.', *Energy and buildings*, vol. 5.1, pp. 31–37.
- Gabriel, K. M. A. and Endlicher, W. R. (2011) 'Urban and rural mortality rates during heat waves in Berlin and Brandenburg, Germany', *Environmental pollution (Barking, Essex : 1987)*, vol. 159, 8-9, pp. 2044–2050.
- Gagge, A. P., Fobelets, A. P. and Berglund, L. (1986) 'A standard predictive index of human response to the thermal environment'.
- GB/T 37529-2019 *Chengshi zongti guihua qihou kexingxing lunzheng jishu [Technical for Climatic Feasibility Demonstration in Master Planning]* [Online]. Available at https://www.cma.gov.cn/zfxxgk/gknr/flfgbz/bz/202209/t20220921_5099223.html.
- Giannakis, E., Bruggeman, A., Poulou, D., Zoumides, C. and Eliades, M. (2016) 'Linear parks along urban rivers: perceptions of thermal comfort and climate change adaptation in Cyprus', *Sustainability*, vol. 8, no. 10, p. 1023.
- Givoni, B. (1997) 'Performance of the “shower” cooling tower in different climates', *Renewable energy*, vol. 10, 2-3, pp. 173–178.
- Givoni, B. (1998) *Climate considerations in building and urban design*, John Wiley & Sons.
- Gobster, P. H. (1995) 'Perception and use of a metropolitan greenway system for recreation', *Landscape and urban planning*, vol. 33, 1-3, pp. 401–413.
- Golany, G. S. (1996) 'Urban design morphology and thermal performance', *Atmospheric Environment*, vol. 30, no. 3, pp. 455–465.
- Gomez-Munoz, V. M., Porta-Gandara, M. A. and Fernández, J. L. (2010) 'Effect of tree shades in urban planning in hot-arid climatic regions', *Landscape and urban planning*, 94(3).
- Grigg, D. (1965) 'The logic of regional systems 1', *Annals of the Association of American Geographers*, vol. 55, no. 3, pp. 465–491.
- Gromke, C., Blocken, B., Janssen, W., Merema, B., Twan, v. H. and Timmermans, H. (2015) 'CFD analysis of transpirational cooling by vegetation: Case study for specific meteorological conditions during a heat wave in Arnhem, Netherlands', *Building and Environment*, vol. 83, pp. 11–26.
- Gulyás, Á., Unger, J. and Matzarakis, A. (2006) 'Assessment of the microclimatic and human comfort conditions in a complex urban environment: modelling and measurements', *Building and Environment*, vol. 41, no. 12, pp. 1713–1722.
- Habeeb, D., Vargo, J. and Stone, B. (2015) 'Rising heat wave trends in large US cities', *Natural Hazards*, vol. 76, no. 3, pp. 1651–1665.
- Hardin, P. J. and Jensen, R. R. (2007) 'The effect of urban leaf area on summertime urban surface kinetic temperatures: a Terre Haute case study', *Urban forestry & urban greening*, vol. 6, no. 2, pp. 63–72.
- Hebbert, M. (2014) 'Climatology for city planning in historical perspective', *Urban Climate*, vol. 10, pp. 204–215.
- Hebbert, M. and Mackillop, F. (2013) 'Urban Climatology Applied to Urban Planning: A Postwar Knowledge Circulation Failure', *International Journal of Urban and Regional Research*, vol. 37, no. 5, pp. 1542–1558.

- Hedquist, B. C. and Brazel, A. J. (2014) 'Seasonal variability of temperatures and outdoor human comfort in Phoenix, Arizona, USA', *Building and Environment*, vol. 72, pp. 377–388.
- Hellmund, P. C. and Smith, D. (2013) *Designing greenways: sustainable landscapes for nature and people*, Island Press.
- Helton, J. C. and Davis, F. J. (2003) 'Latin hypercube sampling and the propagation of uncertainty in analyses of complex systems', *Reliability Engineering and System Safety*, vol. 81, no. 1, pp. 23–69.
- Hilbrandt, H. (2017) 'Insurgent participation: Consensus and contestation in planning the redevelopment of Berlin-Tempelhof airport', *Urban Geography*, vol. 38, no. 4, pp. 537–556.
- Hong, B. and Lin, B. (eds) (2014) *Numerical study of the influences of different patterns of the building and green space on micro-scale outdoor thermal comfort and indoor natural ventilation*, Springer.
- Höppe, P. R. (1993) 'Heat balance modelling', *Experientia*, vol. 49, no. 9, pp. 741–746.
- Höppe, P. R. (1999) 'The physiological equivalent temperature - a universal index for the biometeorological assessment of the thermal environment', *International journal of biometeorology*, vol. 43, no. 2, pp. 71–75.
- Hüttl, R. F., David, K. and Uwe Schneider, B. (2020) *Historische Gärten und Klimawandel*, De Gruyter.
- Huttner, S., Bruse, M. and Dostal, P. (eds) (2008) *Using ENVI-met to simulate the impact of global warming on the microclimate in central European cities*.
- IPCC (2018) *Annex II Glossary-Adaptation*, https://www.ipcc.ch/site/assets/uploads/2018/02/WGIIAR5-AnnexII_FINAL.pdf.
- Ireland, J. D. (2007) *Udana and the Itivuttaka: two classics from the Pali Canon*, Buddhist Publication Society.
- ISO (2005) *Ergonomics of the thermal environment: Analytical determination and interpretation of thermal comfort using calculation of the PMV and PPD indices and local thermal comfort criteria*, International Organization for Standardization.
- Jänicke, B., Milošević, D. and Manavvi, S. (2021) 'Review of User-Friendly Models to Improve the Urban Micro-Climate', *Atmosphere*, vol. 12, no. 10, p. 1291.
- Janković, V. (2013) 'A historical review of urban climatology and the atmospheres of the industrialized world', *Wiley Interdisciplinary Reviews: Climate Change*, vol. 4, no. 6, pp. 539–553.
- Jansson, C. (2006) *Urban microclimate and surface hydrometeorological processes*, KTH.
- Jáuregui, E. (1990) 'Influence of a large urban park on temperature and convective precipitation in a tropical city', *Energy and buildings*, vol. 15, 3-4, pp. 457–463.
- Jendritzky, G., Dear, R. de and Havenith, G. (2012) 'UTCI—why another thermal index?', *International journal of biometeorology*, vol. 56, no. 3, pp. 421–428.
- John Godfrey Saxe (1872) *The Poems of John Godfrey Saxe/The Blind Men and the Elephant - Wikisource, the free online library* [Online]. Available at https://en.wikisource.org/wiki/The_Poems_of_John_Godfrey_Saxe/The_Blind_Men_and_the_Elephant (Accessed 2 July 2024).

- Johnson, G. T. and Watson, I. D. (1984) 'The determination of view-factors in urban canyons', *Journal of Climate and Applied Meteorology*, vol. 23, no. 2, pp. 329–335.
- Jusuf, S. K., Wong, N. H., Hagen, E., Anggoro, R. and Hong, Y. (2007) 'The influence of land use on the urban heat island in Singapore', *Habitat international*, vol. 31, no. 2, pp. 232–242.
- Kleerekoper, L. (2017) 'Urban Climate Design'.
- Klein, R. J. T., Huq, S., Denton, F., Downing, T. E., Richels, R. G., Robinson, J. B. and Toth, F. L. (2007) 'Inter-relationships between adaptation and mitigation'.
- Kolokotroni, M., Zhang, Y. and Watkins, R. (2007) 'The London Heat Island and building cooling design', *Solar Energy*, vol. 81, no. 1, pp. 102–110.
- Kovats, R. S. and Hajat, S. (2008) 'Heat stress and public health: a critical review', *Annu. Rev. Public Health*, vol. 29, pp. 41–55.
- Kratzer, A. (1956) *Das Stadtklima*, F. Vieweg.
- Kuhn, T. S. (1962) 'The structure of scientific revolutions University of Chicago Press Chicago', *Originally published in*.
- Lalic, B. and Mihailovic, D. T. (2004) 'An Empirical Relation Describing Leaf-Area Density inside the Forest for Environmental Modeling', *Journal of Applied Meteorology*, vol. 43, no. 4, pp. 641–645 [Online]. DOI: 10.1175/1520-0450(2004)043<0641:AERDLD>2.0.CO;2 (Accessed 12 July 2018).
- Landeshauptstadt Stuttgart (2022) *Klima in der Stadtplanung* [Online]. Available at <https://www.stuttgart.de/leben/umwelt/klima/klimawandel/klima-in-der-planung.php> (Accessed 28 August 2024).
- Landsberg, H. E. (1947) *Microclimatology. Architectural Forum* 86.3,114-119 [Online].
- Landsberg, H. E. (1981) *The urban climate*, Academic press.
- Larson, L. R., Keith, S. J., Fernandez, M., Hallo, J. C., Shafer, C. S. and Jennings, V. (2016) 'Ecosystem services and urban greenways: What's the public's perspective?', *Ecosystem Services*, vol. 22, pp. 111–116.
- Lehmann, I., Mathey, J., Rößler, S., Bräuer, A. and Goldberg, V. (2014) 'Urban vegetation structure types as a methodological approach for identifying ecosystem services—Application to the analysis of micro-climatic effects', *Ecological indicators*, vol. 42, pp. 58–72.
- Lehnert, M., Geletič, J., Husák, J. and Vysoudil, M. (2015) 'Urban field classification by “local climate zones” in a medium-sized Central European city: the case of Olomouc (Czech Republic)', *Theoretical and applied climatology*, vol. 122, 3-4, pp. 531–541.
- Lenzholzer, S. (2012) 'Research and design for thermal comfort in Dutch urban squares', *Resources, conservation and recycling*, vol. 64, pp. 39–48.
- Li, H., Wang, A., Yuan, F., Guan, D., Jin, C., Wu, J. and Zhao, T. (2016) 'Evapotranspiration dynamics over a temperate meadow ecosystem in eastern Inner Mongolia, China', *Environmental Earth Sciences*, vol. 75, no. 11.
- Li, H., Wolter, M., Wang, X. and Sodoudi, S. (2018) 'Impact of land cover data on the simulation of urban heat island for Berlin using WRF coupled with bulk approach of Noah-LSM', *Theoretical and Applied Climatology*, vol. 134, 1-2, pp. 67–81.

- Li, H., Zhou, Y., Li, X., Meng, L., Wang, X., Wu, S. and Sodoudi, S. (2018) 'A new method to quantify surface urban heat island intensity', *Science of the total environment*, vol. 624, pp. 262–272.
- Li, H., Zhou, Y., Wang, X., Zhou, X., Zhang, H. and Sodoudi, S. (2019) 'Quantifying urban heat island intensity and its physical mechanism using WRF/UCM', *Science of the total environment*, vol. 650, pp. 3110–3119.
- Li, R. and Chi, X. (2014) 'Thermal comfort and tourism climate changes in the Qinghai–Tibet Plateau in the last 50 years', *Theoretical and Applied Climatology*, vol. 117, pp. 613–624.
- Li, X., Zhou, W. and Ouyang, Z. (2013) 'Relationship between land surface temperature and spatial pattern of greenspace: What are the effects of spatial resolution?', *Landscape and urban planning*, vol. 114, pp. 1–8.
- Li, X., Zhou, W., Ouyang, Z., Xu, W. and Zheng, H. (2012) 'Spatial pattern of greenspace affects land surface temperature: evidence from the heavily urbanized Beijing metropolitan area, China', *Landscape ecology*, vol. 27, no. 6, pp. 887–898.
- Lindberg, F., Holmer, B. and Thorsson, S. (2008) 'SOLWEIG 1.0—Modelling spatial variations of 3D radiant fluxes and mean radiant temperature in complex urban settings', *International journal of biometeorology*, vol. 52, no. 7, pp. 697–713.
- Lindsey, G. and Nguyen, D. B. (2004) 'Use of greenway trails in Indiana', *Journal of Urban Planning and Development*, vol. 130, no. 4, pp. 213–217.
- Litton, R. B. (1977) 'River landscape quality and its assessment. In: Proceedings river recreation management and research symposium, USDA Forest Service', *General Technical Report, North Central Forest Experiment Station, USDA Forest Service*, NC-28, pp. 46–54.
- Liu, H. and Weng, Q. (2008) 'Seasonal variations in the relationship between landscape pattern and land surface temperature in Indianapolis, USA', *Environmental monitoring and assessment*, vol. 144, 1-3, pp. 199–219.
- Liu, Z., Wenwen Cheng, C.Y. Jim, Morakinyo, T. E., Shi, Y. and Ng, E. (2021) 'Heat mitigation benefits of urban green and blue infrastructures: A systematic review of modeling techniques, validation and scenario simulation in ENVI-met V4', *Building and Environment*, vol. 200, p. 107939 [Online]. DOI: 10.1016/j.buildenv.2021.107939.
- Lowry, W. P. (1977) 'Empirical estimation of urban effects on climate: a problem analysis', *Journal of Applied Meteorology*, vol. 16, no. 2, pp. 129–135.
- Maggiotto, G., Buccolieri, R., Santo, M. A., Leo, L. S. and Silvana Di Sabatino (2014) 'Validation of temperature-perturbation and CFD-based modelling for the prediction of the thermal urban environment: the Lecce (IT) case study', *Environmental modelling & software*, vol. 60, pp. 69–83 [Online]. DOI: 10.1016/j.envsoft.2014.06.001.
- Maimaitiyiming, M., Ghulam, A., Tiyip, T., Pla, F., Latorre-Carmona, P., Halik, Ü., Sawut, M. and Caetano, M. (2014) 'Effects of green space spatial pattern on land surface temperature: Implications for sustainable urban planning and climate change adaptation', *ISPRS Journal of Photogrammetry and Remote Sensing*, vol. 89, pp. 59–66.
- Malek, E. and Bingham, G. E. (1993) 'Comparison of the Bowen ratio-energy balance and the water balance methods for the measurement of evapotranspiration', *Journal of Hydrology*, vol. 146, pp. 209–220.

- Manavvi, S. and Rajasekar, E. (2022) 'Evaluating outdoor thermal comfort in urban open spaces in a humid subtropical climate: Chandigarh, India', *Building and Environment*, vol. 209, p. 108659.
- Mathey, J., Röbler, S., Banse, J., Lehmann, I. and Bräuer, A. (2015) 'Brownfields as an element of green infrastructure for implementing ecosystem services into urban areas', *Journal of Urban Planning and Development*, vol. 141, no. 3, A4015001.
- Matzarakis, A. (2007) 'Climate, thermal comfort and tourism', *Climate change and tourism-assessment and coping strategies*, pp. 139–154.
- Matzarakis, A. (2012) 'RayMan and SkyHelios model-two tools for urban climatology', *Proceedings MettoolsVIII*, vol. 8, pp. 1–6.
- Matzarakis, A. and Amelung, B. (2008) 'Physiological equivalent temperature as indicator for impacts of climate change on thermal comfort of humans', in *Seasonal forecasts, climatic change and human health*, Springer, pp. 161–172.
- Matzarakis, A., Fröhlich, D., Marcel, G., Christine Ketterer and Andreas Peer (2015) *Developments and applications of thermal indices in urban structures by RayMan and SkyHelios model* [Online].
- Matzarakis, A., Gangwisch, M. and Fröhlich, D. (2021) 'RayMan and SkyHelios model', *Urban microclimate modelling for comfort and energy studies*, pp. 339–361.
- Matzarakis, A., Martinelli, L. and Ketterer, C. (2016) 'Relevance of Thermal Indices for the Assessment of the Urban Heat Island', in *Counteracting Urban Heat Island Effects in a Global Climate Change Scenario*, Springer, Cham, pp. 93–107.
- Matzarakis, A. and Matuschek, O. (2011) 'Sky view factor as a parameter in applied climatology-rapid estimation by the SkyHelios model', *Meteorologische Zeitschrift*, vol. 20, no. 1, p. 39.
- Matzarakis, A. and Mayer, H. (1997) 'Heat stress in Greece', *International journal of biometeorology*, vol. 41, no. 1, pp. 34–39.
- Matzarakis, A., Mayer, H. and Iziomon, M. G. (1999) 'Applications of a universal thermal index: physiological equivalent temperature', *International journal of biometeorology*, vol. 43, no. 2, pp. 76–84.
- Matzarakis, A., Rocco, M. de and Najjar, G. (2009) 'Thermal bioclimate in Strasbourg-the 2003 heat wave', *Theoretical and applied climatology*, vol. 98, no. 3, pp. 209–220.
- Matzarakis, A. and Rutz, F. (2000) *Estimation and calculation of the mean radiant temperature within urban structures* [Online]. Available at <https://scholar.google.de/citations?user=xhgrlf0aaaaj&hl=en&oi=sra>.
- Matzarakis, A., Rutz, F. and Mayer, H. (2007) 'Modelling radiation fluxes in simple and complex environments—application of the RayMan model', *International journal of biometeorology*, vol. 51, no. 4, pp. 323–334.
- Matzarakis, A., Rutz, F. and Mayer, H. (2010) 'Modelling radiation fluxes in simple and complex environments: basics of the RayMan model', *International journal of biometeorology*, vol. 54, no. 2, pp. 131–139.
- Mayer, H. and Höpfe, P. (1987) 'Thermal comfort of man in different urban environments.', *Theoretical and applied climatology*, 38(1), pp. 43–49.

- McGarigal, K. and Cushman, S. A. (2002) 'Comparative evaluation of experimental approaches to the study of habitat fragmentation effects', *Ecological applications*, vol. 12, no. 2, pp. 335–345.
- Mckay, M. D., Beckman, R. J. and Conover, W. J. (1979) 'A Comparison of Three Methods for Selecting Values of Input Variables in the Analysis of Output from a Computer Code', *Technometrics*, vol. 21, no. 2, p. 239 [Online]. DOI: 10.2307/1268522.
- Meehl, G. A. and Tebaldi, C. (2004) 'More intense, more frequent, and longer lasting heat waves in the 21st century', *Science*, vol. 305, no. 5686, pp. 994–997.
- Meir, P., Grace, J. and Miranda, A. C. (2000) 'Photographic method to measure the vertical distribution of leaf area density in forests', *Agricultural and Forest Meteorology*, vol. 102, 2-3, pp. 105–111 [Online]. DOI: 10.1016/S0168-1923(00)00122-2 (Accessed 12 July 2018).
- Middel, A., Chhetri, N. and Quay, R. (2015) 'Urban forestry and cool roofs: Assessment of heat mitigation strategies in Phoenix residential neighborhoods', *Urban forestry & urban greening*, vol. 14, no. 1, pp. 178–186.
- Middel, A., Häb, K., Brazel, A. J., Martin, C. A. and Guhathakurta, S. (2014) 'Impact of urban form and design on mid-afternoon microclimate in Phoenix Local Climate Zones', *Landscape and urban planning*, vol. 122, pp. 16–28.
- Mihalakakou, G., Santamouris, M., Papanikolaou, N., Cartalis, C. and Tsangrassoulis, A. (2004) 'Simulation of the urban heat island phenomenon in Mediterranean climates', *Pure and Applied Geophysics*, vol. 161, no. 2, pp. 429–451.
- Mills, G. (2006) 'Progress toward sustainable settlements: a role for urban climatology', *Theoretical and applied climatology*, vol. 84, 1-3, pp. 69–76.
- Mills, G. (2014) 'Urban climatology: History, status and prospects', *Urban Climate*, vol. 10, pp. 479–489.
- Mills, G., Ching, J., See, L., Bechtel, B. and Foley, M. (2015) *An introduction to the WUDAPT project. In proceedings of the 9th International Conference on Urban Climate* [Online], Toulouse, France. Available at https://www.wudapt.org/wp-content/uploads/2015/05/Mills_etal_ICUC9.pdf.
- Ministerium für Landesentwicklung und Wohnen Baden-Württemberg (2012) *Städtebauliche Klimafibel - Hinweise für die Bauleitplanung* [Online]. Available at https://wm.baden-wuerttemberg.de/fileadmin/redaktion/m-wm/intern/Publikationen/Bauen/Klimafibel_2012.pdf.
- Moore, G. E. (1998) 'Cramming more components onto integrated circuits', *Proceedings of the IEEE*, vol. 86, no. 1, pp. 82–85.
- Morabito, M., Profili, F., Crisci, A., Francesconi, P., Gensini, G. F. and Orlandini, S. (2012) 'Heat-related mortality in the Florentine area (Italy) before and after the exceptional 2003 heat wave in Europe: an improved public health response?', *International journal of biometeorology*, vol. 56, no. 5, pp. 801–810.
- Morakinyo, T. E. and Lam, Y. F. (2016) 'Simulation study on the impact of tree-configuration, planting pattern and wind condition on street-canyon's micro-climate and thermal comfort', *Building and Environment*, vol. 103, pp. 262–275.
- Müller, N., Kuttler, W. and Barlag, A.-B. (2014) 'Counteracting urban climate change: adaptation measures and their effect on thermal comfort', *Theoretical and applied climatology*, vol. 115, 1-2, pp. 243–257.

- Munn, R. E. (1973) 'Urban meteorology: some selected topics', *Bulletin of the American Meteorological Society*, vol. 54, no. 2, pp. 90–93.
- Munn, R. E. (2013) *Biometeorological methods*, Elsevier.
- NDRC (2013) *Guojia shiying qihou bianhua zhanlue [National Climate Change Adaptation Strategy]* [Online]. Available at <https://www.gov.cn/gzdt/att/att/site1/20131209/001e3741a2cc140f6a8701.pdf>.
- NDRC (2022) *Guojia shiying qihou bianhua zhanlue 2035 [National Climate Change Adaptation Strategy 2035]* [Online]. Available at <https://www.mee.gov.cn/xxgk2018/xxgk/xxgk03/202206/W020220613636562919192.pdf>.
- Ng, E. (2012) 'Towards planning and practical understanding of the need for meteorological and climatic information in the design of high - density cities: A case - based study of Hong Kong', *International Journal of Climatology*, vol. 32, no. 4, pp. 582–598.
- Nikolopoulou, M. and Lykoudis, S. (2006) 'Thermal Comfort in Outdoor Urban Spaces: analysis across different European countries', *Building and Environment*, 41(11), pp. 1455–1470.
- Nishio, S. and Ito, F. (2021) 'Proposal of system for calculating sky view factor using Google Street View', *Frontiers of Real Estate Science in Japan*, p. 313.
- Nora, S. (2018) *Stadtklima Stuttgart - eine städtebauliche Klimafibel* [Online]. Available at https://www.klima.tu-berlin.de/dokuwiki/doku.php?id=wiki:staedtebauliche_klimafibel_stuttgart.
- Nouri, A. S., Afacan, Y., Çalışkan, O., Lin, T.-P. and Matzarakis, A. (2021) 'Approaching environmental human thermophysiological thresholds for the case of Ankara, Turkey', *Theoretical and Applied Climatology*, vol. 143, pp. 533–555.
- Nouri, A. S. and Bártolo, H. (2013) *A bottom-up perspective upon climate change— Approaches towards the local scale and microclimatic assessment*, Taylor & Francis: Lisbon, Portugal.
- Nouri, A. S., Costa, J. P., Santamouris, M. and Matzarakis, A. (2018) 'Approaches to outdoor thermal comfort thresholds through public space design: A review', *Atmosphere*, vol. 9, no. 3, p. 108.
- Nouri, A. S. and Matzarakis, A. (2019) 'The maturing interdisciplinary relationship between human biometeorological aspects and local adaptation processes: an encompassing overview', *Climate*, vol. 7, no. 12, p. 134.
- Oehlert, G. W. (2010) *A first course in design and analysis of experiments*.
- Oke, T. R. (1973) 'City size and the urban heat island', *Atmospheric Environment (1967)*, vol. 7, no. 8, pp. 769–779.
- Oke, T. R. (1981) 'Canyon geometry and the nocturnal urban heat island: comparison of scale model and field observations', *Journal of climatology*, vol. 1, no. 3, pp. 237–254.
- Oke, T. R. (1984a) 'Methods in urban climatology', *Applied Climatology*, vol. 14, pp. 19–29.
- Oke, T. R. (1984b) 'Towards a prescription for the greater use of climatic principles in settlement planning', *Energy and buildings*, vol. 7, no. 1, pp. 1–10.

- Oke, T. R. (1995) 'The heat island of the urban boundary layer: characteristics, causes and effects', in *Wind climate in cities*, Springer, pp. 81–107.
- Oke, T. R. (1997) 'Urban environments', *The surface climates of Canada*, pp. 303–327.
- Oke, T. R. (1998) 'Observing urban weather and climate', *Rep. WMO/TD*.
- Oke, T. R. (2006a) *Initial guidance to obtain representative meteorological observations at urban sites*, World Meteorological Organization WMO/TD-No. 1250 [Online]. Available at <https://library.wmo.int/records/item/35333-initial-guidance-to-obtain-representative-meteorological-observations-at-urban-sites>.
- Oke, T. R. (2006b) 'Towards better scientific communication in urban climate', *Theoretical and applied climatology*, vol. 84, 1-3, pp. 179–190.
- Olgay, V. and Olgay, A. (1963) 'Design with climate', *Bioclimatic Approach to Architectural Regionalism*, New Jersey.
- Olgay, V. (2015) *Design with climate: bioclimatic approach to architectural regionalism*, Princeton University Press.
- Ouyang, W., Sinsel, T., Simon, H., Morakinyo, T. E., Liu, H. and Ng, E. (2022) 'Evaluating the thermal-radiative performance of ENVI-met model for green infrastructure typologies: Experience from a subtropical climate', *Building and Environment*, vol. 207, p. 108427 [Online]. DOI: 10.1016/j.buildenv.2021.108427.
- Ozkeresteci, I., Crewe, K., Brazel, A. J. and Bruse, M. (eds) (2003) *Use and evaluation of the ENVI-met model for environmental design and planning: an experiment on linear parks*.
- Page, J. K. (1968) 'The fundamental problems of building climatology considered from the point of view of decision-making by the architect and urban designer', in *Symposium on Urban Climates and Building Climatology, Brussels, Belgium*, pp. 10–21.
- Pantavou, K., Theoharatos, G., Mavrakakis, A. and Santamouris, M. (2011) 'Evaluating thermal comfort conditions and health responses during an extremely hot summer in Athens', *Building and Environment*, vol. 46, no. 2, pp. 339–344.
- Park, M., Hagishima, A., Tanimoto, J. and Narita, K. (2012) 'Effect of urban vegetation on outdoor thermal environment: field measurement at a scale model site', *Building and Environment*, vol. 56, pp. 38–46.
- Patton, D. R. (1975) 'A diversity index for quantifying habitat "edge"', *Wildlife Society Bulletin (1973-2006)*, vol. 3, no. 4, pp. 171–173.
- Patz, J. A., Campbell-Lendrum, D., Holloway, T. and Foley, J. A. (2005) 'Impact of regional climate change on human health', *Nature*, vol. 438, no. 7066, pp. 310–317.
- Perini, K. and Magliocco, A. (2014) 'Effects of vegetation, urban density, building height, and atmospheric conditions on local temperatures and thermal comfort', *Urban forestry & urban greening*, vol. 13, no. 3, pp. 495–506.
- Pflüger, Y., Rackham, A. and Larned, S. (2010) 'The aesthetic value of river flows: An assessment of flow preferences for large and small rivers', *Landscape and urban planning*, vol. 95, 1-2, pp. 68–78.
- Pozas, B. M. and González, F. J. N. (2016) 'Hygrothermal behaviour and thermal comfort of the vernacular housings in the Jerte Valley (Central System, Spain)', *Energy and buildings*, vol. 130, pp. 219–227.

- Price, J. C. (1984) 'Land surface temperature measurements from the split window channels of the NOAA 7 Advanced Very High Resolution Radiometer', *Journal of Geophysical Research: Atmospheres*, vol. 89, D5, pp. 7231–7237.
- Ross, J., Ross, V. and Koppel, A. (2000) 'Estimation of leaf area and its vertical distribution during growth period', *Agricultural and Forest Meteorology*, vol. 101, no. 4, pp. 237–246.
- Roth, A. and Rosenzweig, E. (2020) 'Advancing empirical science in operations management research: A clarion call to action', *Manufacturing & Service Operations Management*, vol. 22, no. 1, pp. 179–190.
- Santiago, J. L., Krayenhoff, E. S. and Martilli, A. (2014) 'Flow simulations for simplified urban configurations with microscale distributions of surface thermal forcing', *Urban Climate*, vol. 9, pp. 115–133.
- Sarrat, C., Lemonsu, A., Masson, V. and Guedalia, D. (2006) 'Impact of urban heat island on regional atmospheric pollution', *Atmospheric Environment*, vol. 40, no. 10, pp. 1743–1758.
- Schubert, S. and Grossman - Clarke, S. (2014) 'Evaluation of the coupled COSMO - CLM/DCEP model with observations from BUBBLE', *Quarterly Journal of the Royal Meteorological Society*, vol. 140, no. 685, pp. 2465–2483.
- Schuetze, T. and Chelleri, L. (2011) 'Climate adaptive urban planning and design with water in Dutch polders', *Water Science and Technology*, vol. 64, no. 3, pp. 722–730.
- Sebastian, H. and Bruse, M. (2009) *Numerical modeling of the urban climate—a preview on ENVI-met 4.0* [Online].
- Shafer, C. S., Lee, B. K. and Turner, S. (2000) 'A tale of three greenway trails: user perceptions related to quality of life', *Landscape and urban planning*, vol. 49, 3-4, pp. 163–178.
- Shanghai Meteorological Service (2018) *Record of the hyperthermal in Shanghai (2018)* [Online]. Available at <http://www.smb.gov.cn/sh/tqyb/gwqk/infodetail/d41e29a9-b3e5-4f56-aad7-42bcb01d3696.html> (Accessed 26 February 2019).
- Shashua-Bar, L. and Hoffman, M. E. (2000) 'Vegetation as a climatic component in the design of an urban street: An empirical model for predicting the cooling effect of urban green areas with trees', *Energy and buildings*, vol. 31, no. 3, pp. 221–235.
- Shashua-Bar, L., Potchter, O., Bitan, A., Boltansky, D. and Yaakov, Y. (2010) 'Microclimate modelling of street tree species effects within the varied urban morphology in the Mediterranean city of Tel Aviv, Israel', *International Journal of Climatology: A Journal of the Royal Meteorological Society*, vol. 30, no. 1, pp. 44–57.
- Shashua-Bar, L., Tsiros, I. X. and Hoffman, M. (2012) 'Passive cooling design options to ameliorate thermal comfort in urban streets of a Mediterranean climate (Athens) under hot summer conditions', *Building and Environment*, vol. 57, pp. 110–119.
- Sievers, U. (2012) *Das kleinskalige Strömungsmodell MUKLIMO_3 Teil 1: Theoretische Grundlagen, PC-Basisversion und Validierung*.
- Sodoudi, S., Zhang, H., Chi, X., Müller, F. and Li, H. (2018) 'The influence of spatial configuration of green areas on microclimate and thermal comfort', *Urban forestry & urban greening*, vol. 34, pp. 85–96 [Online]. DOI: 10.1016/j.ufug.2018.06.002.
- Spagnolo, J. and Dear, R. de (2003) 'A field study of thermal comfort in outdoor and semi-outdoor environments in subtropical Sydney Australia', *Building and Environment*, vol. 38, no. 5, pp. 721–738.

- Spectrum-Technologies (2017) 'Spectrum Watchdog 2900ET Product Manual', 13 September [Online]. Available at <https://www.manualslib.com/manual/1285680/Spectrum-Watchdog-2900et.html#manual> (Accessed 9 December 2023).
- Spronken-Smith, R. A. and Oke, T. R. (1998) 'The thermal regime of urban parks in two cities with different summer climates', *International Journal of Remote Sensing*, vol. 19, no. 11, pp. 2085–2104.
- Stadt, K. J. and Lieffers, V. J. (2000) 'MIXLIGHT: a flexible light transmission model for mixed-species forest stands', *Agricultural and Forest Meteorology*, vol. 102, no. 4, pp. 235–252 [Online]. DOI: 10.1016/S0168-1923(00)00128-3 (Accessed 12 July 2018).
- Stadtklima Stuttgart (2008) *Stadtklima Stuttgart | Klimaatlas Region Stuttgart | Klimaatlas Region Stuttgart (2008)* [Online]. Available at https://www.stadtklima-stuttgart.de/index.php?klima_klimaatlas_region (Accessed 28 August 2024).
- Staiger, H., Laschewski, G. and Grätz, A. (2012) 'The perceived temperature - a versatile index for the assessment of the human thermal environment. Part A: scientific basics', *International journal of biometeorology*, vol. 56, no. 1, pp. 165–176.
- Steuri, B., Bender, S. and Cortekar, J. (2020) 'Successful user-science interaction to co-develop the new urban climate model PALM-4U', *Urban Climate*, vol. 32, p. 100630.
- Stewart, I. D. and Oke, T. R. (eds) (2009) *Classifying urban climate field sites by “local climate zones” : The case of Nagano, Japan*.
- Stewart, I. D. and Oke, T. R. (2012) 'Local climate zones for urban temperature studies', *Bulletin of the American Meteorological Society*, vol. 93, no. 12, pp. 1879–1900.
- Sun, S., Xu, X., Lao, Z., Liu, W., Li, Z., Higuera García, E., He, L. and Zhu, J. (2017) 'Evaluating the impact of urban green space and landscape design parameters on thermal comfort in hot summer by numerical simulation', *Building and Environment*, vol. 123, pp. 277–288.
- Sundborg, Å. (1950) 'Local climatological studies of the temperature conditions in an urban area', *Tellus*, vol. 2, no. 3, pp. 222–232.
- Systems Innovation (2016) *Synthesis* [Online]. Available at <https://de.systemsinnovation.io/post/synthesis> (Accessed 26 January 2021).
- Systems Innovation (2020a) *Paradigm Shift* [Online]. Available at <https://de.systemsinnovation.io/post/paradigm-shift> (Accessed 28 January 2021).
- Systems Innovation (2020b) *Holism&Reductionism* [Online]. Available at <https://www.systemsinnovation.io/post/holism-reductionism> (Accessed 28 August 2020).
- Taha, H. (1997) 'Urban climates and heat islands: albedo, evapotranspiration, and anthropogenic heat', *Energy and buildings*, vol. 25, no. 2, pp. 99–103.
- Taleghani, M., Sailor, D. J., Tenpierik, M. and van den Dobbelsteen, A. (2014) 'Thermal assessment of heat mitigation strategies: The case of Portland State University, Oregon, USA', *Building and Environment*, vol. 73, pp. 138–150.
- Tan, Z., Lau, K. K.-L. and Ng, E. (2016) 'Urban tree design approaches for mitigating daytime urban heat island effects in a high-density urban environment', *Energy and buildings*, vol. 114, pp. 265–274.

- Tang, H., Liu, J. and Zheng, B. (2022) 'Study on the Green Space Patterns and Microclimate Simulation in Typical Urban Blocks in Central China', *Sustainability*, vol. 14, no. 22, p. 15391.
- Terjung, W. H. and O'Rourke, P. A. (1981) 'Relative influence of vegetation on urban energy budgets and surface temperatures', *Boundary-Layer Meteorology*, vol. 21, no. 2, pp. 255–263.
- Thorsson, S., Lindberg, F., Björklund, J., Holmer, B. and Rayner, D. (2011) 'Potential changes in outdoor thermal comfort conditions in Gothenburg, Sweden due to climate change: the influence of urban geometry', *International Journal of Climatology*, vol. 31, no. 2, pp. 324–335.
- Tsoka, S., Tsikaloudaki, A. and Theodosiou, T. (2018) 'Analyzing the ENVI-met microclimate model's performance and assessing cool materials and urban vegetation applications—A review', *Sustainable Cities and Society*, vol. 43, pp. 55–76 [Online]. DOI: 10.1016/j.scs.2018.08.009.
- Tzoulas, K., Korpela, K., Venn, S., Yli-Pelkonen, V., Kaźmierczak, A., Niemela, J. and James, P. (2007) 'Promoting ecosystem and human health in urban areas using Green Infrastructure: A literature review', *Landscape and urban planning*, vol. 81, no. 3, pp. 167–178.
- United Nations (2018) *2018 revision of world urbanization prospects* [Online].
- United Nations Economic Commission for Europe (2017) *Typology of indicators* [Online]. Available at https://unece.org/fileadmin/DAM/stats/documents/ece/ces/ge.42/2017/Seminar/Chapter_3_-_Typology_of_indicators_2017.05.18_-_for_seminar.pdf (Accessed 10 July 2021).
- Vailshery, L. S., Jaganmohan, M. and Nagendra, H. (2013) 'Effect of street trees on microclimate and air pollution in a tropical city', *Urban forestry & urban greening*, vol. 12, no. 3, pp. 408–415.
- van der Maaten, L., Postma, E. O. and van den Herik, H. J. (2009) 'Dimensionality reduction: A comparative review', *Journal of Machine Learning Research*, vol. 10, 66–71, p. 13.
- Verbruggen, A. (2007) 'Glossary JP. In (book section): Annex I', in *Climate Change 2007: Mitigation. Contribution of Working Group III to the Fourth Assessment Report of the Intergovernmental Panel on Climate Change (B. Metz et al.(eds.))*, Cambridge University Press Cambridge, UK, and New York, NY, USA.
- Verein Deutscher Ingenieure (2019) *VDI 3789: Environmental meteorology-Interactions between atmosphere and surfaces: Calculation of spectral short-wave and long-wave radiation* [Online]. Available at https://www.vdi.de/fileadmin/pages/vdi_de/redakteure/richtlinien/inhaltsverzeichnisse/2843469.pdf (Accessed 3 July 2024).
- Verein Deutscher Ingenieure (2022) *VDI 3787, Part 2: Environmental meteorology-Methods for human-biometeorological evaluation of the thermal component of the climate* [Online]. Available at https://www.vdi.de/fileadmin/pages/vdi_de/redakteure/richtlinien/inhaltsverzeichnisse/3354762.pdf (Accessed 3 July 2024).
- Vitruve, Howe, T. N. and Dewar, M. J. (1999) *Vitruvius: Ten Books on Architecture*, Cambridge University Press.
- Vos, C. C., Berry, P., Opdam, P., Baveco, H., Nijhof, B., O'Hanley, J., Bell, C., Kuipers, H. and Nijhof, B. (2008) 'Adapting landscapes to climate change: examples of climate-proof ecosystem networks and priority adaptation zones', *Journal of Applied Ecology*, pp. 1722–1731.

- Walfram-Research (1996) *Kelvin, Lord William Thomson (1824-1907)* [Online]. Available at <https://scienceworld.wolfram.com/biography/Kelvin.html> (Accessed 28 January 2021).
- Wang, Y. and Zacharias, J. (2015) 'Landscape modification for ambient environmental improvement in central business districts—a case from Beijing', *Urban forestry & urban greening*, vol. 14, no. 1, pp. 8–18.
- Wania, A., Bruse, M., Blond, N. and Weber, C. (2012) 'Analysing the influence of different street vegetation on traffic-induced particle dispersion using microscale simulations', *Journal of environmental management*, vol. 94, no. 1, pp. 91–101.
- Wanner, H. and Filliger, P. (1989) 'Orographic influence on urban climate', *Weather and Climate*, pp. 22–28.
- Weng, Q., Lu, D. and Schubring, J. (2004) 'Estimation of land surface temperature–vegetation abundance relationship for urban heat island studies', *Remote sensing of Environment*, vol. 89, no. 4, pp. 467–483.
- Wilmers, F. (1990) 'Effects of vegetation on urban climate and buildings', *Energy and buildings*, vol. 15, 3-4, pp. 507–514.
- Wong, N. H. and Yu, C. (2005) 'Study of green areas and urban heat island in a tropical city', *Habitat international*, vol. 29, no. 3, pp. 547–558.
- World Urban Database (2020) *The World Urban Database and Access Portal Tools project is a community-based project to gather a census of cities around the world.* [Online]. Available at <http://www.wudapt.org/> (Accessed 12 March 2020).
- Xu, H., Huang, Q., Liu, G. and Zhang, Q. (2016) 'A quantitative study of the climate-responsive design strategies of ancient timber-frame halls in northern China based on field measurements', *Energy and buildings*, vol. 133, pp. 306–320.
- Xu, J., Wei, Q., Huang, X., Zhu, X. and Li, G. (2010) 'Evaluation of human thermal comfort near urban waterbody during summer', *Building and Environment*, vol. 45, no. 4, pp. 1072–1080.
- Xu, L. and Yue, W. (2008) 'A study on thermal environment effect of urban park landscape', *Acta Ecol. Sinica*, vol. 28, no. 4, pp. 1702–1710.
- Xu, Y., Ren, C., Cai, M., Ng, E. and Wu, T. (2017) 'Classification of local climate zones using ASTER and Landsat data for high-density cities', *IEEE Journal of Selected Topics in Applied Earth Observations and Remote Sensing*, vol. 10, no. 7, pp. 3397–3405.
- Yamada, T. and Mellor, G. (1975) 'A simulation of the Wangara atmospheric boundary layer data', *Journal of the Atmospheric sciences*, vol. 32, no. 12, pp. 2309–2329.
- Yan, H., Fan, S., Guo, C., Wu, F., Zhang, N. and Dong, L. (2014) 'Assessing the effects of landscape design parameters on intra-urban air temperature variability: The case of Beijing, China', *Building and Environment*, vol. 76, pp. 44–53.
- Yu, Z. W., Guo, Q. H. and Sun, R. (2015) 'Impacts of urban cooling effect based on landscape scale: a review', *Ying yong sheng tai xue bao= The journal of applied ecology*, vol. 26, no. 2, pp. 636–642.
- Zhang, H., Chi, X., Müller, F., Langer, I. and Sodoudi, S. (2019) *Wie wirkt sich der Tiergarten Berlin auf das Wohlbefinden der Menschen aus? eine Studie über den Kühlungseffekt von Grünflächen und den thermischen Komfort der Fußgänger.* [Online]. Available at <https://doi.org/10.1515/9783110607772-015>.

Zhang, X., Zhong, T., Feng, X. and Wang, K. (2009) 'Estimation of the relationship between vegetation patches and urban land surface temperature with remote sensing', *International Journal of Remote Sensing*, vol. 30, no. 8, pp. 2105–2118.

Zhao, J., Luo, P., Wang, R. and Cai, Y. (2013) 'Correlations between aesthetic preferences of river and landscape characters', *Journal of Environmental Engineering and Landscape Management*, vol. 21, no. 2, pp. 123–132.

Zhengming, W. and Dozier, J. (1989) 'Land-surface temperature measurement from space: Physical principles and inverse modeling', *IEEE Transactions on Geoscience and Remote Sensing*, vol. 27, no. 3, pp. 268–278.

Zhou, W., Huang, G. and Cadenasso, M. L. (2011) 'Does spatial configuration matter? Understanding the effects of land cover pattern on land surface temperature in urban landscapes', *Landscape and urban planning*, vol. 102, no. 1, pp. 54–63.